MINERALIZATION AT MOUNT OWEN, CENTRAL NELSON

A thesis
submitted in partial fulfilment
of the requirements for the Degree
of
Master of Science in Geology
in the
University of Canterbury
by

N.A. Newman

University of Canterbury
1979

Photograph: Geoffrey C. Wood

"Leases to the left of them,
Leases to the right of them,
Leases in front of them,
Surveyed and numbered.
Out of the swarm of names,
Good for sharebrokers' games,
What will prove paying claims -
One in a hundred?"

'Taking a liberty with Mr. Tennyson',
The Nelson Evening Mail, March 1882.

CONTENTS

Figure	FIGURES	PAGE

Figure	FIGURES	PAGE

Figure	FIGURES	PAGE

Figure	FIGURES	PAGE

Figure	FIGURES	PAGE
7-1	Fluid inclusion filling vs. temperature plot. Reproduced from Yermakov (1965)	243
7-2	Density vs. temperature plot showing the filling progress of five different inclusions. From Roedder (1972)	243
7-3	Combined data from graphs by Yermakov and Roedder (Figs. 7-1, 7-2)	245
7-4	Increase in critical temperature (ΔTc) for aqueous solutions of NaCl. Taken from Yermakov, (1965)	249
7-5	The formation of secondary inclusions	253
7-6	Secondary inclusions in massive vein quartz	259
7-7	Inclusions in quartz veins	260
7-8	Scanning electron microscope photographs of fracture surfaces of quartz	261
7-9	As Fig. 7-8. Alignment of secondary inclusion pits reveal the locus of healed fractures	262
7-10	Pseudosecondary inclusions with 'bubbles' of liquid CO_2	264
7-11	Primary and secondary inclusions in sample LS-12	266
7-12	Primary inclusions containing an immiscible liquid	267
7-13	Identification of phases in multi-component inclusions	268
7-14	Diagram showing homogenization behaviour for hypothetical inclusions containing only CO_2. (From Yermakov, 1965)	268
7-15	Nucleation of vapour phases in two-liquid inclusions	270
7-16	Paired photographs of inclusions, at room temperature (showing two fluid phases), and chilled (three fluid phases)	271

Table	TABLES	PAGE

LIST OF APPENDIX FIGURES AND TABLES

ABSTRACT

The Lower Paleozoic sequence at Mt. Owen, Nelson, hosts gold and base metal mineralization. The succession comprises the Wangapeka Formation (a black shale and sandstone unit), the underlying Arthur Marble Formation, which in turn rests on a metamorphosed and hydrothermally altered sequence of quartzite, dolomite, and black shales, informally defined here as the Owen Formation. The succession dips steeply westward, away from the adjacent intrusive batholith of Cretaceous Separation Point Granite. Tectonic deformation, metamorphism, and hydrothermal alteration are related to two principal controls: (a) granite intrusion, and (b) confinement of fluid processes beneath the marble.

Study of the disseminated sulphide minerals in the sedimentary rocks shows that whereas the sequence within and above the marble contains only crystalline pyrite, the more altered Owen Formation contains a complex suite of minerals, exhibiting the paragenesis:

pyrite → pyrrhotite → marcasite → pyrite

Base metal ores form both replacement and infilling bodies within, and near, the marble, and comprise argentiferous galena, sphalerite, and minor chalcopyrite; in one deposit a silver-rich tetrahedrite occurs, together with more complex minerals of the fahlore group. Gold is substantially confined to quartz-carbonate veins in the Owen Formation, where it occurs in a hypogene assemblage of marcasite, pyrite, and quartz, which represents late stage deposition. Some gold, which is highly argentiferous, occurs partly in idiomorphic form and is considered to be hypogene; supergene gold is also present. An earlier

report of native bismuth appears to be based on the misidentification of native lead.

Mineralization extended over a wide range of generally declining temperatures and changing fluid composition; precise reconstruction of physico-chemical conditions is difficult due to the effects of retrograde overprinting, and the lack of equilibrium data for the sulphide, carbonate, and silicate systems examined. A study of fluid inclusions provides some precise data on the hydrothermal system; evidence for the existence of a CO_2-saturated fluid during mineral deposition permits the use of filling temperatures without correction for sealing pressure. The measurement of both CO_2 content and salinity for one inclusion permits complete P-T-X evaluation of the local fluid system at the time of sealing:

X_{CO_2} = 15 wt.% X_{NaCl} = 9.3 wt.% T = 312°C P = 790 b

All data are combined in an interpretative model for the mineralization, in which a fluid is produced by intrusion-induced dewatering and dehydration of sediments, and the mobilisation and transport of ore metals is promoted by decarbonation and desulphurization reactions. Structural control by the impermeable marble produces an up-dip, non-recirculatory fluid flow, resulting in intensified alteration and mineralization in the upper Owen Formation.

CHAPTER I

INTRODUCTION

I. GENERAL INTRODUCTION

The area generally known as the Owen Goldfield lies at the headwaters of the Owen River, the northernmost tributary of the Buller River (Figure 1-1). Prospecting during the 1880's located both gold bearing veins and argentiferous base metal occurrences in an area of Paleozoic rocks to the south of Mt. Owen. Several ore bodies were mined during a period of speculative development, 1887-1889, but all attempts failed within a short time due to unprofitable operation. The field was rapidly abandoned, and has since attracted only minor prospecting. The mineralization has not been investigated prior to this project, and very little information on the economic geology was known other than brief observations made by the Geological Survey and Mines Department staff during the mining period.

(1) Scope of the Project

The aims of this project were as follows:

(i) To describe the mineralization and its geological setting.

(ii) To elucidate the controls, conditions, origin, and history of the mineralization.

(iii) To determine the reasons for the failure of the early mining attempts.

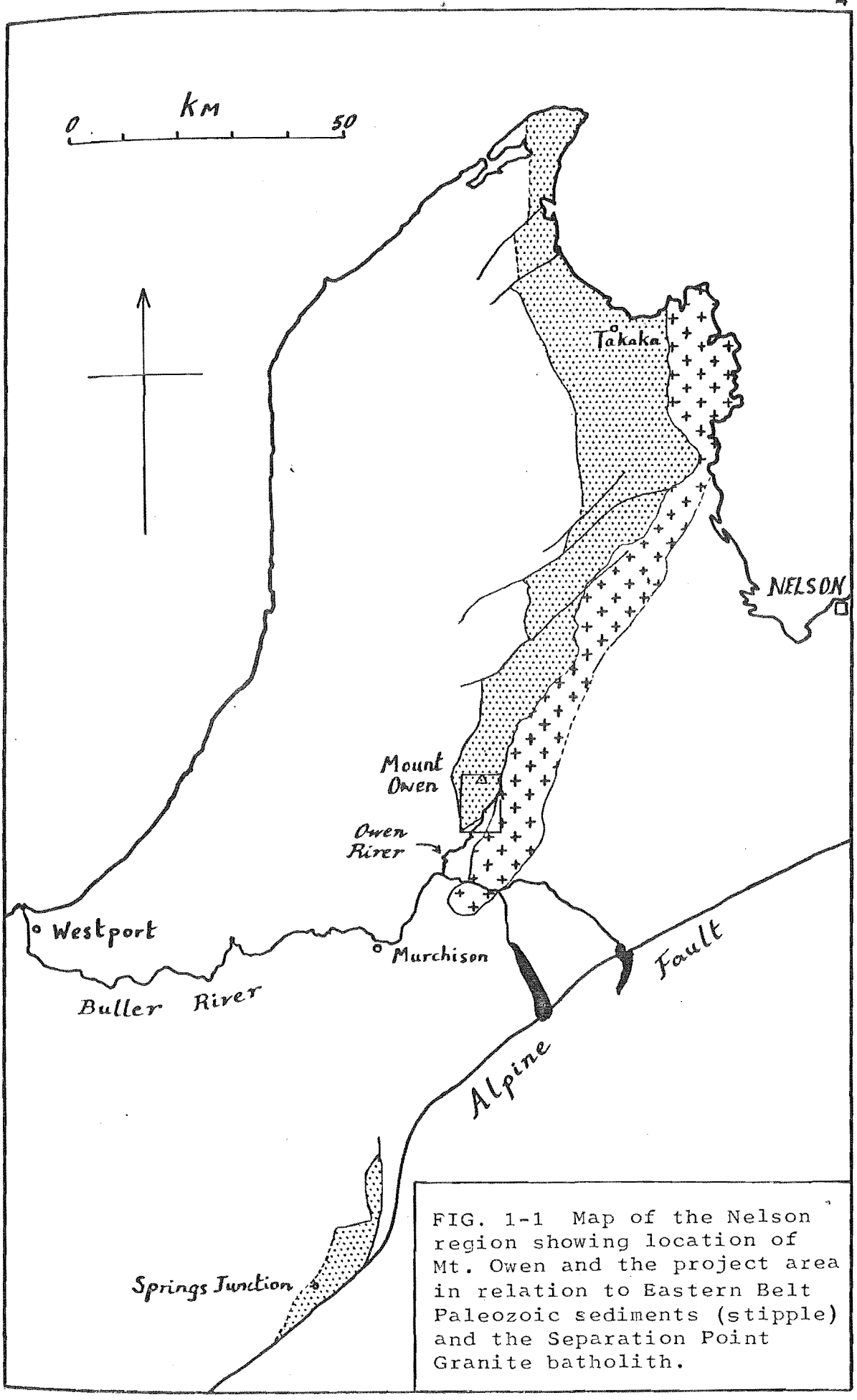

FIG. 1-1 Map of the Nelson region showing location of Mt. Owen and the project area in relation to Eastern Belt Paleozoic sediments (stipple) and the Separation Point Granite batholith.

Because of the lack of previous work, this broad range for the project was considered necessary. This has, however, resulted in a superficial treatment of some aspects, which require more detailed investigation for their proper interpretation. This applies chiefly to the mapping, where considerably more work than was able to be done is required to permit a comprehensive structural interpretation.

II. GEOLOGICAL SETTING AND PHYSIOGRAPHY

(1) Geological Setting

The Owen Goldfield is located on the south-east slopes of the Owen Massif, an area of high country dominated by Mt. Owen (1877 m) and several sub-peaks, all displaying a rugged karst topography incised into thick marble. The Owen Massif represents the southernmost limit of the Eastern Belt (Cooper, 1975), a more or less continuous belt of lower Paleozoic limestones, shales, and their metamorphosed equivalents which extends southward from Takaka (Figure 1-1). The Paleozoic sediments terminate in a blunt, fault-bounded apex against a thick succession of Tertiary rocks, and reappear only at Maruia, 80 km further south.

The rocks of the Owen Massif comprise a relatively simple, upright, succession of three distinct units: quartzites, sandstones and carbonaceous mudstones overlie a thick and continuous marble, which in turn rests upon a more complex unit of predominantly dark, dolomitic shales and sandstones. A general westward dip of the succession south of Mt. Owen exposes the lowermost unit in the headwaters of the Owen River, where the unit is separated from the Separation Point batholith by a fault block of Tertiary sediments. Although mineralization occurs in all three Paleozoic units, the bulk of the gold occurs in veins in the lowermost unit, and the

base metal deposits are concentrated near the base of the marble.

(2) Physiography

The Owen Massif presents a prominent, up-faulted, erosion resistant block, elevated above the surrounding Tertiary rocks. The topography and drainage pattern on the massif are strongly controlled by bedding and jointing in the limestone. Elevated plateaus formed on stripped bedding plane surfaces are deeply incised by solution channels and sinkholes. The eastern margin of the massif terminates in a steep scarp produced by fault-controlled erosion of the westward-dipping succession, forming the narrow valley of the Owen River headwaters. The auriferous veins are found on steep slopes below the escarpment, along both sides of the Owen River, and in the valley of a smaller eastern tributary known as Bulmer Creek (Figure 1-2).

Access is restricted by the steepness of the slopes, with large bluffs common where the marble crops out. Traverses from the valley to the top of the scarp are possible only in a few places. Thick bush is present almost everywhere below 1200 m, except for bluffs and scree slopes and a small area in the south of the region which is farmed. Exposure is poor in areas of bush cover, but considerably better in streams and cliffs, although rarely continuous for more than a few metres.

Many new names for geographic features are introduced in this report to supplement the sparse range of existing locality names. Most new names have been derived from early mining records or local names (Appendix I).

III. HISTORICAL BACKGROUND

Mount Owen was so named by von Haast, who was impressed when he first saw the massif on an expedition in January, 1860. In keeping with his policy of naming prominent features after British geologists, he named the mountain after Richard Owen, a well known contemporary Scottish paleontologist. Haast established that the Owen River, which drained from the mountain, was gold bearing by obtaining a single flake of gold in a panning test (von Haast, 1861).

The gravels of the river were too poor to attract alluvial miners, and no prospecting in the valley is recorded until 1882, when a syndicate of three men (Bulmer, Gibbs and Byrne) announced in Nelson City the discovery of gold bearing quartz in the valley of Bulmer Creek, after spending several years prospecting the region. The short period of development and mining which followed this discovery is not well documented. The summary of these events given below is based on official publications (Handbook of N.Z. Mines, 1887; Black, 1887; Bird, 1887, 1888; Gordon, 1888; Hector, 1888; Park, 1888) and later summaries (Downey, 1928; Williams, 1965), supported by additional details from the files of newspapers of the surrounding districts (The Nelson Evening Mail; The Colonist; The Lyell Times). Personal reminiscence is provided by Lyons (1952), and an excellent background of local history by Brown (1976).

(1) Early Prospecting and Development of the Field

The original party of prospectors made formal applica-

tions for claims in 1882, and the discovery initiated further prospecting. Until 1887 the number of leases in the area slowly increased as further veins were discovered. An increasing population gave rise to a small township, with commercial enterprises set up to serve the prospectors in anticipation of more extensive operations. By late 1887, more than thirty leases had been taken up, and on the results of some good assays, sufficient shareholders' funds were accumulated by some of the larger companies to enable mine development and stockpiling of ore for crushing in batteries which were still under construction. Few assay values for the Owen ores are available, but many of the published results are very high, including one widely publicised value of more than 19 oz/ton (Handbook of N.Z. Mines, 1887). Later assays from the well developed mines show erratic, but generally much lower values. This discrepancy may be partly due to surface enrichment effects, but non-representative sampling was probably the major cause.

The period of 'boom' development at Mt. Owen coincided with major expansion at the Reefton, Lyell, and Wangapeka quartz mining fields. The rise of interest in mining in the Nelson district was marked by the founding of the short-lived Nelson School of Mines (see frontispiece), which was initiated principally by the development of the Owen field (see Black, 1888).

(2) The Mining Period, 1888-1890

In the summer of 1888, the field attracted widespread

attention with the start of crushing at two batteries. Of all the quartz claims taken up (see Map 2), only two were able to sustain crushing operations, the others either waiting to sell their ground to the operating companies, or intending to have their ore crushed by contract.

(a) The Enterprise Lease. The largest company was the Enterprise, which exposed a large but poorly defined vein in a spur on the western side of the valley, immediately south of Halfway Creek. Mine development consisted of three levels from hillside adits, with a winze between levels 2 and 3. Stoping was done in level 1, and possibly level 2. Conditions for working the mine and plant were considered excellent; the crushing battery was set up near the portal of the lowest level (3), and adequate water power was available to operate the plant.

(b) The Wakatu Lease. This lease was located among a group of claims taken up by the original applicants in 1882, and operated on a partly co-operative basis with respect to sharing of the ore transport ropeway and crushing equipment. The other leases of this group (Uno, Bulmer Creek, Natal, Maria Louisa, Chance it, and others) will not be described, but together with the Wakatu may be collectively termed the Bulmer Creek Group. A public crushing battery was erected at the Owen River opposite the mouth of Bulmer Creek, so as to receive ore from many surrounding claims. Here also, the adequate flow and fall of the river permitted the use of water power, provided by a headrace and a short penstock, giving 27 m of fall to drive a double pelton wheel. The Wakatu Company conceded the water rights in return for the

first crushing of 1,000 tons. At several leases in the Bulmer Creek Group, visible specimen gold was reported, and several long drives and cross-cuts were commenced to prove the extent of the veins.

(c) The Golden Crown Lease. A small mine was operated on a hill above the public battery where a winze was sunk on a vein outcrop, a short distance west of Trig GC. A small amount of rich ore was extracted and crushed, but mine development was poor. A low level drive was recommended, but if ever completed, failed to locate the vein.

(d) The Zealandia Lease. This company attempted to work a vein outcropping on the steep slopes north of the Enterprise Lease. Good quartz was found in outcrop workings, but not traced in development drives.

(e) Other Gold Leases. Of the many other gold leases in the area, few contributed any ore for crushing, most being merely prospected and held as speculative ventures.

(f) The Outcome of Crushing. Both batteries commenced operating in early 1888, but on cleaning-up after a few weeks' crushing, very disappointing results were obtained. The Enterprise ore yielded only 0.1 oz/ton (3 ppm), and the Wakatu ore at the public battery performed only a little better. A decline of interest began immediately. Some attempts to improve gold recovery were made, including the dismissal and replacement of some mine managers, but very little further crushing was done. The Enterprise Company cut their losses by selling their plant, while many of the Bulmer Creek leaseholders amalgamated their holdings. Rich ore patches were worked over the next few months in a

period of general decline of operations. It is not known how long the public battery remained working, but it appears that only a few hundred tons of ore was crushed for an average yield of less than 0.2 oz/ton (6 ppm).

(3) The Silver Mining Ventures

During Park's visit to the field when the batteries were crushing, he was shown samples of water-worn galena, found among the gravels of Bulmer Creek. His advice to the miners was to examine the base of the marble for the source of this mineral, and subsequent prospecting revealed a number of small base-metal occurrences at this horizon (Park, 1888). Attracted by high silver values in the ore, a new wave of speculation developed, and claims were taken out around prospects near Trig C, the Bulmer headwaters, lower Fyfe River, and Silverstream (Baigent) Creek. Only in Fyfe River was a workable deposit found, where the 'Welcome' Company rapidly worked out a small body of rich ore. Work at the other locations was restricted to small prospecting operations. The attraction of silver mining appears to have been particularly strong, leases being taken out in two continuous lines, each based on the trend of small ore bodies, projected over a distance of more than 2.7 km in each case. Waves of prospecting recurred over many years, with the development of 'lost reef' legends, of which a classic example is found in Lyons' (1952) description of the locality near Trig C. In 1911, the Mount Owen and Rising Sun Mineral Company was formed by local shareholders, and took over the old leases

in this area, employing a prospector (C.S. Beilby) to drive exploratory adits. These attempts to find an ore body were unsuccessful, although the company persisted for several years. The locality, later known as Beilby's Reef, was subject to a brief investigation in the 1950's (Williams, 1965), and again in 1970.

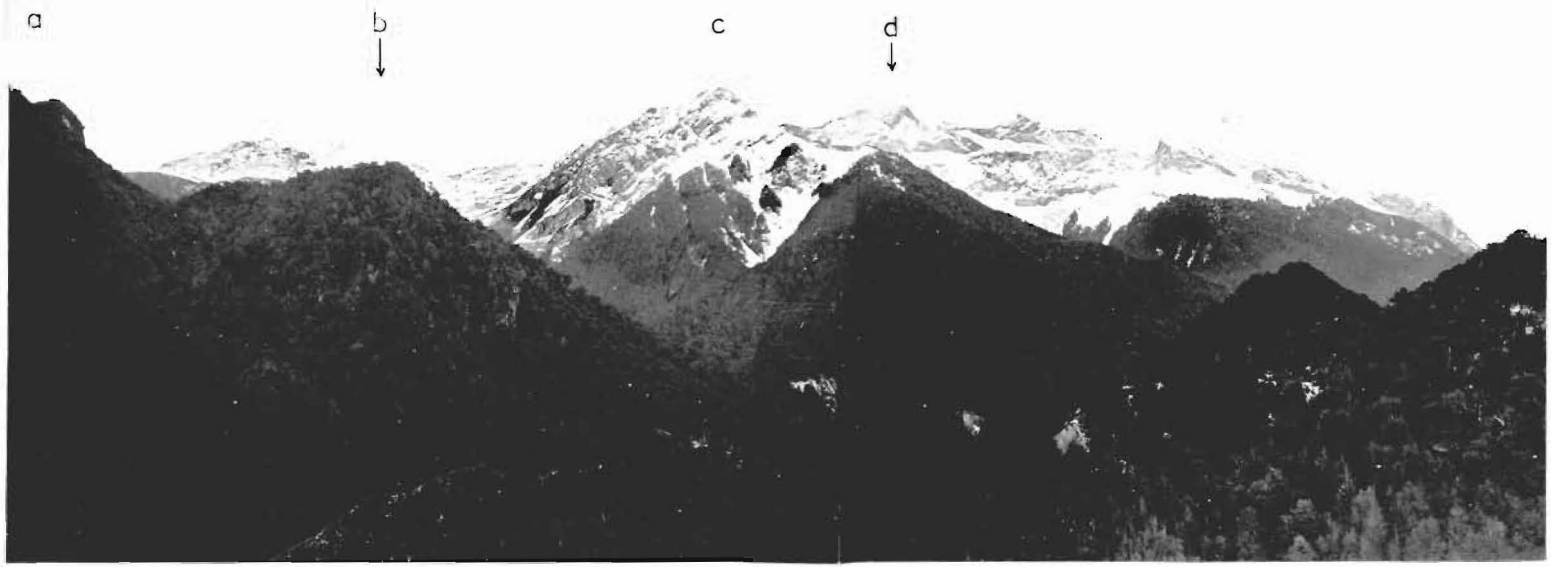

FIG. 1-2 The central part of the Owen Goldfield, photographed from a point above the south bank of Halfway Creek, approximately 350 m east of the Owen River. Features indicated are: (a) flank of Mt. Peru, (b) Bonanza Spur, (c) Sunrise Peak, (d) summit of Mt. Owen. In the valley of Bulmer Creek, which can be seen extending westward behind Bonanza Spur, the snow-covered slumps visible immediately above the ridge in the foreground mark the site of workings by the Uno and Wakatu mining companies.

IV. PREVIOUS WORK

The only significant published investigations of the mineralisation are the brief observations made by the visiting geologists when the mines were operating, and these reports have been referred to above. Only Park (1888) and Hector (1888) include notes on the geology of the area, Park's report including a cross-section (Figure 1-3), a structural interpretation and a geological history. He considered the mineralization to be the result of 'infiltration from the surface' into fissures formed by granite intrusion. His rejection of a purely magmatic origin is surprising, in view of the widespread acceptance of this concept of ore genesis at the time.

During the mining period, the government analyst published announcements concerning the supposed discovery of bismuth in the ores (Skey, 1887, 1888a, 1888b). This and other early observations on the ore mineralogy are reviewed in Chapter V.

Following the decline of interest in the goldfield, no further geological work was done in the area until the late 1920's, when J. Henderson and H.E. Fyfe of the N.Z. Geological Survey undertook field work for the mapping of the Murchison Subdivision. Brief progress reports appeared at the time (Henderson and Fyfe, 1927), and the completed maps were drawn up in 1935, but the text of the bulletin did not appear until 33 years later (Fyfe, 1968). The structural and stratigraphic information provided in this bulletin is discussed in Chapter III.

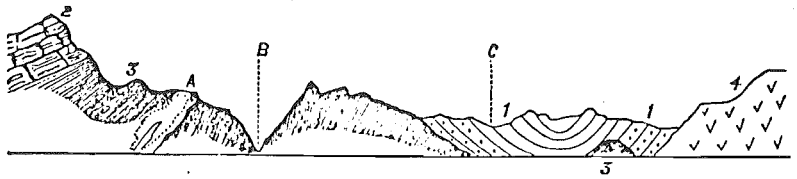

A. Enterprise Claim. B. Owen River. C. Half-way Creek. 1. Cretaceo-tertiary rocks. 2. Limestone. 3. Auriferous slates. 4. Granite (Mount Hope Range).

FIG. 1-3 An east-west cross-section through the Owen Goldfield drawn by Park (1888). The 'limestone' to the left (west) is marble, and the contacts at the margin of the Tertiary rocks are faulted, not sedimentary as shown. Park did not see the shales and slates overlying the marble at Mt. Owen, and did not extend the section to include these units.

Kear (1954) carried out detailed mapping of the Tertiary rocks in the area, and his information concerning Tertiary contacts and faulting has been used in this report (see map 1).

Fyfe's mapping was revised with the issue of the 1:250,000 sheet for the area (sheet 15, Bowen, 1964), and the new stratigraphic interpretations were based on correlation with sequences in the Mt. Arthur region.

The entire Mt. Owen region has recently been re-mapped by the N.Z. Geological Survey for data compilation for sheet S19 (Tadmor), 1:63360 series (Coleman, in press), although the goldfield area will appear on an adjacent sheet, S26 (Hope), in preparation.

CHAPTER II

STRATIGRAPHY

I. STRATIGRAPHIC CLASSIFICATION AND NOMENCLATURE

(1) Previous Classifications

All previous attempts to apply stratigraphic nomenclature to the rocks at Mt. Owen have been limited by the lack of fossils, and have relied on correlation with similar lithostratigraphic units further to the north. A summary of the various classification schemes and ages assigned is given in Figure 2-1.

(a) Park, 1888. Park compared the Owen rocks to those in the Wangapeka-Baton district, and defined lithologic units but did not apply formal names. On the basis of corals from the Wangapeka valley he considered the marble to be Lower Silurian, and the overlying slates and sandstones Upper Silurian, although he did not see this unit at the Owen Goldfield (see Figure 1-2). No age was given to the unit beneath the marble, which he described as 'blue slates, etc.', and 'auriferous slates'. His reason for not attempting age correlation for this unit may be attributed to Hector's (1888) belief that an unconformity existed below the marble. Park recognised the post-Devonian, intrusive relationship of the granite, and suggested a lower Carboniferous age.

(b) Henderson and Fyfe, 1935. On the geological maps drawn up for the Murchison Subdivision bulletin, no distinction of the Paleozoic units at Mt. Owen is made, except for approximate lithological boundaries shown by dashed lines. All of the units are placed within the classification Mt. Arthur Series, and considered to be Upper Ordovician in age. No age is given for the granite.

(c) Bowen, 1964. The issue of the 1:250,000 geological maps for the Nelson region introduced a new stratigraphic interpretation and nomenclature, based mainly on the work of Grindley (1961). The marble at Mt. Owen was classed as Mt. Arthur Marble Formation (Upper Ordovician), the overlying unit Wangapeka Formation (? Silurian), and the underlying unit Flora Formation (Middle Ordovician), all by correlation with similar lithologies at Wangapeka and Mt. Arthur. The sequence of the three formations was termed the Mt. Arthur Group. The granite was named Separation Point Granite (? Carboniferous).

(d) Fyfe, 1968. R.P. Suggate, in editing the text accompanying the long-awaited publication of Fyfe's (1935) maps, provided a revised stratigraphy for the lower Paleozoic rocks of the area. The classification is similar to that of Bowen, but restricted the age of the Mt. Arthur Group to Middle to Upper Ordovician in the light of new fossil evidence, and listed the Separation Point Granite as Cretaceous, after the result of radiometric dating was known (Aronson, 1965).

(e) This Work. When this project was commenced, the

stratigraphic classification as given in Fyfe (1968) was used. During the course of the project, the Nelson Ordovician stratigraphy underwent a major revision, although at the time of writing, the revised scheme has not yet been published (Coleman, in press).

Re-mapping of the Mt. Arthur region by N.Z. Geological Survey staff has recently revealed that the Flora Formation, at the type locality, is a facies of the Wangapeka Formation, which was seen to contain laterally equivalent marble and shale sequences, and to overlie a continuous marble, the base of which is not exposed. The name Wangapeka Formation is to be retained, now embracing an extended range of lithologies including the rocks previously mapped as Flora Formation. The continuous, lower marble is to retain the classification Arthur Marble Formation* (R.A. Cooper, pers comm.).

These two extant formation names appear to remain applicable at Mt. Owen, where a single, thick marble is present, overlying a sequence which is lithologically distinct from any part of the proposed, new Wangapeka Formation. In view of the impending changes to the nomenclature, it appeared undesirable to use the existing scheme. Continued use of the term Flora Formation would lead to confusion by implied correlation with the Flora locality. In abandoning this name, the unit beneath the marble at Mt. Owen could be classified either by correlation with

* Name modified from Mount Arthur Marble Formation by Grindley (1971).

other named units, or by the assignment of a new name.

The only two possible correlatives are the Pikikiruna Schist (Grindley, 1961) beneath the Arthur Marble at Takaka Hill, 65 km north of Mt. Owen, and the Thompson's Flat Formation (Farmer, 1967) which underlies a thin Ordovician marble at Springs Junction, 80 km to the south of Mt. Owen. To adopt the name of the highly metamorphosed Pikikiruna Schist for the much less metamorphosed rocks at Mt. Owen is considered unjustified, irrespective of their possible equivalence. The Thompson's Flat Formation, although bearing strong lithologic similarities with the unit at Mt. Owen, is too remote for reliable correlation in the absence of good evidence of age relationships. The new name Owen Formation has therefore been proposed* for this unit at Mt. Owen, and is used informally throughout this report.

* In a private communication to the N.Z. Geological Survey, October 1975.

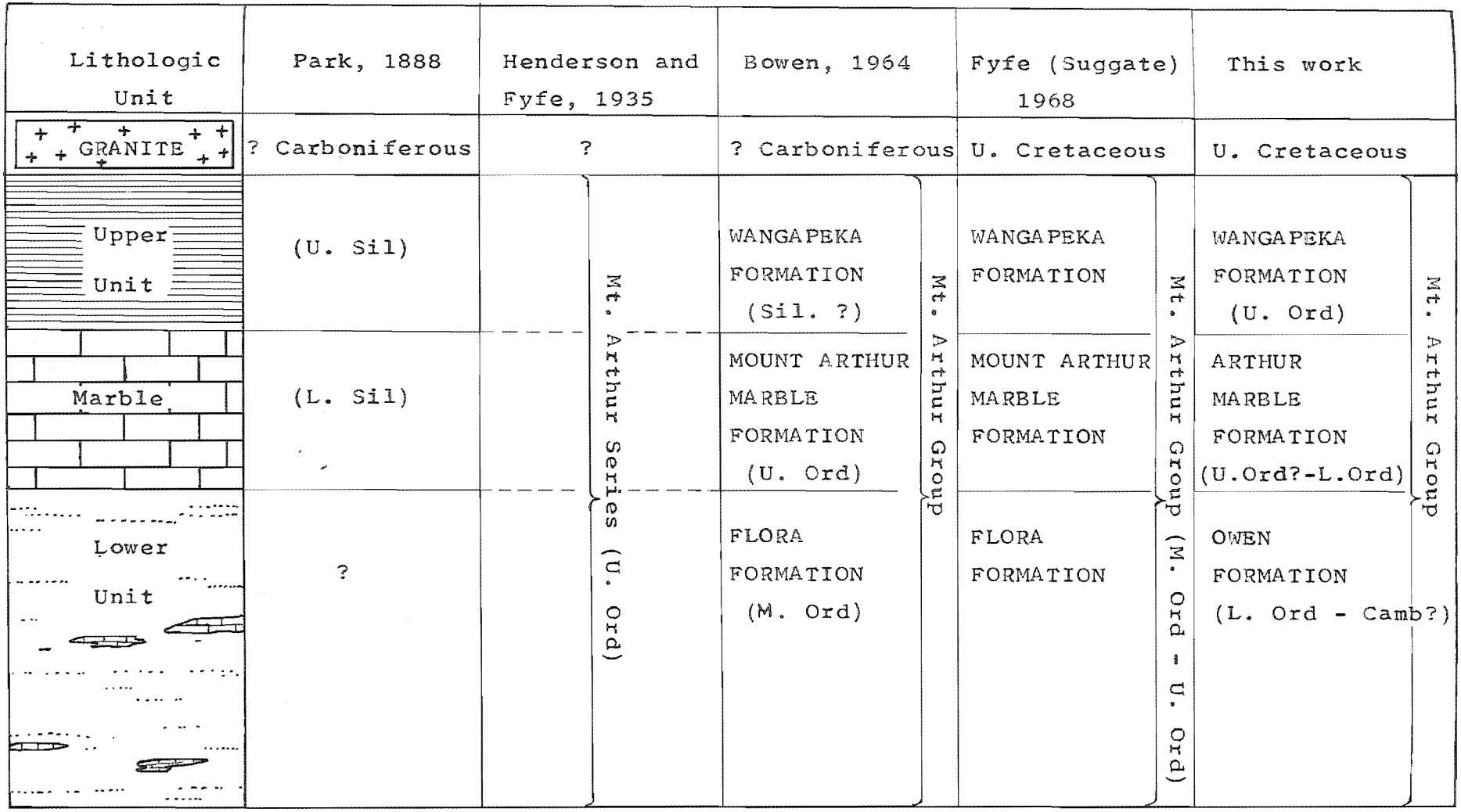

FIG. 2-1 Stratigraphic classification schemes for the Paleozoic rocks at Mount Owen, 1888-1979.

(2) Lithologic Descriptions (see also Figure 2-5)

(a) Wangapeka Formation. Within the project area, this unit comprises a maximum thickness of approximately 600 m of laminated sandstones and mudstones, conformably overlying the Arthur Marble to the south and west of the mouth of Fyfe River. The basal 100 m contains abundant massive sandstone and quartzite beds which rarely exceed a metre in thickness, and which are interbedded with finely laminated carbonaceous mudstone and siltstone (Figure 2-2). Throughout the remainder of the formation, carbonaceous mudstone and fine sandstone lithologies dominate. Stratiform, cubic pyrite is common in all lithologies except massive sandstone, and is especially abundant in units of interlaminated carbonaceous mudstone and siltstone.

Penetrative deformation is restricted to a weak slaty cleavage, and sedimentary structures are well preserved. A variety of sole markings, ripple marks and finely laminated small scale cross-stratification can be seen. More rarely, bioturbate horizons occur. Current indicators reflect a generally west to east flow direction. Load casts, flame structures, and other hydroplastic deformation structures are widespread in the muddy laminae. Intraformational slump folds are present, typically 100-200 mm thick, with axes aligned north-south. These folds close to the east, suggesting a downward paleoslope in that direction giving rise to syntaphral movements.

The sediment composition is dominantly quartz-rich, and no carbonate horizons are known to occur in the project

area. Along Fyfe River, beyond the goldfield area, the Wangapeka Formation appears to grade laterally into, or intercalate with, the marble, forming calcareous shales and impure, carbonaceous marble.

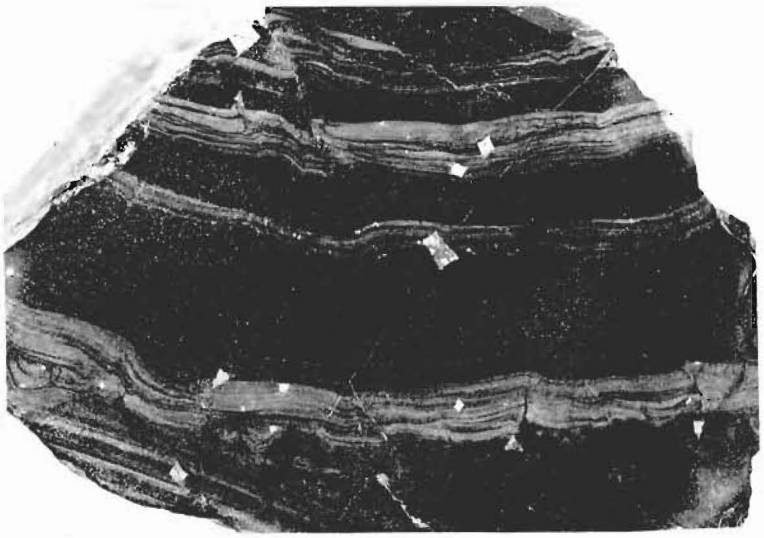

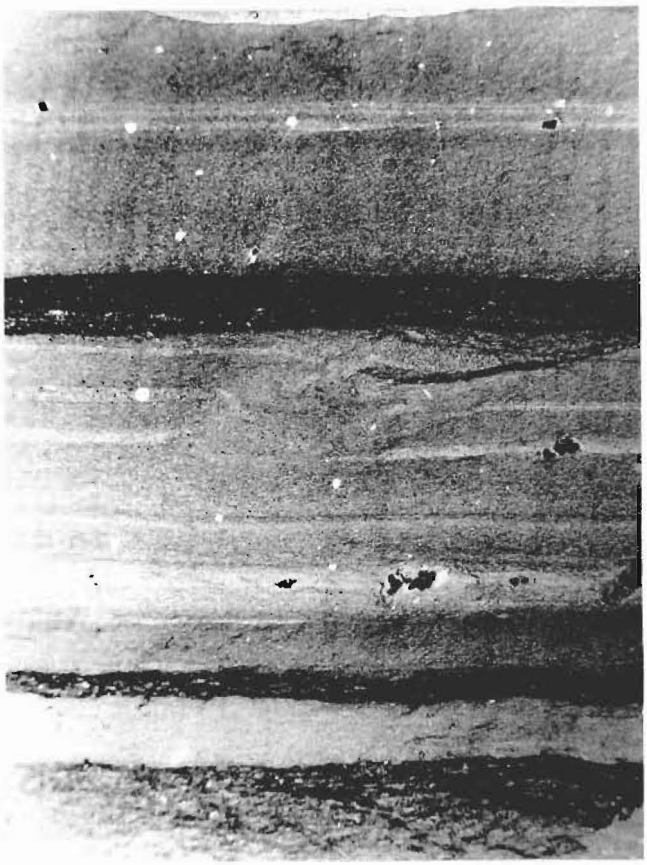

'IG. 2-2 'Black shale' lithologies, Wangapeka Formation.

Upper: A sawcut slab, showing sedimentary structures, deformation structures, and pyrite crystals. Approximately natural size. UC8872

Lower: Fine sedimentary laminations showing stratiform pyrite (black, granular), and dark, carbonaceous laminae. Deformation of the pyrite grains and the surrounding sediment is visible. The central disturbance of lamination may represent a burrow.
A thin section, ppl. x5 UC8868

(b) Arthur Marble Formation. Reliable measurements of the true thickness of this formation are difficult to obtain, due to evidence of possible tectonic thickening. A minimum of 250 m may be considered a conservative estimate, and 500 m a possible maximum. The term Arthur Marble as used in this report represents an informal contraction of the formation name.

The marble contains very few structures, and is predominantly massive. Observations from a number of traverses suggest the following lithostratigraphy:

(i) To the north of the project area, the top of the formation is well exposed, and exhibits a thin bed (1-2 m) of sparry and partly phosphatised marble (Figure 2-3).

(ii) The upper half to one third of the formation contains bands of flint nodules parallel to bedding. The nodules, which stand outprominently on weathered surfaces, range up to fist size, and have rough, irregular margins. An origin from siliceous sponges is possible.

The characteristics of zones (i) and (ii) are absent in the section exposed in Fyfe River, where the marble is massive, with a weak foliation parallel or sub-parallel to bedding.

(iii) A stratigraphic interval below the flint bands, spanning approximately one-third of the formation thickness is massive with few indications of bedding.

(iv) A basal unit, up to approximately 60 m in thickness, is defined by an increasing content of siliceous shale and dolomite as the base is approached. The

impurities are finely interlaminated, and result in a bedding cleavage which is overprinted by a cross-cutting cleavage near the base of the unit to produce a strong lineation (Figure 2-3).

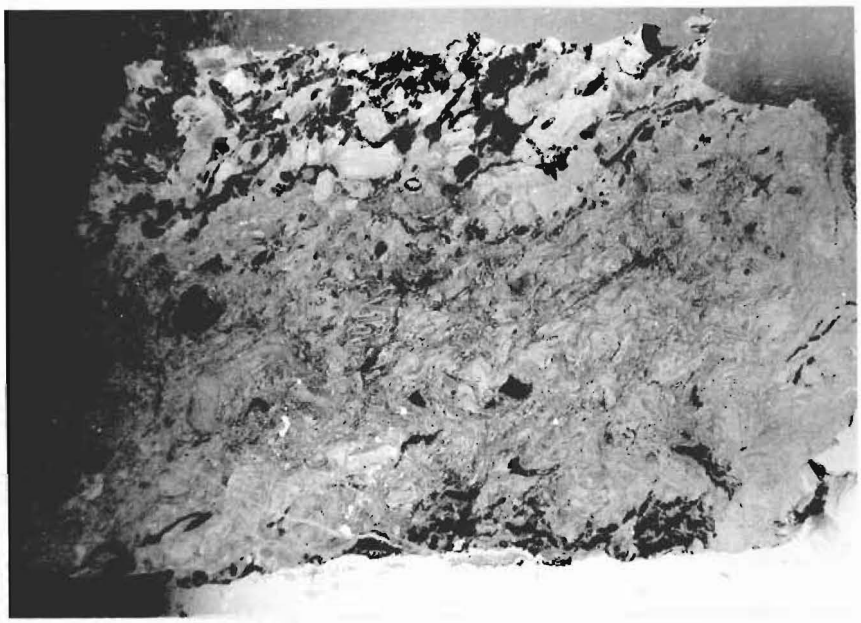

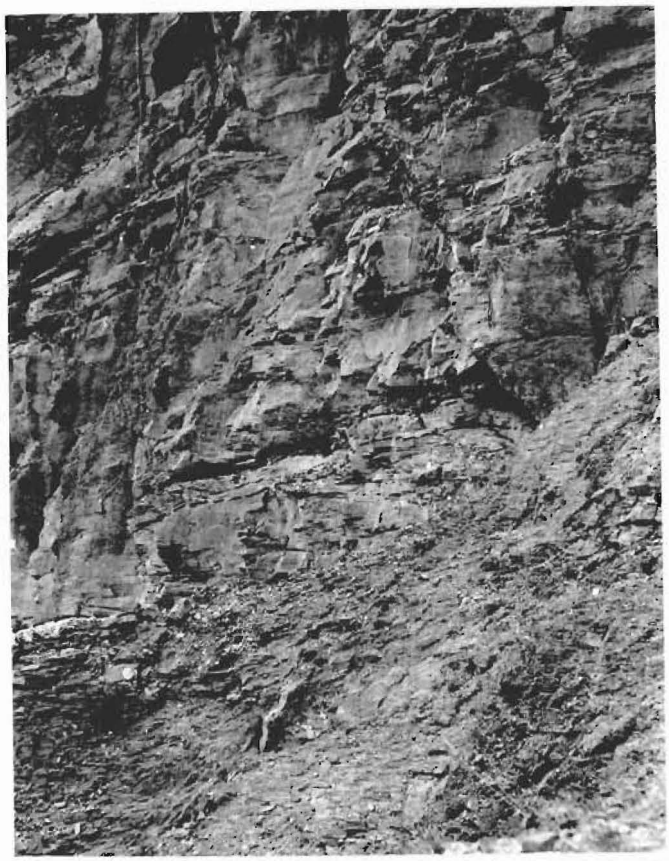

G. 2-3 Lithologic variations in the Arthur Marble
rmation.

per: Phosphatic marble from the uppermost unit, con-
ining shell fragments and dark, carbonaceous organic
tter.
thin section, ppl. x5 UC8874

wer: A section near the base of the formation, south of
ig C, showing a gradation from fissile, impure marble,
wards into a more massive and pure marble. The marble
cut by a basic intrusive sill (indicated) which is
proximately 0.5 m thick.

(c) Owen Formation. At least 750 m of succession are contained in this formation, and if major faulted repetition does not exist, a thickness of approximately 1200 m is indicated. The formation consists of a distinctive and highly varied lithology forming a stratigraphic succession as follows:

(i) The impure carbonate rocks comprising the base of the Arthur Marble terminate at a siliceous unit, which is conveniently defined as the uppermost unit of the Owen Formation, and has been assigned the name Beilby Quartzite. It was in this unit that C.S. Beilby spent several years driving prospecting adits, south of Trig C, at an elevation of 1200 m. The unit consists of recrystallized chert, quartz sandstone, and a coarse chert granule sandstone, interlaminated with dolomite marble and thin shales, and occasionally showing current bedding (Figure 2-4). Ferroan carbonate and pyrite give rise to a red-brown weathering colour. A thickness of more than 100 m outcrops in the cliffs at the head of Byrne stream, but only approximately 70 m is present in a section near Beilby's workings, south of Trig C. South of Bulmer Creek, the unit is difficult to measure, but probably does not exceed 20 m in thickness.

(ii) Below the Beilby Quartzite lies a dolomitic shale of variable thickness, commonly more or less altered to a sericitic composition (see below).

(iii) Dolomitic horizons occur toward the middle of the formation, where one conspicuous and probably continuous

bed of dolomite can be traced. This unit consists of a tough, dark, fine-grained dolomite, containing characteristic pyrrhotite. The name Enterprise Dolomite is used for this unit, the most easily accessible outcrop being in the bank of the Owen River opposite the Enterprise Mine. A thickness of ca. 20-50 m is indicated.

(iv) The Enterprise Dolomite is underlain by an unnamed succession of cleaved mudstones and sandstones, containing thin, discontinuous lenses of dolomitic carbonate and rare intraclastic conglomerates. A strong cleavage is developed in the fine-grained sediments, but fine details of sedimentary structures are often found preserved. Finely laminated horizons occasionally show bioturbation.

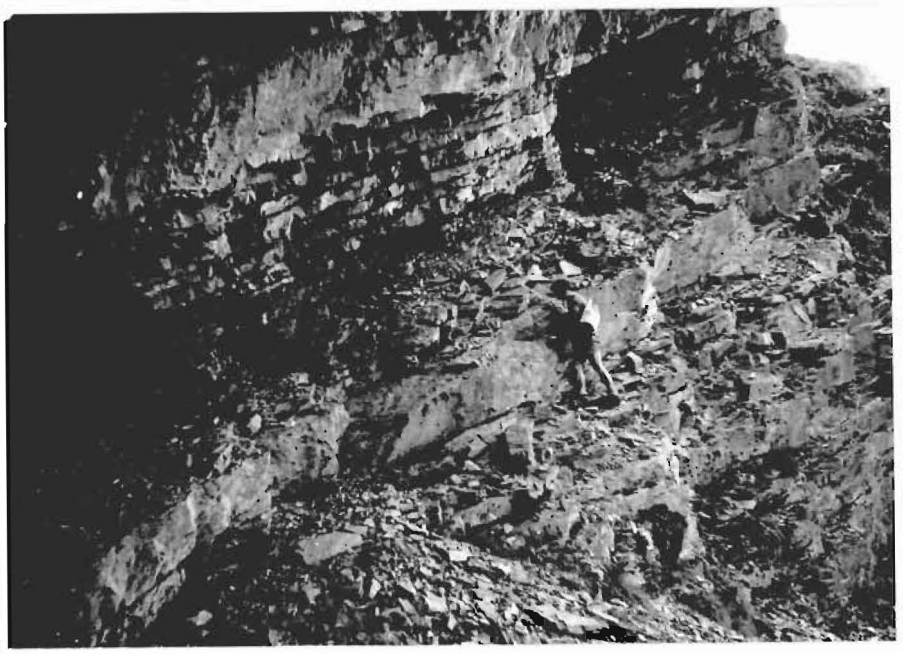

FIG. 2-4 Beilby Quartzite outcropping at the head of Byrne Stream.

Upper: Massive beds of dolomitic quartzite and recrystallized chert near the top of the unit.

Lower: Interlaminated quartzite and carbonate, showing current bedding structures. The massive, pale coloured bed near the hammer handle is a chert-rich lithology which has undergone extreme recrystallization.

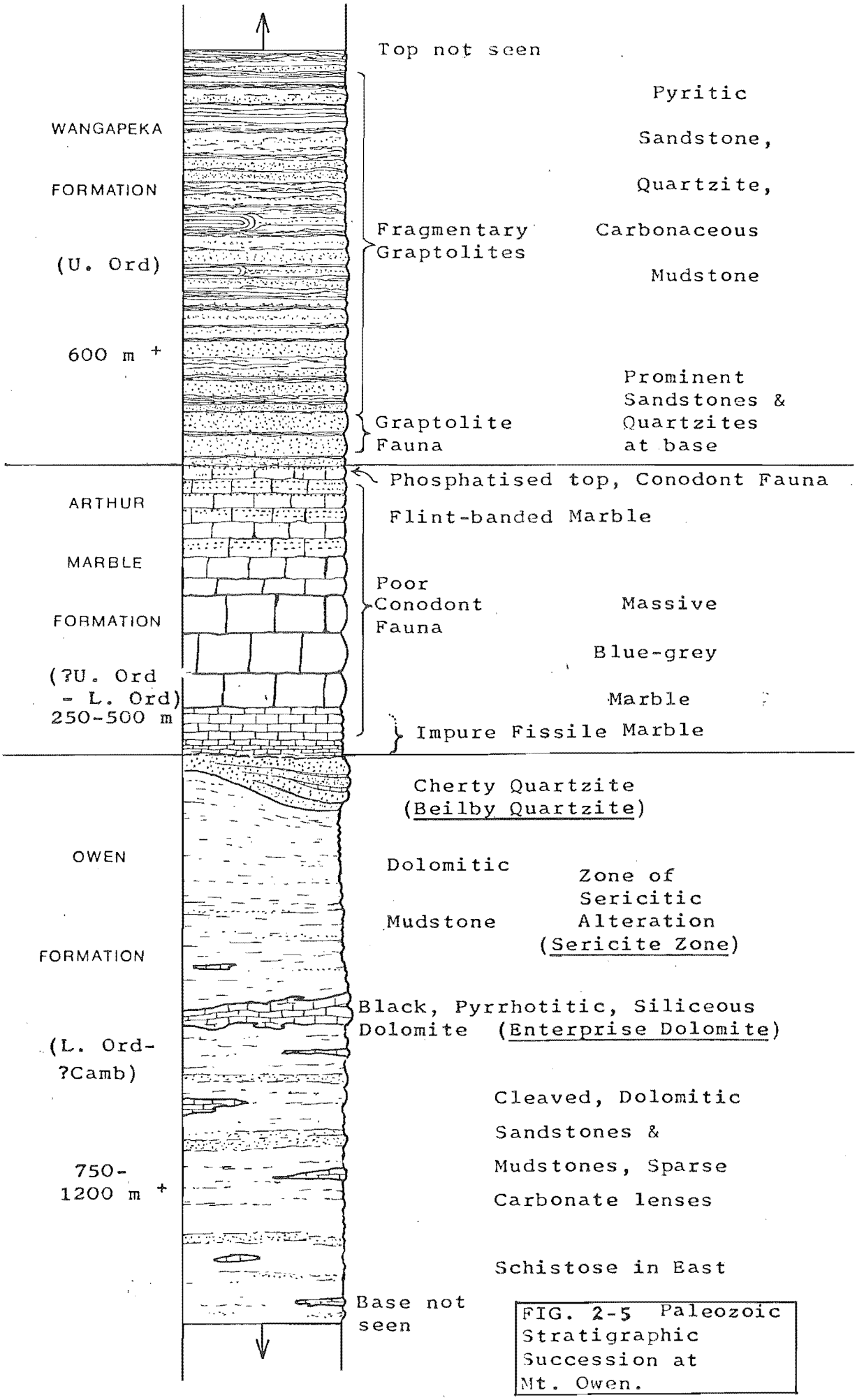

FIG. 2-5 Paleozoic Stratigraphic Succession at Mt. Owen.

(d) Metamorphic Nomenclature for the Paleozoic Sediments.

Both the text of Fyfe's (1968) bulletin and the accompanying maps describe the Owen Paleozoic sediments as schist, subschist and marble. The degree of metamorphism of these rocks (discussed in Chapter VI) is less than that implied by this description. The Wangapeka Formation and the Arthur Marble show very little metamorphism, but the Owen Formation bears a stronger cleavage, and frequently shows a strong lineation. These structures are prominent where recrystallization of carbonates has occurred, thus the schistosity varies markedly with lithologic composition. Fine laminations of sedimentary bedding are often preserved in the carbonate-poor horizons. The use of metamorphic textural names has been avoided where possible in this report.

(e) Basic Intrusives. It is apparent that Fyfe found boulders of basic igneous rock in Frying Pan Creek, and attributed their source to a small area south of Trig EH, which he mapped as 'Basic and Ultrabasic rocks of the Western Mountains'. Re-mapping of the area shows this rock to be extremely widespread, and to occur as thin sills, a metre or less in thickness, throughout the Wangapeka Formation and Arthur Marble (Figure 2-3). The rock is highly altered and often difficult to distinguish from the host lithologies. An intrusive origin is suggested by altered margins in the country rock, where some of the slates have become 'spotted' near the contact,

and also by indications of cross-cutting of the bedding. Identification of the original composition is complicated by the extreme alteration. In hand specimen the rock is dark green with white interlocking feldspars. Thin sections suggest an original composition of a dolerite or alkaline gabbro. Sausseritisation of feldspar and chloritisation of mafic minerals is prominent in all sections examined. Intrusives of similar characteristics were reported by Henderson, et. al. (1959) from the Wangapeka area north of Mt. Owen.

(f) Separation Point Granite. The granite forming the Mt. Hope Range to the east of the Owen River was mapped by Bowen (1964) as Separation Point Granite, following Grindley (1961). This rock has not been studied in detail, but is seen to be consistent with Grindley's description as a massive, leucrocratic, sodic granite. A thin contact zone containing metasedimentary remnants is described in Chapter VI. The main body of granite is extremely uniform, except for thin pegmatites.

(3) Age

(a) Wangapeka Formation. During field work by Fyfe in 1927, poorly preserved graptolites were seen in a boulder in Fyfe River, but the specimen was not retained. In 1965, a collection of graptolites was made from a horizon 15 m stratigraphically above the top of the Arthur Marble Formation, at a locality approximately 4 km north-west of Mt. Owen. Species of Dicellograptus and Climacograptus were identified from which a probable Eastonian age was deduced (Johnston et. al., 1965).

A number of graptolites have since been collected by the writer from the Wangapeka Formation south of Fyfe River. The fossils are most abundant along the ridge near Trig EH, occurring for 150 m west, and 300 m north-east of the trig. The best collections were obtained at the north-east end of this zone, 30-50 m stratigraphically above the marble. Fragmentary graptolites were found at many exposures elsewhere in the formation, but were too poorly preserved for collection. The graptolites were, in every case, preserved as chlorite films, or more rarely, as impressions. Most of the specimens were diplograptids, but other families were also represented (Figure 2-6). Identifications, kindly provided by Dr. R.A. Cooper of the N.Z. Geological Survey, were made as follows:

Fossil record No. S26/f580, University collection No. UCM 764/1-4

? Orthograptus sp.

? Glyptograptus sp.

? Climacograptus sp.

? Amplexograptus sp.

Fossil record No. University collection No.
UCM 765/5,6

Dicranograptus sp.

Glyptograptus sp.

A Gisbornian-Eastonian age is indicated, but preservation is not good enough to permit the recognition of diagnostic species. During early 1978, the writer assisted Dr. Cooper in collecting graptolites from several small, in-faulted remnants of Wangapeka Formation approximately 2 km west of Mt. Owen. A pyritised and relatively well preserved fauna was found at a similar stratigraphic horizon to that described for the other localities, and included the following:

Dicranograptus sp.

Dicellograptus sp.

Climacograptus sp.

Orthograptus ex. gr. calcaratus

Climacograptus bicornis, sensu Riva

(R.A. Cooper, pers. comm.)

This assemblage confirms the age restriction of Gisbornian-Eastonian, with a most probable age of upper Gisbornian (Upper Ordovician). These dates refer to a relatively narrow stratigraphic zone near the base of the Formation. No information is yet available to indicate the time span represented by the remainder of the Wangapeka Formation at Mt. Owen.

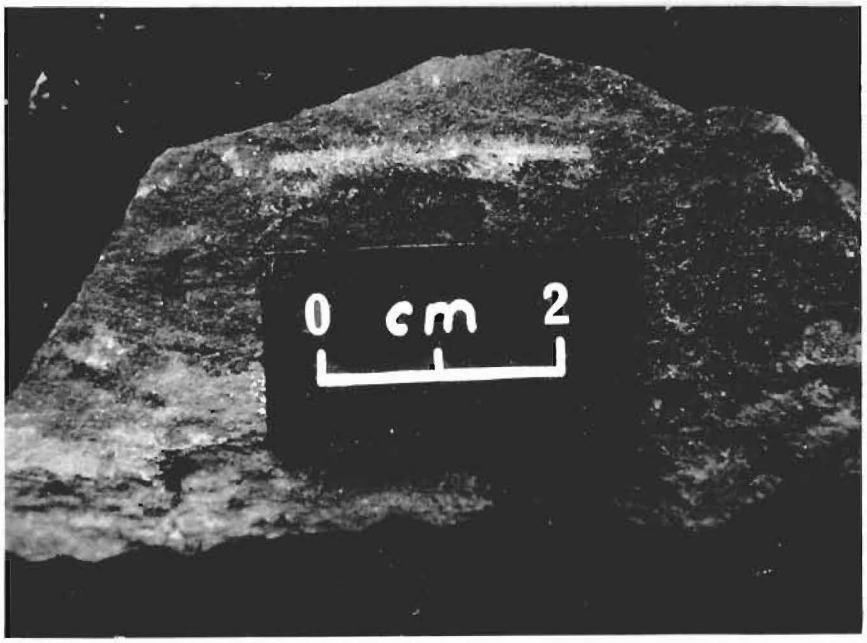

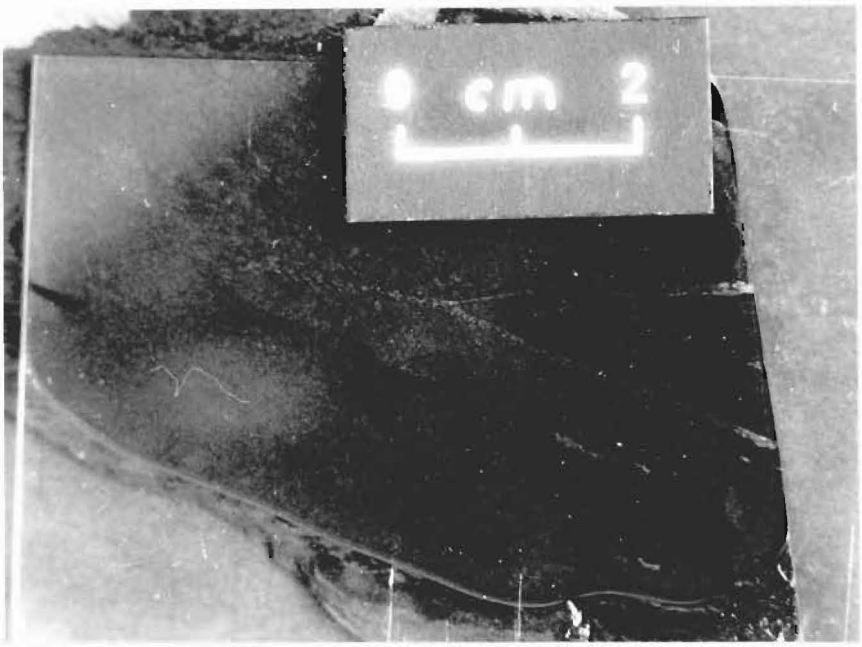

'IG. 2-6 Graptolites from the Wangapeka Formation, ıorth-west of Trig EH.

'pper: ? Orthograptus sp. (UCM 764/4).

ower: Dicranograptus sp. (UCM 764/5).

(b) Arthur Marble Formation. No macrofossils are known from this formation at Mt. Owen, but thin sections show rare bioclastic remains. Recent work by staff of the N.Z. Geological Survey has revealed the presence of acid-insoluble microfossils which show promise in dating this unit. Conodonts from the top of the marble indicate an upper Llanvirnian age. Poorer faunas from lower in the sequence do not provide good age-diagnostic indentifications, but provisional results suggest a probable restriction of upper Tremodocian-Arenigian for the lowermost samples. Dolomitic carbonates from the Owen Formation have, to date, produced no fauna (microfossil data from Simes, 1977 and pers. comm.).

The indicated range of ages spans a considerable time period, possibly due to the presence of time-compressed sequences at the top of, and perhaps within, the marble. The absence of dates for the Owen Formation is regrettable, as this unit may also span a long period, possibly with a compressed sequence represented by the Beilby Quartzite. Faunal identifications are severely restricted by the poor preservation of the fossils. It is hoped that further sampling will provide additional information.

(c) Igneous Rocks. The basic sills at Mt. Owen are probably contemporaneous with similar intrusives further north, which penetrate Devonian strata, and may be correlatives of intrusives of the Riwaka Complex, mapped by Grindley (1971) as ?Upper Carboniferous.

The Separation Point Batholith has been radiometrically dated as ca. 90-100 m.y. (mid Cretaceous) by Rb-Sr and K-Ar methods (Hulston and McCabe, 1972).

(4) Correlation with Other Areas

Possible correlation of the Owen Formation-Arthur Marble sequence with the Pikikiruna and Springs Junction area on lithostratigraphic grounds alone has been discussed. The lithology of the Pikikiruna Schist is obscured by advanced metamorphism. The Thompson's Flat Formation, which consists of dolomitic mudstones, sandstones, quartzites, conglomerates and marble lenses, shows strong affinities with the lithology of the Owen Formation. Provisional identifications of conodonts and trilobites (Simes, 1977 and pers. comm.; Cooper et al., in prep.) from the Springs Junction rocks provides useful age data. The marble overlying the Thompson's Flat Formation contains a relatively good Llandelian conodont fauna in its uppermost beds, and is therefore probably the equivalent of at least part of the Arthur Marble at Mt. Owen. The lower part of the Thompson's Flat Formation contains Upper Cambrian trilobites and conodonts, again suggesting a time-compressed sequence. If the successions at both Springs Junction and Mt. Owen are continuous, the Owen Formation may be partly or entirely Cambrian in age.

(5) Significance of Inferred Stratigraphic Correlation

Some aspects of the inferred stratigraphic relationships

of the Paleozoic rocks at Mt. Owen may be of fundamental significance to concepts of the origin of mineralisation in the area. These aspects are as follows:

(i) The succession at Mt. Owen may represent a very long period of slow deposition of fine grained sediment, much of which is non-terrigenous. A long, stable period of tectonic inactivity would favour the retention of pore water at depth in the accumulated sediments.

(ii) The Owen Formation may overlie, grade into, or represent, metal-rich volcanoclastic sediments of the Haupiri Group, which have been regarded as source rocks for gold and base-metal mineralisation.(Grindley and Wodzicki, 1960).

The possible role of these factors as fundamental elements of a sedimentary source for ore genesis is examined and discussed in Chapters IV and VIII.

CHAPTER III

STRUCTURE

I. PREVIOUS STRUCTURAL CONCEPTS

Beneath the base of the Beilby Quartzite lies a zone of pelitic rock which commonly shows evidence of metasomatic alteration. Where this alteration is intense, the rock has a light, bleached appearance, frequently with a brown or pink colouration due to ferric weathering products or ankerite, but occasionally tinted green by chlorite. Sericite and ankeritic dolomite are ubiquitous, occasionally to the exclusion of all other minerals, and carbonaceous matter is always absent. The name sericite zone is used in this report, denoting an essentially stratigraphically controlled zone characterised by this alteration.

Hector (1888) attributed this zone to a weathered surface unconformably overlain by the marble, although this view was not shared by Park. Williams (1965) interpreted early field observations in terms of Grindley's concepts of thrusting, suggesting the presence of a low-angle thrust plane beneath the marble. This idea is again proposed in the text of Fyfe's (1968) bulletin, where an angular discordance between the marble and the underlying rocks is inferred from the following evidence:

(i) The plane of contact north of Bulmer Creek could be projected into marble at the escarpment south-east of Mt. Owen.

(ii) The discordance between dips in the Owen Formation (Park's cross-section, Figure 1-2), and in the marble (Park's measurements near Mt. Owen).

(iii) 'The boundary between these rocks is such that a low angle thrust would produce'.

(iv) An impression of overthrusting is gained from viewing the bluffs beneath the escarpment south-east of Mt. Owen (Figure 3-1).

FIG. 3-1 Bluffs at the head of Byrne Stream, as viewed from a point approximately 200 m east of Trig C. Massive Arthur Marble forms the steep cliffs at the skyline, and the summit of Mt. Owen (centre), overlying bedded units of the Beilby Quartzite which forms the top of the Owen Formation. The boundary between the formations is shown by a dashed line, to the right of which the marble appears to be downthrown by faulting. Several small offsets are not shown.

II. STRUCTURAL REAPPRAISAL

(1) Evidence for Stratigraphic Continuity

The structural interpretation quoted above concludes with the remarks; '... the evidence for overthrusting is admittedly weak and a simpler explanation may be found...'. Little field work is required to show that the evidence for overthrusting is largely invalid. Both folding and faulting severely limit the orthographic projection of measured attitudes. To project the contact plane near Bulmer Creek to the scarp at Mt. Owen is to span a distance of nearly three km, and from Park's cross-section at the Enterprise mine to Mt. Owen is more than 5 km. Over this distance the dip of both the marble and the underlying rocks becomes shallower to the north, and the units are downthrown to the east by steeply dipping faults. Traverses from Owen Formation to Arthur Marble are difficult to achieve, but complete sections can be observed in several places. Sections across the contact were examined at the head of Byrne and Fagan's streams, and above Beilby's workings, and an almost complete section above the Enterprise mine. In all sections, no evidence of unconformable contact could be found. The Owen Formation becomes carbonate-rich near the Beilby Quartzite, which is partly intercalated with carbonate beds. The quartzite can be seen to grade upward into impure, fissile marble, which in turn grades upward into massive marble.

The sericite zone may represent a horizon of localised

movements, but is unlikely to locate a major thrust. The thickness of the zone varies considerably, as does the degree of alteration; in Fagan's Stream it is barely represented, while below Trig C at least 100 m is well defined. Local development of the zone can be correlated with intensified hydrothermal veining, and both veining and alteration may be related to original permeability and/or composition, as discussed in Chapters VI and VIII. In Fagan's Stream, a sequence of grey-brown dolomitic mudstones is seen to extend upwards to the siliceous base of the marble, no abrupt lithologic changes being detectable.

(2) Folding

(a) Wangapeka Formation. Small slump folds in the Wangapeka Formation appear to be intraformational features related to syndepositional movement. Below Trig EH, some small scale, gentle to open folding of the bedding (Fleuty classification) about north-south axes is visible. The relationship with cleavage is uncertain, but the axes parallel those of the slump folds, and a wet-sediment deformation origin may apply. Along Fyfe River, to the west of the area mapped, both the Wangapeka Formation and the Arthur Marble are known to exhibit close, similar style folding on a scale of less than a metre. The rocks examined in the east are, by comparison, undeformed, and generally reflect the attitude of the upper contact of the marble (Figure 3-2). The large-scale structure shown by the upper marble horizons north of Fyfe River is seen to be an upright, gently folded syncline, revealed by the stripped bedding surfaces.

FIG. 3-2 Upper unit of the Arthur Marble incised by Fyfe River to form a steep-sided gorge (right) and overlain by Wangapeka Formation, the sequence dipping south-west towards Frying Pan Creek (left). The line of contact runs approximately along the top of the marble bluffs. Tertiary rocks form the slump-scarred hills in the background.

(b) Arthur Marble Formation. Structure within the marble is more complex than that seen in other formations. Continuous escarpment exposure from the Owen River and Bulmer Creek suggests an absence of megascopic folding. Traverses through the plateau regions, however, show both upright open folds, and tight to isoclinal recumbent folds (Figure 3-3). Many of the latter are extremely slender, elongate structures, suggesting a soft sediment deformation origin, and at least some of the folding may be due to gravity-controlled deformation prior to lithification. Additional complication is introduced by small scale, intra-formational, low angle thrusting, which is seen to be vertically repetitive.

Analysis of the deformation within the marble would require considerable field work and detailed mapping beyond the scope of this project. Field observations of the gross structure indicate that, at least in the project area, the deformation of the marble is largely internal, and is not developed to the same extent within the other formations.

(c) Owen Formation. Field observations show a considerable range in bedding/cleavage angles, indicating a phase of folding which predated or accompanied cleavage formation. No fold closures showing a genetic relationship to cleavage could be found, except small, irregular folds on a scale of less than a metre (Figure 3-4) where the cleavage is axial planar. These folds may be parasitic to larger, unrecognised structures.

Harmonic folding may exist to the east of the Owen

3-3 Overfold in Arthur Marble, on the western
of an anticline 2 km west of Mt. Owen summit.
old is viewed looking north along the axis.

'IG. 3-4 Minor folds exposed in Bulmer Creek, near
pring Creek. The folds are south-plunging structures
'ith an axial plane cleavage.

River, where traces of gentle folds were seen in outcrops on the relatively well-exposed hill opposite the Enterprise mine. An attempt was made to measure the orientation of this folding by the stereographic plotting of cleavage poles (Figure 3-5). The results are inconclusive, due to the considerable scatter of the plotted points. Shearing and brecciation appears to have caused block dislocation and rotation effects, possibly in combination with drag folding. The spread of cleavage poles indicates folding about an axis plunging moderately to the south-west. The small number of bedding attitudes also plotted show a similar pattern. Some minor fold axes, however, plot to the east of south, possibly as a result of earlier folding. Measurements from areas separated by large distances show little structural relationship; the proper analysis of structure by stereographic methods can be expected to require careful definition of structural domains. Variation of deformation style with lithologic character and large-scale cleavage refraction may add further complications. Multiphase deformation, including some post-cleavage folding, appears to have affected the Owen Formation, especially in easternmost outcrops.

(3) Faulting

The location of major faults at the margins of the Paleozoic rocks has been well established by the work of Fyfe, and later by Kear (1954), who also projected faults seen in the surrounding Tertiary rocks for some distance

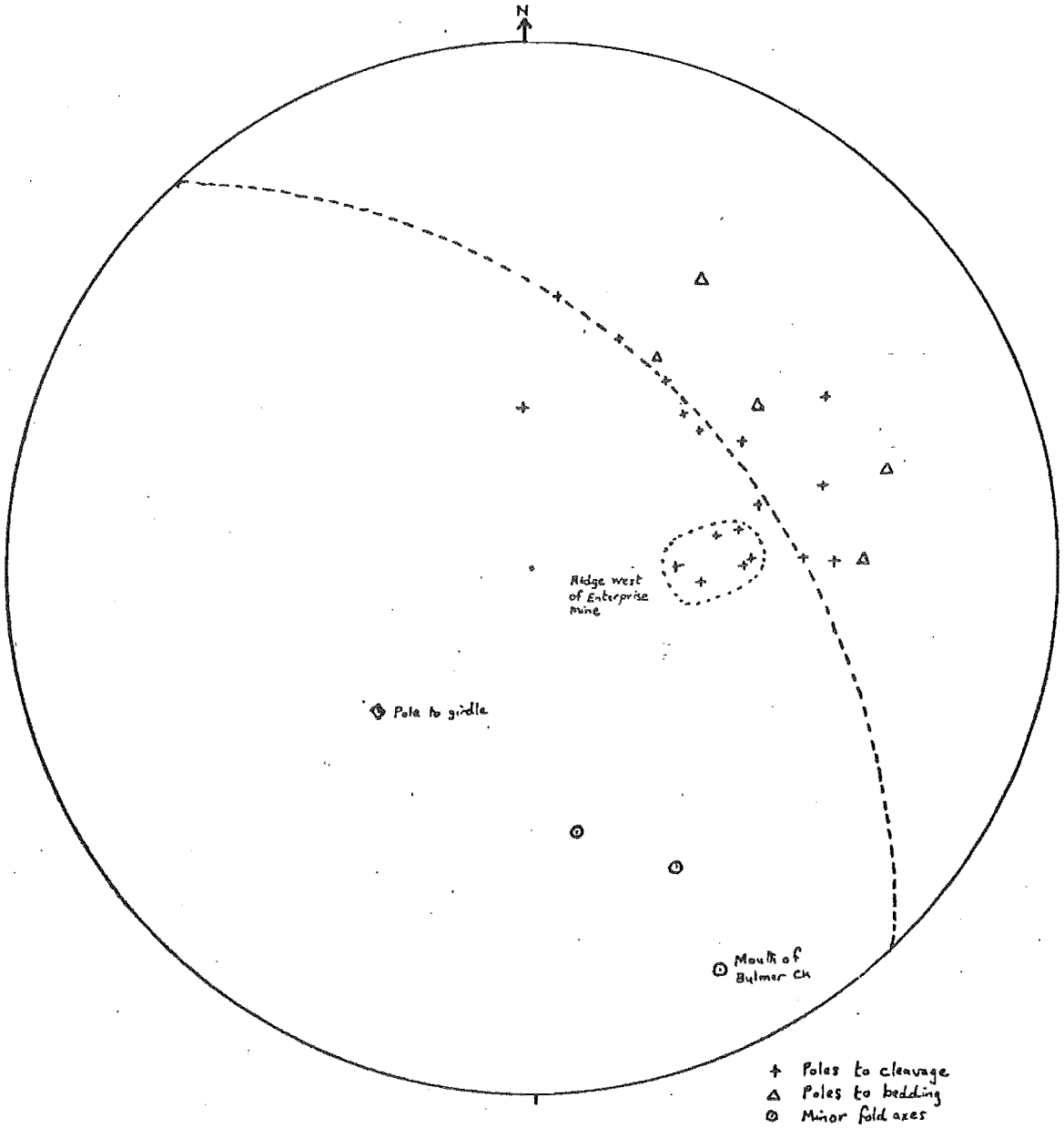

FIG. 3-5 Stereograph of poles to cleavage and to bedding, Owen Formation. Points are measured on the hillside east of the Owen River, opposite the Enterprise mine, except where shown otherwise. Three minor fold axes are also shown. See text.

into the basement. The Owen Fault, bounding the Paleozoic rocks to the south-west, appears to be a single, simple displacement (see Map 1). A major displacement is also located at the western margin of the Separation Point Granite, where a fault zone consisting of several closely spaced fault planes is indicated by thin slivers of differing metasedimentary and Tertiary rock types near Trig CK. Further west, and sub-parallel to the faulted granite margin, multiple northeast-southwest faulting occurs near the contact of the Paleozoic basement with the narrow strip of Tertiary rocks. Neither the interpretation of Henderson and Fyfe (1935), nor that of Kear (1954) is considered satisfactory for faulting along this zone. The major displacement recognised (Map 1) is similar in its northern part to Henderson and Fyfe's Bulmer Fault, but otherwise follows a course mapped by Kear. The name Baigent Fault is considered appropriate. The westward flexure of this fault to the south of the area is matched by a similar flexure in the granite boundary fault, possibly indicating a 'bulge' in the granite margin at depth. One or more faults which appear to diverge from the Baigent Fault to trend north-west, produce a major downthrow of the Arthur Marble north of Byrne Stream. This downthrow is reflected on a small scale by numerous faults cutting the marble north of Trig C. These faults show little vertical displacement, but juxtapose bedding of different attitudes. This may be due to rotational movements, or more probably, horizontal movement within gently folded bedding. A prominent fault

breccia is developed by one such fault in the base of the cliffs immediately south of Trig C, where the fault plane descends from the quartzite into the more easily fractured sericite zone (Figure 3-6).

The time, and order, of displacement on the faults is uncertain. Kear's work indicates considerable movement on some of the major faults during Tertiary time. All major faults die out northwards, reflecting the major downwarping of the tectonically active Tertiary basin to the south-west of the area.

Additional, unmapped faults are suspected from breccia zones, erosion features, and indications of repetition of units. This applies especially to the section exposed in the Owen River north of Bulmer Creek, where numerous shear zones cut a dark, siliceous carbonate which is probably a continuation of the Enterprise Dolomite. Bedding in this area strikes parallel to the trend of the faulting pattern, which obscures any fault displacements which may occur.

Displaced blocks of Paleozoic strata exist below Trig PH and Trig C, but some doubt remains as to whether these represent fault blocks or large-scale slumping. The block below Trig PH, which consists of marble with underlying quartzites and mudstones, is bounded by breccia zones and is considered to be emplaced by complex faulting, although this is difficult to prove from field evidence. The smaller block of displaced marble at Trig C is probably slumped.

FIG. 3-6 Fault breccia developed at the base of the Beilby quartzite, approximately 100 m south of Trig C. Vertical displacement does not exceed 50 m.

(4) Cleavage and Metamorphism

The Wangapeka Formation exhibits a single slaty cleavage, with an associated simple flattening shown by graptolite distortion and pyrite cube pressure fringes (Chapter IV). Some shear movements are suggested by slight cleavage refraction and pyrite brecciation. Rarely, this cleavage is seen to be overprinted by a weak fracture cleavage with quartz infillings. The slaty cleavage is prominent in massive mudstones, commonly forming an angle of less than 20° with bedding, but is present as a bedding cleavage in the shales. Sandstone units show no cleavage.

Cleavage within the Arthur Marble is not well defined. Rare remnants of bedding show evidence of transposition and flowage, but in general the unit must be considered massive and uncleaved.

Cleavage is commonly observed throughout the Owen Formation, but bedding in this unit is often obscured, especially in pelitic lithologies. Bedding in sandstone units is usually well preserved, and can be traced in carbonate lithologies by fragments of transposed laminae or pyrrhotite knots after stratiform pyrite. In most lithologies the cleavage is accompanied by a bedding foliation, the combination of these structures causing a pronounced, penetrative lineation, which commonly destroys all traces of both planar structures in pelitic units. The lineation structure is extremely well developed in siliceous carbonate at the base of the Beilby Quartzite, where a 'molar tooth'

pattern is displayed in sections perpendicular to the lineation (Figure 3-7). Silty laminae show a 'pencil' structure, forming sub-circular rods. The bedding is generally disrupted; muddy laminae have flowed around the rods, and are streaked into thin, exaggerated flame structures. The 'molar tooth' structures are not known from other horizons within the formation, but the lineation is often visible, forming pencil-like fragments at shattered outcrops.

Specimens of Owen Formation which retain bedding lamination show a simple, penetrative strain-slip cleavage (Figure 3-8), occasionally with evidence of shear as shown by cleavage refraction (Figure 3-9). A pebble of phyllite shows an earlier schistosity enclosed in porphyroblastic quartz-chlorite knots (Figure 3-10), about which the dominant, later cleavage can be seen as a crenulation cleavage. An older schistosity was also revealed by porphyroblastic chloritoid from phyllite near Trig GC. The cloritoid (discussed in Chapter VII) predates the cleavage and preserves the earlier structure in helicitic textures and by a weak preferred orientation (Figure 3-11). Careful examination of some phyllitic carbonates showed traces of an earlier schistosity in pressure shadows about pyrrhotite knots (Figure 3-12).

The lowermost units of the Owen Formation contain rare examples of pre-cleavage quartz veining. Thin veins occur with a marked crenulation due to shortening (Figure 3-13),

FIG. 3-7 'Molar tooth' lineation structures in an impure, siliceous dolomite. The structures are commonly seen in situ at the base of the Beilby Quartzite, but are more clearly seen in partly weathered stream boulders, an example of which is shown cut perpendicular to the lineation. UC8875

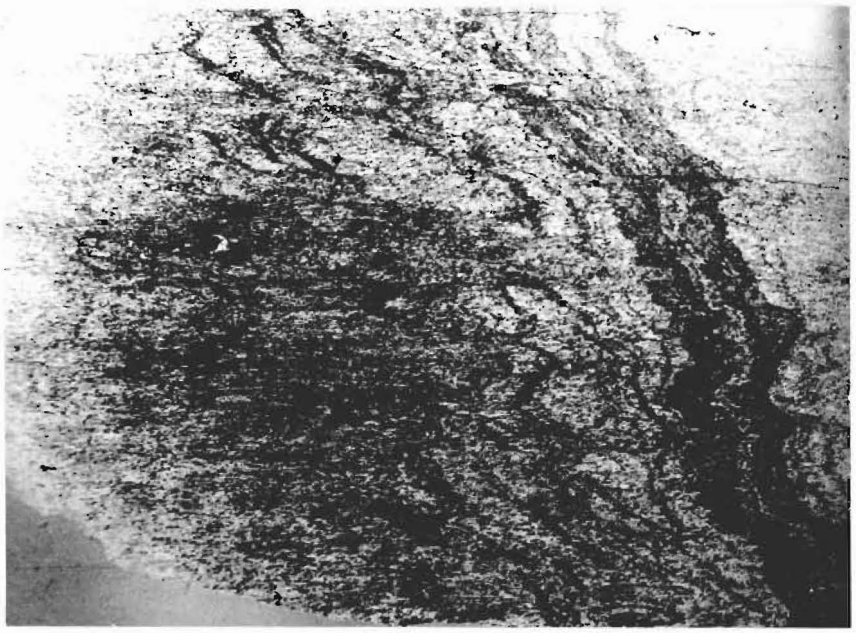

'IG. 3-8 Strain-slip cleavage in a silty lithology of
:he Owen Formation.
thin section, ppl. x5 UC8876

IG. 3-9 Cleavage in impure Enterprise Dolomite,
howing refraction.
thin section, ppl. x5 UC8877

Both specimens cut from stream boulders)

FIG. 3-10 Strain-slip cleavage traces deflecting around quartz-chlorite porphyroblasts which enclose an older foliation. A thin quartz veinlet, originally sub-parallel to the earlier foliation has been crenulated, and transposed by shear.
Specimen cut from a stream pebble, probably from the lower Owen Formation.
A thin section, ppl. x5 UC8880

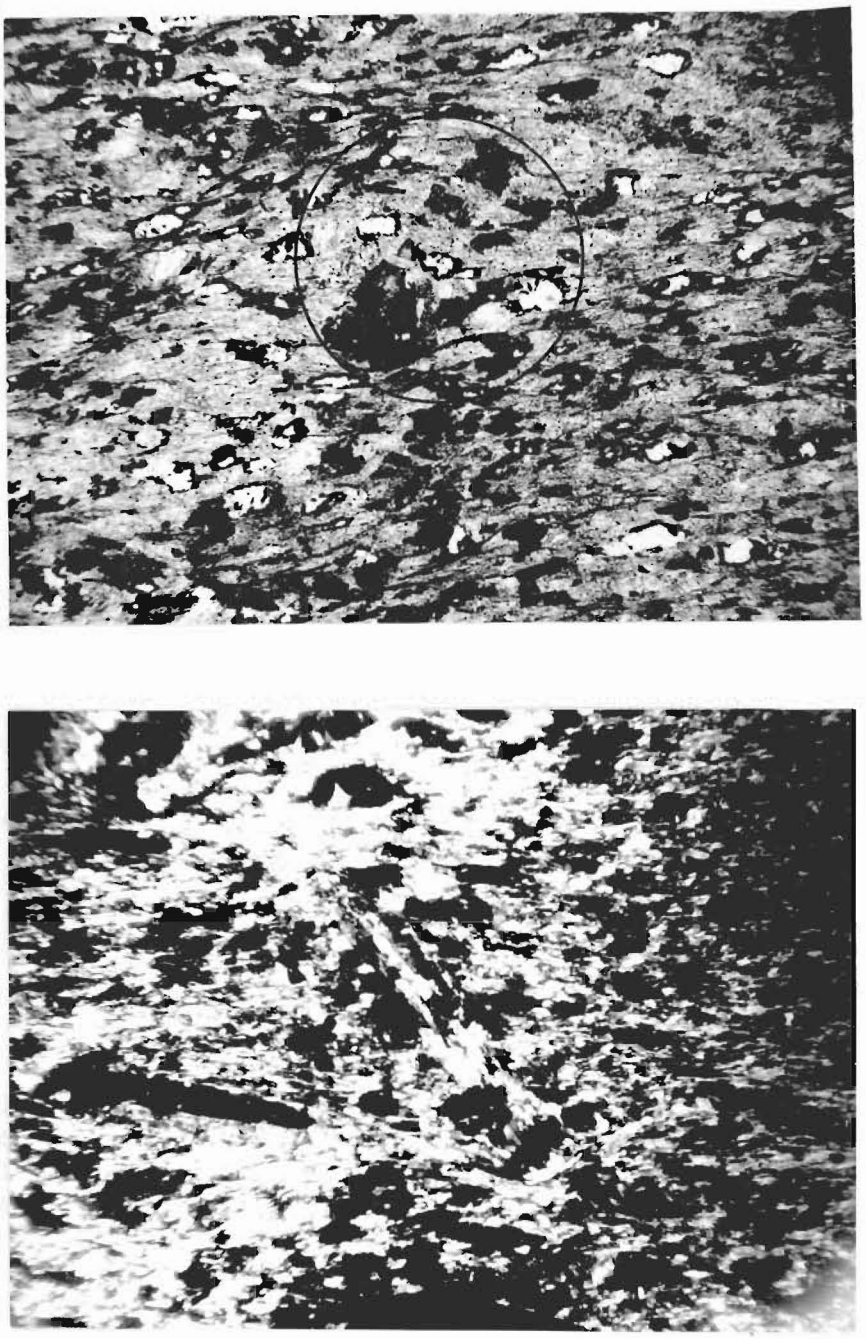

FIG. 3-11 Chloritoid in schistose material from near Trig GC. UC8881

Upper: A chloritoid lath (circled), fractured and offset by cleavage. Syntectonic metamorphism has caused partial replacement of the chloritoid at the fractures. The groundmass is principally sericite and quartz, and the clear spots are voids produced by the weathering out of a constituent which was probably a carbonate.
A thin section, ppl. x50

Lower: A chloritoid lath and intergrown muscovite aligned with a foliation which predates cleavage.
A thin section, xpl. x50

FIG. 3-12 Enterprise Dolomite, showing traces of an early foliation preserved in the pressure shadow of a pyrrhotite bleb, and surrounded by a later cleavage. A thin section, ppl. x20 UC8879

and dilation fractures due to extension (Figure 3-14). In addition, the quartz-chlorite porphyroblastic pebble shows a crenulated veinlet, originally infilling a fracture parallel to the earlier schistosity. This evidence suggests that the overprinted foliation marks an earlier cleavage (Figure 3-10).

The metamorphic alteration of the Wangapeka Formation and Arthur Marble in terms of mineralogical change is negligible. A simple metamorphic assemblage in the Owen Formation (discussed in Chapter VI) indicates lower greenschist facies thermal metamorphism. Biotite is restricted to rocks east of the Enterprise Dolomite, and chloritoid is found only in a narrow north-south zone near Trig GC. Metamorphic chlorite is also present, but is accompanied by chlorite from hydrothermal alteration in the more permeable units. Pyrrhotite is also a product of metamorphism, and is found throughout the formation up to the base of the Beilby Quartzite. The formation of pyrrhotite is known from assemblages of both regional metamorphism (Carpenter, 1974), and contact aureoles (Neumann, 1950). Only two phases of metamorphism can be recognised at Mt. Owen; an early one, resulting in the formation of chloritoid, chlorite, and possibly biotite, and a later syntectonic event creating the cleavage. It is difficult to establish from which phase the pyrrhotite dates. Pyrrhotite forms streaks aligned parallel to the cleavage, but as this mineral is easily deformed, it may have predated cleavage.

FIG. 3-13 A veinlet seen near Trig GC, crenulated by deformation accompanying cleavage formation. Considerable shortening in the plane of the vein is indicated.

FIG. 3-14 Fracturing at the margin of a vein such as described above (Figure 3-13), reveals extension fractures oriented perpendicular to the crenulation lineations. A stream boulder, UC8878

(5) Relation to Regional Metamorphic and Tectonic Events

The metamorphism affecting the sediments at Mt. Owen appears to be due to contact effects from the nearby Separation Point Granite. This is suggested by the rapid decrease in metamorphic grade, both westward and upward through the succession. The occurrence of chloritoid may be compared with occurrences reported by Grindley (1971) from areas of Rangitatan thermal metamorphism near intrusive plutons to the north. He also reports that the metamorphic mineral growth proceeds mimetically on older S-surfaces developed in the Tuhuan orogeny, the Rangitatan cleavage being limited to non-penetrative strain-slip structures.

Cleavage in the Owen Formation appears to have a strain-slip origin, but is sufficiently well developed to be penetrative and obliterate an earlier foliation. As no more recent cleavage is known, the cleavage in the Owen Formation probably represents Grindley's (1971) 'Third Movement Phase', which is defined as accompanying post-intrusive Rangitatan deformation and chlorite-zone retrograde metamorphism. It is difficult to interpret the 'molar tooth' structures of the Owen Formation except in terms of upward fluid flow. A water-escape process is suggested by the apparent hydroplastic behaviour, and by comparison with similar structures previously described by Braddock (1970) and Clark (1970). The time of formation of the structures in the Owen rocks remains in doubt. The lineation is clearly a result of the intersection of a penetrative cleavage with bedding, but the

delay of water escape until mid-Cretaceous time is difficult to envisage, even if the Arthur Marble acted as a permeability barrier. A number of possible interpretations must be considered, as follows:

(i) Cleavage as defined by the 'molar tooth' structures represents a Tuhuan water-escape event, and is neither related to, nor overprinted by, the cleavage in the remainder of the formation.

(ii) The situation represented in (i) above, but with reactivation of the Tuhuan cleavage by Rangitatan movement.

(iii) The 'molar tooth' structures represent Rangitatan water-escape, and are directly related to the cleavage throughout the remainder of the Owen Formation.

(iv) The structures represent Rangitatan cleavage formation by a mechanism other than water-escape, but modified by subsequent fluid flow processes.

Much of the evidence presented above suggests that significant differences may exist between the tectonic-metamorphic history of the Mt. Owen area and that of other Eastern Belt sediments further north interpreted by Grindley (1971). These differences may arise from two causes: the Owen area is geographically remote from the areas investigated by Grindley, and may have escaped major Tuhuan diastrophism by being to the south of the area subject to overthrusting. Secondly, the Mt. Owen area is in close proximity to the flank of the Separation Point Granite, which appears to have controlled the Rangitatan

deformation in this zone. No structural equivalent of the Owen Formation is known, except for highly metamorphosed schists where much of the tectonic record has been obliterated.

The inferred metamorphic-tectonic sequence for the Owen rocks can thus be summarised as follows:

Event	Time
Syntaphral slumping and folding	Syndepositional
Folding and shearing in Arthur Marble (and Owen Formation?)	Tuhuan Orogeny
Early cleavage (bedding?)	Rangitatan Orogeny
Contact metamorphism	
Minor quartz veining	
Crenulation cleavage, followed by mimetic mineral growth	
Shearing and principal vein formation	
Further shearing, brecciation, minor folding	
Major faulting	Tertiary

(6) Structural Control of Vein Location

The distribution of veins in the Owen area can be simply demonstrated by a composite map of mining leases (Map 2), from which it is seen that the gold-mining leases are almost completely restricted to the Owen Formation. Sparse veins in the Wangapeka Formation near the mouth of Frying Pan Creek were prospected with poor results, and later abandoned and taken over by silver prospectors. The

veins in this locality show little relationship to structure, and to some extent are tensional features, possibly caused by differential strain near the contact with the underlying marble.

In the text of Fyfe's (1968) bulletin, the concentration of veins within the Bulmer Creek group of leases is noted, and correlated with a possible 'syncline crest'*. This structure cannot be confirmed, nor can any major tectonic structure be related to vein distribution. Field observation shows almost all veins in the Owen Formation to occupy shear zones parallel or sub-parallel to bedding, and to be located between the Enterprise Dolomite and the Beilby Quartzite. The sericite zone is commonly veined, and possibly hosts the major vein systems at the Enterprise and Uno leases, where widespread alteration can be seen. In each case, it is not clear whether the sericite zone is represented as a downfaulted block, or merely by local downward extension of the zone around fractures locating the major veins. The sericitic country rock at the Enterprise lease is stratigraphically too low to represent the zone, but together with the Zealandia lease, may be part of a downthrown fault block associated with the displaced strata below Trig PH. A vertical fault is known immediately east of the Enterprise mine, and the interpretation of downfaulting is selected as the most probable.

*trough?, axis?

The Bulmer Creek group veins may also be similarly down-faulted, with a probable major displacement in Uno Creek. Veins prospected below the Enterprise Dolomite show little or no sericitic alteration of the wall rocks, and usually contain poor gold values. An exception is the Golden Crown lease where good prospects were obtained from a large vein, apparently very low in the stratigraphic succession.

The base metal occurrences show definite lithologic control by the Arthur Marble, the mineralization being located near the base of, or within, this unit (see Chapter V).

CHAPTER IV

DISSEMINATED MINERALIZATION

The Paleozoic rocks at Mt. Owen contain a complex suite of authigenic, disseminated metalliferous minerals. These minerals were investigated to determine any relationship to the origin and formation of the vein-associated minerals (Chapter V). The term mineralization is used in a broad sense to include disseminated minerals occurring in low concentration. The minerals are principally iron sulphides; all other metalliferous sulphides, i.e. those of economic interest, are described as ore minerals, ore sulphides, and where applicable, foreign sulphides.

I. WANGAPEKA FORMATION

The only major disseminated mineralization within the Wangapeka Formation is pyrite, which occurs abundantly in a typical 'black shale' situation, as described in Chapter II. Stratiform pyrite concentrations, with individual cubes ranging up to 10 mm in size are common. The features exhibited by these crystals provide information on the diagenetic and deformational events during, and after, pyrite growth.

(1) Pyrite Morphology

Two remarkable specimens, illustrated in Figures 4-1

and 4-2, are of particular interest. The first is a 5 mm pyrite cube in a partly weathered, interlaminated dark carbonaceous mudstone ('shale') and quartz-rich siltstone (Figure 4-1). A sawcut section shows partial oxidation in zones, pseudomorphing continuations of the shale laminae through most of the crystal. The preservation of fine sedimentary detail indicates replacement of the host sediment by pyrite, without discernible disturbance of the surrounding sediment. The pseudomorphed lamination revealed in the pyrite lacks the deformation of the surrounding host rock, where the laminations show thickness variation, flame structures, and a small-scale warping attributed to a phase of hydroplastic deformation. The thickness of the pseudomorphed laminae is not measurably different from the sediment laminae immediately beyond the cube margins, indicating that crystal growth was substantially post-compactional. Preferential oxidation of the replaced shale laminae may be due to the inclusion of platy grains from the host sediment, creating an incipient permeability during weathering. Alternatively, a slight compositional variation inherited from the replaced sediment may exist. Ramdohr (1969) lists various causes for zoning in pyrite, but no significant investigation of this subject has been made. The writer can find no previous report of matrix replacement structures within pyrite crystals.

Superimposed on the lamination in the cube is a poorly defined concentric zoning, also shown by a variation in oxidation. The outermost zone consists of a thin, oxidation resistant rim which is not traversed by the lamination

pseudomorph zones. Other pyrite crystals, when examined in polished section, showed this rim as a distinct zone of coarse anhedral inclusions of non-reflective material, weakly aligned parallel to the crystal margins (Figure 4-3). Most cubes also showed a high density of inclusions at the crystal centres.

The second notable hand specimen is that shown in Figure 4-2. Within the bedding of a quartzite, moulds of pyrite crystals are preserved that show evidence of a complex growth pattern. Lithification appears to have arrested growth in the quartzite, but 'epitaxial overgrowth' continued at, and possibly above, an interface with a mud layer which has been weathered away.

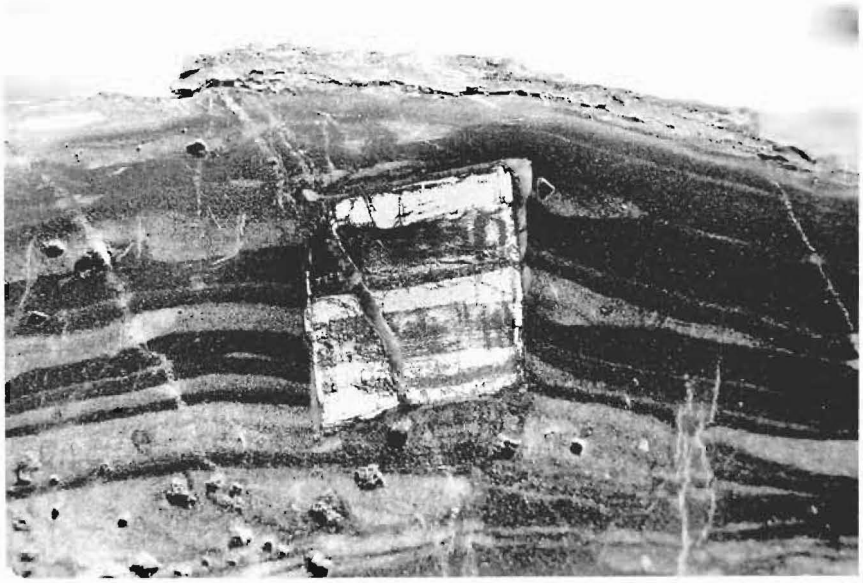

FIG. 4-1 A pyrite crystal in interlaminated siltstone and mudstone of the Wangapeka Formation, south of Fyfe River. Partial oxidation of the pyrite reveals perfect replacement of the sedimentary laminations. Weak concentric zoning is also visible. Refer to text for discussion. A sawcut slab, x 4 UC8866

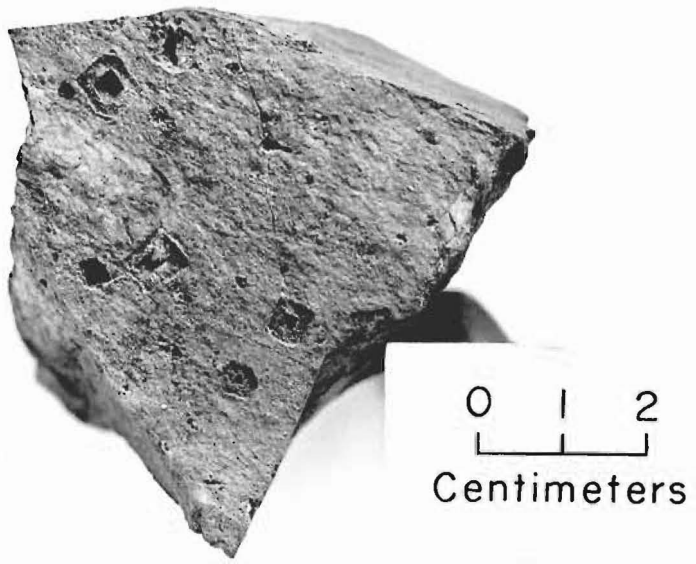

FIG. 4-2 A weathered bedding surface of quartzite from the Wangapeka Formation. Pyrite crystals grown at a mud-sand interface have undergone 'epitaxial overgrowth' in the less competent lithology. The structures are interpreted as indicating arrested pyrite growth due to lithification of the sandstone. See Figure 4-9. UC8867

Cessation of growth of all pyrite was possibly caused by the commencement of a period of deformation within the host rock, which resulted in rotation and brecciation of the crystals. The resulting stress inhomogeneity at the pyrite margins has produced quartz 'jackets' or pressure fringes (redefined, Spry 1969). The nature and extent of the pressure fringe reflects the competence of the host lithology. This relationship is demonstrated by the features of three pyrite crystals, each from a different lithology within a single hand specimen (Figures 4-4, 4-5b, 4-6a). All sections were cut perpendicular to bedding, and at a high angle to cleavage.

Pyrite from quartzite (Figure 4-4) shows little or no post-growth modification, including quartz jacketing. The example from muddy sandstone (Figure 4-5b) shows a well defined, simple pressure fringe, with slight rotation. Pressure-solution effects are visible, forming irregular, corroded surfaces on the pyrite approximately parallel to the cleavage in the sandstone. The 90° angular separation of the pressure fringe and the pressure-solution zones is well shown.

The third example (Figure 4-6a) consists of a polished section of pyrite in carbonaceous mudstone, the least competent lithology. Pressure fringes are well developed, and some solutions effects are visible. Also within mudstone are found pyrite crystals showing irregular and assymetrical fringe growth, fringe dislocation, and pyrite brecciation (Figure 4-5a), reflecting shear stress during growth of the

quartz fringes. Corrosion of pyrite has taken place at more than one set of surfaces, resulting in very anhedral grain shapes.

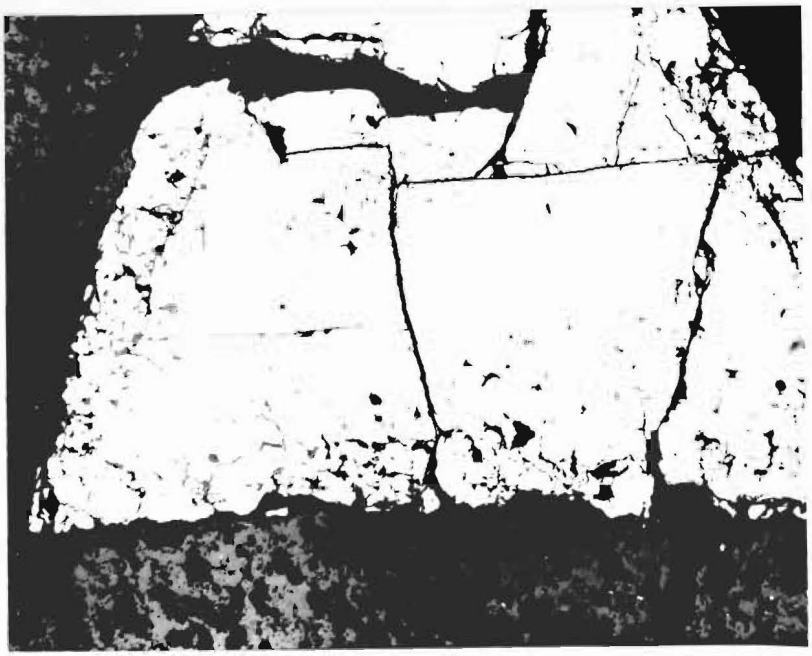

FIG. 4-3 Pyrite in siltstone, Wangapeka Formation, in polished section. An inclusion-rich outer zone is interpreted as a late growth phase.
ppl. x40 UC8872

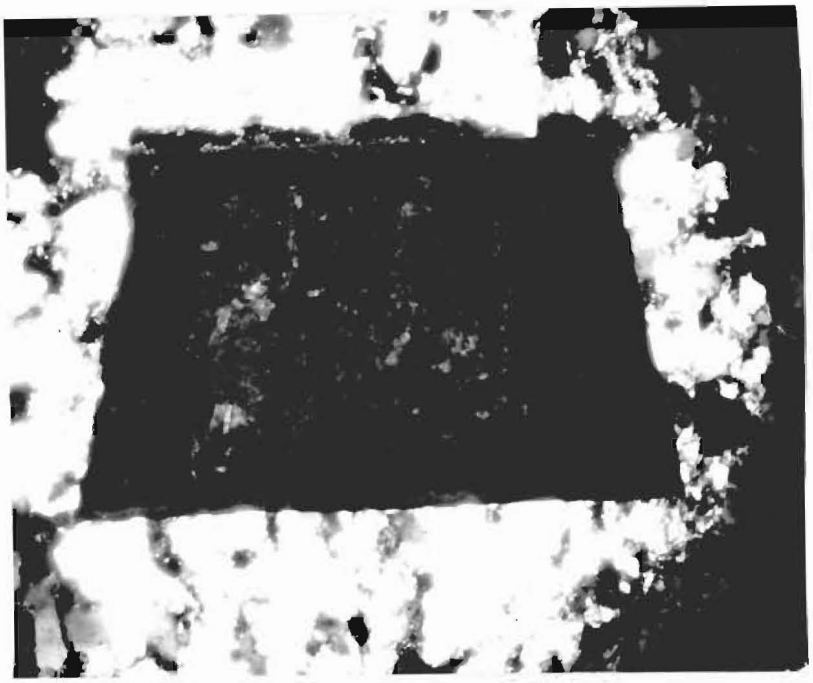

FIG. 4-4 Two-stage pyrite growth revealed in a hematite pseudomorph in weathered quartzite. Quartz jacketing and retrograde effects are negligible, apparently due to the competent nature of the lithology.
Thin section, ppl. x70 UC8869

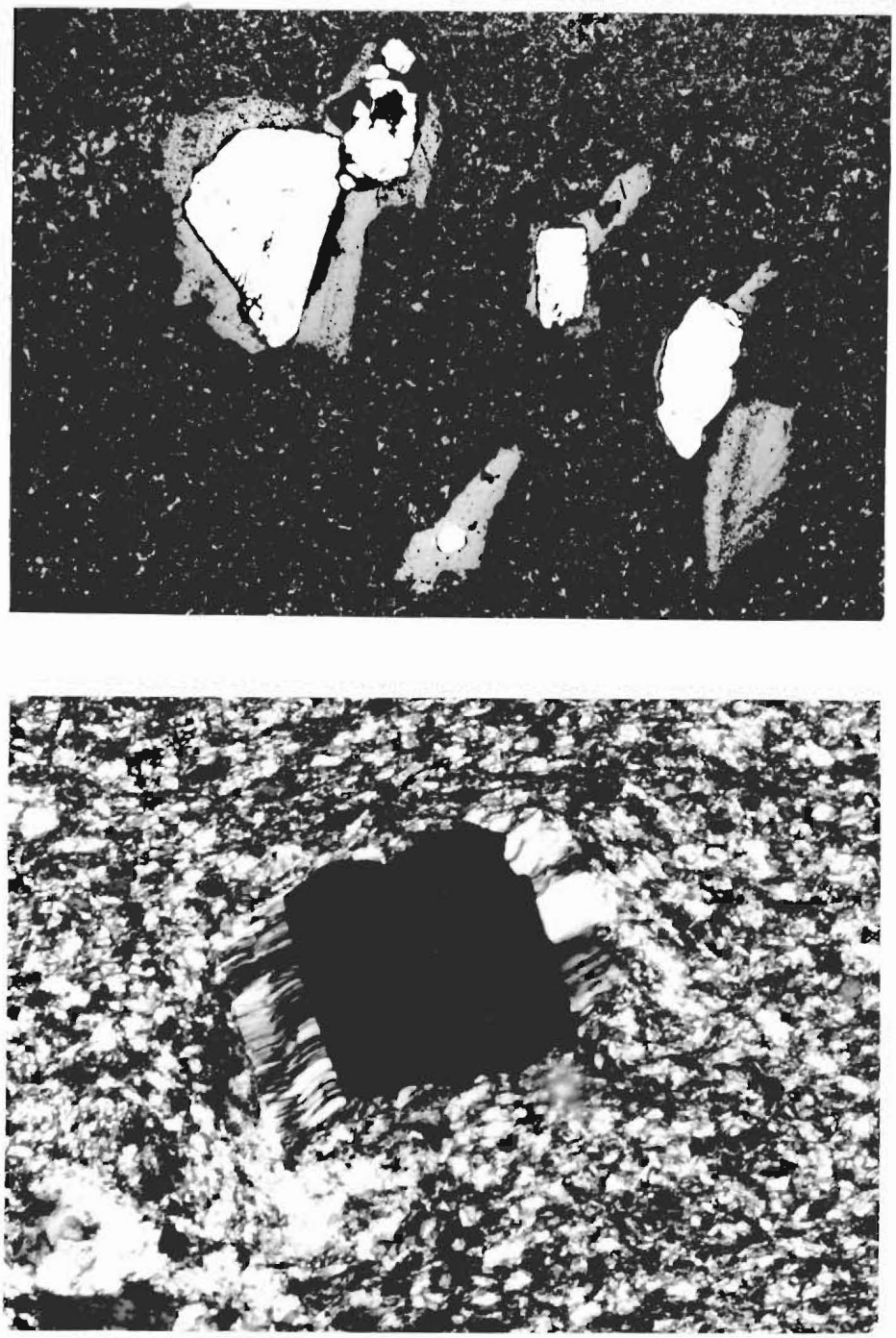

FIG. 4-5 Quartz 'jackets' developed on pyrite cubes, Wangapeka Formation. Pressure-solution effects are visible, and in (b) show an angular relationship with the pressure fringes which suggests that the two effects arise from a common stress situation.

(a), Upper: Mudstone.
Polished section, ppl. x64 UC8870

(b), Lower: Sandstone.
Thin section, partly xpl. x175 UC8868

(2) Inclusions within Pyrite

Reflection microscopy reveals some interesting aspects regarding the distribution and composition of inclusions within the pyrite crystals. As described above, inclusions broadly define two concentric zones. The outer, or 'rim', zone is characterised by angular inclusions of both quartz and a nonreflective material which is probably carbon. This zone is often poorly developed, or absent as in Figure 4-6a. In contrast, the central (or 'core') zone could be recognised in every example. The inclusions of the core consist of rounded to euhedral blebs of quartz and foreign sulphides (Figures 4-6, 4-7). Of the latter, sphalerite and chalcopyrite are most common, but other mineral phases are present, tetrahedrite and pyrrhotite being tentatively identified. Figure 4-6b shows an unidentified phase coexisting with sphalerite. Inclusions within the core tend to show equilibrium textures, the quartz occasionally forming perfect euhedra (Figure 4-7a). The small size of the inclusions made identification difficult, and in many cases impossible; the application of electron probe microanalysis may be of great value in this respect, but such analysis was not attempted.

The following consistent observations concerning foreign sulphide inclusions were noted:

(i) Inclusions are characteristic of the core, but are not restricted to this zone.

(ii) The sulphide inclusions in the core are predominantly chalcopyrite; those beyond the core are predominantly

sphalerite.

(iii) The small pyrite crystals within massive mudstone are noticeably more inclusion-rich than the larger crystals within the coarser lithologies.

(iv) Inclusion composition for the mudstone pyrite favoured chalcopyrite, with sphalerite being the more common in pyrite from the coarser lithologies.

(v) Both the inclusion/host abundance ratio, and the chalcopyrite/sphalerite ratio appeared to vary from one lamination to another, as seen within single polished sections.

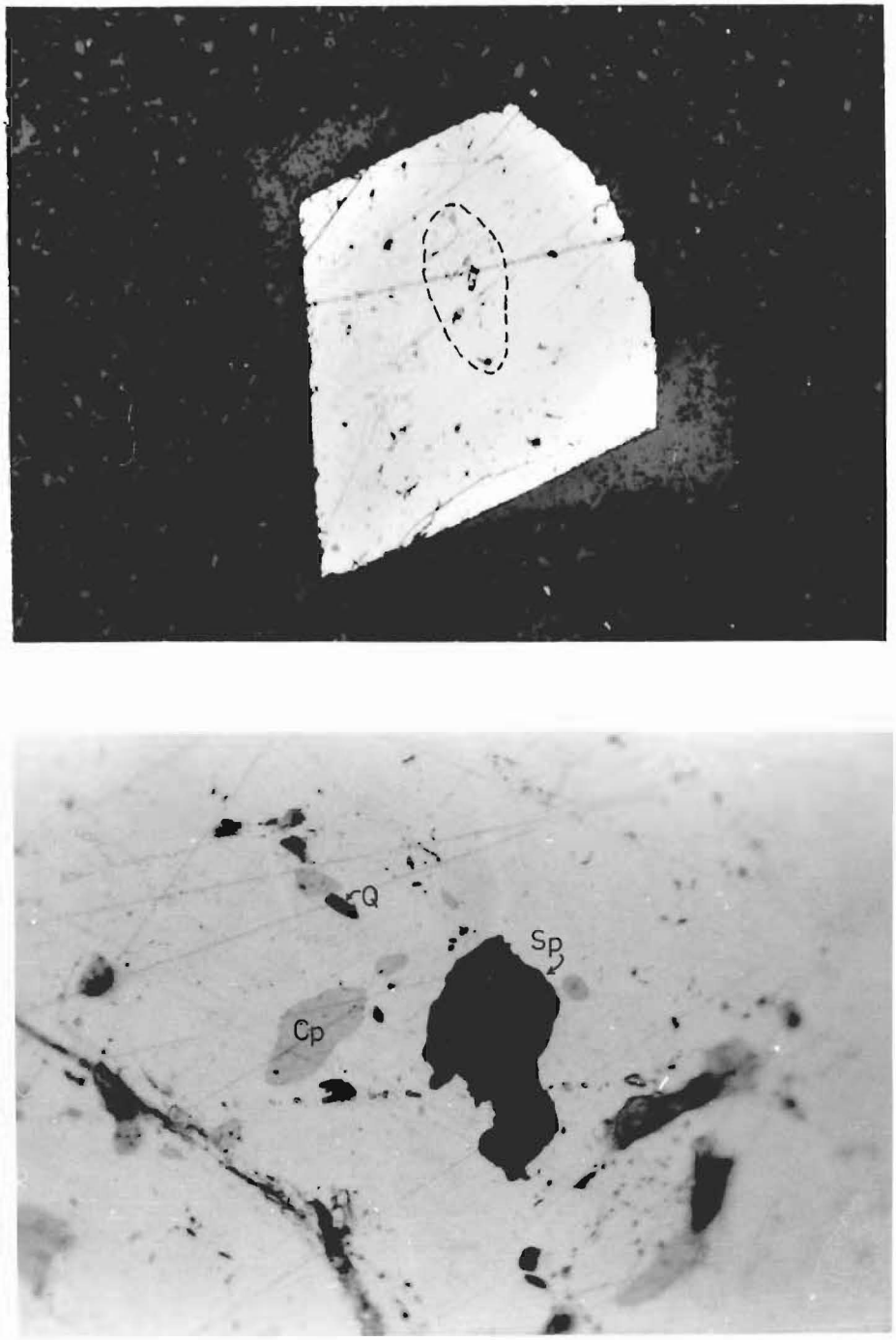

FIG. 4-6 Sulphide inclusions in pyrite. UC8870

(a), Upper: Pyrite in polished section, showing a central core of foreign sulphide blebs (indicated). Other, randomly distributed inclusions are quartz. Pressure fringe growth and corrosion of the host crystal are evident. ppl, x130.

(b), Lower: Central inclusion zone in a pyrite crystal (detail). Rounded blebs of quartz, chalcopyrite, and sphalerite are identified. The sphalerite is host to an unidentified mineral of low reflectance, possibly zincite. Polished section, ppl, oil. x1600

Cp; chalcopyrite, Sp; sphalerite, Q; quartz

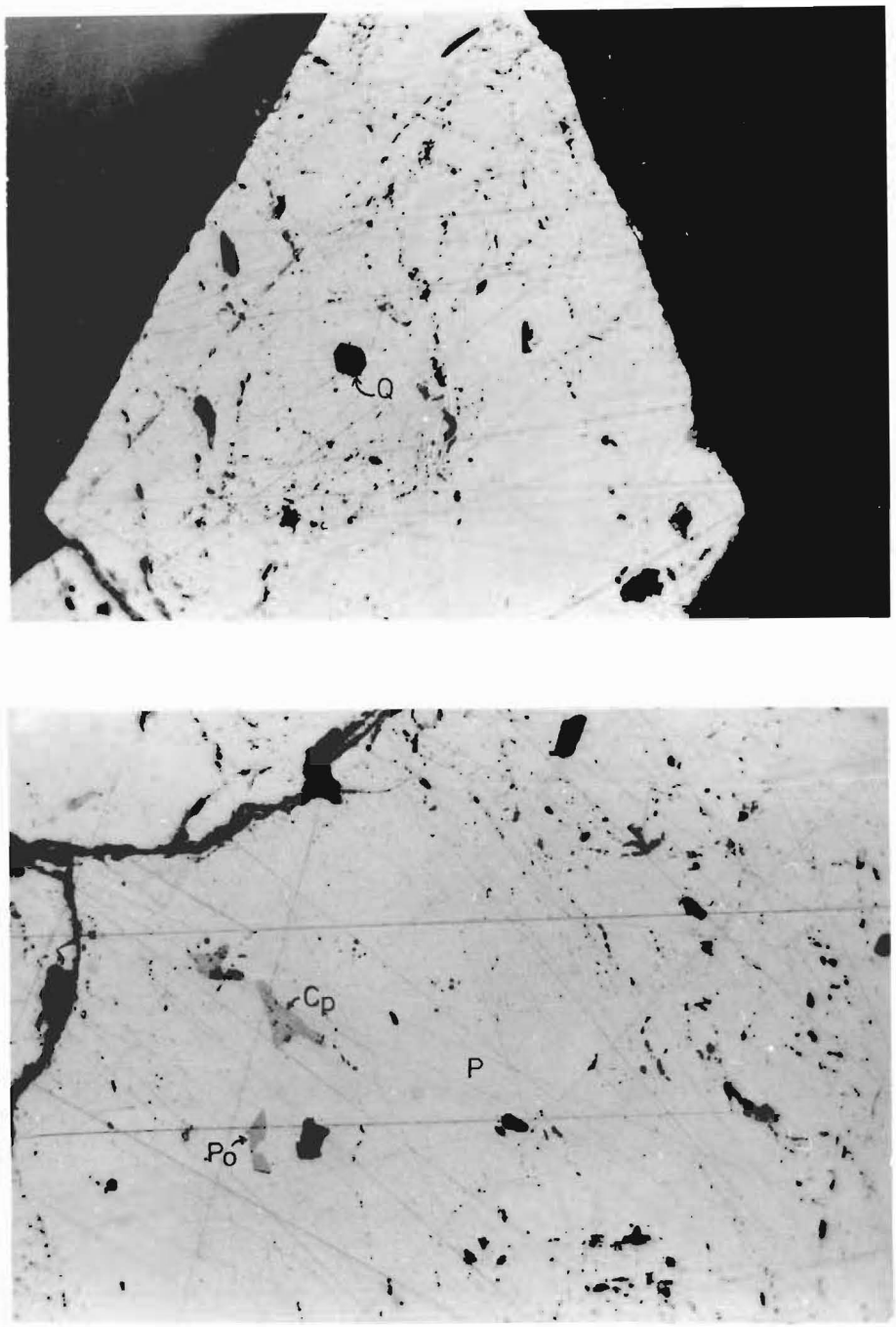

FIG. 4-7 Inclusions showing euhedral sections. UC8870.

(a), Upper: Quartz inclusion showing hexagonal section.

(b), Lower: Euhedral pyrrhotite and anhedral chalcopyrite. These minerals, being of very similar hardness and reflectance, appear almost identical with monochrome photography. They can be readily distinguished under the microscope by means of colour and optical properties.
Polished sections, ppl, oil. x640

P; pyrite, Po; pyrrhotite

(3) Retrograde Effects

Both during and after the formation of the quartz pressure fringes, the pyrite crystals underwent retrograde modifications. The most prominent physical modifications comprise fracturing and brecciation, which is developed to the greatest extent in the mudstones and siltstones. These effects are therefore related to lithologic competence, as are the pressure fringes described above. The elongation of 'knots' comprising pyrite crystal clusters or fragments of brecciated pyrite crystals reflects the extension parallel to the plane of tectonic cleavage. The effect of shear is also evident where extreme brecciation and displacement of pyrite fragments has occurred. Numerous examples of multiple fringe growth and fringe dislocation (Figure 4-5) suggest that several movements have been induced by a changing stress field during sediment deformation.

Geochemical modifications have also occurred, by pyrite dissolution (or 'corrosion'), and replacement. These effects are clearly related to the deformation, either as direct pressure-solution (Figure 4-5), or by replacement of pyrite by quartz along fractures. This replacement did not develop uniformly, but produced a 'patchy' texture, occasionally showing some control by the weak pyrite {001} cleavage. Fracturing and replacement has produced some examples of redistribution of foreign sulphides (Figure 4-8), but there is no evidence of the introduction of fresh sulphide from outside the crystals. Furthermore, the geochemical system at the time of replacement appears to have

been buffered against the dissolution of the other sulphides, a phenomenon frequently observed in sulphide systems and adequately explained in terms of solubility and reaction equilibria. Within the mudstone horizons, there are abundant examples of total dissolution of pyrite crystals, leaving a quartz bleb - the contracted and recrystallized pressure fringe - containing a smaller bleb of coalesced foreign sulphide (Figure 4-8).

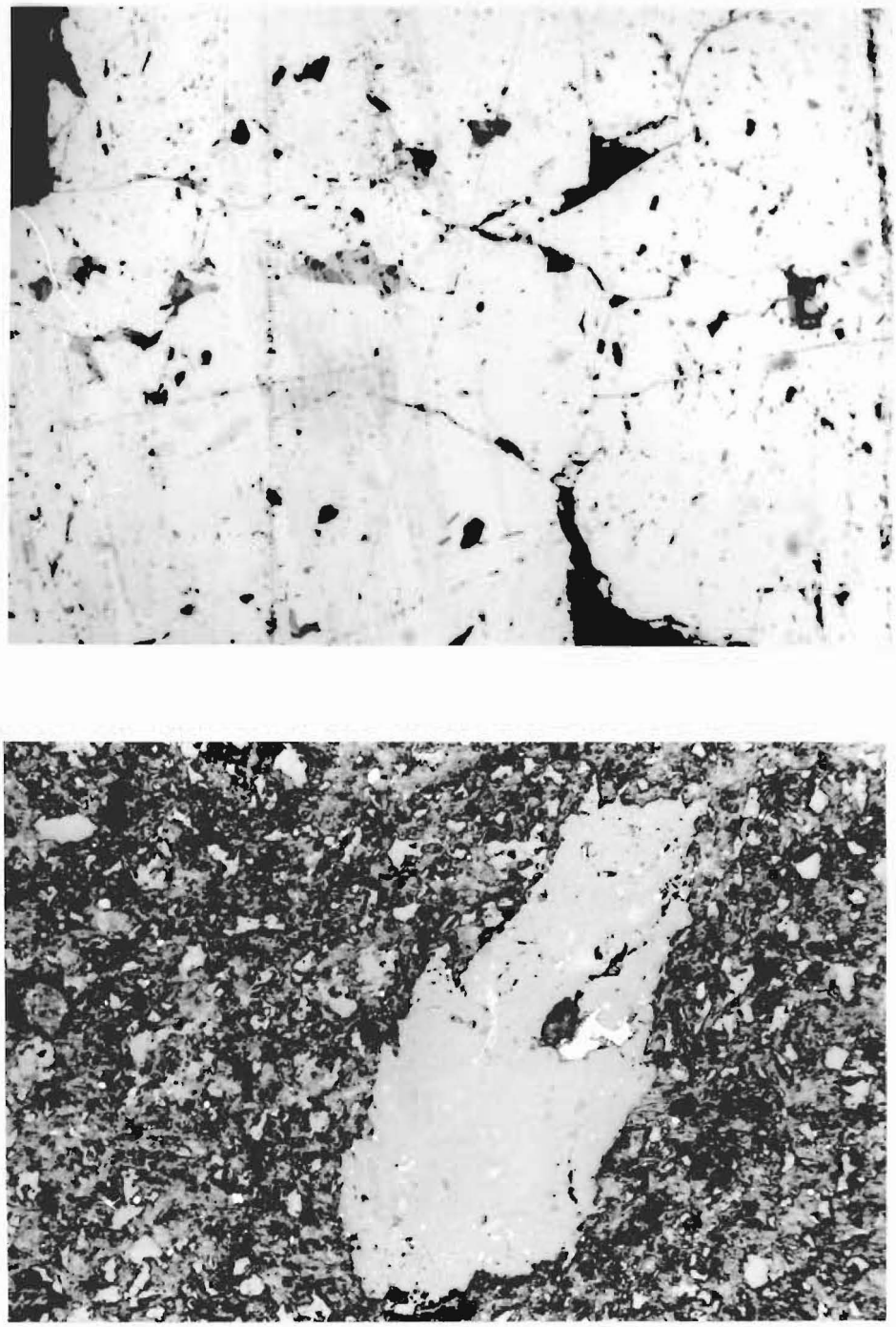

FIG. 4-8 Retrograde effects on pyrite crystals.

(a), Upper: Brecciation, resulting in partial replacement of pyrite by quartz and redistribution of foreign sulphide inclusions. UC8868

(b), Lower: Solution of pyrite. In this example, total loss of pyrite has taken place, leaving the coalesced and recrystallized pressure fringe. The chalcopyrite inclusions remain as a single bleb enclosed by the quartz. Sphalerite remnants are less common, and therefore may have been less stable in conditions which caused pyrite corrosion. UC8870
Polished sections, ppl. x250

(4) Growth History

The morphology and structure of the pyrite crystals indicates a two-stage development. The first commences with the core and is followed by a period of relatively stable, uniform growth by perfect replacement of the surrounding sediment. There is no evidence of disturbance of the sedimentary laminae by crystallization forces. Replacement textures indicate the crystals to be substantially post-compactional in origin. Similarly, the concentric growth zoning shows a history of isomorphous growth from a cube form established when the crystals were less than 20% of their final size.

A separate and later growth phase is indicated by the sharply 'stepped' crystals which occupied the moulds of the hand specimen shown in Figure 4-2. The inclusion-rich rims recognised in polished section are probably related to the same late growth period, but as none of the 'stepped' crystals remain, this association is unprovable. Replacement evidence shows all the pyrite - with the possible exception of the outermost rim - to predate the deformation of the host sedimentary laminae. This deformation ultimately caused the development of pressure fringes, brecciation, and in some cases corrosion of the pyrite. Figure 4-9 summarises the growth history, as reconstructed for the specimens of Figures 4-1 and 4-2.

Although the occurrence of pyrite in sediments has been the subject of considerable study and experimentation, very little has been published regarding the growth of

coarse crystalline pyrite, and even less regarding inclusions in pyrite. The very earliest stage of growth is represented by the core zone. Evidence already presented indicates that if any pre-compactional nucleus existed, it was very small in relation to the final crystal dimensions. This concept must be reconciled with the evidence from the cores, which suggests a rapid accumulation of a microcrystalline or amorphous mass of sulphide which crystallized sufficiently rapidly to prevent alignment, expulsion, or further coalescence of the included material.

(i) Cubic growth by replacement of surrounding sediment.

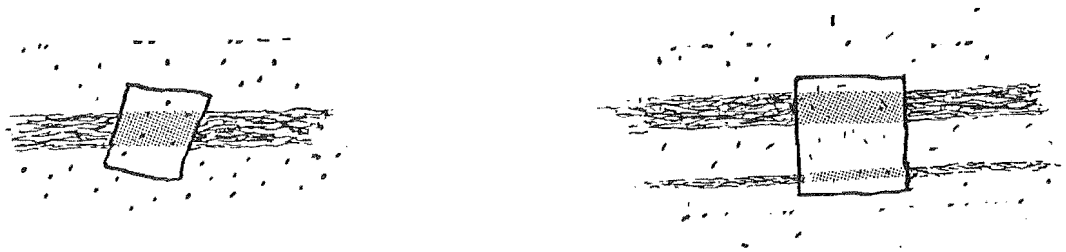

(ii) Inclusion-rich rims; imperfect replacement.

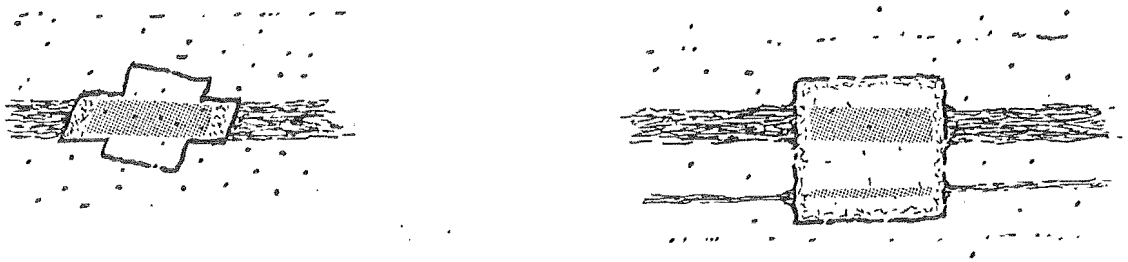

(iii) Deformational effects. Tectonic rotation, fracturing, replacement, and quartz jacketing.

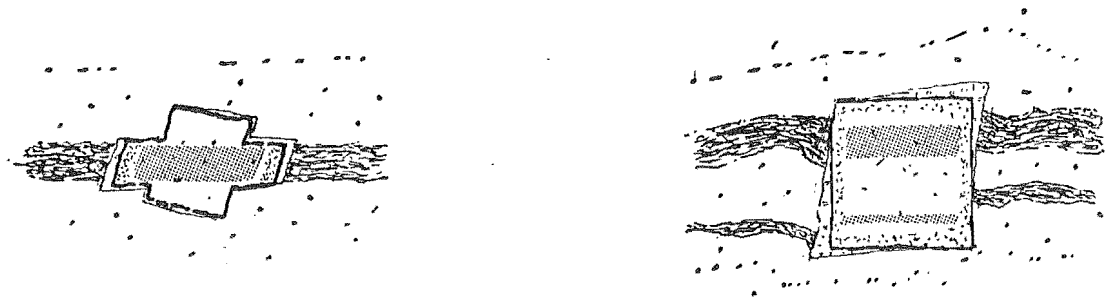

Sandstone, Siltstone.

Carbonaceous mudstone ('black shale').

Pyrite replacing mudstone

FIG. 4-9 Stages of pyrite growth and modification in laminated shales of the Wangapeka Formation, as exemplified by the specimens UC8866 (right) and UC8867 (left). See also Figures 4-1, 4-2.

Much has been written on the formation of fine sedimentary pyrite as a diagenetic mineral. Berner (1970) summarises this work and shows that the pyrite forming in the uppermost surface layers of modern carbonaceous sediments develops by reaction of metastable, intermediate iron monosulphide species with elemental sulphur. As this sulphur is produced by the oxidation of hydrogen sulphide, the reaction is unlikely to persist at depth. It is conceivable that the core material of the Wangapeka Formation pyrite accumulated as a sulphide gel, during or immediately following a monosulphide stage. Non-iron sulphides could be included due to co-precipitation phenomena. The possible presence of pyrrhotite (Figure 4-6) may represent a relict mineral from this early, sulphur-deficient phase.

The only previous report of primary sulphide inclusions in pyrite known to the writer is that of Arnold et. al. (1973). This work includes a description of coarse crystalline pyrite in sandstone of the famous Almaden mercury locality in Spain. Pyrrhotite and cinnibar inclusions are located in the pyrite 'nuclei', having been trapped during early growth. The included sulphides were considered to have precipitated and coexisted in equilibrium with the pyrite, but the chemistry of the process was not discussed.

Without further investigation, the exact origin of the cores in the Wangapeka Formation pyrite must remain uncertain. Whether development commenced with a monosulphide phase, or by simple precipitation of disulphide, or by some combination of the two processes cannot be established

on the evidence to hand.

The stage of uniform cubic crystal growth is more easily understood. The cubes developed by replacement during an episode which was substantially post-compactional, but preceding a phase of movement which resulted in a plastic deformation of the sediment. Hydroplastic deformation structures within the mudstone horizons suggest that the retained water content was high. A concentric zonation within the cubes (from an unknown cause) indicates fluctuations in the physical or chemical environment. Growth of this major part of the pyrite crystals almost certainly took place below the zone of oxidation where sulphurization transitions might occur, and probably proceeded by direct migration of near stoichiometric FeS_2 solutions. The sparsity of inclusions between the core and rim zones may represent contributions by factors such as extremely slow and stable growth, elevated temperatures, and highly favourable replacement conditions at the active crystal margins. The fact that no 'rejected' material accumulated at the margins supports the latter possibility. The presence of many, comparatively large, pyrite crystals within thin sandstone laminae requires a situation of significant sulphide mobility via solution transport. Such a situation would be consistent with 'wet' sediments, especially if a flow was provided by slow and continuous expulsion of water. A late, accelerated phase of dewatering accompanying initial sediment deformation could be expected to produce the inclusion-rich rims.

Many features relate pyrite crystal growth to permeability. The greater cube growth in the sand and silt horizons compared to that of the mudstone, and the higher core/crystal ratio in the mudstone pyrite both suggest that the post-core growth was dominant in the coarser sediment. Initially, the mudstone would have the lesser permeability, but would supply the bulk of the water, which on compaction would migrate along the coarser grained laminae. Advancing cementation in the sandstone appears to have arrested pyrite growth. The 'stepped' crystals of the sample shown in Figure 4-2 indicate that for a period there existed an unusual situation wherein the permeability of some sandstone beds was reduced to less than that of the adjacent mudstone laminae (see Figure 4-9). This condition would result in an immense increase in local pressure gradients acting on any remaining fluid in the mudstone, with a resulting increase in fluid flow in this material, although the absolute permeability would remain low.

An alternative explanation lies in the assumption that inter-layer movements maintained horizons of high permeability in thin mudstone laminae. Strain at such lithologic discontinuities is expected, and certainly took place during later times as shown by the brecciation and disturbance of pyrite crystals. The one objection to movement-induced permeability is the lack of evidence of disturbance to the growing pyrite, the moulds of which show perfect symmetry.

From whatever cause, permeability rather than sediment

composition appears to be the dominant control on pyrite growth, by limiting the availability of pore fluid which presumably transported the sulphide constituents to the growing cubes. Compaction-expelled pore water as an agent of ore mineral transport has been accepted by a number of authors, notably Noble (1963) and Stanton (1972).

Advancing deformation halted pyrite growth, and stress inhomogeneity at the margins of the rigid cubes resulted in the quartz pressure fringes. A marked change in chemical conditions at, or immediately following this time is apparent, as pyrite has become unstable, suffering 'corrosion' at the points of maximum compression. Movement, particularly within the more plastic mudstone laminae, caused severe brecciation of pyrite.

If the pyrite crystal growth can be related to a time of post-compactional high permeability, this growth must be considered diagenetic. The transition from diagenetic effects to metamorphic effects is difficult to define, being gradational. In this case, the change may be marked by the onset of deformation and the cessation of pyrite growth.

(5) Significance to Concepts of Ore Genesis

A number of aspects relevant to ore genesis may be recognised in this study of pyrite. Although fluid transport of sulphide in permeable sediments appears to be the probable cause of crystal growth, some consideration should be given to the source of the pyrite components. The wide-

spread and intimate distribution of the crystals within the sediment is evidence for an internal source; that is, the sulphide was derived from the host sediment. Major growth of the crystals probably took place during conditions of late diagenesis rather than metamorphism, with no evidence of any significant breakdown of iron-bearing minerals. Furthermore, the sulphur source must be identified.

The pyrite was seen to occur in two forms. The relatively large, cubic crystals are concentrated in the sand and silt laminae, as described. In addition, the muddy laminae contain very abundant, fine-grained pyrite, ranging in size from ca. 50μ to less than 1μ . Some of the largest grains of this fine material show pyritohedral form, but most exist as polycrystalline aggregates. The smallest grains show a framboidal texture (Figure 4-10), indicating that this fine-grained pyrite is of syngenetic or early diagenetic origin (Love 1964, 1967).

This line of reasoning provides grounds for the postulate that the coarse crystalline pyrite grew by a simple redistribution of existing pyritic material. Fine framboidal and polycrystalline pyrite may have become unstable during late diagenesis, going into solution when individual grains were highly stressed. Thus pressure-solution effects could provide the driving force for continuous crystal growth, by yielding a slow and constant supply of sulphide, sufficient to saturate the fluid system with

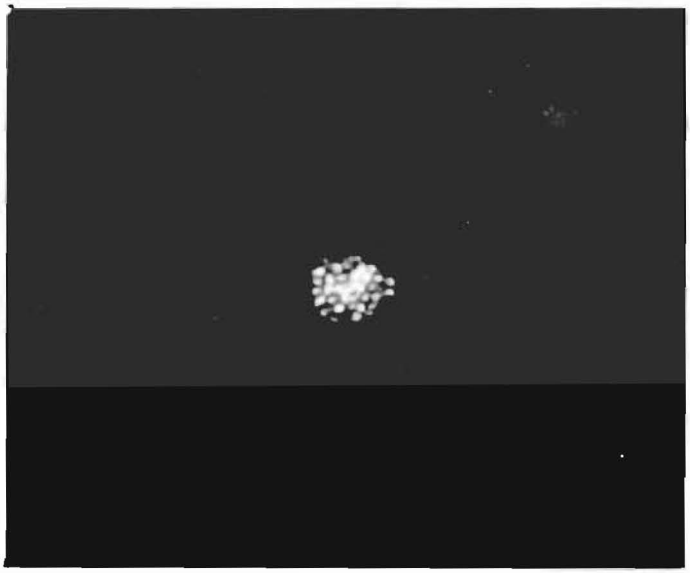

FIG. 4-10 Framboidal pyrite visible within recrystallized quartz in silty mudstone, Wangapeka Formation. The framboid is approximately 4 u in diameter. Polished section, partly xpl, oil. x2500 UC8870

respect to FeS_2. Framboidal pyrite survives in the mudstone laminae, where intergranular stresses would be minimal.

The significance of the foreign sulphide inclusions is worthy of further discussion. These sulphide blebs appear to be associated only with the cube cores, and as suggested, may represent a component of primitive sulphide masses. The apparent association of consistent Cu/Zn ratios of included sulphide with individual sedimentary horizons indicates a syndepositional origin. Carbonaceous mudstones, and particularly 'black shales' are known to have a high ore metal content (Vine and Tourtelot 1970), which may arise from complementary processes of sedimentary precipitation and absorption as discussed by Bernard (1964). The formation of the sulphide inclusions comprises a small scale, primary concentration of ore minerals, which could readily become available for transport and further concentration in the event of a later metamorphic or metasomatic episode. For the rocks of the Wangapeka Formation under discussion, host crystal retrograde effects have not proceeded far enough to significantly remobilize these sulphides. Remnant foreign sulphide persisting after complete solution of the host (Figure 4-8) suggests that the chemical system may be 'buffered' against mobilization of some ore minerals while sufficient pyrite remains. Such concepts of mineral stability and transport are well known from studies of the converse situation, where ore sulphides

are deposited from incoming solutions by replacement of stratiform pyrite, in both diagenetic and metamorphic environments.

II. ARTHUR MARBLE FORMATION

Disseminated mineralization within the Arthur Marble is almost non-existent. Apart from alteration zones at the margins of the intruding dikes and sills, only rare fine-grained pyrite is detectable in hand specimens. Most samples, however, when dissolved in acid yield a small amount of minute pyrite aggregates in the residues. These aggregates vary from irregular to framboidal shapes, made up of many small pyritohedral grains (see Figure 4-11). Similar residues from the marble remnant at the granite margin near Trig CK yielded small euhedral grains of both pyrite and monoclinic pyrrhotite, identified by X-ray diffraction.

The low sulphide content of the marble contrasts sharply with that of the nearby 'black shale' lithologies. Sulphide mobility in the marble appears to be very low; the survival of polygranular pyrite aggregates may be attributed to a lack of fluid-controlled processes, in response to a rapid and extreme reduction in permeability on burial. Additionally, the effect of intergranular stress would be small in comparison to that in the non-carbonate units. The pyrrhotite from marble near Trig CK is almost certainly a product of thermal alteration of pyrite, accompanied by recrystallization to euhedra.

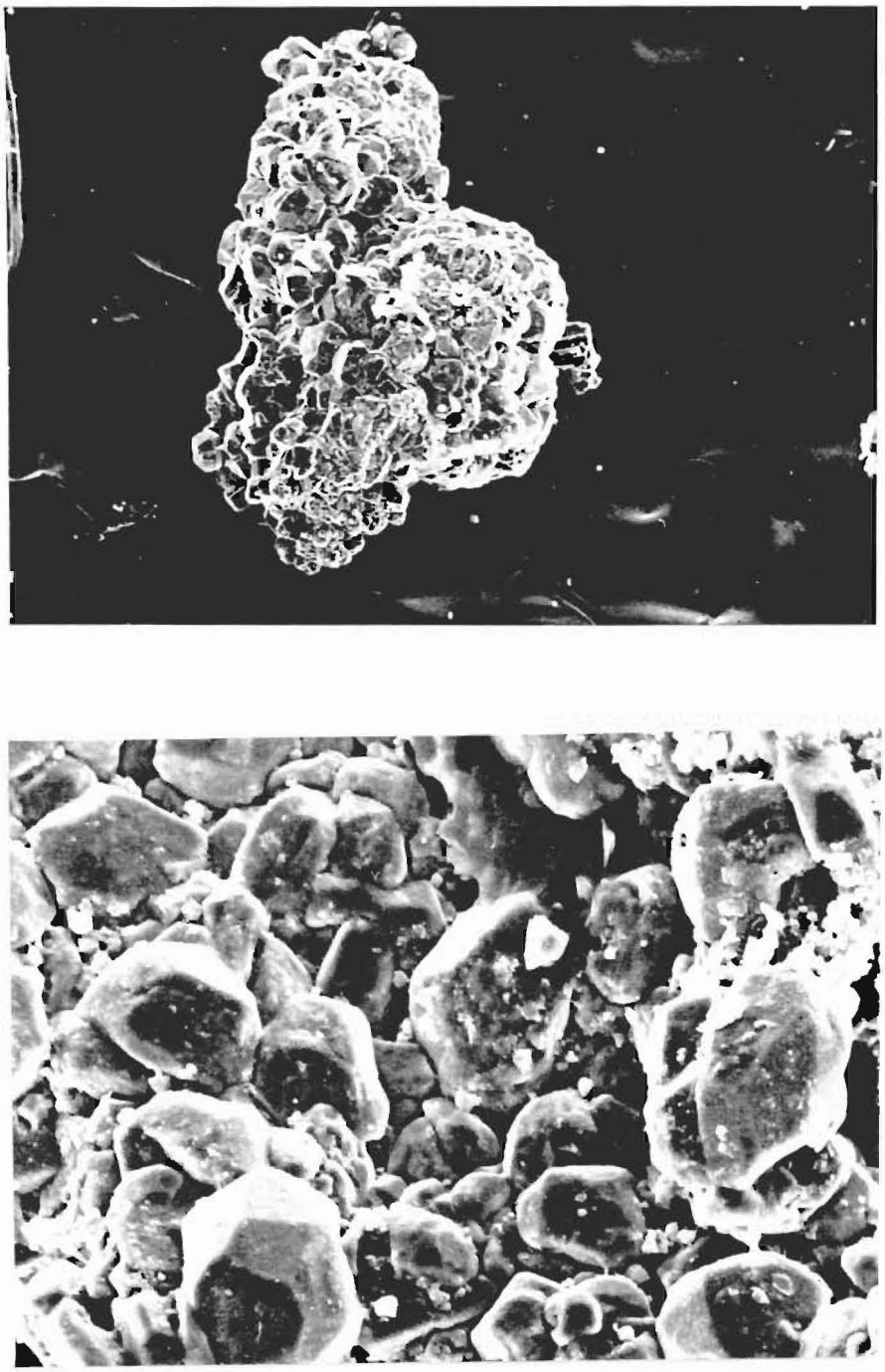

FIG. 4-11 Pyrite aggregates from Arthur Marble, obtained from acid-insoluble residues. Photographed with the scanning electron microscope.

Upper: x150

Lower: Surface detail, x750

III. OWEN FORMATION

This formation has undergone the greatest metamorphic and hydrothermal alteration, and it therefore contains the least well preserved original sedimentary structures. Overall, the lithology is similar to that of the Wangapeka Formation, although more carbonate-rich.

(1) General Description

The uppermost unit, the Beilby Quartzite, contains minor siderite within recrystallized cherty material, and a small amount of pyrite grown at intergranular boundaries where some permeability is retained along stylolitic sutures (Figure 4-12). Throughout the remainder of the formation, the disseminated mineralization is dominated by iron sulphide blebs, generally with a marked elongation parallel to cleavage. The mineralogy of these blebs was investigated by polished section and X-ray diffraction (see Table 4-1). Three iron sulphides were detected; pyrrhotite, pyrite, and marcasite. These minerals all occurred so similarly as to be usually indistinguishable by visual inspection of hand specimens, but a consistent pattern of occurrence emerged after the analysis of a number of specimens from a wide area. Pyrrhotite is restricted to the Enterprise Dolomite, which also contains lesser amounts of the other two sulphides, of which marcasite is the more abundant. Marcasite occurs along 'healed' fractures within the dolomite, along with infillings of carbonate, and

occasionally chlorite. At the margins of the dolomite unit, pyrrhotite gives way to marcasite and pyrite, which are found throughout the remainder of the formation. The disulphides occur together, or as pyrite alone.

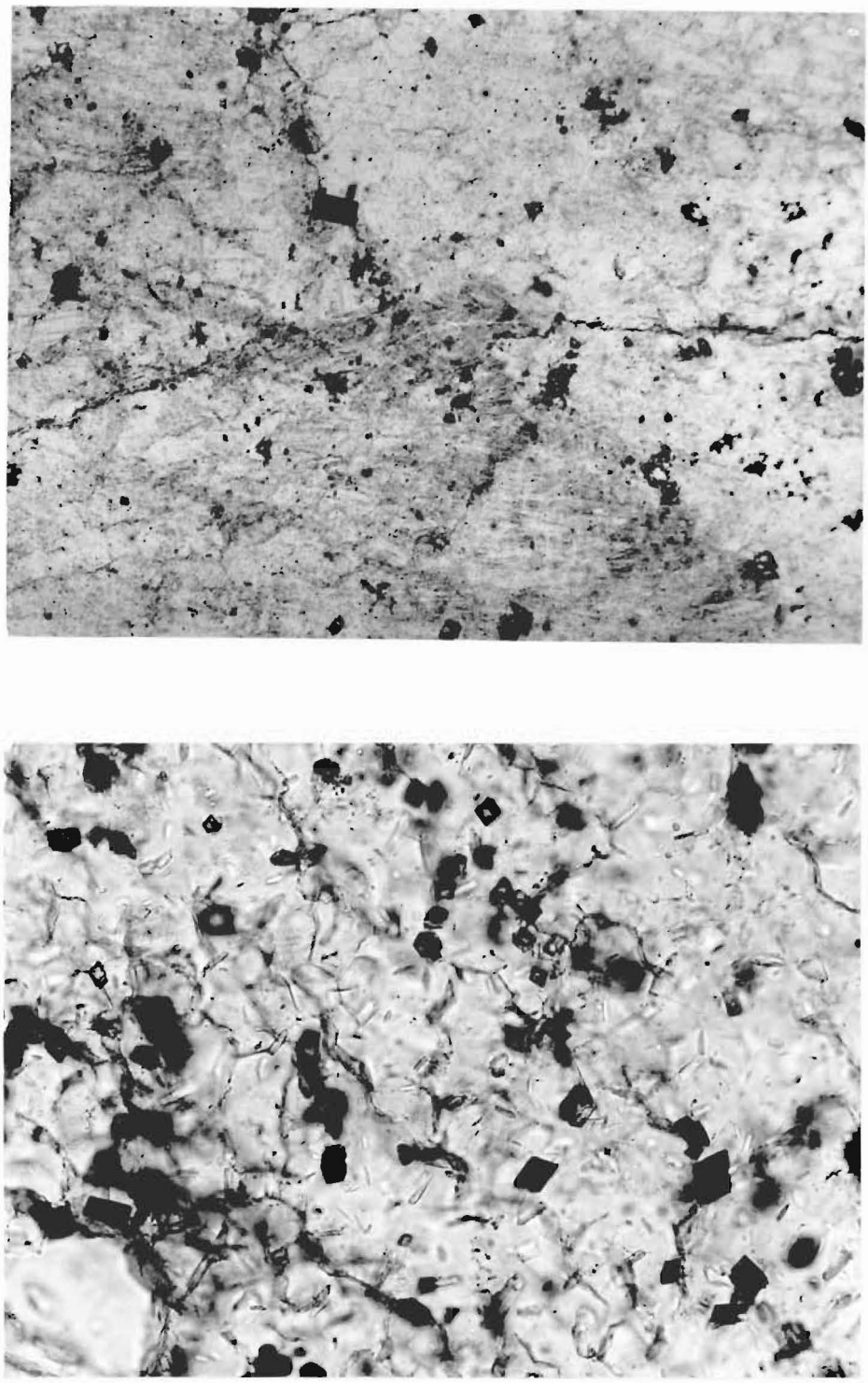

FIG. 4-12 Disseminated mineralization in Beilby Quartzite, Owen Formation.

Upper: Pyrite grown at a permeable, stylolitic boundary between polycrystalline quartz grains, which may represent recrystallized chert.
Thin section, ppl. x40 UC8884

Lower: Detail of the quartz grains, showing abundant siderite rhombs and sericite flakes.
Thin section, ppl. x400 UC8882

Rock type	Po	Mc	Py	Example
Sericite zone	—	—	●	UC8901
Enterprise Dolomite (uppermost)	○	●	●	UC8905
" "	●	—	—	UC8879
" "	●	○	—	UC8906
" "	—	●	○	UC8907
Siliceous carbonate below dolom.	—	●	●	UC8892
Carbonate lens " "	—	○	●	UC8905
Phyllite " "	—	—	●	UC8904

Po: pyrrhotite
Mc: marcasite
Py: pyrite
● abundant
○ trace only
— not detected

TABLE 4-1 Summary of sulphide composition for rocks of the Owen Formation, as determined by optical microscopy and X-ray diffraction. For optical determination, the samples were prepared as polished sections and examined with a polarizing microscope. Samples for X-ray diffraction were separated by coarse crushing followed by gravity separation and fine grinding.

(2) Origin and Paragenesis

There can be little doubt that the sulphide blebs were derived from original stratiform pyrite, via a pyrrhotite stage. Figure 4-13a shows a specimen of Enterprise Dolomite with sedimentary bedding marked by pyrrhotite blebs which are individually elongated parallel to cleavage. Another specimen (Figure 4-13b) contains a pyrrhotite mass with a distinct rhomb-shaped cross section, possibly representing a relict pyrite cube shape. (Examples of pyrrhotite pseudomorphs after pyrite have been collected by the author from lower Paleozoic rocks in similar situations elsewhere in Nelson).

The occurrence of pyrrhotite as a metamorphic mineral after pyrite is well known. The limit of this conversion in regional metamorphic terranes has been proposed as a metamorphic isograd, located slightly below the biotite isograd (Carpenter, 1974; see also Figure 4-14). Pyrrhotite also occurs in broad aureoles beyond the zone of silicate alteration around intrusive granites, and is considered a sensitive indicator of thermal metamorphism (Neumann 1950). Such zoning cannot be traced in the Owen area, due to complications of structure and lithologic variation.

The abundant marcasite occurring in association with the pyrrhotite is consistent with the known alteration products of pyrrhotite in retrograde conditions (Edwards, 1953, Ramdohr, 1969). The widespread coexistence of

marcasite with pyrite suggests that most, if not all, the pyrite has resulted from marcasite inversion. A paragenetic sequence -

pyrite ⟶ pyrrhotite ⟶ marcasite ⟶ pyrite

can therefore be defined. The first transition is essentially a desulphurization reaction, and must be attributed to metamorphism. The second and third transitions apparently arise from a widespread metasomatic phase of retrograde metamorphism.

Pyrite-free marcasite is found accompanying the pyrrhotite in the dolomite unit, usually as separate blebs, although rare examples of pyrrhotite altering to marcasite were noted. Elsewhere, marcasite and pyrite occur together, with marcasite being most abundant in the low-permeability, carbonate-rich horizons. The intimate association of marcasite with well recrystallized minerals within fresh rock indicates a definite hypogene origin, although some marcasite accompanying near-surface pyrrhotite specimens may be due to weathering. Both pyrrhotite alteration and marcasite inversion have been inhibited in the dolomite, presumably due to the extremely low permeability of this unit. The chemical environment may also contribute to their stability. The more permeable lithologies, particularly the sericite zone, exhibit break-up of the sulphide blebs, and sulphide deposition as fine filaments parallel to cleavage, and as coarser infillings in cross-cutting fractures. Marcasite is rare in these zones, due to either inhibited formation or more advanced inversion.

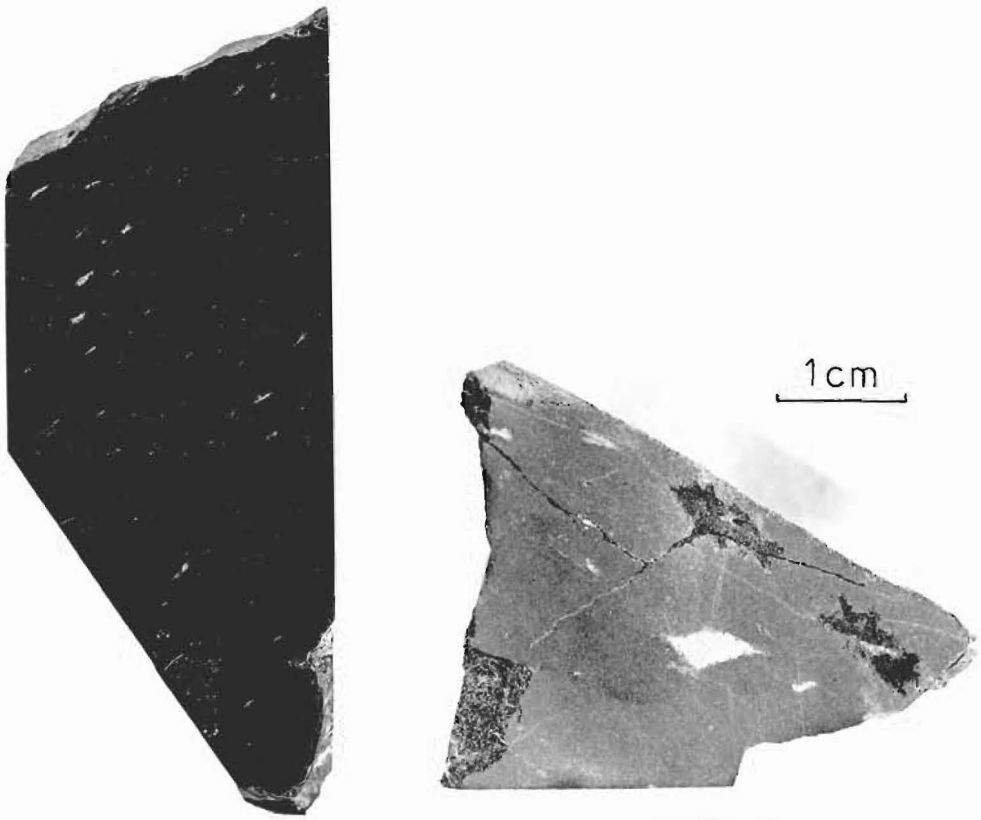

FIG. 4-13 (a) Dolomitic mudstone from the Owen Formation showing pyrrhotite formed by in situ alteration of stratiform pyrite. The sedimentary laminations are horizontal, but the individual pyrrhotite blebs are elongate parallel to cleavage, approximately 45° to bedding. Natural size. UC8877

(b) Dolomitic mudstone with pyrrhotite pseudomorphing a former large pyrite crystal. The section is cut perpendicular to the axis of maximum strain elongation. UC8890

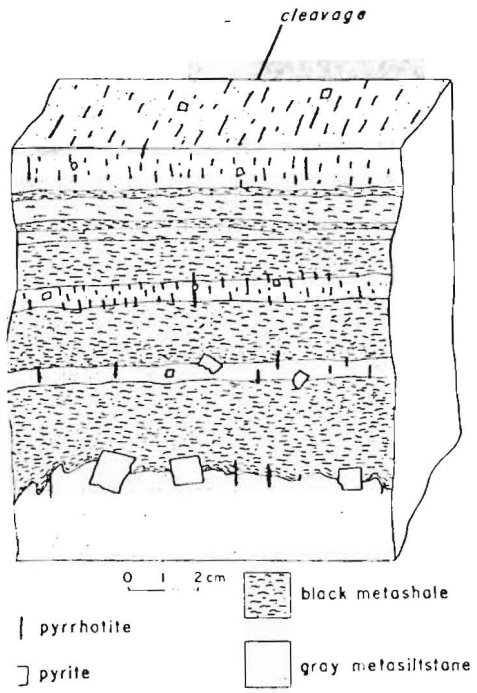

FIG. 4-14 (left) An example of pyrite-pyrrhotite conversion in response to regional metamorphism, observed in late Precambrian sediments of Tennessee. The conversion is incomplete, as remnant pyrite remains.
From Carpenter (1974).

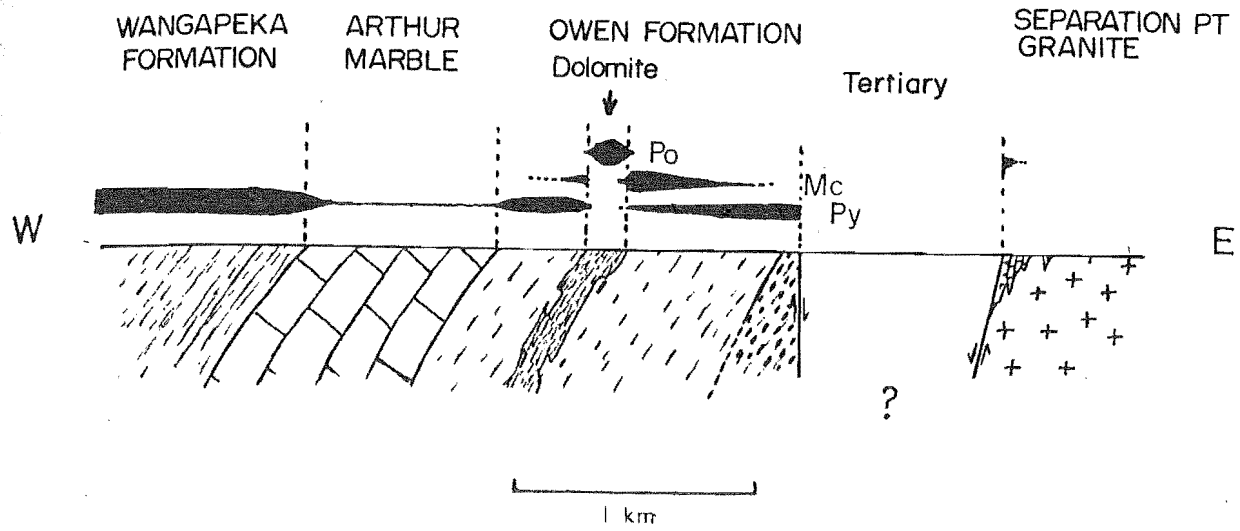

FIG. 4-15 A theoretical and ideal east-west section through the central goldfield region of Mt. Owen, showing type and approximate abundance of disseminated iron sulphides. Pyrite was originally abundant in the pelitic rocks, but sparse in the marble. Prograde thermal metamorphism caused alteration of pyrite to pyrrhotite throughout all but the uppermost (and westernmost) Owen Formation. Later retrograde, hydrothermal effects converted pyrrhotite to marcasite, and possibly pyrite. Further pyrite has reappeared by marcasite inversion in zones of higher temperature (east) and higher permeability (west). The extremely impermeable dolomite has resisted retrograde changes to the sulphides, preserving pyrrhotite.

(3) Sulphide textures

(a) Pyrrhotite. Except for the rare examples of relict cubic shape described above, the pyrrhotite occurs as elongate streaks which often exceed 20 mm in length. Rapid oxidation makes this mineral difficult to find in field exposures. With cross-polarized light, polished sections of pyrrhotite show a moderate foam texture, consisting of mosaics of grains showing abundant equiangular triple junctions. This tendency toward an equilibrium texture is indicative of considerable post-deformational annealing, as discussed by Stanton (1972).

The pyrrhotite mineralogy is further discussed in Chapter VIII.

(b) Marcasite-Pyrite. The blebs which contain these minerals form elongate streaks similar to those described for pyrrhotite, although some show evidence of greater recrystallization to produce more compact sulphide 'knots'. Recrystallization of both sulphide and surrounding host rock minerals is most pronounced in the carbonate-rich rocks, where some euhedral termination structures are formed by pyrite pseudomorphs after marcasite. Many of these recrystallized knots retain an impressive mosaic of marcasite with well developed lamellar twinning in a groundmass of pyrite (Figure 4-16).

The distribution of marcasite within individual sulphide blebs is not random. Two preferred distribution

characteristics are recognised; grains are concentrated at either the edge of a bleb, or at the centre. Marcasite at the margin commonly occurs as few, discrete and well recrystallized grains, whereas the central concentrations show textures varying from a few isolated crystalline grains to a rim of crystals surrounding a microcrystalline mass (Figures 4-17, 4-18).

These textures must be interpreted in terms of both initial products of pyrrhotite alteration, and the later products of inversion and recrystallization. The microcrystalline cores suggest that at least the final stage of pyrrhotite alteration produced an initial disulphide product in the form of a disordered mass.

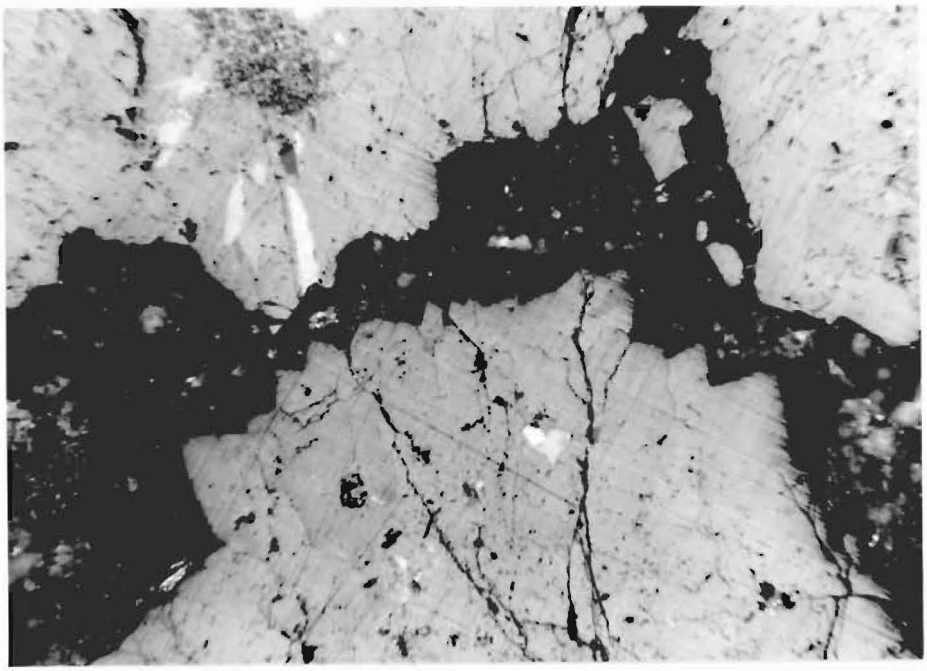

FIG. 4-16 Textures of marcasite-pyrite blebs in Owen Formation sediments.

Upper: Massive sulphide, showing characteristic lath-like twins of marcasite in a mesostasis of pyrite (medium grey). Polished section (PS510), partly xpl. x120 UC8893

Lower: Pyrite with relict marcasite grains. The acute terminations against carbonates (dark) are indicative of former marcasite. Considerable marcasite inversion since original crystallization is inferred.
Polished section (PS503), partly xpl, oil. x180 UC8892

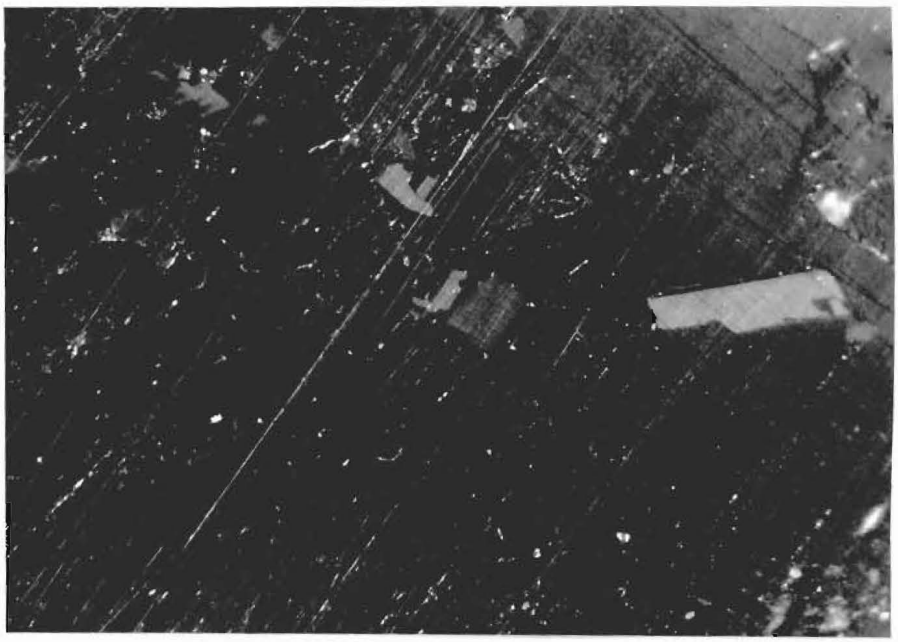

FIG. 4-17 Marcasite distribution within sulphide blebs in the sediments of the Owen Formation, showing partial inversion and recrystallization. PS503, UC8892

Upper: Marcasite crystals grown at the edge of a sulphide bleb, against well recrystallized quartz and carbonates (light grey). The sulphide mesostasis is pyrite (medium grey).
Polished section, partly xpl, oil. x640

Lower: Relict euhedral crystals at the centre of a sulphide bleb.
Polished section, partly xpl, oil. x640

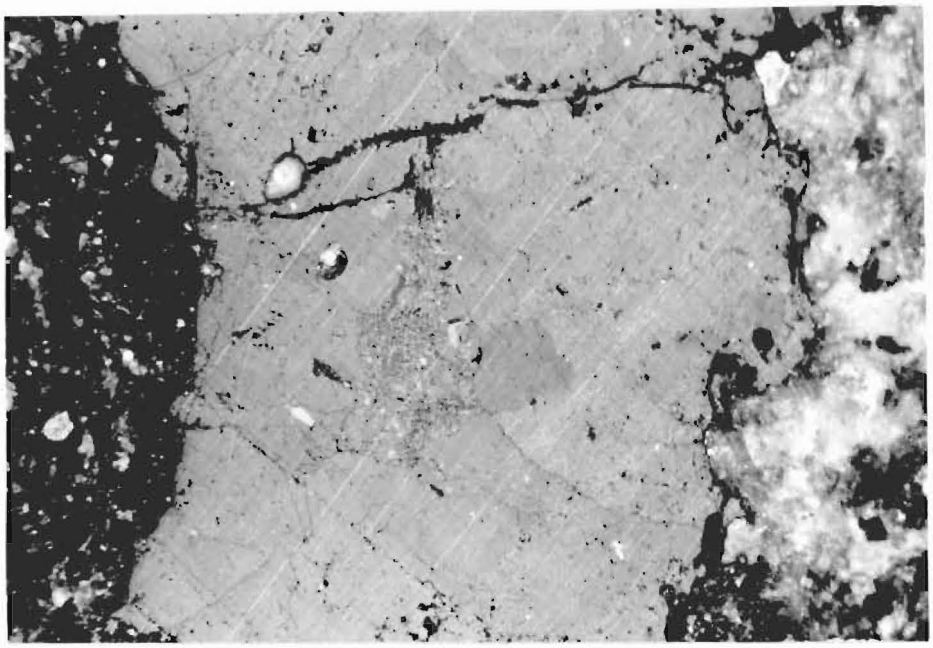

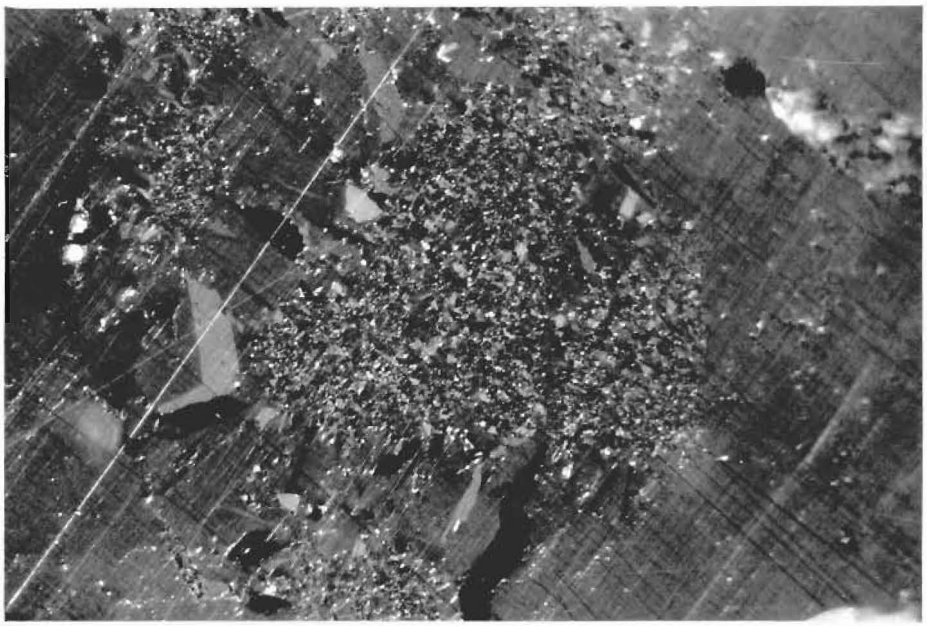

FIG. 4-18 Marcasite in sulphides of the Owen Formation (continued). PS503, UC8892

Upper: Marcasite as a microcrystalline mass at the centre of a pyrite bleb.
Polished section, partly xpl. x120

Lower: Detail of above.
Partly xpl, oil. x640

The inward progression of restructuring involving recrystallization and/or marcasite inversion, from the outer edge of the sulphide masses, may have isolated the core zone against further modification. Marcasite at the bleb margins appears to have survived due to the establishment of relatively large crystals, but other factors may be important. A weak surface anisotropy of the pyrite surrounding the marcasitic cores shows the pyrite grains to be relatively large and well recrystallized. The extent to which this characteristic is inherited from pre-existing marcasite is uncertain.

(c) Non-Ferrous Sulphides. Small amounts of chalcopyrite, sphalerite, and other sulphides occur in close association with the iron sulphide blebs. Their pattern of occurrence and composition provides strong evidence that these minerals were derived at least in part from foreign sulphide inclusions in the original pyrite, and are thereby equivalent in origin to the inclusions described for the Wangapeka Formation pyrite. In the Owen Formation, these minerals are frequently not enclosed by the iron sulphide, and therefore cannot be classified as inclusions except in the sense of implied origin.

The non-ferrous sulphides are illustrated in Figures 4-19, 4-20. The best examples were seen in the pyrrhotite blebs, where conspicuous concentrations of chalcopyrite are commonly located at the points of maximum elongation. Chal-

copyrite, and ?tetrahedrite, were seen to form intergranular films and interstitial grains at triple junctions within the pyrrhotite. Similarly, sphalerite forms small rounded grains along host grain boundaries.

Noticeably less foreign sulphide was found in association with the marcasite-pyrite blebs, where the ore minerals were usually separated from the host bleb or only partly in contact with it. Chalcopyrite was once again the most abundant ore mineral, the sphalerite being present as very small grains, commonly scattered throughout the host rock surrounding the iron sulphides. Some examples of sphalerite replacing host rock minerals were noted.

If the non-ferrous sulphide was originally present as inclusions in pyrite, similar to what has been described from specimens from the Wangapeka Formation, this material has been subject to considerable redistribution throughout the successive alteration of the host sulphide and surrounding rock. Much of this redistribution may be due to recrystallization, such as the apparent expulsion of included sulphide to the extremities of the pyrrhotite blebs. Some remobilisation of ore metals in solution is probable, as indicated by the apparent depletion of ore sulphides in the more permeable, sericitic rocks. The host sulphides also have been extensively remobilised (Figure 4-21), replacing country rock minerals such as carbonate and biotite.

Remobilisation may account for the chalcopyrite-rich and sphalerite-poor characteristic of the pyrrhotite. The evidence from the Wangapeka Formation suggests that sphalerite is removed from the host sulphide in preference to chalcopyrite. Alternatively, metamorphic addition of copper may have taken place, but proof of this is difficult to establish.

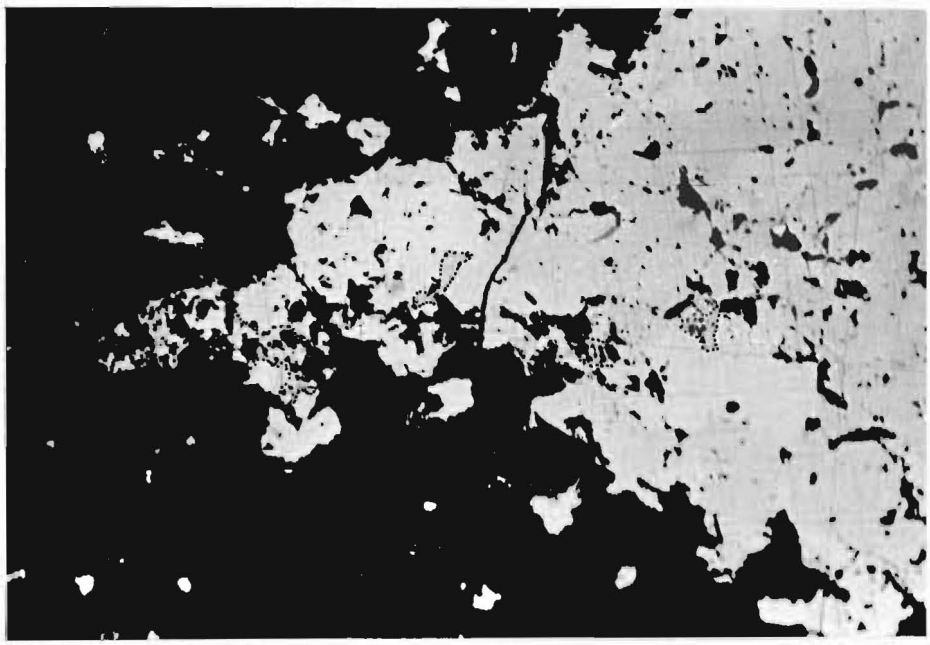

FIG. 4-19 Non-ferrous sulphides in disseminated sulphide blebs, Owen Formation. PS502, UC8890

Upper: Chalcopyrite (outlines dotted) concentrated in the 'apex' of a pyrrhotite mass in dolomitic mudstone. The matching saw-slab is illustrated in Figure 5-13b.
Polished section, ppl. x100

Lower: Detail of the pyrrhotite. Non-ferrous sulphide inclusions occur at intergranular locations, especially at triple junctions. Chalcopyrite inclusions are indicated by arrows.
Partly ppl, oil. x640

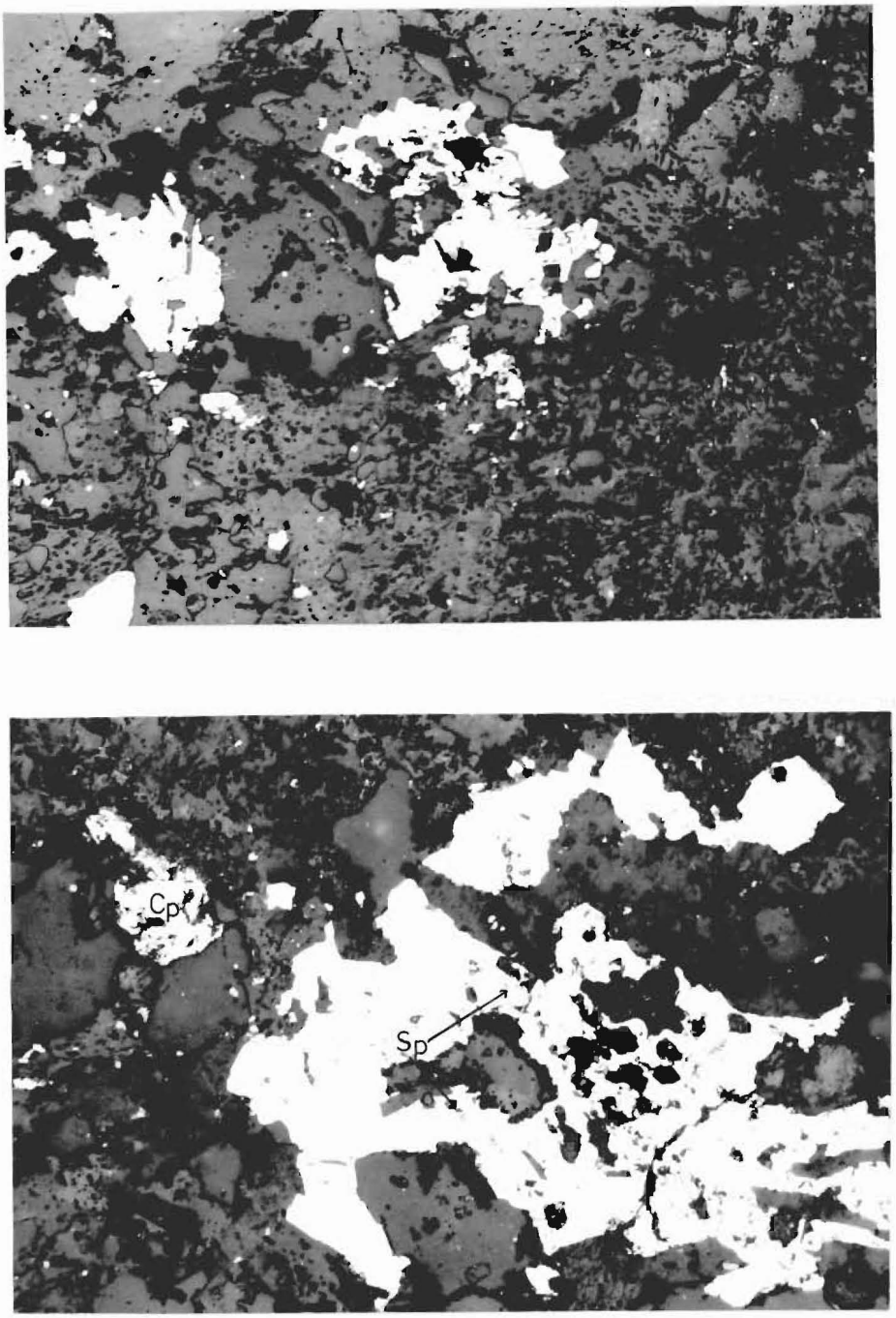

FIG. 4-20 Non-ferrous sulphides associated with disseminated and partly remobilized marcasite-pyrite blebs in dolomitic mudstone, Owen Formation. The ore sulphides are commonly detached from the disulphide blebs. UC8893

Upper: Showing chalcopyrite (Cp).
Polished section (PS510), ppl. x120

Lower: Showing chalcopyrite, and small amounts of sphalerite (Sp).
Polished section (PS510), partly xpl. x120

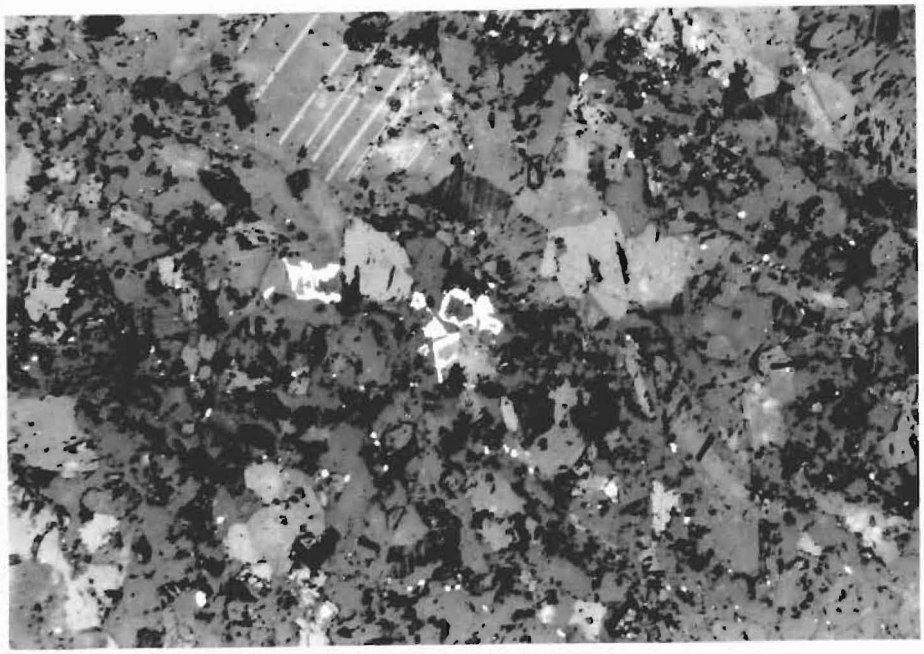

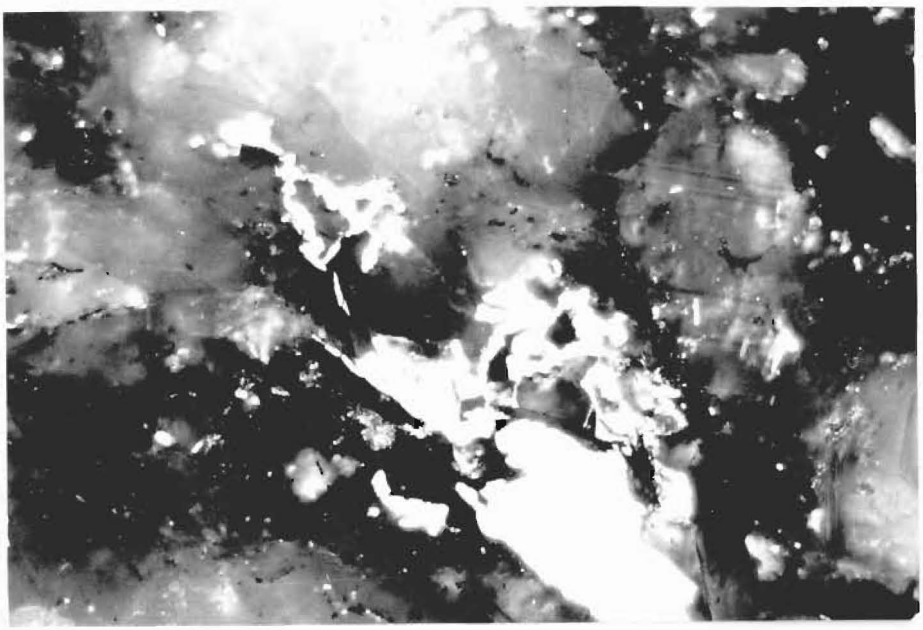

FIG. 4-21 Remobilisation of disseminated sulphides, Owen Formation. Replacement of country rock minerals, including ferroan carbonates and biotite, may be a result of the diffusion of liberated sulphur during the pyrite to pyrrhotite transition. Considerable remobilisation also occurred during the resulphurization phase, and the replacing pyrite shown above may date from either event.

Upper: Polished section (PS503), partly xpl. x250 UC8892

Lower: Polished section (PS510), partly xpl, oil. x640 UC8893

IV. DISCUSSION

This study of disseminated mineralization is considered important for two principal reasons. Firstly, the observations provide some insight regarding the mobility, accumulation, and stability of sulphides in sediments under conditions ranging from diagenesis to metamorphism. Secondly, the alteration of the disseminated sulphides can be used to trace the history of a metamorphic event which became pervasively hydrothermal, or metasomatic, during the waning phase.

The stratiform sulphides of the relatively unmetamorphosed Wangapeka Formation provide a useful indication of the pre-metamorphic characteristics of the Owen Formation sulphides. Advancing metamorphism caused alteration of pyrite to pyrrhotite, probably by desulphurization as suggested by the alteration of other iron-containing minerals to sulphide in the surrounding sediment. Recrystallization within the dolomite horizons has preserved pyrrhotite by preventing retrograde alteration of sulphides enclosed by this unit. Elsewhere, the degree of retrograde alteration can be seen to be a function of rock permeability. Restoration to the disulphide state was a result of what can be recognised as a widespread, low temperature hydrothermal event, which gave rise to a major episode of vein formation caused by contemporaneous fracturing, as described in the following Chapter (V).

The successive alteration and restructuring of the disseminated sulphides has permitted the release of significant amounts of ore minerals. Similarly, the release and migration of sulphur-bearing species may have been important in 'scavenging' the surrounding sediment, extracting metals from silicates and creating sulphides which would be readily available for mobilisation by a subsequent hydrothermal phase.

CHAPTER V

VEIN MINERALIZATION

This term is used to cover all mineralization having a direct relation to vein-forming processes, and includes minor replacement and infilling in addition to the well defined quartz lodes. Vein location and vein structures have been partly described in Chapter III, and a history of prospecting and mining activities presented in Chapter I. Some duplication of these details in this section is unavoidable.

The veins at Owen can be divided on the basis of emplacement and ore petrography into two types; one characterised by base metal sulphides and association with carbonate rocks, and the other a gold-bearing quartz occurring in generally non-carbonate lithologies. A summary of the vein-associated mineralization is given in Figure 5-1.

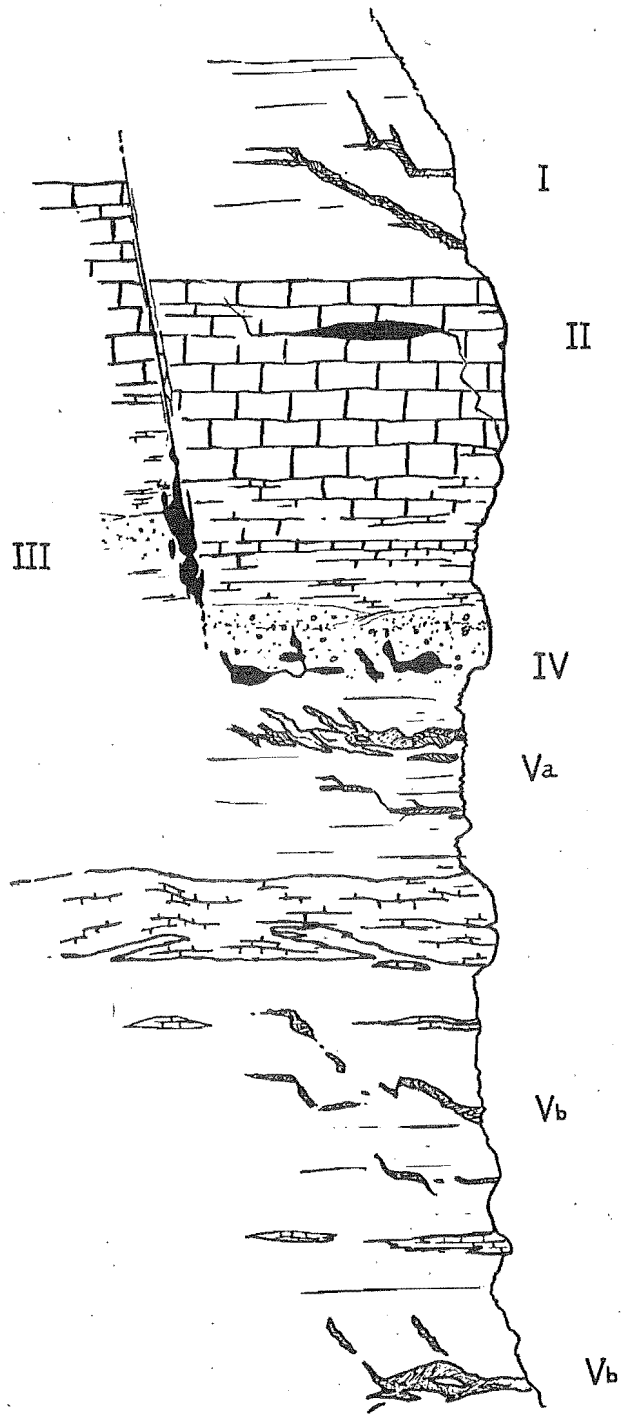

FIG. 5-1 Summary of distribution and classification of vein-associated mineralization at Mt. Owen. Base-metal veins are shown as solid black, gold-quartz veins are hatched.

I. Weakly auriferous quartz veins in Wangapeka Formation
II. Base-metal replacement orebodies in Arthur Marble (Welcome lode).
III. Base-metal mineralization of fault zone (Silverstream lode).
IV. Base-metal mineralization at the base of the Beilby Quartzite (Beilby's reef, etc.).
Va. Major gold-quartz mineralization in sericite zone of Owen Formation (Enterprise, Zealandia vein systems).
Vb. Lesser gold-quartz mineralization in remainder of formation (Murchison, Golden Crown veins, etc.).

I. BASE METAL VEINS

This group consists of a number of mineralized locations, exhibiting a pyrite-sphalerite-galena assemblage which is accompanied by minor chalcopyrite, generally high silver values, and moderate gold values. Of several known locations of this type, one is within the Arthur Marble, but the remainder all occur within a narrow zone immediately beneath the Beilby Quartzite and partly extend up into this unit. This zone marks a gradational contact between the sericite zone and the overlying quartzite. The rock is both carbonate-bearing and siliceous, but has an abundant sericite-chlorite content and a marked permeability.

(1) Emplacement

(a) Beilby's Reef. The northernmost occurrence is so named after the prospector C.S. Beilby, although the local name is 'The Rising Sun', after the name of the company which employed Beilby to drive prospecting adits. This is the best known base metal locality in the district, and is situated at 944944 among steep bluffs approximately 200 m south of Trig C. It is the only such deposit to be described by Williams (1965) who presents a brief description drawn from the reports of Park (1888), and from a more recent unpublished report prepared in the 1950's. Williams reports Park's silver assays at 12,300 oz/ton, which is misleading and possibly misprinted. Park referred to a

range of values from 12 to 300 oz/ton for samples from a number of base metal prospects in the area. Williams' description of the mineralization is as follows:

> 'Between the marble and the slates is a splintered zone of bluish schistose slate; this zone of fracture seems to extend several hundred feet below the marble contact, but silicification is most intense close below it, where a sparingly mineralized quartz occurs in the form of a stockwork occupying a complex jointing and shearing pattern.'

This description is somewhat misleading. Fracturing around the Beilby locality comprises faulting, brecciation, and shear zones with infilled tension gashes (see also Structure, Chapter III). Much of this deformation controlled mineral deposition which consists of open space fillings with some minor wall rock replacement, forming many small discontinuous stringers and veinlets which only rarely show thickening to more than 0.2 m. Some veinlets are parallel to bedding, and some are parallel to cleavage, while others occupy fractures and breccia zones which cross-cut both of these structures. It is probable that much of the 'silicification' mentioned by Williams refers to the Beilby quartzite, where the recrystallized chert-rich horizons closely resemble hydrothermal silica.

Similar deformation locates other base-metal localities along this stratigraphic zone, but poor exposure and difficulty of access impedes examination. A discovery was reported in 1888 south of Beilby's reef near Bulmer Creek, where some impressive galena specimens were collected and

leases taken out. The location has remained lost since the mining days due to thick vegetation and much talus and stream debris in the bottom of the valley, but probably represents a repetition of the Beilby's reef mineralization.

(b) The Silverstream Lode. A shallow shaft sunk near a stream which became known as Silverstream (now officially Baigent Creek) intersected base metal ore during the prospecting of 1888. This locality (919872) is at the southern extremity of the Owen Paleozoic rocks, in an area of structural uncertainty due to poor exposure. The mineralization appears to be associated with a major fault or fault zone, which is marked by a coarse blocky breccia in the streambed near the shaft (Figure 5-2). The ore textures also indicate a fault zone deposit which has been subject to considerable post-mineralization movement. Fragments of quartzite and sericitic material from the breccia and an obscure outcrop of highly cleaved and altered slate immediately east of the breccia suggest that a sliver of upthrown Owen Formation is now emplaced against the Arthur Marble and Wangapeka Formation which outcrop to the west.

Partial infilling and flooding of the shaft prevents access to the workings and few details of the exposed mineralization are available from records, but a linear lode structure may be assumed from the surviving descriptions of the orebody, which was grandly named 'The New Anaconda'

FIG. 5-2 A coarse blocky breccia near the shaft on the Silverstream lode, Baigent Creek. A north-south trending fault of major displacement apparently locates this mineralization, and the breccia contains blocks of quartzite and calcareous slate similar to the uppermost Owen Formation.

at the time of the excavations. The line of leases taken out to the north and south of the discovery is parallel to the trend of major vertical faults in the vicinity.

(c) The "Welcome" Orebody. A further discovery of the 1888 prospecting was a vein of massive galena outcropping in the gorge of Fyfe River (930898). The vein, described as being 14 inches (0.34 m) wide at the outcrop, appears to have been a tabular body which rapidly pinched out in all directions, located along a fissure parallel to the bedding in the Arthur Marble. The ore, which was highly argentiferous, has been completely worked out by outcrop workings and a short drive with up-dip stoping. Only thin veins of galena remain in the workings, but two large hand specimens of rich ore containing more than 80% of galena were found near the mouth of the drive. Very little quartz veining or fracturing can be found at this deposit, which appears to have formed principally by replacement of marble.

(2) Mineralogy

Good specimens displaying ore and wall rock characteristics were obtained from the three main localities described above. No chemical analysis of these ores was attempted, as the sulphide mineralogy was determined in polished section, and many assay results are available for the precious metal content.

The "Welcome" ore is distinct from all others, in both composition and textures. The mineralogy of this lode

is comparatively simple; massive, coarse-grained galena was accompanied by a little quartz, pyrite is restricted to traces in the lode margins, and sphalerite appears to have been absent. Minor covellite is present as films in galena cleavages and as small cubic inclusions. The specimen sectioned was probably from the surface workings, as a thin crust of supergene minerals is present on one face, therefore the covellite is almost certainly an alteration product of original chalcopyrite. Other supergene minerals include malachite, azurite, cerussite, minium, and traces of metallic gold (Figure 5-3). The restricted mineralogy, the coarse-grained ore texture, the scarcity of gangue minerals, and the nature of the host rock all indicate a replacement origin for this orebody.

Ores from the deposits located near the base of the quartzite show a consistent galena-sphalerite-pyrite assemblage, with chalcopyrite as a minor component. The Beilby's reef specimens are generally pyritic, but commonly show a dominance of one base metal sulphide in individual veinlets. Abundant quartz, chlorite and sericite are present as gangue minerals. Calcite veins are also present, but are unmineralized and are probably of supergene origin (see Chapter VI). Polished specimens prepared from veinlets around the Beilby's reef locality (PS 506) and in the basin further north all show sphalerite and galena replacing brecciated pyrite (Figure (5-4). Fracture infilling relationships indicate that galena, in part, post-dates sphalerite, and there is also evidence for much

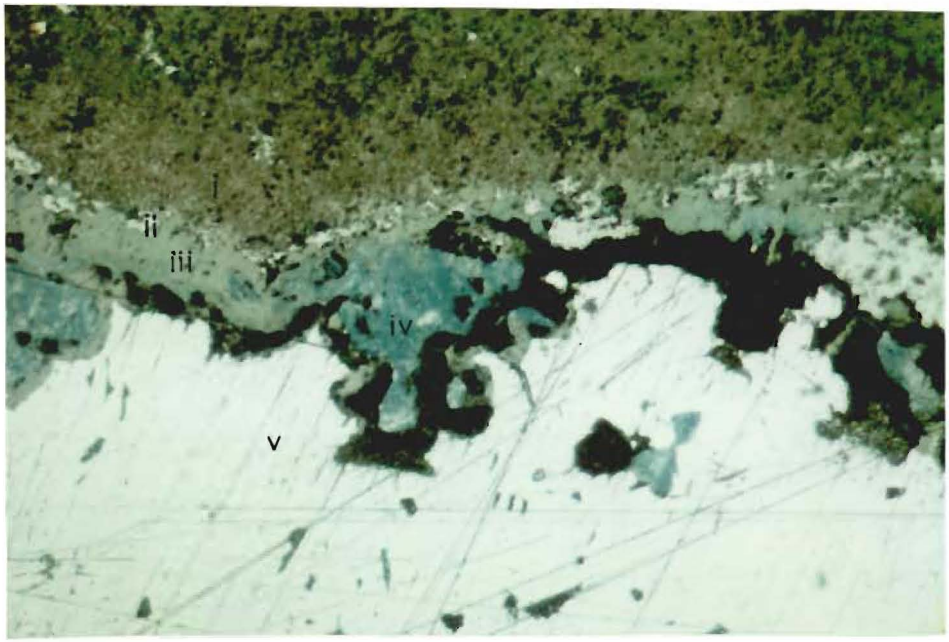

FIG. 5-3 A contact of massive galena and silicified wall rock from the Welcome orebody, Fyfe River. Zoned supergene alteration can be recognised, as follows:

(i) Silicified wall rock.
(ii) Hematite (discontinuous, bright).
(iii) Cerussite.
(iv) Covellite (blue). Dark areas are voids created on polishing, possibly the site of a friable secondary mineral.
(v) Unaltered galena, containing sparse patches of covellite.
Polished section (PS511), Ektachrome, ppl. x120 UC8886

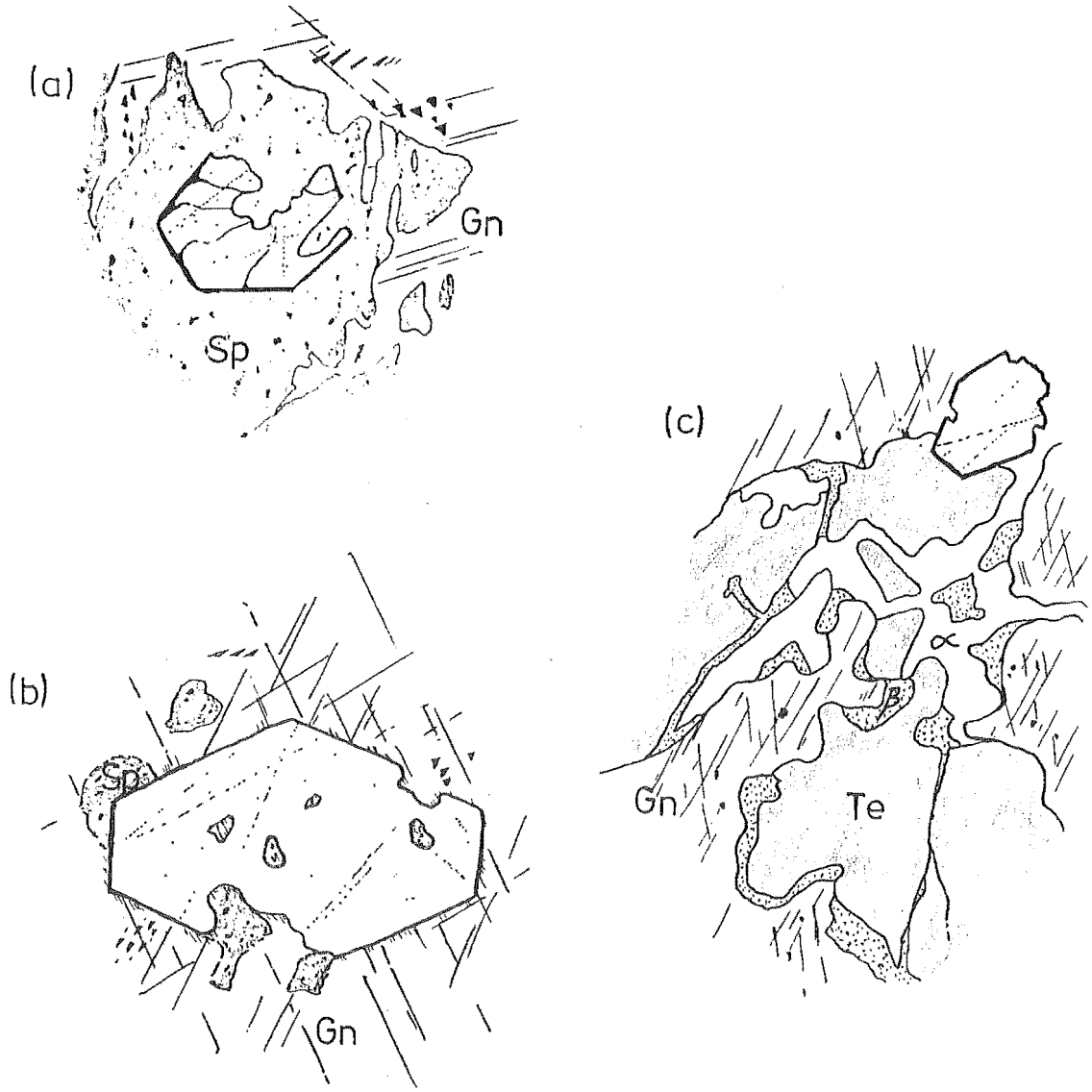

FIG. 5-4 Paragenetic relationships seen in the sulphides of the base metal ores.

(a) Pyrite (euhedral section) is partly replaced by sphalerite (Sp) which is in turn infilled and partly replaced by galena (Gn). A vein sample from the Beilby's Reef locality.
Drawn from a polished section (PS506), x100 UC8887

(b) The same sequence seen in the Silverstream ore. Some sphalerite and galena was included in the pyrite during growth, either by simple enclosure or by sporadic replacement.
Drawn from a polished section (PS503), x160 UC8888

(c) Complex relationships of unmixing and replacement involving minerals of the 'grey copper ores' (see text). A tetrahedrite (Te) infills and possibly replaces galena, and is accompanied by unidentified exsolved minerals $\propto$ and β. β is possibly chalcopyrite. Silverstream ore.
Drawn from a polished section (PS504), oil, x640 UC8888

contemporaneous deposition. The chalcopyrite is associated with the sphalerite, and shows textures which suggest, but do not prove, exsolution. Where wall rock replacement has occurred, fine pyrite appears to precede the deposition of the ore sulphides.

Similar evidence is shown by the ores of the Silverstream lode, which are more complex. Good specimens collected from a small dump near the shaft show the dominant sulphide to be galena. Microgranular sulphide textures and intermixed fragments of brecciated quartz and country rock indicate fault zone deformation.

The pyrite of the Silverstream ore shows some unusual characteristics in polished section. Crystal development as $\{111\}$ and $\{110\}$, and possibly combinations of the cube, $\{100\}$, and the pyritohedron, $\{210\}$, is indicated by the abundance of hexagonal and pentagonal cross-sections (Figure 5-5). These crystals also show large, rounded inclusions of ore sulphides near their centres. The structures are attributed to the enclosure of ore sulphide during an early, rapid phase of pyrite growth, followed by later recrystallization. This interpretation is supported by rare examples of pyrite showing a 'cruciform' core and included sulphides, and also skeletal cubes which enclose a large amount of sulphide matrix (see Figures 5-5, 5-6). These growth characteristics are apparently combined with replacement of pyrite by the surrounding sulphide. Thus the indicated orebody history is one in which pyrite grew

rapidly with contemporaneous deposition of sphalerite and galena, and was later partly replaced by these and other sulphides. The resulting crystal defects were rounded and partly eliminated by recrystallization. Later brecciating events caused some infilling and replacement by quartz, in a chemical environment in which pyrite was particularly unstable, as indicated by cubic quartz pseudomorphs in a base metal sulphide matrix.

Some of the minor mineral phases could not be identified by optical means, and electron probe microanalysis was employed in an attempt to obtain semiquantitative data on the composition of these minerals. Unfortunately, a shortage of time and defects in the analytical equipment prevented a proper study of the mineralogy, but sufficient information was obtained to indicate the presence of members of the complex 'grey copper ores'. The most abundant unknown mineral was tentatively identified as tetrahedrite from optical properties, although the hardness and reflectance lay outside the range of published values. Analysis showed the presence of copper, antimony, silver, and to a lesser extent zinc and traces of bismuth (Figure 5-7). The mineral is therefore almost certainly one of the fahlore group, and the classification as a tetrahedrite*

* According to Ramdohr, the fahlore group comprises the tetrahedrite-tennantite series, for which the basic member is considered to be Cu_3SbS_3, with substitution as follows: (continued over)

member appears justified. The mineral shows spectacular unmixing textures, with ?chalcopyrite and other phases forming exsolved rims and central inclusions. At least four mineral phases remain unidentified, some of which are illustrated in Figure 5-8.

Proper investigation of these minerals must await future work. It is clear, however, that the tetrahedrite has a high silver content, and probably comprises the principal silver-bearing mineral in these deposits. The tetrahedrite also appears to have been initially very rich in copper and antimony, both of which have unmixed on cooling or in response to substitution on cooling. The unmixing products include a rare, highly reflectant antimony mineral which may be native antimony.

* (continued)

Ag, Zn, Fe, Hg, Ni, Co	for Cu
As, Bi, Sn, Ge	for Sb
Te	for S

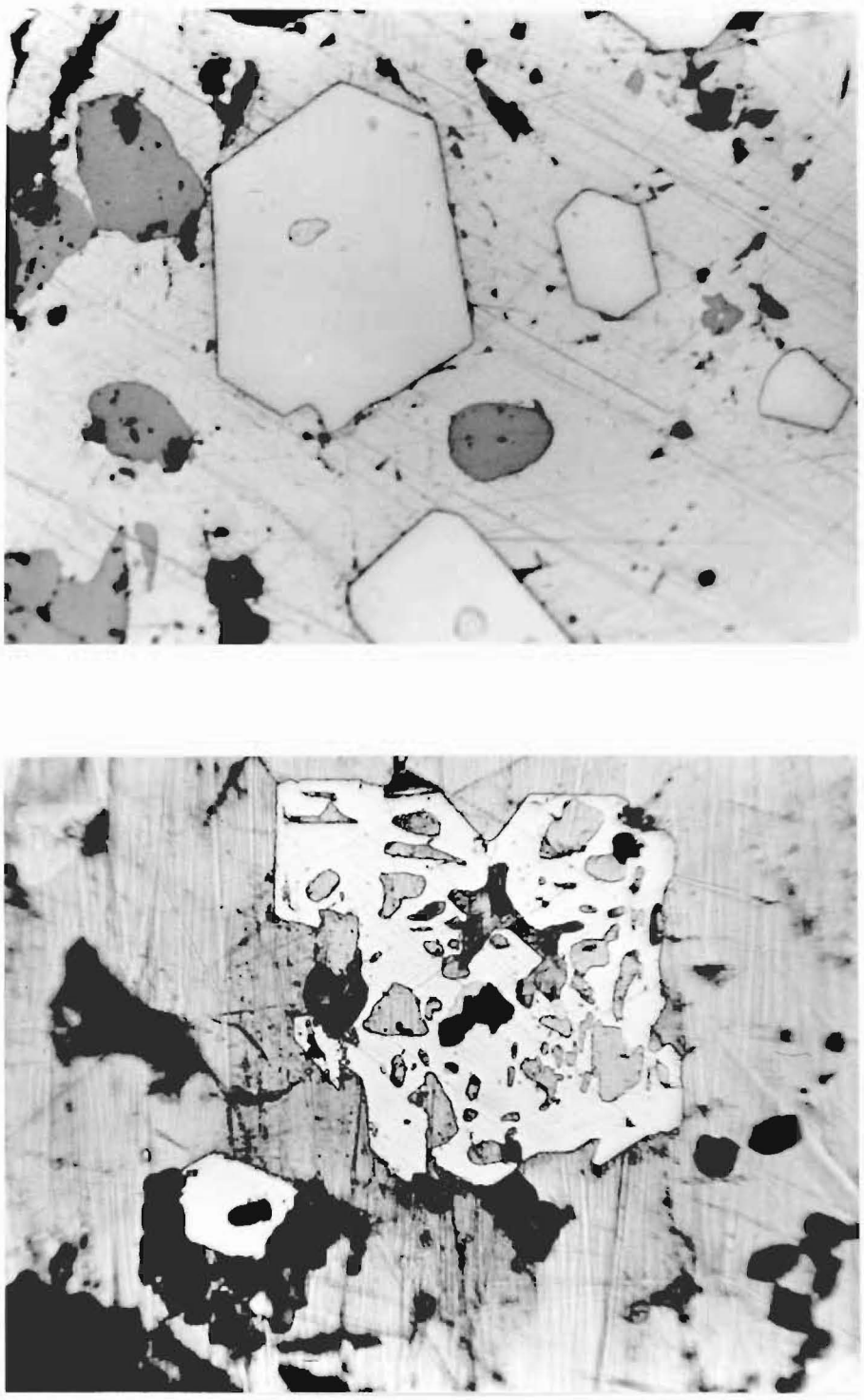

FIG. 5-5 Pyrite textures in Silverstream ore. UC8888

Upper: Euhedral pyrite enclosing ore sulphide blebs.
Polished section (PS505), ppl. x250

Lower: 'Skeletal' pyrite enclosing sulphide matrix. Some replacement is also evident.
Polished section (PS504), ppl, oil. x640

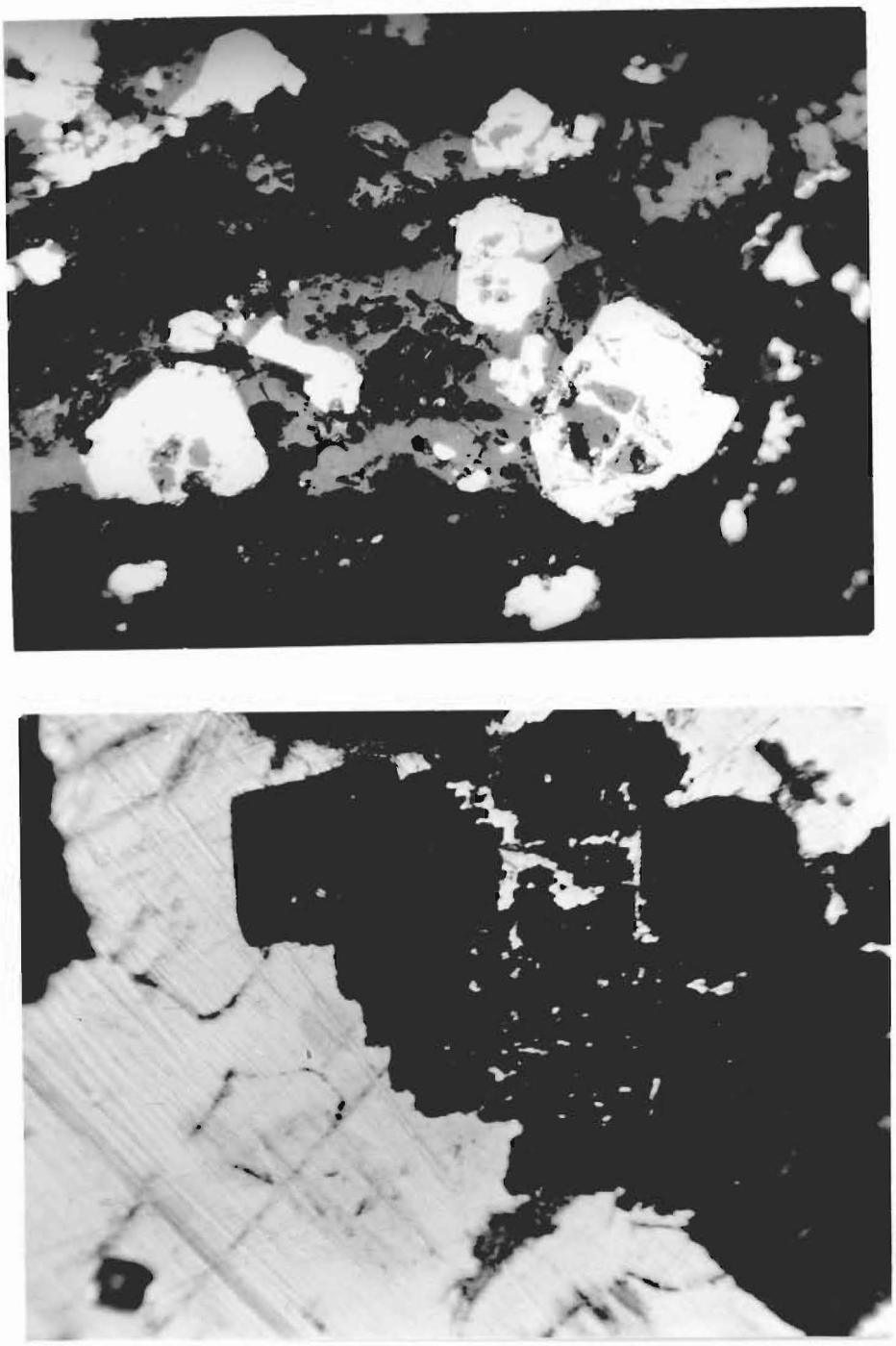

FIG. 5-6 Pyrite textures in Silverstream ore (continued).

Upper: The presence of rare pyrite with cruciform cores, enclosing and surrounded by sphalerite and minor galena, provides further evidence for an early stage of 'skeletal' pyrite growth. The resulting structures appear to have been infilled by the rapid deposition of other sulphides, followed by later idiomorphic growth to produce the euhedral rims.
Polished section (PS504), ppl, oil. x400 UC8888

Lower: Pyrite, which has been partly replaced by galena (light grey), has later been replaced by quartz (dark).
Polished section (PS504), partly xpl, oil. x400 UC8888

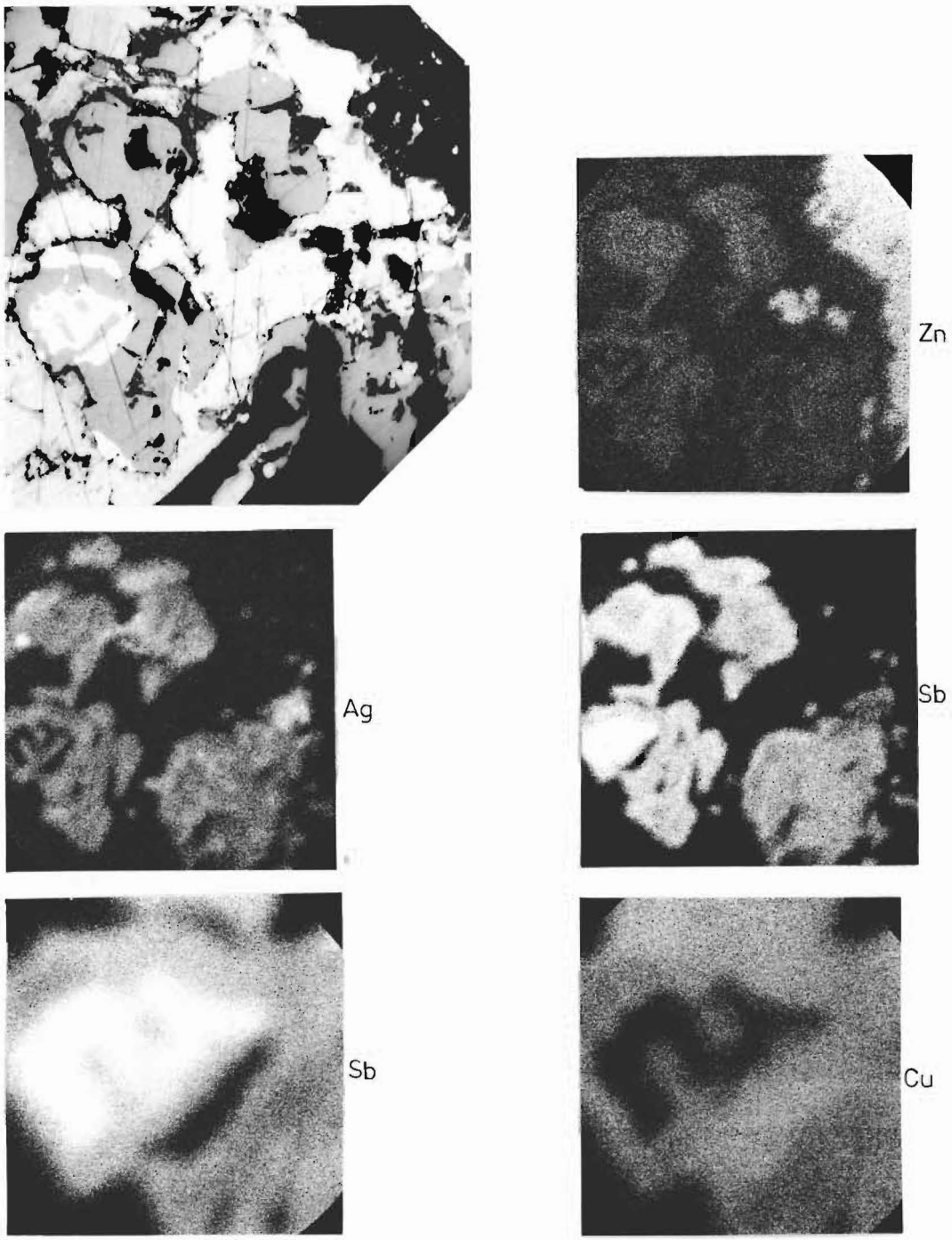

FIG. 5-7 Results of semiquantitative electron probe microanalysis of an inclusion of unknown minerals in galena of the Silverstream ore (PS 504, UC8888).

Top left: Optical photomicrograph. Note that the central mineral is of much greater reflectance than the galena (light grey mesostasis).
ppl, oil. x640

The other photographs are backscatter maps of the same field, recorded for the elements as shown above, from the display of a JOEL microanalyser. The two final maps (bottom) are greater magnifications of the highly reflectant mineral, which may be antimony metal.

The foreshortened perspective is due to the inclined take-off angle of the detector. Instrumental problems resulted in a poor resolution.

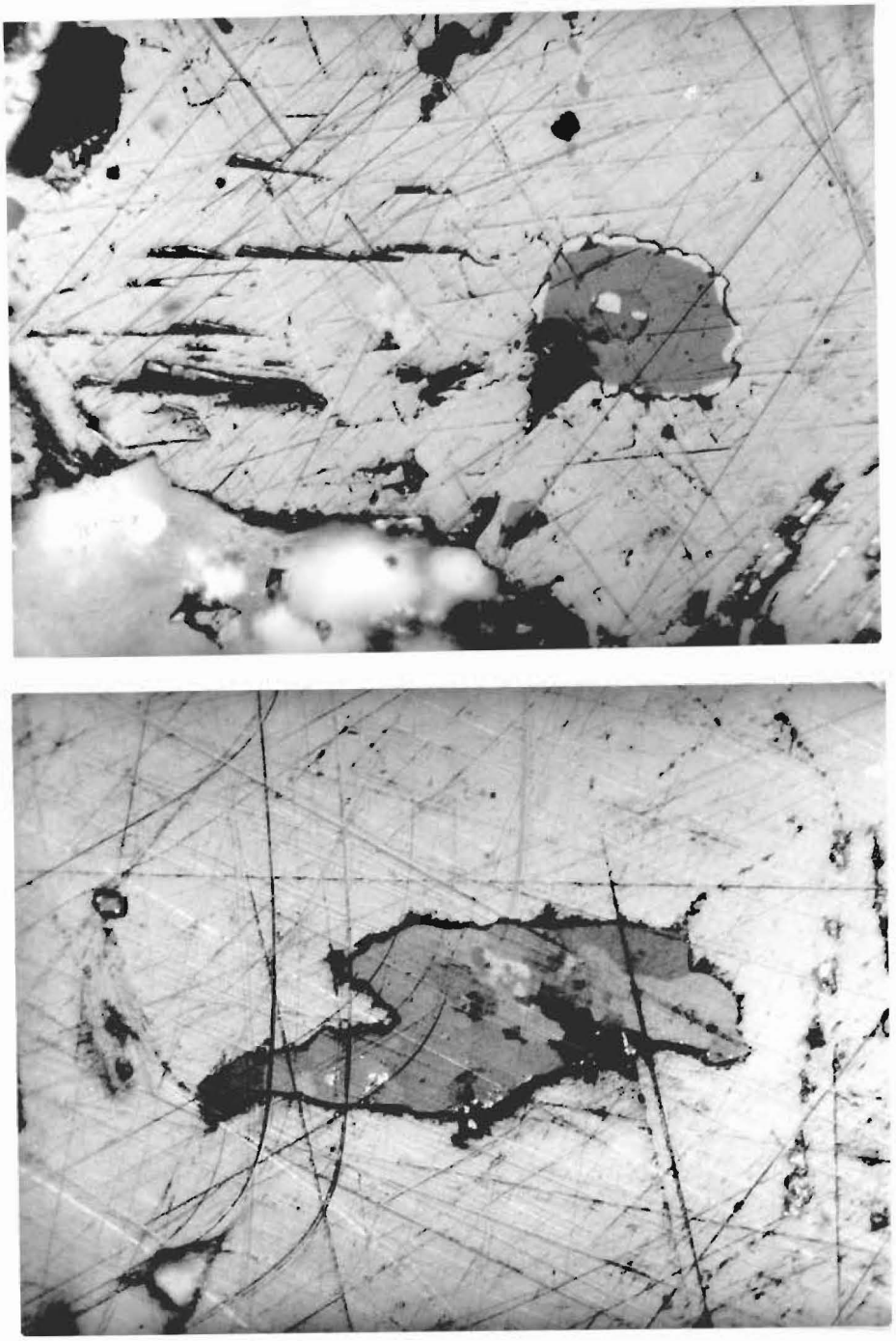

FIG. 5-8 Inclusions of unidentified minerals in galena of the Silverstream ore, showing unmixing textures. Unfortunately, the photographs had to be taken before a proper polish could be made.
Polished sections (PS 504), UC8888

Upper: Tetrahedrite (medium grey) exolved to produce both core and rim zones of two additional minerals, α (dark grey) and β (light grey, ?chalcopyrite). See Figure 5-4.
Partly xpl, oil. x640

Lower: Further unknown mineral species, some of which are strongly anisotropic.
Partly xpl, oil. x640

II. AURIFEROUS QUARTZ VEINS

These veins are distinguished as a separate group having a quartz or quartz-carbonate gangue, some degree of gold mineralization, no essential association with carbonate rocks, and a general absence of base metal minerals. Some overlap in the classification of these veins is represented by the pyritic, base metal-poor veins of the Beilby's Reef locality. The auriferous quartz veins do not intersect the Arthur Marble, but occur in the formations above and below this unit, and are thereby divided into two groups.

(1) Wangapeka Formation

The veins within this formation in the Owen Goldfield are substantially restricted to a relatively small area near the junction of Fyfe River and Frying Pan Creek. Vein occurrence diminishes abruptly to the west, and beyond Trig EH only rare, small-scale veins can be found. This distribution is reflected by the excavations of the early prospectors, whose shafts and trenches are found only in this small area.

The veins are open space fillings of quartz with sparse pyrite, some breccia zones showing more intense pyritic mineralization. The lack of fresh exposures prevents a complete analysis of the vein mineralogy. An examination of the surface outcrops and weathered, broken ore from prospecting excavations suggests that the mineralization is restricted to iron sulphides, quartz, and some

sparse carbonates. The host rocks show very little alteration, except where shearing at the vein margins brecciates mudstone. Gold mineralization of the veins is widespread but weak, although some values were sufficiently high to encourage trenching and driving.

(2) Owen Formation

The gold-bearing veins of this formation were the focus of attention during the days of prospecting, and formed the basis for the establishment of the goldfield. Veins are found throughout the unit, but show a variation in distribution and characteristics with host lithology. The zone between the Beilby Quartzite and the Enterprise Dolomite contains the highest density of veins, and is host to some very large lode structures such as the vein systems of the Enterprise, Zealandia, and Uno Creek mines. Veins below this zone are auriferous, but rarely contain workable values.

Weathering has made the collection of unoxidised vein samples difficult except where fresh material is exposed by streams. A number of old workings gave relatively good access to underground exposures, but in most cases sulphide and carbonate minerals showed considerable alteration after remaining exposed to a combination of air and groundwater for more than 85 years. Both vein structures and vein mineralogy were best exposed during the period of mining, but unfortunately the geologists who did visit the field at the time left only brief records of what they saw, and no specimen collections are known to have survived. The

reports of the freshly exposed veins and ores show the influence of contemporary attitudes to mining geology; descriptions were usually limited to accounting for the difficulties of mine working or poor gold recovery. These reports are, however, still considered to be a useful source of information.

(a) Vein Emplacement. Structural aspects of the veins are first mentioned in the Handbook of N.Z. Mines 1887, where earlier reports by W.C. Wright, a mining engineer, were drawn upon. A brief description states that the veins have well defined hanging-walls which contain the bulk of the gold, and are delineated by a 'slate selvage', while the foot-walls varied in orientation. The reports of Park (1888) and Hector (1888) provide more detailed observations on the exposed vein systems. Apparently Park introduced the concept of the veins being 'bedded segregations, having in all cases the strike and underlie of the country.' The intended meaning of the term segregations is unclear, but one may assume that Park wished to indicate a distinction from simple, planar infillings, as he continues, '....segregated veins, unlike true fissure-lodes are very uncertain in their behaviour in the direction of dip.' Hector examined the Enterprise workings, and described the vein system simply as an irregular vein without definite walls.

The degree of deformation impressed these early observers; Park recorded:

> 'All over the field the auriferous slates are much slickensided and broken, and the quartz

> itself encloses large bodies of slate, and frequently contains.... so much shattered slate as to seriously reduce the returns of gold per ton when calculated on the total quantity of stone put through the stampers.'

Similarly, Hector noted:

> 'The general feature of this part of the field (the Bulmer Creek leases) is the irregular and broken character of the reefs, both as to the direction and thickness.... They do not appear to run in continuous lines, but are displaced by frequent and extensive dislocations due to surface-drooping of the mountainside.'

These observations refer chiefly to the veins exposed in the Uno, Wakatu, and Enterprise mines, where both vein formation and country rock sericitisation is intense. These characteristics give rise to vein multiplicity, and at the Uno-Wakatu area, considerable slumping, causing displaced blocks of vein material. Shearing and replacement within the vein systems has caused the abundance of country rock inclusions and vein irregularity noted above.

The alteration and fracturing of the country rock has greatly accelerated the collapse of the workings at these mines, and also enhanced the alteration of exposed ores. An additional obscuring effect is the widespread precipitation of calcite on the walls of underground workings, due to the leaching of carbonate country rock and ores by supergene water. In some drives, 'cave pearls' exceeding 10 mm in diameter have formed since excavation. The only formerly producing mine in the sericite zone which remains accessible is the Enterprise. Entry to the workings can be gained only at the third or lowest level, where the vein was reported to break up into a number of separate struc-

tures, and yielded erratic gold assays which averaged to a poor value. No stoping was attempted at this level, but a prospecting drive towards the south has been constructed at the end of the tunnel, revealing only small veinlets. A winze connecting the second and third levels remains in good order, but the portals to all upper levels are slumped over. Removal of all the rich surface ore prevents examination of the original outcrop, thus exposure of the entire Enterprise vein system is limited to the single drive at level three. Although a large lode structure can be recognised, the margins are poorly defined, splaying out into small stringers which vary greatly in thickness. The characteristic of a well defined hanging-wall as noted in the Mining Handbook could not be recognised and may apply to a specific mine of the Bulmer Creek group, where there was much development work during Wright's visit of 1886. A number of shear zones sub-parallel to bedding can be seen in the Enterprise drive. Where these structures show post-mineralization movement some roof instability results, but where the vein material is continuous the workings are very stable.

Veins below the sericite zone are generally smaller and more clearly defined. The drive at the Murchison lease near the mouth of Bulmer Creek is still open, revealing a profuse array of small veins which are characterised by little development of either wall rock alteration or wall rock replacement. Infilling in response to shearing appears to be the dominant process of vein formation.

Post-depositional movement has been extensive, producing truncated veins and repeatedly 'stepped' or en echelon offsets. It is this widespread small-scale shearing which frustrated the efforts of the prospectors and miners. A great many trenches and prospecting drives can be found on the hillsides below Trig SP, where attempts have been made to follow veins and small leaders which pinch out or end abruptly. Similar reasons account for the failure of low level drives to intersect known lodes, in contradiction to measurements made at outcrop or at higher mine levels.

(b) Gangue Mineralogy. A report by Black (1887) is the first to describe the gold ores in any detail. He was impressed by the weathering characteristics of the lodes, and reported:

> 'Another peculiarity of the Owen stone is the extraordinary proportion of iron pyrites it carries at lower depths, to which air has not yet had free access. This mineral has been mostly oxidised to brown oxide of iron .... by the removal of which a cavernous, or vesicular, or rough porous character is impressed on the quartz, which with the rusty colour of the remaining oxide of iron, gives it an unusual appearance, and renders it easily crushed.'

Much of the porosity and oxide formation noted would be due to the decomposition of iron-rich carbonate, and it is surprising that this mineral was not distinguished from the quartz. Many Owen Formation veins, and especially those in and near the sericite zone, contain abundant ferroan dolomites and ferroan calcite, which weathers to produce masses of limonite and the rough porosity seen in near-surface quartz. Only Park noted the vein carbonates,

which he quoted as evidence for vein formation by downward percolation, stating; '.... and in support of this assumption it may be mentioned that in the claims immediately under, or near the junction of, the limestone the quartz is largely mixed with veins of calcite.'

The remainder of the gangue minerals consist of muscovite and chlorite, neither of which are mentioned in previous reports. Both are common, but achieve abundance only in the areas of intense alteration. Sericitic mica is very widespread, and is almost invariably present as an alteration product at vein margins and country rock inclusions. Larger flakes frequently occur at quartz and carbonate grain boundaries, often imparting a specular sheen which on casual examination can be mistaken for gold. Chlorite is less widespread, but plentiful in the principal veins where it occasionally forms platy green masses several centimetres in diameter and vermicular aggregates in quartz and carbonate. A more detailed examination of some gangue minerals is presented in Chapter VI.

(c) Sulphide Mineralogy. The vein sulphides are the minerals most severely affected by oxidation. In the absence of any recent excavation, great difficulty was experienced in obtaining representative samples for study. It is regrettable that at the time of mining the mineralogical examinations were so cursory and no permanent collection was retained. Black was content to describe the sulphides collectively as 'iron pyrites', but both Hector and Park, who visited the field during crushing, refer

indirectly to arsenopyrite. Hector confuses the Enterprise and Wakatu workings, but relates that in one of the mines 'the stone is highly charged with arsenical pyrites which decomposes to a blackish powder that has a strong smell.' Similarly, Park noted 'In the solid the quartz contains a large percentage of sulphide and arsenide of iron, and occasionally cupric sulphide.' In polished sections which contain fresh sulphides, no arsenopyrite can be recognised, nor can this mineral be detected by X-ray diffraction. The sections show sulphide masses consisting of pyrite in intimate combination with marcasite, closely resembling the disseminated sulphide blebs described from the country rock. Typical textures show crystals of marcasite arranged in radiating form about a dark, fine-grained, porous mass which does not polish and oxidises rapidly. The marcasite 'rosettes' lie in a mesostasis of pyrite which shows features suggesting marcasite inversion (Figure 5-9). The marcasitic sulphide is widespread and forms fracture infillings accompanying late-stage quartz, implying a low temperature hypogene origin. Cubic pyrite is not common in the gold ores, but is seen as small crystals at the margins of the sulphide masses (e.g. Figure 5-9b), suggesting that pyrite was formed partly penecontemporaneously with marcasite and partly by marcasite inversion. The fine-grained material is seen to be invariably marcasitic where the grains are large enough for optical determination, and everywhere shows a tendency to rapid oxidation; this material is therefore considered to consist of poorly

crystallized marcasite. The linear and segmented textures exhibited by some of these masses (Figure 5-10) may be due to early marcasite structures, now modified by recrystallization.

Semi-quantitative scans by X-ray fluorescence show arsenic to be present in the sulphide but at levels not exceeding a few hundred parts per million. As neither pyrite nor marcasite accept significant amounts of arsenic into their lattice structures, this element probably occurs either as a component of mineral inclusions which are too small to resolve, or concentrated in the microcrystalline marcasite, perhaps by recrystallization processes.

This study of the ore mineralogy, which is based on a limited amount of fresh sulphide together with much oxidised sulphide and associated pseudomorphs, boxwork structures and leached quartz, indicates that marcasite and inversion-derived pyrite form the principal sulphide minerals. Marcasite is known to oxidise more rapidly than pyrite, particularly when present in a very fine-grained form. Specimens which oxidise in this way commonly emit a strong smell. These characteristics, combined with the lack of cubic crystals, and indications of poor amalgamation may have resulted in a misidentification when the early geologists reported arsenopyrite. The reports indicate a general lack of concern for accuracy in identifying orebody minerals. The 'cupric sulphide' mentioned by Park may refer to either chalcopyrite or its supergene derivative covellite, both of which were seen to form

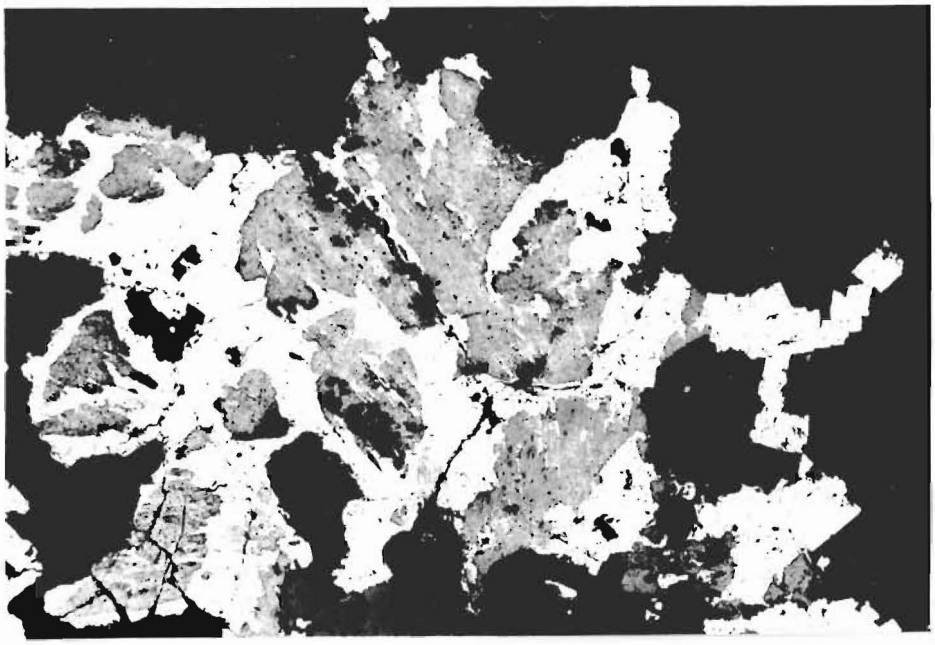

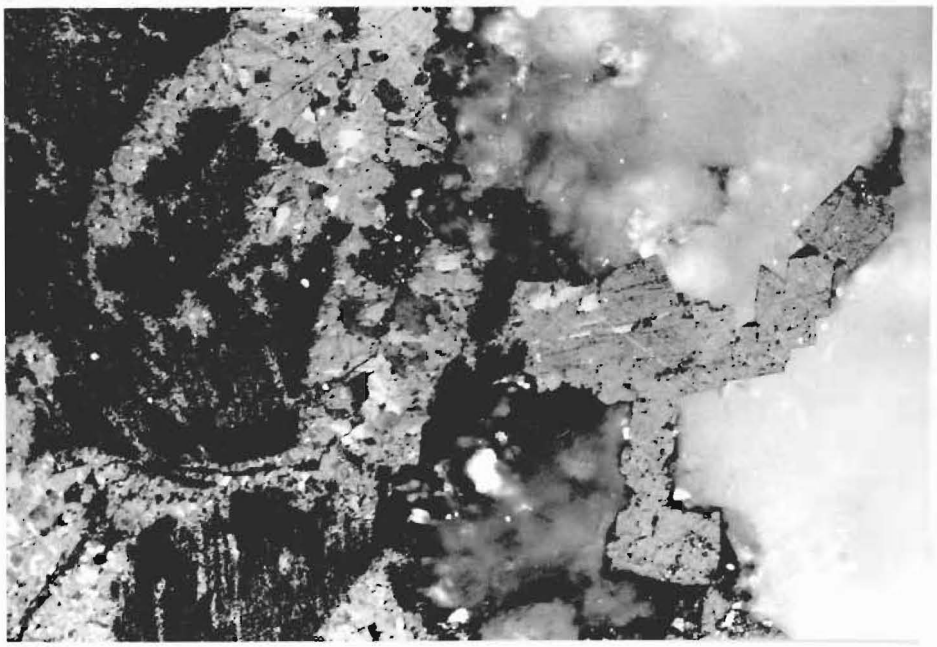

FIG. 5-9 Marcasite-pyrite sulphide in the auriferous quartz veins, Owen Formation. PS507, UC8894

(a), Upper: Sulphide textures typical of the late stage quartz veins. Patchy, irregular zones of poorly crystallized marcasite are surrounded by massive crystalline disulphide. The surrounding gangue is quartz. Polished section, ppl. x64

(b), Lower: Detail of the right-hand margin of the above field, as seen in cross-polarized light. The bulk of the sulphide is predominantly marcasite, except for the euhedral extremities where only pyrite exists. The cubic sections suggest penecontemporaneous growth of the dimorphs. xpl. x130

FIG. 5-10 Detail of the poorly crystallized marcasite. The cause of the planar fabric and segmentation is unknown, but may be inherited from early growth structures in the original marcasite, perhaps modified by strains induced by recrystallization.
Polished section (PS508), ppl. x64 UC8895

small veinlets (1-2 mm) in association with the iron sulphides. Rare grains of sphalerite and galena were also found, associated with a quartz-calcite gangue.

(d) Native Metals. The only notable distinction of the Owen Goldfield in the mineralogical literature is in providing New Zealand's sole record of in-place native bismuth (Morgan and Bartrum, 1913; Williams, 1965). This was first reported by the dominion analyst, from amalgamation tests on quartz samples collected by Hector during 1886, the results being announced in the 22nd Annual Report of the Colonial Museum and Laboratory (1887), and independent publications (Skey, 1887, 1888a, 1888b). The metal was apparently identified only in bullion alloys from amalgamation tests, such as the 'bismuthic gold' described and exhibited by Skey in 1888, when the following analysis was given:

Gold	78.41%
Silver	5.62
Bismuth	14.81
Copper	Traces
Loss	1.16
	100.00

After Skey's publications, no further reports of Owen bismuth are known other than references by other authors to Skey's work. Considerable confusion is evident as to whether bismuth occurred as a true bismuthic gold*, or

* It is now known that the maximum solid solution of Bi in Au is <1% (Wise, 1964).

associated with gold as a discrete metal.

X-ray fluorescence analysis of some Owen ores indicates that bismuth concentrations are low. Three vein samples were carefully checked against standards, producing the following results:

Sample	Location	Bi, ppm
LS-01	North of Beilby's reef, near Trig C.	72 ± 10
LS-04	Pyritic vein, Wangapeka Formation.	< 15
LS-08	Pyritic Enterprise ore.	<15

The high value for LS-01 reflects the base metal influence, and is not unexpected. The other samples have levels which are below the detection limit of the analytical method. Similar analyses of alluvial gold and stream sediment concentrates from near the lodes failed to detect any bismuth, even when the grains were mounted and sectioned to expose fresh surfaces. Small flakes of a soft, white metal were found, which on analysis proved to be lead. These flakes were scarce in number but were consistently found with gold in situations which indicated that an artificial origin was most unlikely. A single grain of gold was found which showed adhering particles of a malleable material identical in appearance to the lead, but unfortunately the specimen was lost before determinative tests could be made.

Nuggets of native lead, bearing fragments of gold were collected from the Collingwood district and described by Skey (1889), soon after the last reports of the Owen bismuth. It appears probable that Skey mistook lead for

bismuth in the Owen samples, particularly if the identification was based on the very small sample described in the initial announcement (Skey, 1887). The test reactions of the two metals are very similar, especially with respect to oxidation and solubility in nitric acid.

There is considerable evidence for hypogene enrichment of the Owen gold-bearing veins, giving rise to native metals. Much of the gold taken from near-surface zones was obviously due to such enrichment, as indicated by assay values and some petrological data (see below). The lead is almost certainly of supergene origin, as are the traces of native copper noted by Hector. The same author observes that open face and outcrop workings at the Enterprise mine gave a 'foul amalgam' which he attributed to bismuth on the basis of Skey's determination. Such surface ores would be host to any native metals in the orebody. The existence of native bismuth in this situation is doubtful, the usual occurrence for the metal being primary hypogene. At this level of investigation, the presence of metallic bismuth or gold-bismuth combinations cannot be disproved. From the available evidence, however, confusion of this element with lead appears to be the best explanation.

Hector carefully recorded the extraction process at one of the Owen batteries, visiting the plant soon after crushing began. From the discharge of the stampers, a concentrate was collected on blanketed tables. This material was periodically collected and re-tabled, and finally ground in berdens with mercury. During this grinding, a fraction of

the concentrate was removed by stirring with a large magnet. Samples assayed from various stages of this process (Table 5-1) show high gold values for most fractions listed as being separated by a magnet, and particularly for the portion separated during berdanning. An almost equal amount of mercury accompanied the gold, and indications of 'bismuth' varied proportionately with the gold. These associations may be easily accounted for in terms of the escape of partially amalgamated gold, lead, and possibly mixed particles of the two metals.

The reason for the occurrence of a magnetic concentrate is not clear. It is difficult to account for a magnetic mineral in the ore; pyrrhotite, or fine-grained magnetite as a pyrrhotite alteration product would have these properties, but are unknown in the ore specimens. Hematite and limonite accompany the enriched gold, but could not be separated from the ore with the low-intensity magnets available at the time of crushing. Hector does not describe the magnetic concentrate, nor indicate what proportion of the ore it represents. The only source envisaged for this fraction is the abrading cast iron of the crushing and amalgamating machinery, which could be expected to produce sharp splinters and flakes which may have gathered particles and coatings of the soft, malleable native metals.

A further native metal may be listed if the suspected native antimony in the Silversteam ore is included. This occurs as minute inclusions (Figure 5-7) exsolved from

tetrahedrite, and would therefore be of hypogene origin. Without further microanalysis, the identification is uncertain.

RESULTS of ANALYSES of SEVEN SPECIMENS of SLIME, &c., from the Wakatu Mill.—Lab. No. 4777.

Lab. Sub-no.	Particulars of Sample.	Gold per Ton.	Remarks.
1	Slime after berdannings, considered as waste	1dwt. 14gr. ..	Traces of mercury.
2	Magnet cleanings after berdanning	..	Good indication of mercury and good reaction of bismuth.
3	Magnet residue after berdanning, top-blanketing	Gold found not enough to weigh	Sample too small to allow a good weighing of gold.
4	Magnet cleanings before berdanning, from top-blanket washings	Several small specks of free gold	Ditto.
5	Magnet residue, top-blanketings before berdanning	1oz. 12dwt. 12gr. ..	Mercury nearly 2oz. per ton.
6	Waste removed by magnet during berdanning	39oz. 19dwt. 12gr.	Mercury 36oz. 8dwt. per ton; bismuth approximately ½oz. per ton.
7	Residue after washing top-blankets	1oz. 6dwt. ..	Mercury easily found.

TABLE 5-1 Descriptions and analyses of samples of quartz taken from various stages of treatment after crushing at one of the Owen batteries. The samples, collected by Hector during his visit to the field, were probably taken from the Enterprise battery, not the 'Wakatu' as stated. The analyses were compiled by W. Skey, dominion analyst, who had previously announced the discovery of native bismuth. Considerable loss of mercury and partly amalgamated gold is indicated, although the fraction of the total throughput these concentrates represent is not given. (From 23rd Annual Report of the Colonial Museum and Laboratory, 1888.)

III. GOLD MINERALIZATION

(This section refers to the veins of the Owen Formation only)

(1) Alluvial Gold

Due to the scarcity of visible gold in the vein ores, alluvial gold was collected for study by panning in the Owen River, a few hundred metres below the Enterprise mine. Sediment from crevices in the exposed bedrock at the banks of the stream was panned to a heavy concentrate, which was further concentrated in the laboratory by panning with a watchglass, followed by drying, magnetic separation, and hand picking under a binocular microscope. This treatment provided a large number of gold grains and also the lead flakes previously described.

(a) Morphology of Gold Grains. Approximately 10% of the gold particles showed smooth faces, often comprising partial or complete crystal forms. Several near-perfect crystals as octahedra and elongate rhombdodecahedra up to ca. 2 mm in length were found, with some larger grains showing indications of this form but obliterated by the growth imperfections and abrasion (see Figure 5-11). The preservation of fine detail and smooth surfaces on some of the smaller grains indicates that at least some of the gold was transported in larger, protective host mineral grains which have since been broken down and removed by solution. The sediment which yielded both the unabraded gold and the lead flakes was collected from deep streambank crevices;

limonite accumulation and partial cementation indicated decay of sulphides and a long period of undisturbed repose since active transport. Some limonite adhering to the gold showed crystalline pseudomorphs, apparently reflecting an original iron sulphide host (see Figure 5-11 h).

(b) Composition of Gold Grains. The unabraded grains showed considerable variation in colour when compared with the abraded grains, which showed little variation. A number of different coloured grains were examined in polished section, which revealed that many had a thin rim which was more densely coloured than the grain interior (Figure 5-12). The differences in depth of colour were interpreted as being due to a variation in silver content, a characteristic confirmed by scanning the sectioned grains with an electron probe microanalyser. For two grains which showed this inhomogeneity, semiquantitative count rate scans were made, indicating a composition of 20 wt. % and 31 wt. % Ag respectively for the grain interiors (see Figure 5-13). This estimation must be regarded as approximate, being based on simple count rates without standardisation or absorption correction, and by assuming the grains to consist of only gold and silver. Proper quantitative analysis would also require a higher degree of surface polish.

The gold-rich rims are almost certainly due to silver depletion of the outermost surfaces by oxidation processes. Such characteristics are known from many examples of weathered argentiferous gold as described by Edwards (1954),

and investigated by microanalysis and discussed by Desborough (1970), and Desborough *et al.* (1971).

These analytical results suggest that some of the metal will fall into the class of *electrum*, for which the minimum silver content is variously defined as 18% (*Dana's Textbook of Mineralogy*), 20% (*Handbook of Geochemistry*, VII pt III), and 30% (Ramdohr).

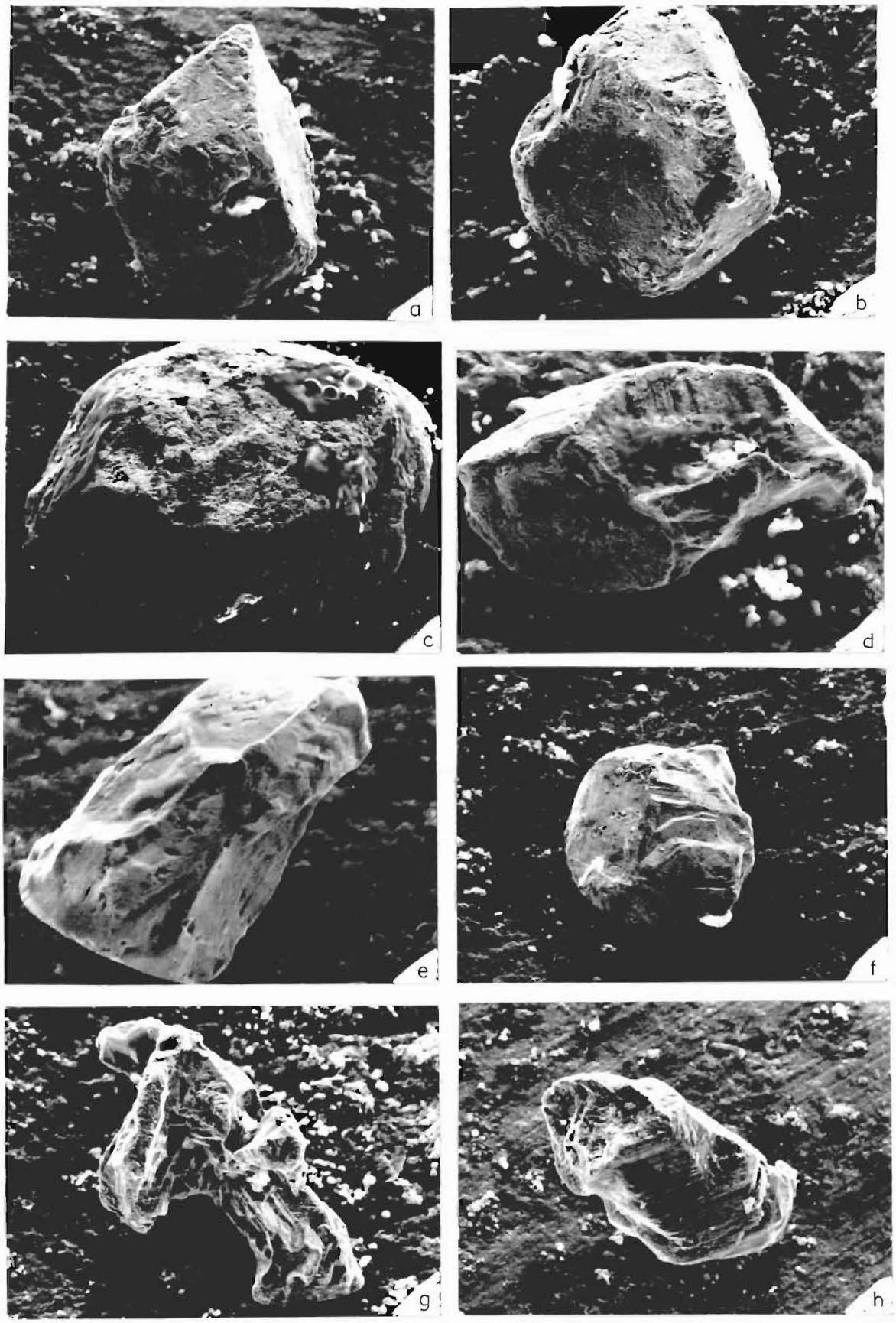

FIG. 5-11 Crystalline alluvial gold grains, photographed with a scanning electron microscope. UC8896

(a), (b) Octahedra.
(c), (d) Elongate rhombdodecahedra.
(e), (f), (g), (h), grains showing some crystal structure of uncertain form. The grain in (h) is surmounted by a remnant of limonite which pseudomorphs crystalline sulphide. a,b,f,h; x90 c; x60 d,e,f; x130

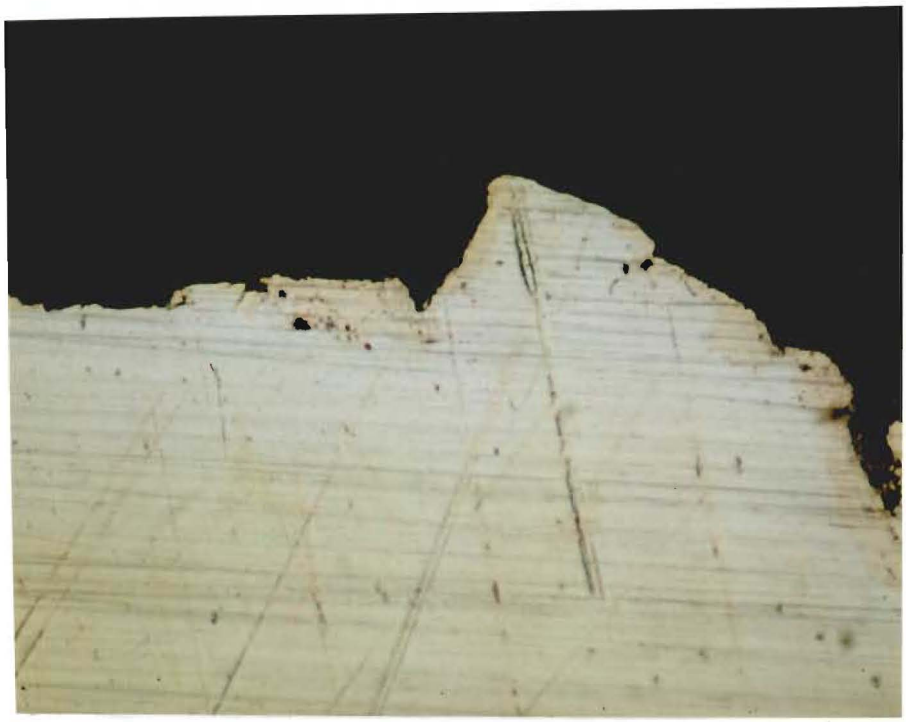

FIG. 5-12 The edge of an alluvial gold grain in polished section. The more densely coloured rim is due to supergene silver depletion. Some porosity in the grain appears to be essential for significant penetration of the depletion process. Such porosity may be either an initial depositional texture or a property induced by abrasion.
Polished section (PS509), Ektachrome, ppl, oil. x500

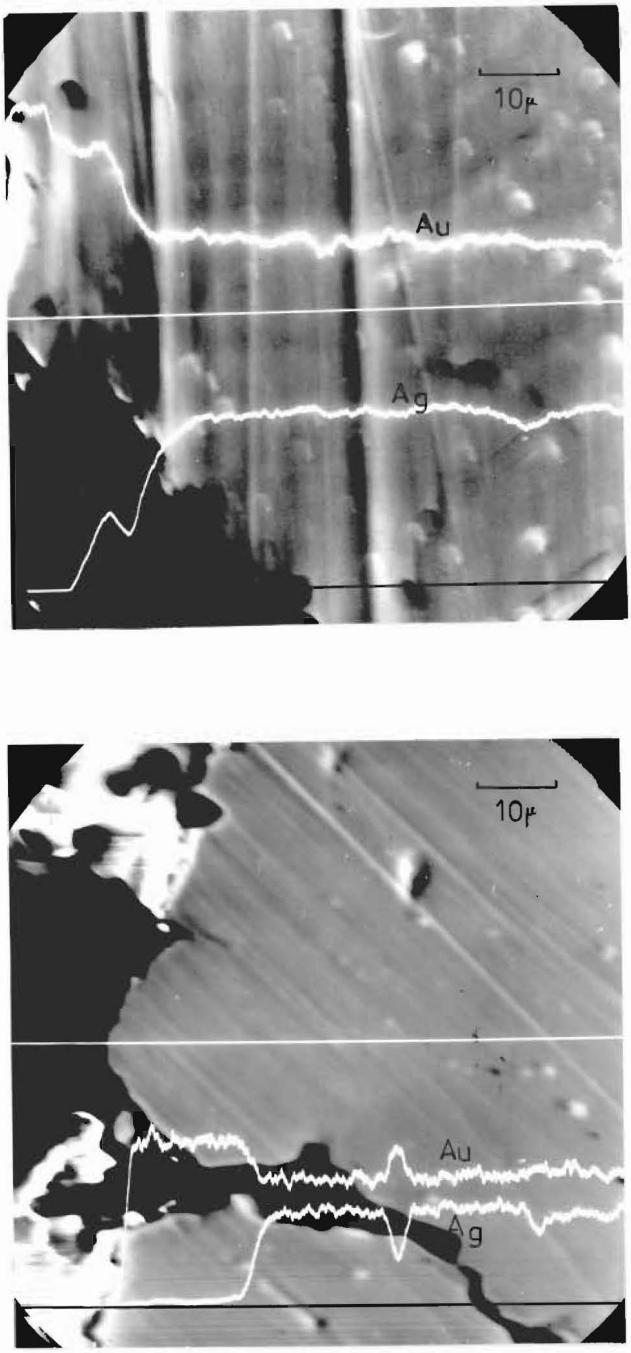

FIG. 5-13 Confirmation of silver depletion by electron probe microanalysis. Graphical displays for microanalyser scans across the edge zone of sectioned gold grains, showing results for gold and silver. An antipathetic relationship is clearly shown. The straight white lines mark the scan paths, and the black lines indicate the base line for the count rate traces. PS509

(2) Gold in Veins

Although a large amount of quartz was examined both in the field and in the laboratory, only two specimens were found to contain visible gold. A very small particle was seen in the rim of secondary minerals of the galena specimen from the Welcome mine, and is probably of supergene origin. Some larger particles accompany iron sulphides in massive vein quartz from the Owen Formation (sample LS-24, a large stream boulder near the mouth of Bulmer Creek, see Figure 5-14).

These larger grains show imperfect crystal sections, and may represent the source of the crystalline gold in the stream sediments. Iron sulphides form the surrounding host mineral, which would provide protection for the smaller gold grains during transport, later weathering away to leave undamaged crystal surfaces preserved.

Some uncertainty remains regarding the paragenetic relationship between the gold and the host sulphide. The ore specimen is partly weathered, and the gold grains are seen to be associated with pores or voids, and surrounded principally by limonite. The host sulphide is marcasitic pyrite which has probably undergone considerable marcasite inversion. The ore is, therefore, typical of the sulphide-bearing Owen Formation quartz as described, except for the presence of the gold and a small amount of chalcopyrite and its supergene derivatives. Some gold-iron disulphide contacts remain, showing smooth boundaries which continue

into the zones of gold-hematite contact. In addition to the subhedral gold grains, anhedral gold is present as small veinlets which project from the grain surfaces into the surrounding sulphide, and also minute 'lumpy accretions' on the otherwise smooth grain margins.

There is very little authoritative literature available regarding the processes of particulate gold deposition. Various authors infer the growth of crystalline and argentiferous gold to be a medium to low temperature hypogene process (Petrovskaya, 1971, Desborough et al., 1971), and this is also suggested by Boyle (1968), who studied the occurrence of silver. From observations on a number of Russian gold-bearing ores, Petrovskaya postulates the association of simple gold crystal forms with deposition at great depth, the crystals showing progressively greater complexity and a higher silver content with formation at shallower depths. An entirely supergene origin for the Owen gold crystals is therefore considered unlikely, especially as the microanalysed argentiferous grains have homogenous interiors.

Supergene gold deposition cannot, however, be completely discounted; surface quartz enrichment has definitely occurred to some extent as shown by old assay values. Furthermore, the evidence of the native lead and copper indicates supergene metallogenesis. The anhedral 'additions' to the crystalline gold grains may have such an origin. Late supergene attack and removal of gold is

revealed by the presence of corrosion cavities (Figure 5-15), which probably developed in the oxidising environment prevailing during the formation of the nearby limonite. Gold removed in this way could presumably be reprecipitated on nucleating centres provided by gold particles in the reducing zone. Careful specimen polishing and further microanalysis may resolve this uncertainty.

On the basis of the available evidence, a late stage, low temperature hydrothermal origin is assigned to the gold grains. The gold has been deposited either contemporaneously with the marcasitic pyrite as open space fillings in the quartz, or deposited after the sulphide by replacement. The association of gold grains with the pores and voids seen in polished section supports both origins, and it appears possible that both processes of hypogene deposition operated during orebody formation. The small gold veins near the margins of the grains have definitely formed by replacement, but as suggested above, this may be supergene.

(3) Gold in Rocks: The Search for a 'Carlin-Cortez' Deposit

During the early stages of field work for the project, the writer was impressed by the possible existence at Mt. Owen of the characteristic features of what is now termed a 'Carlin-Cortez' gold deposit. This term is taken from the name of two large gold mines in northern Nevada, established in the 1960's to exploit large orebodies con-

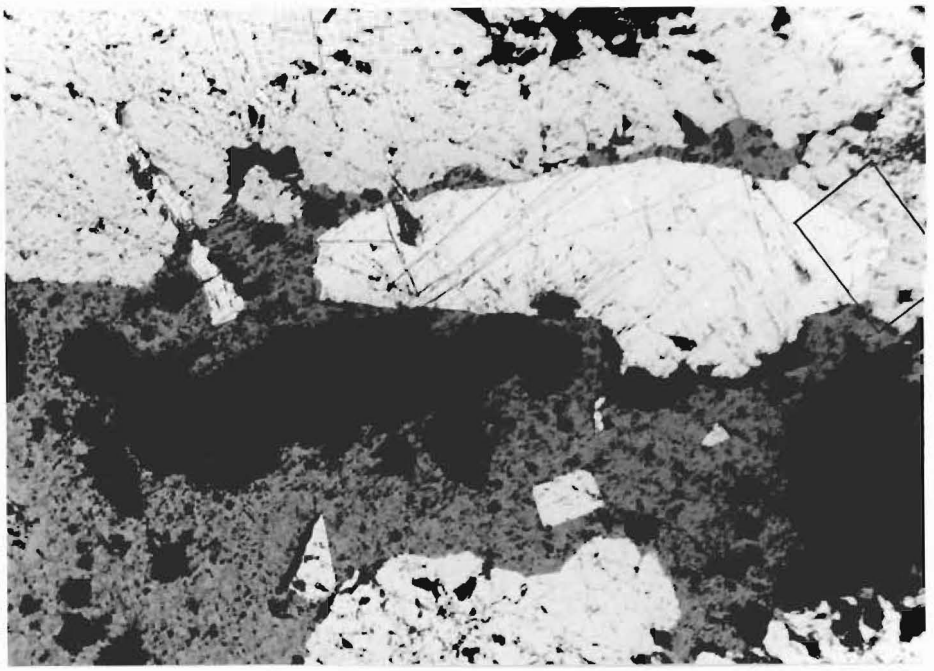

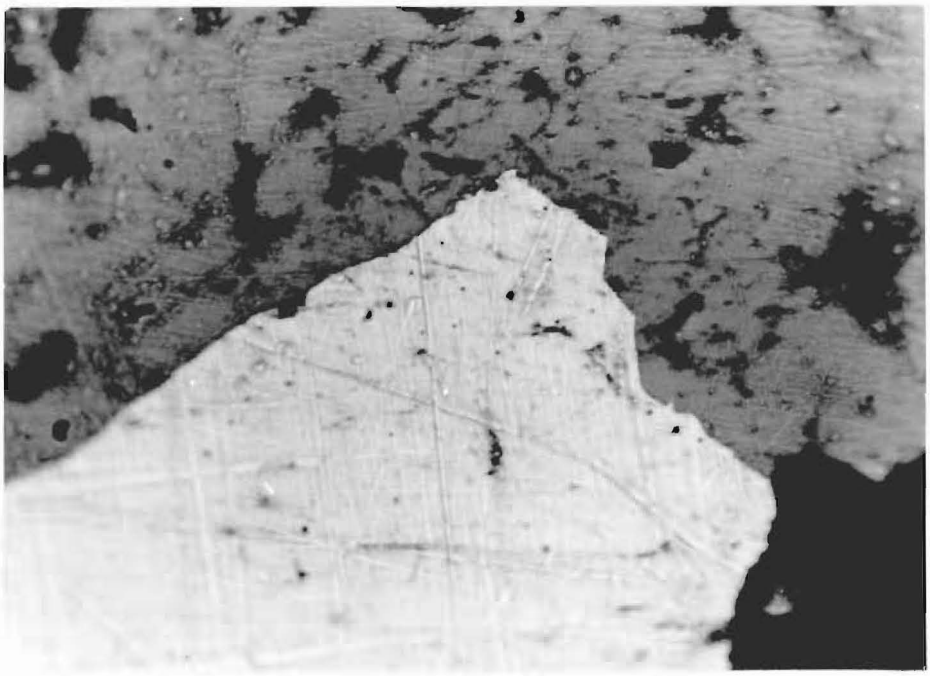

FIG. 5-14 Gold (white) in marcasitic pyrite (light grey) and supergene limonite (dark grey). The gold shows an overall subhedral outline (upper) and also some 'lumpy' anhedral areas and veinlets which appear to be later additions to an original crystalline grain. Where a gold-sulphide boundary is preserved (lower), smooth crystalline faces can be seen.
The sample is from a stream boulder resting in the bed of Bulmer Creek. PS508, UC8895

Upper: Polished section, ppl. x250

Lower: Detail of above (indicated), ppl, oil. x1400

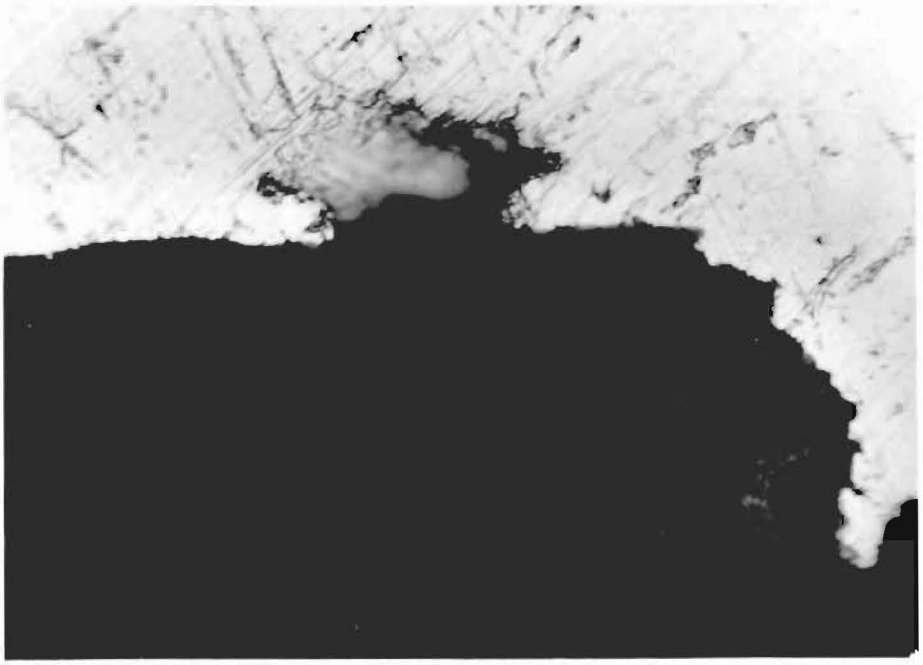

FIG. 5-15 Detail of the margin of the gold grain shown in Figure 5-14. A corrosion cavity in the gold is not infilled by limonite; locally strong acid oxidizing conditions are inferred. PS508, UC8895
ppl, oil. x1400

taining workable concentrations of disseminated gold in epithermally altered siltstones and limestones. Micron to submicron sized gold particles occur in the rock, with accompanying enrichment in metals such as Sr, Ba, Cu, Sb, and Hg. A complete description of the Cortez deposit can be found in Wells et al. (1969), and a similar treatment of the Carlin deposit in Radtke and Sheiner (1970) and Radtke et al. (1972). The two deposits differ in some aspects of lithology, but the essential characteristics are as follows:

(i) Proximity to intrusive igneous bodies which constitute the source of the hydrothermal alteration.

(ii) A zone of 'bleached' sediments as a result of widespread hydrothermal alteration.

(iii) The presence of carbon in the host sediments prior to alteration. This carbon is partially or completely lost by oxidation processes during alteration in the bleached zone.

(iv) The presence of dolomitic carbonates in the host rocks.

(v) The existence of both stratigraphic and structural controls. (A massive limestone body forms a capping to a bleached zone at the Cortez deposit).

(vi) The introduction of iron sulphides into the host rock.

(vii) Enrichment by Au, Ag, Sr, Ba, and various transition metals.

The coexistence of many of these characteristics at Mt. Owen in a situation closely resembling that of the Nevada orebodies suggested the possible existence of an auriferous horizon.

(a) Methods. The discovery of mineralization of this type can be achieved only by the recognition of geochemical anomalies, as described by Warren and Hajek (1973), who also used biogeochemistry with some success. A small-scale geochemical search program was included in the project to test the possibility of gold enrichment at Mt. Owen. Due to the limitations of laboratory time, the decision was made to analyse directly for a gold anomaly, with reconaissance sampling of the most favourable lithologies. Rock samples were collected from several horizons within the Owen Formation, one from the main body of the marble, and two from the Wangapeka Formation. All possible care was taken to avoid including obviously mineralized material from the samples. At some locations, this was difficult due to the abundance of small veinlets.

Sample preparation consisted of fine grinding, and roasting to decompose sulphides. Some research was spent in selecting the optimum analytical method, and the results of this are presented as Appendix II of this report. To determine the very low levels of gold in rocks, radiometric methods such as neutron activation or isotope dilution are commonly used. As these methods require sophisticated equipment which is not locally available, a procedure based

on atomic absorption was devised. The essential features of this procedure are:

(i) Sample attack and digestion by aqua regia.

(ii) Analyte concentration from a large sample (50-100 grams) by solvent extraction, using methyl isobutyl ketone (MIBK).

(iii) Determination by atomic absorption, calibrated by means of internal standards ('spiking') to overcome interferences and non-atomic absorption.

(b) Results. With careful operation, gold concentrations in the order of 10^{-3} ppm* may be successfully measured with the method used. Forquartz-rich rocks containing few acid-soluble components, standardisation is simple, but where large amounts of the sample pass into solution some difficulties are encountered with non-linearity, non-atomic absorption, and also with the solvent extraction process.

When this work was commenced, the planned sampling and analytical program was much more extensive than the work subsequently carried out. Regrettably, the time involved in processing the samples proved excessive, and the program had to be severely contracted. The need for improvements to the extraction method for samples containing a high carbonate, iron, or other heavy metal content was indicated, and such improvements are recommended in Appendix II. Some

* To avoid confusion of U.S. and U.K. billions, concentrations are quoted in parts per million throughout.

of the high values reported from the highly calcareous samples may be erroneously enhanced due to the difficulties described above, and should therefore be treated with caution; planned reanalysis to check for errors was not possible. Values for slates and quartzites are presented with greater confidence. Repeat analyses for some of these samples indicate a reproducibility to within an error of 0.0004 ppm at gold levels ca. 0.003 ppm. A summary of the results appears in table 5-2.

The establishment of background values is difficult, mainly due to the lack of accurate data on the gold content of rocks. DeGrazia and Haskin (1964) quote values for a number of different rocks and recent sediments (table 5-3) and show that a relatively restricted range of concentrations occurs for most materials except where significant inhomogeneity affects detrital sandstones. Warren and Hajek used a background of 0.005 ppm for soil samples from an area of volcanic arenites and mudstones in British Columbia. The concentrations indicated by the Wangapeka Formation samples and the unaltered mudstones of the Owen Formation suggest that a similar background could be applied to the Mt. Owen area.

Without further analyses, it is difficult to establish whether or not the higher values indicated at and near the sericite zone constitute a gold anomaly. This difficulty is due in part to the necessity of sampling a sequence of layered rocks of widely differing composition, and by the

fact that any widespread alteration probably occurs parallel to this layering. Some uncertainty must remain regarding the validity of the high gold results in Table 5-2, although it is unlikely that all the values are exaggerated to the extent by which they exceed the lower background indicated by the other samples. From a consideration of the characteristics of the mineralization and alteration at Mt. Owen, and by comparison with the known Carlin-Cortez deposits, the permeable horizons near the base of the marble comprise the most probable host for disseminated gold mineralization. In conclusion it can be stated that a gold-enriched zone may exist, but no such zone of economic grade is indicated by the samples analysed.

Some months after the field and laboratory work for this aspect of the project was completed, a commercial prospecting company examined the area, having independently recognised the potential for gold mineralization of this type after researching existing published and private reports which describe the geology. Company staff visited the area and made brief excursions during which some sampling was done. The results of the subsequent analyses are not available, but no further work was done on this venture.

To the best of the writer's knowledge, no other analytical work of this type has been undertaken for research purposes within N.Z. There are many useful modifications to the approach taken in this project, if this topic is to

be re-examined at Mt. Owen or elsewhere. These are:

(i) An improved analytical method to overcome the difficulties and uncertainties of gold determination in acid-soluble samples (see Appendix II).

(ii) Examine gold distribution by biogeochemical means. Warren and Hajek (1973) indicate that plant ash may be enriched in gold by a factor of 50 to 100 times the concentration in the soil-producing rock. A similar enrichment occurs for arsenic and some other elements.

(iii) Pursue a geochemical approach based on some of the other elements characteristic of Carlin-Cortez mineralization which present fewer analytical difficulties than does gold, especially in areas of carbonate-rich rocks.

TABLE 5-2 Indicated gold concentrations in rocks from Mt. Owe Determination by atomic absorption as described in Appendix II

Sample	Gold (ppm)
Dark quartzitic mudstone, Wangapeka Fmn.	0.0030
Dark carbonaceous mudstone, " "	0.0043
Massive Arthur Marble (middle)	0.0023 (note 1)
Impure Arthur Marble (basal)	0.003 (")
Beilby Quartzite, calcareous	0.0068 (note 1,2)
Sericite Zone, Owen Formation	0.066 (note 2)
Calcareous slate, " "	0.017 (" 1)
Dolomitic mudstone, " "	0.0025
Quartzitic mudstone, " "	0.0039

Notes: (1) Results possibly exaggerated due to highly calcareous sample.
(2) Possible contamination by small scale vein material

TABLE 5-3 Averaged gold concentrations of some common rock types and sediments, as determined by neutron activation analysis. From DeGrazia and Haskin (1964).

Rock Type	Gold (ppm)
Acid igneous and metamorphic	0.0024 ± 0.0018
Basic igneous and metamorphic	0.0026 " 0.0006
Mid-Atlantic Ridge basalts	0.010 " 0.0003
Carbonates	0.0025 " 0.0014
Shales	0.0047 " 0.0016
Sandstones	0.006 " 0.0035
Pealgic clays	0.012 " 0.007

IV. DISCUSSION

Two types of veins have been distinguished on the basis of ore mineralogy. Different ore and gangue assemblages for these vein types reflects different chemical environments, and possibly different temperatures, of ore deposition. The invariant association of the base metal veins with the marble is the most obvious correlation of orebody mineralogy and host rock composition. Fluid inclusion data (Ch. VII) suggests that the base metal veins were formed at higher temperatures than the other veins. This is consistent with the indications of much late-stage low temperature mineralization of the auriferous quartz veins, which appears to have overprinted any high temperature characteristics by the formation of secondary inclusions, and possibly by sulphide and gangue replacement (see Chapters VI, VII, and VIII).

A sequence of mineral deposition which reflects generally waning temperatures and changing fluid chemistry can be recognised from paragenetic evidence of cross-cutting and replacement in the major gold-bearing veins of the Owen Formation, as follows:

(i) An early phase of veining characterised by unmineralized quartz and dolomitic carbonate, sericite, and chlorite.

(ii) A later phase of calcite and quartz with traces of base metal sulphides.

(iii) A third phase consisting of quartz, possibly with

some calcite. The quartz is host to marcasitic pyrite, gold, and traces of chalcopyrite.

(iv) A final phase of hydrothermal deposition may be represented by cross-cutting veins of pure calcite which occasionally form drusy coatings on the walls of incompletely filled fissures. A single specimen of acicular aragonite (UC 8883) in this form was found near the Uno Creek workings.

The marcasitic pyrite is the only mineral group identified as a host to gold. The occurrence of marcasite as a hypogene mineral is not common, but examples have been recorded from the Freiberg ores (Germany) in Dana's System of Mineralogy, and from other localities by Newhouse (1925). Ramdohr lists 'melnikovite marcasite' as a poorly crystallized form which rapidly tarnishes and develops sulphate efflorescence when exposed to air. This description is consistent with the observed characteristics of the samples from the Owen Formation, and also with Hector's impressions of the sulphides in the ore he saw being crushed. Combined marcasite-pyrite sulphide is recorded as a late primary mineral in the Renison Bell orebody (Tasmania) by Stillwell and Edwards (1943), who associate the appearance of this phase with the hypogene breakdown of earlier-formed pyrrhotite. This association has been confirmed in more recent times in other orebodies by Fryklund (1964) and Grove et al. (1972).

Deposition of vein marcasite may be correlated with

the formation of disseminated marcasite in the surrounding sediments of the Owen Formation, the latter effect almost certainly being the result of pyrrhotite breakdown. As to whether any of the vein sulphide formed in response to in situ pyrrhotite breakdown is unresolved, as the existence of pyrrhotite as an ore sulphide is not entirely refutable. Although it appears unlikely that no trace of pyrrhotite would remain as inclusions or pseudomorphs, an exhaustive analysis of the mineralogy cannot be claimed, due to the lack of fresh ore specimens. Furthermore, the source of the magnetic concentrate from the crushing batteries remains in some doubt. Edwards' (1954) description of hypogene marcasite arising from pyrrhotite includes an observation that the onset of deposition of this type coincides with the appearance of hydrothermal carbonates, '.... in which the excess iron of the pyrrhotite is accommodated'. The unmineralized earlier deposits of quartz and ferroan dolomites may therefore originate during a period of pyrrhotite breakdown in which the system was sulphur-deficient. Iron not stabilized as sulphide in the rock could pass into solution, contributing to the widespread development of the ferroan carbonates (see Ch. VI). The lack of iron in later carbonates is consistent with the onset of sulphide deposition, suggesting that sulphur was then being added to the fluid system.

The correlation of the mineralization sequences of the base metal veins and the auriferous veins is obscure. Host

rock composition appears to have been the dominant factor in determining deposition, as marcasite is absent from the base metal orebodies, yet cubic pyrite is abundant. A reasonable hypothesis is to consider sulphide deposition to have developed contemporaneously in both deposits.

The complete sequence of carbonate and quartz deposition within the area is undoubtedly more complex than that described, which may apply to only the later phases of a long history of hydrothermal alteration and deposition. The last sulphide phase, the marcasitic pyrite, is of particular interest in acting as host to the primary gold mineralization, a characteristic which is apparently unrecorded for this sulphide in New Zealand. It is conceivable that such auriferous marcasite may occur at epithermal gold-bearing localities elsewhere in Nelson, as the observers who recorded early mining information rarely attempted to distinguish different iron sulphides, and modern investigations may fail to identify the dimorph because of rapid and advanced oxidation.

Additional discussion on the time and source of mineralization, gold distribution, and prospects for commercial operations is presented in Chapter VIII.

CHAPTER VI

EVIDENCE FROM SOME SPECIFIC MINERAL ASSEMBLAGES

I. SULPHIDES

(1) Minerals of the System Fe-S

(a) Pyrrhotite: Identification and Composition. Pyrrhotite survives only in the impervious dolomitic horizons, its former widespread occurrence in the Owen Formation being defined by sulphide pseudomorphs (Ch.IV). Specimens collected for study were obtained from these few horizons, and may not be fully representative of the original suite. Initial identifications were made by reflection microscopy and confirmed by x-ray diffraction.

Natural pyrrhotites occur in a large number of phases which differ in composition and crystal structure. A comprehensive review of the known phases and their interrelationships is provided by Power and Fine (1976). The dominant pyrrhotite phases resulting from metamorphic and hydrothermal processes are the hexagonal and monoclinic forms, which may be distinguished by x-ray diffraction in accordance with a method established by Arnold and Reichen (1962), and later used and extended by other workers. Hexagonal pyrrhotites produce a (102) reflection which forms a single sharp and symmetrical diffractometer peak,

the position of which is dependent on the metal:sulphur ratio. Monoclinic forms produce a split peak, corresponding to reflections from (408), (228) and ($\bar{4}$08), ($\bar{2}$08) (Arnold, 1966).

A complete evaluation of the x-ray indicated structure and composition of the Owen pyrrhotites may produce useful information, but such an evaluation was considered beyond the scope of the project. Partial diffraction charts are reproduced (Figure 6-1), showing peaks in the d=2.1 Å region which include the characteristic reflections described above. A split peak occurs with a spacing of approximately 0.25 °2θ (Co kα radiation). Together with other peaks, this forms a characteristic pattern for monoclinic pyrrhotite, for which calculated d spacings suggest a relatively sulphur-enriched form. Bulk composition of monoclinic pyrrhotite may be estimated by the method of Arnold and Reichen (1962) whereby sample heating is employed to produce hexagonal symmetry, and the metal content determined from the position of the resulting single (102) peak. Several pyrrhotite-bearing rock samples were heated prior to crushing, to prevent oxidation. Heat treatment was maintained for 20 minutes at 500° C, a process similar to that found to be adequate by Wright (1966). Diffraction traces for the heat-treated samples are included in Figure 6-1. Slow cooling destroyed the split peak completely, but quenching yielded a single sharp peak for which d=2.0566$\pm$ 0.0018 Å. If this is taken to be the true (102) reflection,

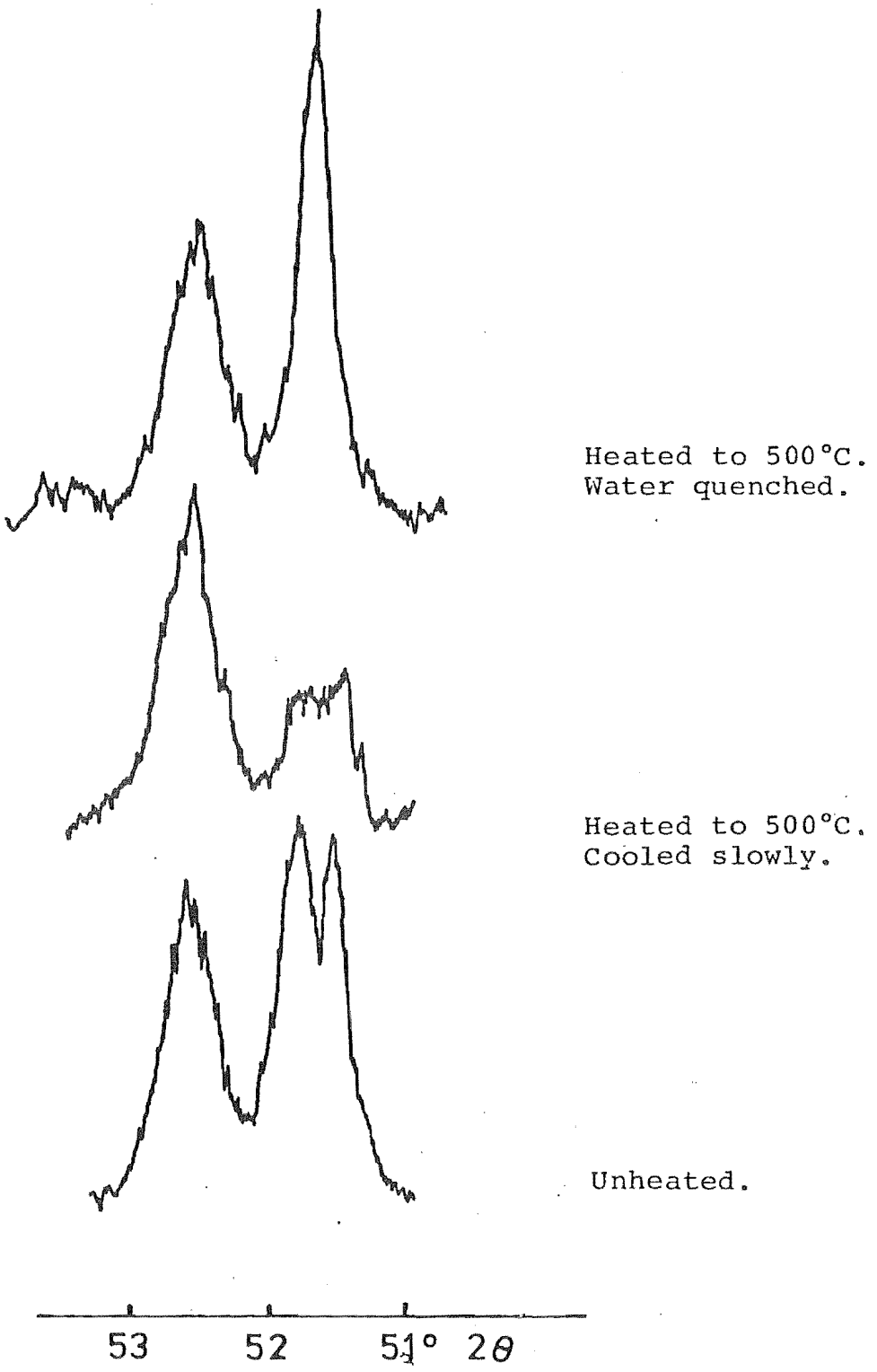

FIG. 6-1 XRD readouts for pyrrhotite from Enterprise Dolomite. (UC8879) Monoclinic symmetry is indicated. (Co k∝ radiation, 1/2°/ minute).

the lattice dimension converts to a composition of 46.5±0.15 atomic % Fe (Arnold and Reichen 1962, Figure 1), indicating extreme Fe deficiency.

A further means of distinguishing the two dominant pyrrhotite forms is provided by the differing magnetic properties. The ferrimagnetism of the monoclinic form is distinct, and permits separation with a hand magnet. In contrast, hexagonal pyrrhotite is antiferromagnetic. This test may be refined for use with polished sections under the microscope, by applying a very fine slurry of magnetic powder and noting adherence to the pyrrhotites. A magnetic slurry was prepared and applied to several polished sections, following the method used by Carpenter (1974), who acknowledges the earlier work of Cameron and Van Rensberg (1961) where the preparation was used as a final buffing agent. The origin of the technique can be traced to work by Bitter (1931), who developed a magnetite powder method to investigate magnetic domains. Within the specimens tested, no non-magnetic pyrrhotite could be detected, indicating that the mineral is present in wholly monoclinic form. Figure 6-2 shows a field of polycrystalline pyrrhotite with the adhering coating which reveals not only the equigranular foam texture but also a fine linear magnetic structure within each grain. The presence of these lineations is apparently unrecorded in the literature, and no definite cause can be assigned. There is a number of possible causes, such as the presence of a lamellar inter-

FIG. 6-2 Pyrrhotite (white) in dolomite, with an adhering coating of magnetite powder after treatment with a slurry for the detection of magnetic minerals. The pyrrhotite is shown to be of monoclinic form. The coating reveals individual crystalline grains and a fine linear magnetic structure of uncertain origin.
Polished section (PS502), ppl. x130 UC8890

growth of two phases (Bennet, et al. 1972), or fine twin-banding (Nakazawa et al. 1975). A further possibility emerges from the original work by Bitter (1931), who detected similar linear fields on the surface of synthetic materials and identified linear magnetic inhomogeneities as the cause. A close similarity between the structures in Figure 6-2 and those illustrated by Bitter is noted.

(b) Pyrrhotites: Geothermometry. Since early work on the pyrrhotite solvus (Arnold 1962), many complications have emerged, resulting in considerable uncertainty regarding the application of geothermometry to natural phases (Barton and Skinner 1967). This uncertainty is especially associated with monoclinic pyrrhotite. Furthermore, the Owen pyrrhotite appears to be anomalously sulphur-rich, and has probably undergone advanced retrograde modification. For these reasons, no attempt has been made to derive numerical temperature estimates with this mineral.

(c) Significance of the Fe-Sulphide Assemblage. The origin of the Owen Formation pyrrhotite from authigenic, stratiform pyrite is well established. The pyrite to pyrrhotite conversion is the principal record of a metamorphic event, yet the conditions of pyrite breakdown cannot be determined with sufficient precision to be of value in reconstructing the metamorphic conditions during this event. The progress of knowledge concerning the thermal stability of pyrite may be seen as a classic example of the evolution

of an experimentally-determined concept from simplicity to complexity. Early work on the simple Fe-S system (Kullerud and Yoder 1959, Kullerud 1959) indicated pyrite to pyrrhotite transition temperatures of 743°C at 10 b pressure, and 575°C when the vapour pressure was only 2 mm Hg (2.6×10^{-3} b). Field evidence indicated that this transition could occur at lower temperatures, and experiments by Lambert (1973) showed the presence of additional chemical species in the system to be significant in this respect, not only by lowering the sulphur fugacity but also by altering the pyrite decomposition reactions. This effect was especially marked when both coal and water were added to the charge, producing conversion temperatures as low as 355°C at the system's vapour pressure. The pressure elevation of conversion temperatures remained relatively constant at ca. 16°C/kb.

Although no limits to the physical and chemical conditions of metamorphism may be defined from the sulphide assemblage, the breakdown of the Owen Formation pyrite may be seen as a response to:

(i) Elevated temperatures.

(ii) Lowered pressures.

(iii) Major changes in chemical conditions serving to reduce the sulphur fugacity and stabilise pyrrhotite or pyrrhotite-forming intermediate species.

All of these effects are envisaged as a result of granite intrusion and accompanying uplift of the adjacent rocks.

As indicated in Chapter IV, some doubt remains as to the time of pyrrhotite formation with respect to cleavage development. Decomposition of pyrite probably predates cleavage, and is contemporaneous with the growth of the pretectonic silicates (chloritoid, chlorite, etc.) Wherever pyrrhotite occurs in non-calcareous mudstone in situations where cleavage can be seen to form a moderate angle with bedding laminae, these laminae deflect around the elongate margins of the sulphide blebs. Conversely, the pyrrhotite in calcareous mudstone shows pressure shadow effects, possibly inherited from a more strain-resistant pyrite precursor. Graf and Skinner (1970) demonstrate that pyrrhotite flows plastically when stressed whereas pyrite shows a brittle response. No evidence of pyrite brecciation can be recognised in the specimens, and all the structures of the pyrrhotite blebs and the surrounding sediment are consistent with plastic flow (Figure 6-3). Wherever initiated, however, pyrite decomposition has proceeded to completion prior to the end of the cleavage-forming event. The sharp cut-off of pyrrhotite formation at the base of the marble demonstrates the restricting effect of this unit on the processes operating beneath it.

Evidence from the hydrothermal stage is the more abundant. The widespread conversion of pyrrhotite to marcasite and pyrite comprises the principal record of this period, but hydrothermal alteration almost certainly influenced the characteristics of the pyrrhotite prior to marcas-

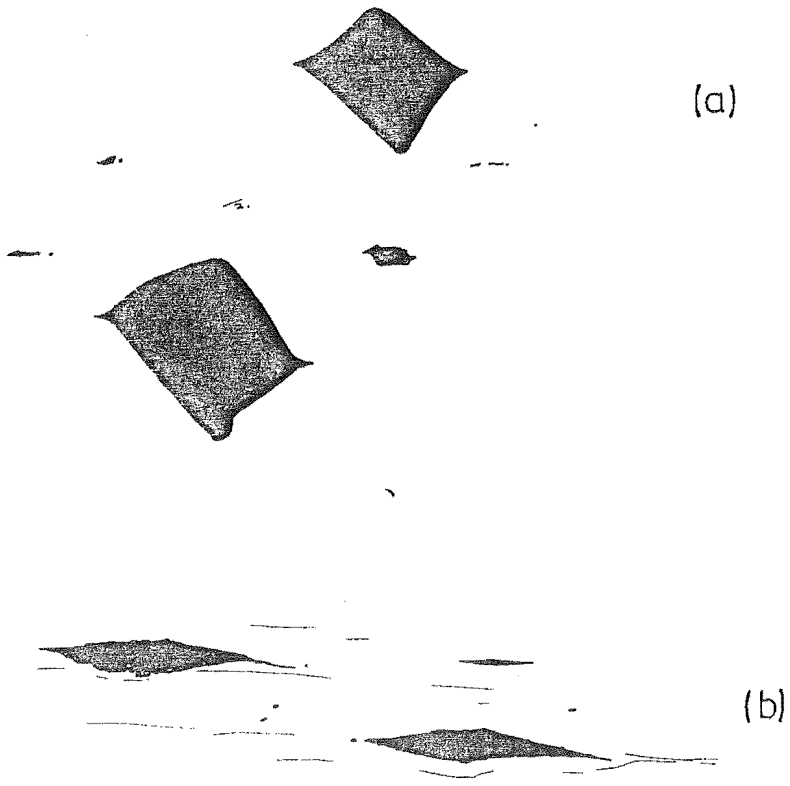

FIG. 6-3 (above) Pyrite pseudomorphs after pyrrhotite pseudomorphs of original authigenic pyrite, seen in rock of the sericite zone.

(a) View perpendicular to cleavage.
(b) View in plane of cleavage.

Drawn from a stream boulder, twice natural size. UC8908

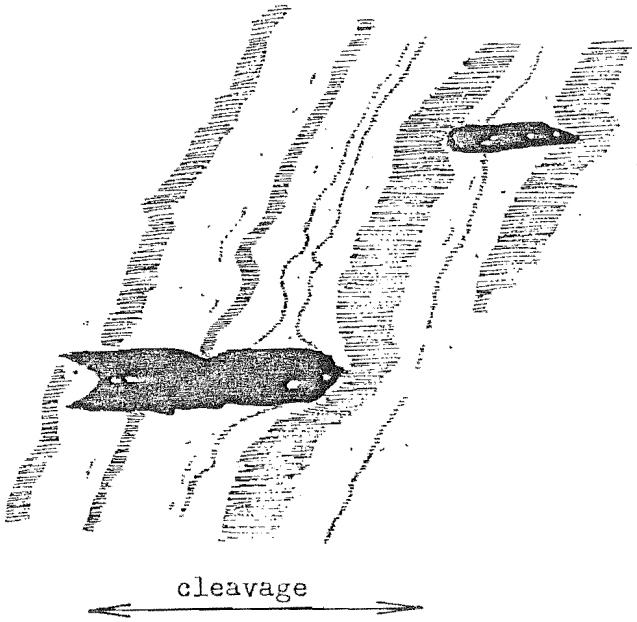

FIG. 6-4 (left) Pyrrhotite blebs in cleaved, laminated mudstone. The dark mudstone laminae (hatched) show displacement about the pyrrhotite (black), which probably predates cleavage. Viewed in the plane of cleavage (indicated).
Drawn from a stream boulder, twice natural size. UC8909

itisation. X-ray studies of the Owen pyrrhotite, although inconclusive, indicate an unusually sulphur-rich composition. With the exception of magnetic properties, this pyrrhotite shows close similarities with an anomalous monoclinic form reported by many authors and reviewed by Power and Fine (1976). Such pyrrhotite is widespread and characteristic of low temperature environments. The upper limit of monoclinic pyrrhotite stability has been established as ca. 250°C, above which the hexagonal form exists. Temperatures for the Owen rocks definitely exceeded this limit during hydrothermal activity, and the pyrrhotite assemblage probably developed in the hexagonal form.

On cooling, the reaction:

hexagonal pyrrhotite + pyrite → monoclinic pyrrhotite

may proceed at or below the 250°C inflexion point (Kisson and Scott 1972). Resulphurization as an agent of hydrothermal activity would have promoted this reaction to the extent that hexagonal pyrrhotite did not survive anywhere except as traces in the impermeable carbonates of the skarn zone at the granite margin, where both forms of pyrrhotite coexist. Reconstruction of the details concerning the resulphurization episode is complicated by the uncertainty of the time and rate of the recrystallization of the dolomitic horizons. Although the recrystallization process has ultimately reduced the permeability to the extent of creating a chemically closed system for the pyrrhotites, their composition has been altered to the sulphur-rich limit, but no co-

existing pyrite formed.

The pyrite-marcasite mineralogy has been described in Chapter V. Low temperature alteration of pyrrhotite is proposed as a primary cause of marcasite development, which took place as both in situ alteration of country rock sulphide, and hypogene deposition, probably in reponse to chemical buffering of the fluid system. The physico-chemical conditions controlling marcasite deposition are insufficiently known to derive precise values for the corresponding hydrothermal phase. The indicated progression and overlap of the pyrite-marcasite depositional sequence and partial marcasite inversion suggests that this period of hydrothermal alteration spanned a wide range of pressure-temperature conditions. The deposition and survival of marcasite does provide some limitation on temperature estimates. Experiments by Ramdohr (1969) show that marcasite will slowly invert to pyrite above 350°C, but the mineral can be synthesized 'above 250°C'. Formation at lower temperatures is more commonly observed. Assuming 350° to be an upper limit for marcasite stability, no post-mineralization event can have imposed higher temperatures. This reasoning therefore precludes the possible existence of the mineralization prior to the intrusion of the nearby Separation Point Granite. As the marcasite limit of 350° is probably too high, the evidence for the mineralization as a product of post-intrusive hydrothermal activity becomes difficult to refute.

(2) Minerals of the System Fe-Zn-S

(a) Theoretical Considerations. Sphalerite is widespread in the Owen Formation. This mineral commonly includes FeS as a solid solution to an extent determined by the temperature and pressure of formation or recrystallization. The simple temperature dependence of the FeS content as proposed by Kullerud (1953) has long been abandoned for geothermometry purposes, and much research has been expended to determine the controls on sphalerite composition. This knowledge remains incomplete, particularly at low temperatures and with respect to the effect of chemical environment. Sulphur fugacity is known to be a major control on the FeS content, and most attempts at temperature-pressure reconstruction based on sphalerite composition rely on the presence of coexisting pyrrhotite and pyrite as a sulphur fugacity buffer.

(b) Investigation of Sphalerite Composition. Regrettably, no specimen from the Owen rocks can be found fulfilling the above requirement. The widespread occurrence of pyrrhotite, however, may have provided some degree of buffering. The only hand-specimen sized sphalerite samples available were from the base metal veins, and from one specimen (UC 8885, Silverstream Lode) small flakes of the mineral were removed for analysis. These flakes were examined with a binocular microscope and any material with metalliferous inclusions rejected. Four samples were prepared in this manner, then dissolved in acid and the result-

ing solution analysed for Zn and Fe by atomic absorption. As the required result was only the Fe/Zn ratio, weighing and quantitative solution preparation was unnecessary except for simple calibration standards, and a sample size of less than 0.01 gram was possible. Electron microanalysis facilities were not available at the time, and although the method used is considered to be of high accuracy, it will incur the disadvantages of bulk analysis in spite of the small sample size.

The results were as follows:

Sample	1	7.0	mole %	FeS
"	2	6.9	"	"
"	3	10.4	"	"
"	4	6.2	"	"

(c) Discussion. In view of the analytical method, the values appear to be relatively constant; the high result for analysis (3) may be due to the inclusion of pyrite or chalcopyrite in the sample. Some degree of sulphur fugacity control may be implied. The coexisting iron sulphide is exclusively pyrite, thus the local sulphur fugacity would be higher, and the Fe content of the sphalerite lower, than if pyrrhotite had been present when the sulphides developed.

The pressure-temperature dependence of the Fe content of sphalerite has been partly clarified by Scott (1973). The FeS levels have been shown to be constant between 300° and 500°C for pressures below 5kb in the pyrrhotite/pyrite buffered systems (Figure 6-5). Although these data permit geobaric reconstructions within these limits (e.g.

Berglund, et al. 1974), the work of Scott cannot be extended for use at lower temperatures. An indication of the low temperature relationships is provided by work by Browne and Lovering (1973), wherein sphalerites from an active hydrothermal field (Broadlands, N.Z.) were examined. Approximate temperatures and pressures of formation were obtainable by direct measurement. Corresponding analyses show that the sphalerite pyrrhotite/sphalerite pyrite phase boundary deflects sharply to the low-FeS region between 250° and 280°C (Figure 6-6). The pressure values accompanying these data are low (ca. 100b) but nearly isothermal boundaries can be expected to follow this trend. The known pressure dependent changes in mole % FeS in sphalerite above 300°C are small (approximately 1.4 mole %/kb) compared to the temperature dependent deflection indicated by Browne and Lovering (less than 12 mole %). Below 300°, the pressure effect probably diminishes progressively.

The absence of pyrrhotite in the Owen base metal deposits requires the sphalerites to plot to the right of Browne and Lovering's phase boundary, which if accepted as correct, will provide minimum formation temperatures. If the compositional range 6-7 mole % FeS is taken to be representative of the sphalerite analyses above, the boundary curve implies a corresponding minimum temperature range of approximately 180° - 220°C. Unfortunately, these values must be read from the extreme lower end of the boundary, where the uncertainty of the data increases. Errors in this

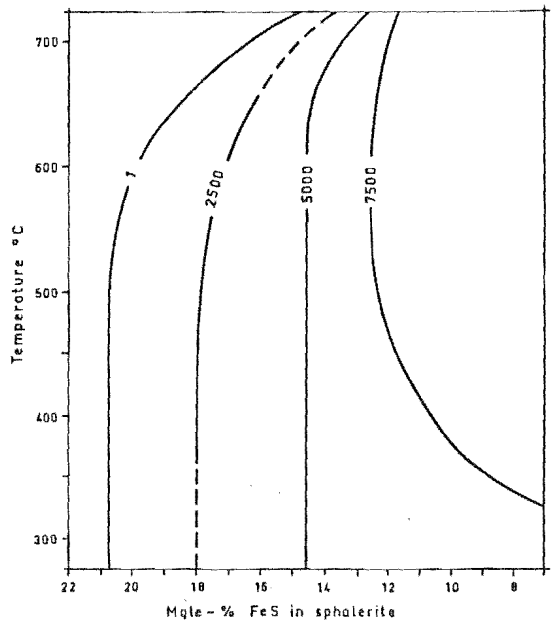

FIG. 6-5 FeS Isobars for Sphalerite above 300°C.
After Scott, (1973).

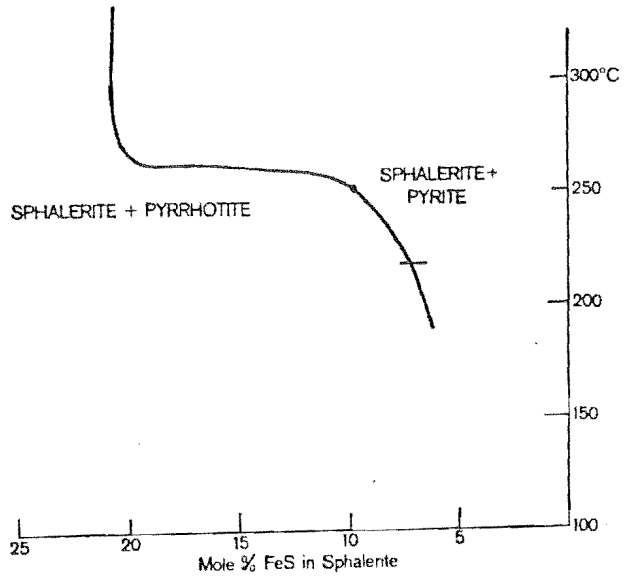

FIG. 6-6 Temperature-Composition phase boundary for Sphalerite, Pyrite and Pyrrhotite at low pressures, below 300°C.
Adapted from Browne & Lovering (1973), Figure 3.

temperature estimation may arise from:

(i) Higher pressures for the Owen sphalerite as compared with Browne and Lovering's calibration.

(ii) A sulphur fugacity significantly higher than the level controlled by pyrrhotite/pyrite buffering.

The effect of either situation will be positive, i.e. a higher temperature indication will result. Therefore, unless the phase boundary is seriously in error, the temperature range of 180° - 220°C may be accepted with some confidence as providing a minimum deposition temperature. If the higher value of 10.4 mole % FeS is accepted as a true sphalerite composition, a varying sulphur fugacity caused by fluctuation of temperature, pressure, or other causes is implied, and deposition temperatures above approximately 260° must be envisaged.

A further study of the Owen sphalerites is considered warranted, both to investigate the base metal ores by more extensive analysis, and if microanalysis is employed, to examine the small sphalerite inclusions in the disseminated sulphides. The sphalerite in the pyrrhotite may prove especially suitable, as sulphur fugacity buffering is suggested by the pyrrhotite composition.

(3) Other Sulphide Systems

Other systems defined by the sulphides occurring in the Owen rocks are of little value in determining physico-chemical conditions of deposition and subsequent history. Exceptions to this may be represented by some of the minor

phases within the base metal ores, where several unmixing textures are preserved. Insufficient identification precludes their use for these purposes at this stage of the investigation. One may suggest that if the phases were identified, little data concerning their paragenesis would be available, due to the complex mineralogy of the fahlore systems.

II. CARBONATES

Introduction

During the early stages of field work, a marked variation in the appearance of some vein carbonates was noted. Some were of a darker colour and were more weathering-resistant than others, and showed a limonitic coating on weathered surfaces. Many of the deeply weathered vein outcrops showed porous limonite pseudomorphs of rhombohedral carbonates.

These characteristics and simple field tests indicated the presence of dolomites. X-ray diffraction determined both calcite and dolomite in vein samples, and also showed widely varying proportions of these two minerals in the country rock. Apart from very small amounts of siderite in the Beilby Quartzite, and a single specimen of vein aragonite (Ch. V), calcite and dolomite were the only carbonate minerals found. These carbonates are widespread in the project area, and comprise major rock-forming and vein-forming minerals. Their close association with the mineralization justifies more than the cursory report of their occurrence that has been given in Chapters II, IV and V. The carbonates have therefore been investigated with respect to their distribution and composition, and an attempt is made to use these data to elucidate the hydrothermal history of the rocks.

(1) Carbonate Mineralogy

Dolomite will accept large amounts of Fe as a substitution for Mg. The terminology used for carbonate minerals in this report follows a widely adopted recommendation by Goldsmith (1959) that dolomites with more than 20% Fe substitution for Mg be termed ankerites. As the Owen carbonates span a wide range of composition, the term dolomite is used to cover all the double carbonates of the ankerite series where the specific composition is unknown.

Both Fe and Mg substitute for Ca in calcite, for which the corresponding adjectives ferroan and magnesian are applied where this substitution is significant. Mn also commonly substitutes for Ca in both calcite and dolomite, but as shown below this effect is too small to require a modification of the mineral names.

(2) Carbonate Geochemistry

(a) Carbonate Systems: A Brief Outline. The carbonates of concern to most natural rock and vein studies are those represented by the end members of a quaternary system; calcite $CaCO_3$, magnesite $MgCO_3$, siderite $FeCO_3$, and rhodochrosite $MnCO_3$. Analyses of Owen samples show contribution by Mn to be relatively insignificant (see below), thus the complication of a quaternary system is avoided, permitting evaluation in terms of the more common ternary system.

Solid solution in the binary system $CaCO_3$-$MgCO_3$ has been investigated by Harker and Tuttle (1955a, 1955b), and

Goldsmith et al. (1955). The aspect of interest in this system is the occurrence of magnesian calcite, which is known to be present in carbonates of organic origin and also from environments where calcites form or equilibrate at elevated temperatures in the presence of available Mg. The system $CaCO_3$-$FeCO_3$ has been similarly investigated by Goldsmith et al. (1962) and Rosenberg (1963), and a definite temperature dependence determined for ferroan calcites, which are not formed in low temperature environments. Continuous solid solution in the binary system $MgCO_3$-$FeCO_3$ is known from the work of Rosenberg (1963b), but minerals of this series have little application to this project.

A special solid solution series of the ternary system is represented by the dolomites, which have been investigated chiefly by Rosenberg (1967, 1968). Members of this series undergo progressively increasing substitution of $MgCO_3$ by $FeCO_3$ with increasing temperature, but maintain an almost constant $CaCO_3$ mole fraction. Much remains unknown concerning the low temperature origins of dolomite, but the ankerite varieties are restricted to metamorphic, hydrothermal, metasomatic, and magmatic environments, except in unusual sediments such as coal where both ankerite and siderite are common (Smythe and Dunham 1947).

(b) Measurement of Carbonate Composition. The relative ionic radii of the metals of the rhombohedral carbonates is as follows:

$$Ca > Mn > Fe > Mg$$

In the case of calcite, therefore, substitution by any of the other metals causes a decrease in cell size, with a corresponding increase in 2θ reflection angles. Conversely, substitution of Mg in dolomite by Fe or Mn will increase the cell size, reducing the 2θ angles. Composition in terms of substitution by any one element may therefore be determined by precise X-ray diffraction measurements. Appendix III contains graphs relating carbonate composition to (104) angles for Cu $k\alpha$ radiation, taken from the data of various authors.

(c) Method. Chippings were taken from a number of carbonate-bearing rock and vein samples from throughout the project area, although most samples examined were from the carbonate-rich Owen Formation. Carbonate vein minerals were almost completely restricted to this unit. A dolomite specimen from Mt. Burnet, N.W. Nelson, was included for purposes of comparison. The sample chips were ground to a fine powder from which smear plates were prepared for X-ray diffraction. Using Cu $k\alpha$ radiation and medium slits, scans were made over the range 29° to 32° 2θ to measure the (104) reflections of the principal rhombohedral carbonates. Goniometer calibration was carefully checked against the (101) reflection of quartz, which formed a minor component in most samples. The scan rate selected was 0.5°/minute.

To check the extent of Mn substitution in all the car-

bonates, and the ratios of Fe to Mg substitution in calcite, small portions of some samples were dissolved in dilute hydrochloric acid and the resulting solution analysed for these metals by atomic absorption. The validity of such analyses is limited by the sample purity, as non-carbonate inclusions may contribute the analyte metals, particularly in the case of dolomites where heating is required for dissolution. Some rock samples were analysed, in addition to the relatively pure vein materials, the carbonate content being considered as total acid solubles. The results were calculated to mole % values based on the major carbonate phase, and are tabulated below.

(d) Results. All X-ray measurements are presented in Table 6-1, where peak shifts from the pure end-member calcite and dolomite reflections are shown as $\Delta 2\theta$ values. Peak positions are considered reproducible to within $\pm 0.005°$ for strong, sharp peaks, and at least $\pm 0.01°$ for all others except where very imperfect peaks occur as discussed below. Where more than one carbonate is present in a sample, the relative peak heights provide an indication of the relative proportions of each mineral. Some examples of diffraction traces are given (Figure 6-8). A diagrammatic representation of carbonate distribution, condensed from the data of Table 6-1 is given as Figure 6-7.

TABLE 6-1 (104) Peak shifts .

XRD No.	Description and Location of Sample			$\Delta 2\theta$cal.	$\Delta 2\theta$dol.	Id/Ic
1	Rocks Biosparite, uppermost Arthur Marble near Mt Owen summit.		UC8874	0.02 (b)	-	C
2	Uppermost Arthur Marble near trig EH, Fyfe River.		UC8910	0.04	-	C
3	Black marble interfingering with shales, Fyfe River.		UC8911	0.025	-	C
4	Massive Arthur Marble above trig C.		UC8912	0.03	-	C
5	Massive Arthur Marble north of Fyfe River.		UC8913	0.05	-	C
6	Lower Arthur Marble breccia, Byrne Stm.	(i) Fragments	UC8916	0.05	-	C
7	As above.	(ii) Matrix	UC8916	0.06	-	C
8	Lowermost, laminated, fissile, Arthur Marble, head of Byrne Stm.		UC8914	0.06	~0.03 b	0.06
9	Beilby Quartzite, trig C.		UC8915	0.045(b)	-	C
10	Uppermost sericite zone, trig C.		UC8917	~ 0.07 b	~0.13 b	>20
11	As above, wall rock to sphalerite vein.		UC8918	~ 0.035(b)	~0.15 b,s	0.3
12	Sericite zone, Enterprise mine.		UC8923	-	0.10(b↓)	D
13	Carbonate lens above Enterprise Dolomite, near Enterprise mine.		UC8924	0.04(b↑)	-	C
14	Carbonate lens containing pyrrhotite, Lower Spring Creek.	(i)	UC8927	~ 0.12 b	-	C
15	As above.	(ii)	UC8927	0.005(b↑)	-	C
16	Carbonate lens near mouth of Spring Creek.	(i)	UC8928	0.16	~0.10 b	0.5

TABLE 6-1 continued

17	As above.	(ii)	UC8928	0.05 b↑	~0.11 b 0.4
18	Enterprise Dolomite, opposite mouth of Zealandia Creek.	(i)	UC8891	0.06 b	0.10(b↑) 1.3
19	As above.	(ii)	UC8891	0.16 b↑	0.015 b↑ 1.0
20	Carbonate-rich shale beneath dolomite, near Uno Creek.		UC8892	0.06(b↑)	0.08(b↑) 0.2
21	Carbonate lens, mouth of Bulmer Creek.		UC8905	0.06 b	0.145 b 1.0
22	Carbonate lens, Golden Crown mine.		UC8899	~0.105b,s?	0.153 b↑ 0.7
23	Skarn zone marble containing garnet, near trig CK.		UC8929	0.0 (b↑)	- C
24	As above, but from further west.No garnet.		UC8930	0.10	- C
25	Igneous dike, base of marble, head of Byrne Stream.		UC8926	~0.15 b	- C
26	Mt. Burnet.			0.017(b↑)	0.133 >20
Veins					
27	Clear crystals forming drusy infillings. Near trig C.		UC8919	0.032	- C
28	Vein in igneous dike, Fyfe River.		UC8925	0.015	- C
29	Vein in Beilby Quartzite near Beilby mine.		UC8920	0.052(b)	0.132 14
30	As above.	(i) Creamy carbonate	UC8921	0.042	0.095 b 0.05
31	As above.	(ii) Light milky carbonate	UC8921	0.065	- C

TABLE 6-1 continued

32	Vein from sericite zone, near Beilby's reef locality. (i) Creamy carbonate.	UC8902	0.06	-	C
33	As above. (ii) Dark brown carbonate.	UC8902	~0.125 s?	0.13	1.2
34	As above. Light creamy veinlet.	UC8903	0.085	-	C
35	Clear crystals from late veins in Enterprise mine.	UC8898	0.052	-	C

Notes:

All 2θ values refer to true peak shifts, not 2θ - 2θstandard.

Symbols are as follows:

- Phase not detected.
- b Broad peak.
- b↑ Broadened on high angle side.
- b↓ Broadened on low angle side.
- s Split or multiple peak.
- ( ) Effects slight
- ~ Poor or weak peak, measurement approximate.
- Id/Ic Ratio of (104) peak intensities for dolomite and calcite.
- C Only calcite detected.
- D Only dolomite detected.

From the diffraction results, the following salient points emerge:

(i) Only calcite and dolomite-ankerite phases are present.

(ii) A large range in composition for both minerals is indicated by the peak shifts for both rock and vein samples. This range persists to a small scale, i.e. between samples taken from the same outcrop, and in some cases between samples taken from a single hand specimen.

(iii) Calcite is the ubiquitous carbonate. The occurrence of calcite only, is common, but almost all the dolomitic specimens contained both carbonates.

(iv) Peak broadening, often with skewness and in some cases peak multiplicity was exhibited by the reflections of both carbonates in both rock and vein samples. For calcite peaks, these effects were most pronounced when coexisting dolomite was present. All rock-specimen dolomites showed peak broadening, but most vein dolomites produced relatively well-defined peaks.

The results of the chemical analyses are summarized in Table 6-2, and are discussed below. The most significant point to emerge from these analyses is the low Mn values, which indicates that the errors incurred by neglecting this element are very small.

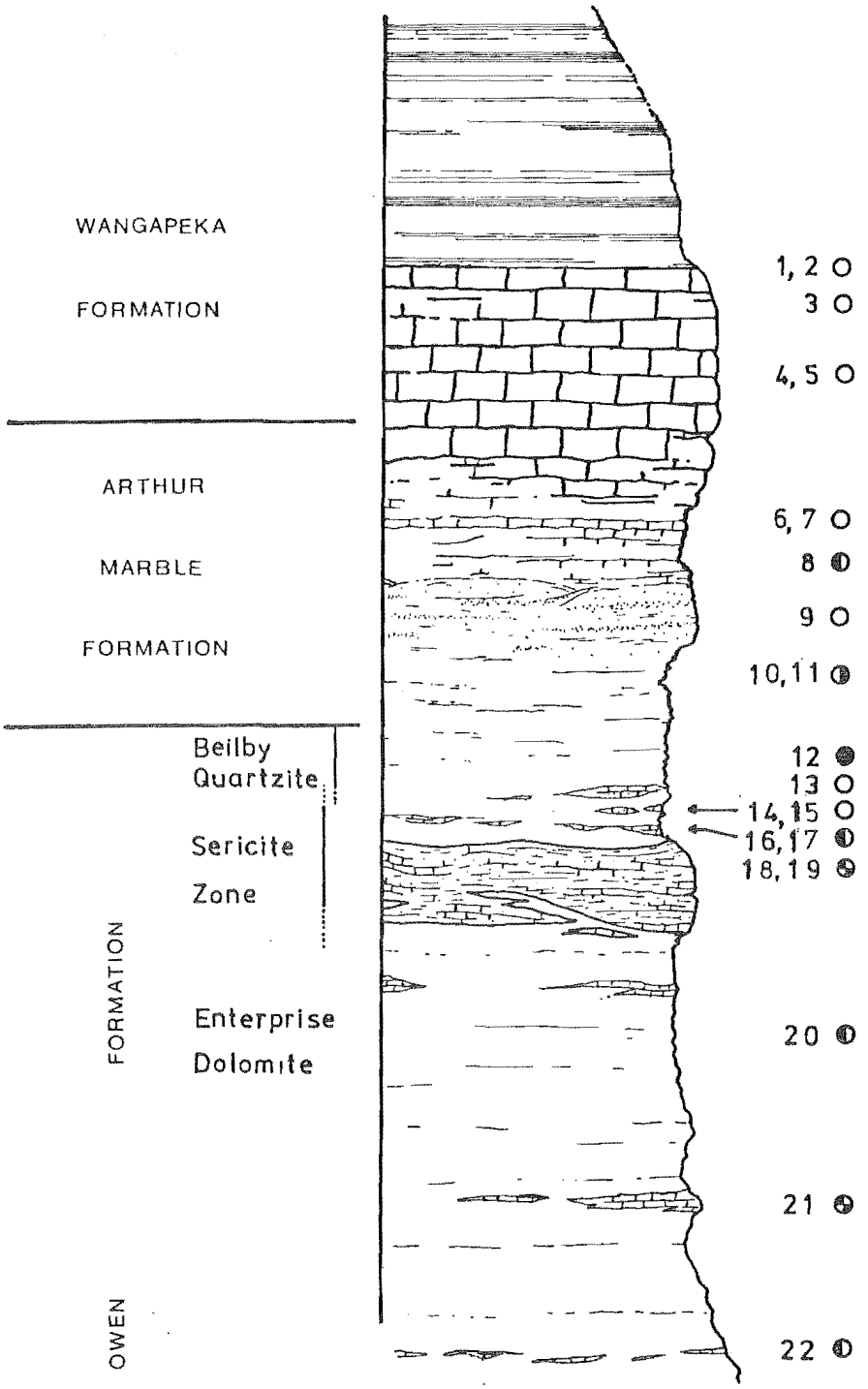

FIG. 6-7 Lithostratigraphic distribution of carbonates in country rocks at Mt. Owen. Numbers refer to Table 6-1.

O Calcite only

● Dolomite only

◐ Calcite dominant

◑ Dolomite dominant

◒ Subequal proportions

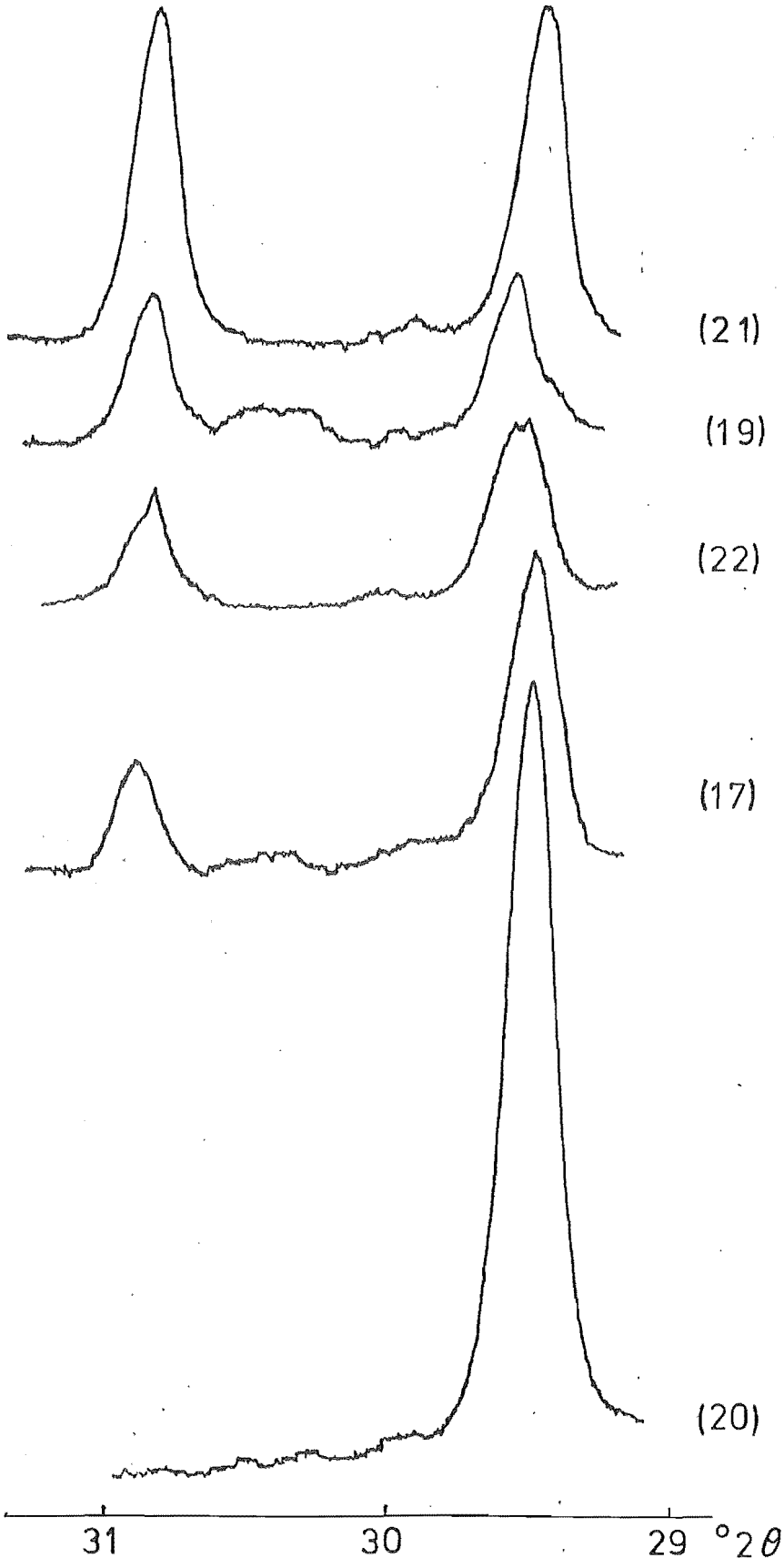

FIG. 6-8 Diffractometer traces of (104) peaks of carbonates from country rocks.

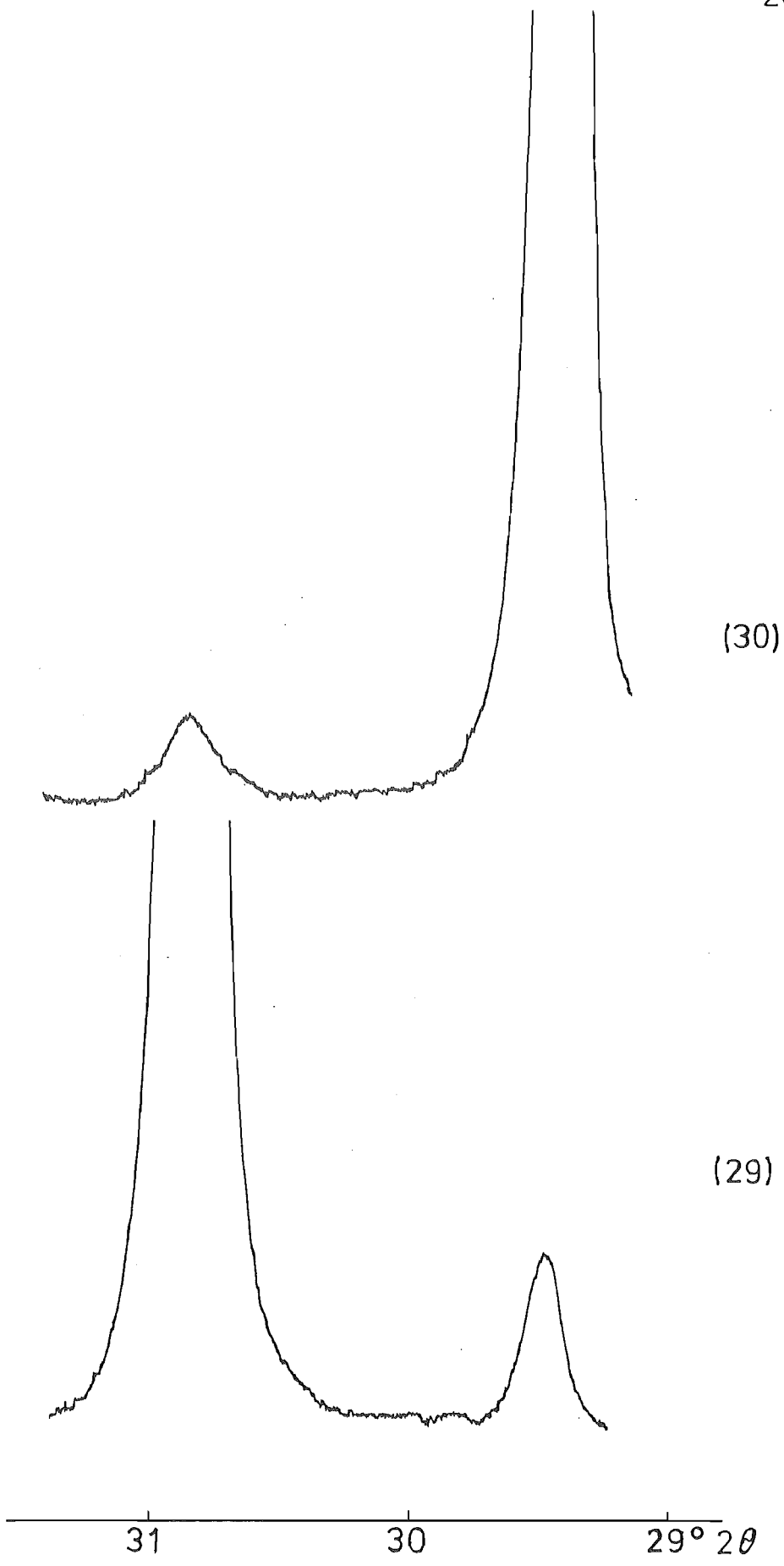

FIG. 6-8 continued. Diffractometer traces of (104) peaks, vein carbonates.

(e) Discussion. The peak characteristics described above are unlikely to be due to disordered 'protodolomites' (which are reported from Cretaceous and younger rocks Goldsmith and Graf 1958), and are almost certainly due to compositional variations arising from one or more of the following causes:

(i) Original, pre-metamorphic compositional variations remaining due to incomplete equilibration during the period of elevated temperatures.

(ii) Disequilibrium developed during cooling.

(iii) Disequilibrium with material added by hydrothermal or supergene processes.

Persistence of much relatively unaltered organic carbonate is suggested by the highly calcitic samples. The Arthur Marble specimens (1) to (6) form a characteristic group with small peak shifts. The very fine grain size, reflecting a micritic origin, is consistent with the homogeneity and attainment of equilibrium inferred from the sharp peaks of samples (2) to (6). Sample (1), however, is a biosparite containing coarse shell fragments, and shows peak broadening. Where solution effects are dominant, as in the matrix of the marble breccia (sample 7), a greater degree of substitution is noted.

Samples (23) and (24) are supposedly Arthur Marble, taken from the highly metamorphosed remnant at the flank of the granite at Trig CK. Sample (23), which contains garnets and other high grade metamorphic minerals, shows

a peak shift of 0.0°, the only sample to contain pure calcite. One must assume that the metamorphic conditions prevailing have 'purified' the calcite, incorporating all Ca-substituting metals into stable silicates. Sample (24), taken from an outcrop further from the granite contact, contained no garnets and showed a comparatively large peak shift. The lower equilibrium temperatures have apparently been only sufficient to promote increased substitution.

Dolomitization is restricted to horizons beneath the marble, where the greater permeability was probably the most important control on this process. The interlayering of dolomitic and dolomite-free carbonate horizons is surprising, and illustrates that dolomitization was highly selective and incomplete. Such characteristics are indicative of subsequent dolomitization, which either resulted from, or was extended by, the hydrothermal-metasomatic events in the area. Dolomite is abundant within and near the Enterprise Dolomite unit, and also in parts of the sericite zone, from which the only sample of calcite-free dolomite was taken (sample 12). Enhancement of dolomitization in the sericite zone by hydrothermal activity is probable, as prominent vein dolomite is found within this zone and the immediately overlying units.

Coexisting calcite in the sericite zone shows only a moderate degree of substitution, and may result from late, low temperature deposition, or perhaps in some cases supergene material. In contrast, the calcites in the less altered dolomitic lithologies show a high degree of substi-

tution.

Chemical analysis was used to investigate the composition of the carbonate fraction of four country rocks and three vein samples (Table 6-2). The calcite-rich specimens were analysed for Mn, Mg and Fe, and the dolomite-rich specimens were analysed for Mn and Fe alone. These specimens also appear in the X-ray table (6-1) and the corresponding peak shift values are included in Table 6-2. In the case of calcite (analyses a-e) the change in lattice dimensions is seen to be a result of substitution by all three metals, Fe, Mg and Mn. The effect of Mn is very small, this element being present to a maximum extent of only 0.15 mole %. No data are available to show the effect on d spacings of combinations of different substituting elements, but as the two-component systems all exhibit linear plots of Δd vs concentration, it is reasonable to assume that the effect of such combinations will be additive. Thus, columns in Table 6-2 are included to show the X-ray predicted composition if the substitution were:

(i) Mg only.

(ii) Fe only.

In each case, the $\Delta 2\theta$ values appear too high. A further two columns list:

(iii) total substitution represented by the sum of Mn+Mg+Fe carbonates.

(iv) The expected $\Delta 2\theta$ value for this total substitution. This final peak shift value is much closer to the measured

TABLE 6-2

Partial analysis of Rock and Vein Carbonates.
For explanation of symbols see Table 6-1.
All compositions expressed in mole %.

	XRD No.	Description	Composition* Mn	Mg	Fe	$\Delta 2\theta$	$I_{\perp}/I_{\parallel}$	Predicted monosubstitution $MgCO_3$	$FeCO_3$	$\sum Mn+Mg+Fe$ and CO_3 expected $\Delta 2\theta$	$\Delta 2\theta$ measured $-\Delta 2\theta$ expected
(a)	27	Pure vein calcite	0.038	0.29	0.46	0.032	C	1.0	1.4	0.79	0.02	0.012
(b)	34	Vein calcite	0.15	1.27	1.37	0.085	C	2.7	3.7	2.79	0.07	0.015
(c)	24	Marble near skarn zone	0.053	1.56	0.88	0.10	C	3.2	4.3	2.49	0.065	0.035
(d)	1	Slightly impure marble	0.026	0.40	0.23	0.02	C	0.7	0.9	0.66	0.015	0.005
(c)	2	Slightly impure marble	0.029	0.67	0.39	0.04	C	1.3	1.7	1.10	0.026	0.014
(e)	21	Carbonate lens	0.23	n.d.	31.8	0.145	1.0	see text			(note 1)	
(f)	10	Sericitic carbonate	0.09	n.d.	43.1	0.13	>20	"	"			
(g)	29	Vein dolomite	0.39	n.d.	37.3	0.13	14	"	"			

Notes:

*Calcite components calculated as carbonate, $..CO_3$

Dolomite components calculated as $Ca..(CO_3)_2$

1: Calculated as dolomite

n.d: not determined

shifts, although these remain consistently high. A standard positive reading error incurred in the diffraction and peak measurement procedure may be included. Sample inhomogeneity is also possible, as separate powders were prepared for each analytical method.

Analyses (f), (g) and (h) refer to the dolomite specimens, of which (f) proved to contain a large amount of calcite, and is therefore of use only to show the range of $MnCO_3$ levels. The results of the three specimens are calculated as mole % dolomite, and should be valid for (g) and (h) which contain only traces of calcite.

The X-ray determination of natural dolomite compositions is still subject to considerable uncertainty. The products of ideal experimental systems involving high temperature synthesis have (104) peak shifts which show a linear relationship with Fe substitution. Such a plot has been verified and published by Rosenberg (1967). Natural ankerites, however, depart from this ideal correlation by showing excessive peak shifts at high Fe contents. Experimental systems containing excess reactants in the form of several stable phases of the $CaCO_3$-$MgCO_3$-$FeCO_3$ ternary, produce dolomites which show more natural characteristics. Rosenberg attempted to synthesize dolomite end-members of a three-phase zone of the carbonate ternary (Figure 6-9) and obtained satisfactory results only above 350°C due to long equilibration times at lower temperatures. The resulting dolomites showed a progressive increase in Fe substi-

tution with temperature, and also a progressive increase in $CaCO_3$ beyond the 50 mole % level. Such an excess of $CaCO_3$ has been reported in highly ferroan natural ankerites (Rosenberg 1960, Goldsmith et al. 1962) and appears to be one cause of the excessive peak shift. Rosenberg's (1967) plot of 'ideal' synthetic dolomites is reproduced below as Figure 6-10 (dashed line), with additional data from member ankerites (unlabelled circles). Also plotted is a point for the ankerite standard of the JCPDS X-ray powder diffraction file, card 12-88, for which both composition and d spacings are accurately determined. These points, in combination with the invariant point for pure dolomite, $CaMg(CO_3)_2$, define the locus of a regular curve which deflects away from the linear plot of the 'ideal' ferroan dolomites.

Analysis (h) was performed on vein dolomite of high purity which yielded no insolubles and showed a peak intensity ratio of $I_{calcite}/I_{dolomite}=14$. When this sample is plotted on Figure 6-10 the point falls very close to the curve described above. Sample (f) is obviously impure, containing large amounts of calcite and some sulphide. Sample (g), although almost calcite-free, contained only 15% soluble carbonate, and much sulphide Fe is probably included in the analysis. For these reasons, no attempt was made to add the data from these samples to Figure 6-10.

The three dolomite analyses indicate that Mn contents are low, the highest value of 0.39 mole % being recorded

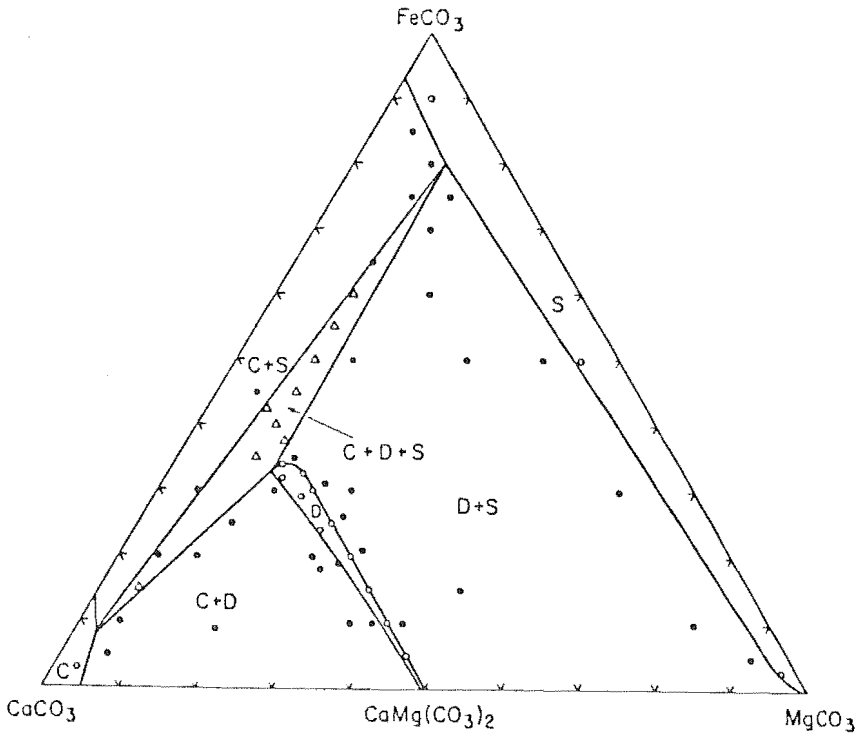

Subsolidus relations in the system $CaCO_3$-$MgCO_3$-$FeCO_3$ at 450°C. D—dolomite solid solution; C—calcite solid solution; S—siderite-magnesite solid solution. Open circles, one-phase; filled circles, two-phase; and triangles, three-phase assemblages.

FIG. 6-9 Carbonate ternary diagram and caption from Rosenberg (1967, Figure 1).

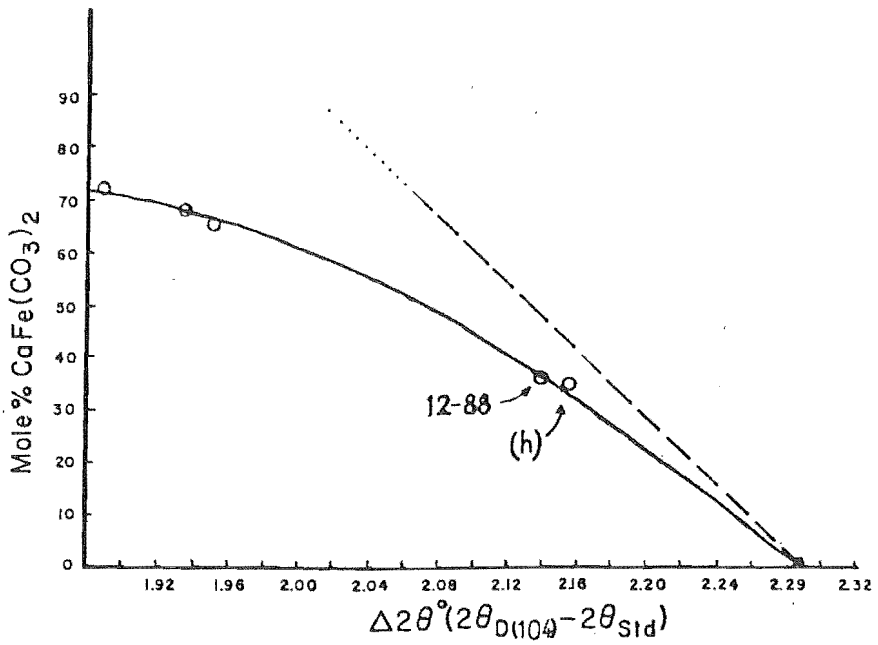

FIG. 6-10 Modified graph from Rosenberg (1967, Figure 2). The abscissa has been extended to accommodate the end-member dolomites (Table 6-3) and a curve constructed through these and other points considered to represent natural dolomites. See text.

for the vein sample, which probably reflects the order of Mn concentration for the 'open' hydrothermal system.

Both the range in dolomite composition and the peak broadening and skewness characteristics may be attributed to the combined effect of country rock equilibration, metasomatism, and hydrothermal deposition over a wide range of temperatures. As the peaks of the vein carbonates show little broadening and no skewness, these characteristics in the case of the country rocks are seen as evidence for both incomplete equilibration and continued carbonate reaction with other minerals and pore fluids as temperatures declined.

The Mt. Burnet deposit consists of massive, metamorphosed dolomite, described by Bishop (1967) but not yet investigated by geochemical or petrological studies. A specimen of the quarried material (analysis 26) proved to be an ankerite of high purity and narrow compositional spread, as indicated by a very sharp, symmetrical peak. This marked contrast with the Owen samples may be attributed to the differences in metamorphic history and geochemical environments. For the Mt. Burnet material, an initial composition of relatively high purity and homogeneity, a long and relatively isothermal equilibration during regional metamorphism, and a low permeability and general lack of hydrothermal reaction are the probable distinguishing factors. Bishop does not discuss the origin of the Mt. Burnet dolomite, but believes it to be pre-metamorphic.

The Owen dolomitization may have been either pre-metamorphic or syn-metamorphic, but the early characteristics are almost certainly modified and overprinted by the period of hydrothermal activity.

(3) Carbonate Systems and Geothermometry

Reference has been made to the temperature dependence of the degree of substitution in both calcite and dolomite. The possible use of carbonate minerals for geothermometry has been recognised since the early work of Goldsmith et al. (1955) and Graf et al. (1955).

(a) Dolomites. Studies by Rosenberg have partly evaluated dolomite substitution in this respect. He reports (1967):

> 'For natural compositions lying within the ternary system, the $FeCO_3$ content of dolomite might provide an approximate formation temperature for the three-phase carbonate assemblages and a minimum formation temperature for one- and two-phase carbonate assemblages. However, these temperature estimates will be highly imprecise, even where the $MnCO_3$ content is negligible due to .... the limited data below 450°C'.

As far as can be determined, temperature-dependent relationships between natural carbonates below 450° remain poorly understood at the time of writing. In a further publication, Rosenberg stresses that the presence of $MnCO_3$ affects the ternary system phase boundaries so as to yield apparent dolomite formation temperatures which are too low. In addition, the effect of excess $CaCO_3$ in the dolomite structure remains undetermined.

The temperature-composition relationship of low-Mn natural dolomites is best represented by the graph of Figure 6-11, taken from Rosenberg (1968, Figure 1). The dolomite end-members of Table 6-3 (Rosenberg 1967) define the left-hand phase boundary along which lie the dolomites of maximum substitution. The curve is accurately known down to only 400°C, but the trend is indicated to 350° where a sharp deflection to lower Fe compositions is evident. Using the 'natural dolomite' curve constructed in Figure 6-10, and neglecting Mn, a range of compositions for Owen dolomites is presented in Table 6-4. When this range is applied to Rosenberg's T-X graph, the Fe-rich members will fall near an extension of the dolomite boundary curve in the 350°C region (Figure 6-11). This may provide some indication of the maximum temperatures of major ankerite equilibration.

The above procedure is based on successive approximations and assumptions based on scant data, and the possibility of large errors in the resulting temperature estimates is therefore acknowledged. Until improved and extended data from carbonate systems are available, more precise geothermometry using these minerals is not possible.

(b) Calcites. The temperature dependence of the level of substitution of Ca in calcite presents another possible geothermometer. Carbonate binary systems are well understood (Harker and Tuttle 1955b, Goldsmith et al. 1962,

Temp (°C)	$\Delta 2\theta$ $[2\theta_{(211)} - 2\theta_{s.d.}]$	Composition (mole %) $FeCO_3$	$MgCO_3$	$CaCO_3$
350	not measured	<25	—	—
400	2.03 ±0.01	30	16.5	53.5
450	1.950±0.005	33	13	54
500	1.934±0.005	34	11.5	54.5
550	1.890±0.01	36	9	55

Table 6-3 Data for end-member dolomites, taken from Rosenberg (1967, Table 1).

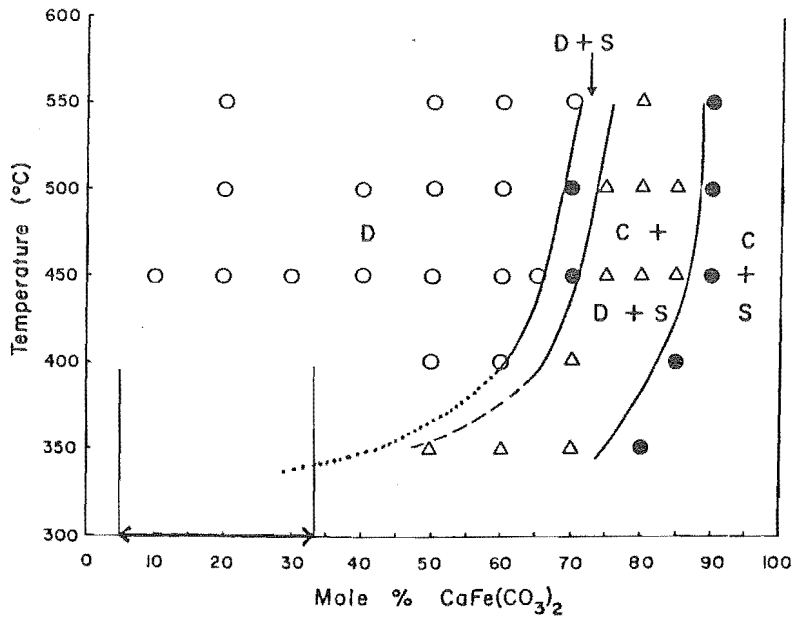

Subsolidus relations on the join $CaMg(CO_3)_2$-$CaFe(CO_3)_2$. D—dolomite solid solutions; C—Ca-rich solid solutions; S—Ca-poor solid solutions. Open circles, one-phase; filled circles, two-phase; and triangles, three-phase assemblages.

FIG. 6-11 Figure and caption adapted from Rosenberg (1968, Figure 1). The dolomite boundary, located by the data from the table above, has been extrapolated (dotted line). The trend of this boundary below 400° is indicated by the known trend of the adjacent boundary. These two curves should converge at lower temperatures; also indicated is the range of indicated dolomite composition for the Owen rocks and veins. The Fe-rich end of this range intersects the extrapolated curve just below the 350° isotherm. The dotted curve and the composition range are the only modifications to Rosenberg's figure.

TABLE 6-4

Determination of $CaFe(CO_3)_2$ in Dolomites, using the curve of Figure 6-10.

XRD No.	$\Delta 2\theta^*$	$CaFe(CO_3)_2$ mole %
Rocks		
19	0.015	5
8	0.03	8
20	0.08	21.5
12	0.10	26.5
16	0.10	26.5
18	0.10	26.5
17	0.11	28.5
10	0.13	33.5
21	0.145	37
11	0.15	37.5
22	0.153	38
26 (Burnet)	0.133	34
Veins		
30	0.095	6.5
33	0.13	33.5
29	0.130	33.5

*Peak shift

Rosenberg 1963), but little information dealing with calcite composition in ternary systems is available. Considerable uncertainty remains concerning the degree of substitution in the presence of other minerals. Harker and Tuttle (1955b) produced some limited data on the composition of calcites coexisting with pure magnesian dolomite, and an attempt to use these for determining metamorphic equilibration temperatures has been made by Barron (1974). Barron's work, originally presented as part of a PhD thesis, represents the only attempted application of carbonate geothermometry known to the writer. Regrettably, much of the reasoning in his paper is unclear, but the method was considered worthy of close examination with the intention of adapting the procedure to obtain geothermal information from the Owen calcites. A careful examination of Barron's publication revealed a number of serious errors which have apparently received no attention in the succeeding literature. A brief criticism is therefore considered justified, commencing with an outline of the geothermometric method used, as follows:

(i) Coexisting natural calcite-ankerite mixtures are analysed by X-ray diffraction, and peak shifts converted to maximum mono-substitution values (Table 6-5). The resulting $FeCO_3$ and $MgCO_3$ limits for the calcites are plotted as joins on a partial carbonate ternary (see Figure 6-12).

(ii) Temperature points are added to the $MgCO_3$-$CaCO_3$ margin of the diagram. These points are taken from Harker

Compositions of calcite-ankerite pairs

Sample number[a]	Calcite $\Delta 2\theta$	$FeCO_3$ (mole %)	$MgCO_3$ (mole %)	Ankerite $\Delta 2\theta$	$CaFe(CO_3)_2$ (mole %)	Amended values $FeCO_3$ (mole %)	$MgCO_3$
46225	0.78	2.5	4.3	2.15	44	2.3	1.8
46226	0.88	6.5	10.5	2.22	21	6.6	4.5
46227	0.77	2.3	4.0	2.22	21	1.9	1.5
46288	0.83	4.5	7.8	2.22	21	4.5	3.4
46118	0.79	2.8	4.9	2.22	21	2.8	2.1
46229	0.83	4.5	7.8	2.21	24	4.5	3.4

[a] Five figure numbers refer to specimens in the collection of Sydney University.

TABLE 6-5 From Barron (1974, Table 1), with amended values added (right-hand columns).

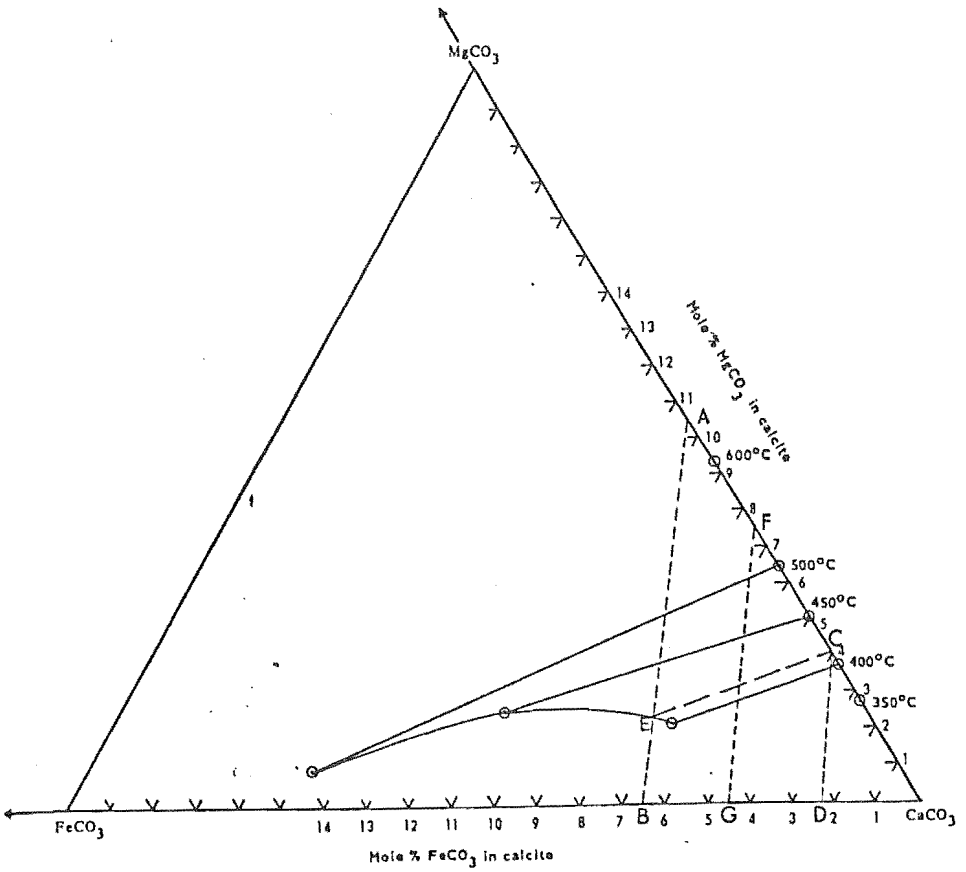

Solid solution limits of $FeCO_3$ and $MgCO_3$ in calcites co-existing with dolomite-ankerite at 400° C and 500° C (solid lines). *A–B* represents the maximum substitution limits of $MgCO_3$ and $FeCO_3$ in the Sofala calcites and *C–D* represents the minimum substitution limits. The overlap of these compositions occurs along the line *C–E* which coincides with the solvus isotherm of 415° C

FIG. 6-12 From Barron (1974, Figure 1).

and Tuttle's binary (Appendix III, Figure 2) and cover the range 300°-600°C, thereby requiring considerable extrapolation to lower temperatures from the original data which terminated at 500°.

(iii) Points are plotted for calcite end-members from Rosenberg's (1967) ternary diagrams for 400°, 450° and 500°C.

(iv) $MgCO_3$ isotherms are constructed between the three corresponding binary- and ternary-derived points.

(v) Obscure reasoning then follows in which the calcites with maximum and minimum substitution limits are considered to define corresponding ranges of possible equilibration temperatures which somewhat fortuitously overlap along a single isotherm, thus producing a temperature with a possible error limited to that arising from X-ray measurement uncertainties only.

Apart from the questionable validity of the final deductions, the work appears to be so affected by incorrect and inaccurate data that the results must be regarded as erroneous. Criticism of the principal defects may be summarised as follows:

(i) The maximum $FeCO_3$ in calcite values (Barron, Table 1) are inaccurate.

(ii) The $MgCO_3$ in calcite values (Barron, Table 1) are incorrect. Barron's table is reproduced as Table 6-5, together with amended values measured from Figure 1, Appendix III. That Barron's values are incorrect is

immediately apparent when the $MgCO_3$ levels are seen to be greater than the $FeCO_3$ levels. As the ionic radii of the metals involved are known to have the relationship Ca >Fe >Mg, less $MgCO_3$ than $FeCO_3$ is required to give the same calcite lattice dimensions.

(iii) The use of Harker and Tuttle's T-X data for magnesian calcite introduces considerable inaccuracy, the original values being given to the nearest 0.5 mole %. Goldsmith et al. (1955), who published a similar plot and discussed its possible use for geothermometry, considered the curve to be satisfactory only for calcites where $MgCO_3$ substitution is greater than 5 mole %. Barron's calcites all fall below this limit.

(iv) The values obtained by extrapolation of Harker and Tuttle's curve are doubtful. The curve becomes very linear below 550°C and to estimate the position by 'assuming a regular solution' (Barron 1974), considerable uncertainty must be incurred, which should be expressed by an error range in the final result.

(v) Measurements of ternary calcite compositions are described as being taken from Rosenberg's (1967) Figure 4, which is reproduced as Figure 4, Appendix III. Barron re-plots these points on the partial ternary to the nearest 0.1 mole %. To estimate the position of the three-phase triangle calcite apices to such a degree of precision is unjustified, especially as these positions vary between Rosenberg's own diagrams (Rosenberg 1967, Figures 1,3,4).

(vi) Barron (1974) does not consider the effect of $MnCO_3$, nor even quote the degree of Mn substitution in the calcites.

(vii) The experimental data are derived from systems which were rapidly quenched. No consideration is given to the possibility of reaction reversibility and continued re-equilibration during declining temperatures.

(viii) A considerable spread in calcite composition is exhibited by only six samples. As the total range of calcite composition is important to Barron's method, it appears that a greater number of analyses would have markedly altered the final estimation.

This work cannot, therefore, be accepted as a model of calcite geothermometry for the Owen samples. The apparent reluctance of other workers to attempt such geothermometry supports the view that the data are inadequate for a satisfactory understanding of the T-X relationships, particularly below 500°C where most hydrothermal carbonate suites originate. Further development of ternary data would be useful, especially for $FeCO_3$ substitution which has a higher composition vs. temperature gradient than that of $MgCO_3$. (Appendix III, Figure 3).

The comparatively low degree of substitution for the calcites of Table 6-2 is not unexpected, as these samples were considered to represent low-temperature veins and relatively pure carbonate lithologies. The indicated calcite substitution for other veins and rocks (Table 6-1) is

also low, and if the T-X information from the $CaCO_3$-$FeCO_3$ and $CaCO_3$ binaries is accepted as an approximate indication of natural systems, one of the following processes is suggested:

(i) Low Fe or Mg concentration caused a deficit of these metals in the systems in which the calcites deposited or equilibrated.

(ii) The calcites suffered retrograde equilibration at lower temperatures.

In either case, the condition would be accentuated by Fe-consuming reactions which would compete with calcite for the available Fe. As suggested in Chapters V, and VI pt. I, such reactions may have been common in the Owen rocks. Operation of process (ii) is further supported by the indication that dolomites may be relatively metastable at moderate and low temperatures (Goldsmith et al. 1962). The relatively pure vein carbonates would be less affected by either of the above processes, being formed in a chemical system which is comparatively open during deposition, and almost completely closed afterwards. No exsolution of dolomite (Goldsmith et al. 1955) was confirmed, and the peaks are sufficiently well defined to provide an accurate indication of substitution. If the depositional systems were not deficient in Fe and Mg, it would appear that most hydrothermal calcite deposition occurred at low temperatures, below approximately 200°C.

Were there sufficient data available for satisfactory

interpretations, carbonate studies would be ideally suited to electron probe microanalysis. Determination of substitutions within a single beam spot to avoid the contamination problems of bulk analysis would provide a useful support to X-ray analysis, and possibly promote a better understanding of the interrelation of coexisting natural carbonate minerals.

(4) Aragonite

As noted in Chapter V, a single specimen of vein aragonite was found near old mineworkings at Uno Creek. This mineral occurred as an open-space filling, producing drusy fracture coatings of acicular crystals. An origin from either late hypogene or supergene processes is possible, aragonite being known from both low-temperature hydrothermal suites, and those produced by secondary alteration of ore deposits and dolomitic or other magnesian rocks. If hypogene, the deposition of this mineral probably represents a very late hydrothermal stage, the most favourable range of aragonite crystallization being regarded as 50° to 80°C (Deer, Howie and Zussman, 1962b).

(5) Biaxial Calcite

Thin sections of carbonate lithologies from the lower Arthur Marble and Owen Formation contained a number of calcite grains displaying a distinct biaxial character. This property was confirmed and measured with a universal

stage by David Shelley* (pers. comm.), who interpreted the occurrence as possible evidence of inversion of high pressure metamorphic aragonite. This view was proposed in a publication (Shelley, 1975), quoting the occurrence as a personal communication from the writer (this work). Shelley's interpretation was not supported by the writer, since lack of other evidence for such extreme pressure or burial was considered to conflict with, although not disprove, the pre-existence of metamorphic aragonite.

Biaxial calcite has been attributed to several other causes; these are now listed and reviewed by Turner (1975), who recognises strain as the only origin, and states, '... there is nothing to suggest that natural inversion of aragonite to calcite favours biaxiality in the latter'.

* Metamorphic Petrologist, Geology Department, University of Canterbury.

III. SILICATES

(1) Metamorphic Silicates

(a) Wangapeka formation and Arthur Marble. These units show very little mineralogical alteration, which is surprising when the proximity and size of the nearby granite batholith is considered. Recrystallization, degradation of clay minerals and the growth of minor sericitic mica and rare chlorite are the only changes which can be considered metamorphic, and no useful indicator of pressure-temperature conditions is recognised.

(b) Owen Formation. Within the rocks beneath the marble, the range of silicate mineralogy is comparatively restricted, but evidence of thermal metamorphism is recognisable. The following minerals are assigned to this origin.

(i) Biotite. This mica is found only in the impermeable dolomitic horizons, and is occasionally abundant, but always subordinate to muscovite. Small biotite flakes, up to approximately 0.1 mm, are visible in thin section and cause a recognisable shift in the basal mica x-ray diffraction peaks.

(ii) Muscovite. White mica is the most widespread silicate within the Owen Formation, being common in all rock types. Except in hydrothermal veins, the grain size rarely exceeds 0.1 mm, therefore the mineral falls within the classification sericite (Winchell 1951). The extent of muscovite development during metamorphism is difficult to ascer-

tain. Deer et al. (1962a) conclude that muscovite is comparatively uncommon in thermal metamorphism, but is favoured by water-rich conditions. The bulk of the sericitic, permeable lithologies can be related to a history of alteration in which sericitisation was the principal reaction.

(iii) Chlorite. A metasomatic-hydrothermal origin also accounts for most of the chlorite occurring in the rocks of the Owen Formation, but some rare examples are characteristic of thermal metamorphism. A stream boulder of carbonate-rich mudstone shows porphyroblastic chlorite in thin section, wherein the porphyroblasts appear to enclose a fabric which has been cross-cut by a weak schistosity (see Ch. III). The outcrop is unknown, but the lithology is representative of the middle-to-lower Owen Formation. Traces of chlorite seen in the Enterprise Dolomite and adjacent units may also have a thermal metamorphic origin.

(iv) Chloritoid. This mineral is restricted to the extreme eastern exposures of the Owen Formation, near the summit of Golden Crown Hill where it occurs as porphyroblasts consisting of anhedral crystals, and radiating, twinned laths. The assistance of Dr. D. Shelley is gratefully acknowledged in identifying this mineral in thin section. X-ray diffraction produced a pattern consistent with this identification.

A study of the occurrence of chloritoid by Halferdahl (1961) indicates that although a metasomatic origin is pos-

sible, isochemical metamorphism to greenschist grade is the common environment of formation. Chlorition is recognised as an important marker of low to middle grades of metamorphism (Winkler 1967, p.94), but very little is known regarding the minimum conditions of formation. Halferdahl sees chloritoid as 'one of the earliest new minerals to develop in either regional or contact metamorphism', but indicates only an approximate correlation of the mineral's appearance with lower greenschist conditions. Although the effect of pressure is uncertain, formation temperatures exceeding ca. 380°-400°C are inferred. Chloritoid is a relatively uncommon mineral, developing in rocks of a restricted chemical composition. Such lithologies are rich in Al_2O_3 and FeO components, and contain little SiO_2, CaO, MgO, or other alkalis. The occurrence at Golden Crown Hill is surprising in view of the abundant quartz in the country rock, and of the nearby dolomite-calcite lenses. The occurrence of chloritoid, as described and illustrated in Chapter III, appears to predate cleavage, and cannot be related to stress. This is consistent with Halferdahl's conclusion that chloritoid is not a stress-induced mineral, but conflicts with Grindley's (1971) report of the association of chloritoid with shear zones in other areas of Rangitatan plutonism. Local variations in the abundance of chloritoid in the Pikikiruna Schist have been attributed to differences in both bulk composition and contact metamorphic conditions (Ghent, 1968).

Chloritoid appears to be the highest grade metamorphic indicator occurring in the Owen Formation, common associate minerals, e.g. staurolite, being absent. The possibility of the destruction of such minerals must be considered, in view of the evidence of retrogressive metamorphism.

(c) The Contact Zone. The thin strip of contact-metamorphosed sediments at the western margin of the granite contains a high temperature 'skarn' mineral suite. Over approximately 100 metres, a progression may be traced from recrystallized marble to mafic-rich, foliated granite. Recognisable structure within the marble remnant indicates that sedimentary layering is orientated sub-parallel to the intrusive margin; the pattern of progressive alteration with decreasing distance to the contact is therefore complicated by the original lithological variations. The rocks within this zone have been examined only briefly, and are considered to be of little importance to the mineralization or metamorphic history of the principal block of sediments further west. Thin sections revealed the following minerals:

(i) In marble; garnet, diopside, epidote, muscovite.

(ii) In schistose hornfels, closer to the granite contact; biotite, ?clinozoisite, zoisite, hornblende, diopside, tremolite, sillimanite, scapolite, microcline, Ca-rich plagioclase, sphene.

The foliated granite, which grades westward into diorite, contains characteristic biotite, hornblende, sphene and apatite and forms a thin zone traceable along the entire

length of the faulted western granite margin in the Owen area, irrespective of whether metasediments are present or absent. A marginal contact-assimilation zone is inferred. It is notable that major fault movement has followed this contact zone very closely.

The lack of continuity of Paleozoic rocks between the granite and the goldfield is unfortunate. Further evidence from pelitic rocks within the intermediate aureole would have assisted the investigation of the metamorphic history of the Owen Formation.

(2) Post-Metamorphic Silicates

This section refers to the Owen Formation only, as the rocks from other units contain insignificant post-metamorphic minerals. Chlorite and white mica are the only silicates which can be directly associated with the stage of hydrothermal deposition and alteration. The composition and distribution of these mineral groups has been investigated by means of x-ray diffraction.

(a) White Mica. The most obvious mineral of hydrothermal association is sericite, which is abundant within and near the orebodies, and which defines the sericite zone (Chapter III). Diffraction patterns for the sericitised country rock closely resemble those of the more highly altered wall rock adjacent to the veins. The x-ray indicated composition was that of muscovite, and although the polymorph type could not be ascertained, the 2M configura-

tion is considered most probable.

The distribution of the micas is illustrated by the low-angle diffraction data for a suite of specimens (Table 6-6). Diffraction traces from a selection of these samples are reproduced (Figure 6-13), representing a range of rock types extending from the Enterprise Dolomite, through sericitised country rock to wall rock from the Enterprise Mine. These data are most readily appreciated by examining the 10 Å peaks of the six diffraction traces shown in Figure 6-13. The uppermost trace (3) has a large peak at 8.7° due to biotite; the other five, representing a sequence from sericite zone country rock to vein mica, all show a prominent muscovite peak at 8.8-8.9°. Samples from near the veins (6,8) show an additional peak near 9.2° due to coexisting paragonite, but coarse-grained mica intergrown with hydrothermal quartz and carbonate from the veins shows only muscovite peaks. Both Table 6-6 and Figure 6-13 show evidence of a progressive shift in the principal basal reflection peaks for the white micas with increasing proximity to the vein systems, indicating a compositional trend. Following the method of Zen and Albee (1964), the composition of white mica can be determined by interpolation on the muscovite-paragonite linear regression, using d(002) values. Composition is expressed as a ratio of interlayer alkalis (Table 6-6, column 5). Sericites from near the vein walls show a decrease in K in favour of Na (and/or Ca); coexisting paragonites show an increase in K. The coarse vein

TABLE 6-6

10 Å Peak XRD Data from Representative Samples, Owen Formation

Sample No.	Description		$^{\circ}2\theta_{(002)}$*	$d_{(002)}$	$\frac{K}{K+Na+Ca}$	Other Minerals Present
1	Chloritoid-bearing country rock, Trig GC	(Mu)	8.80	10.05	~1	Qtz, Dol, Ctd
2	Enterprise Dolomite	(Bt+Mu)	8.80	—	—	" " tr. Chl
3	" "	(Bt)	8.75	10.107	—	" " "
4	" "	(Bt)	8.75	10.107	—	" " "
5	Chloritic carbonate above Enterprise Dol.	(Mu+Bt)	8.76	—	—	" Cal, Chl
6	Sericite zone, near Enterprise Mine	(Mu)	8.85	9.99	0.92	Cal, Dol, tr.Chl
7	" " " " "	(Mu)	8.85	9.99	0.92	" " Chl
		(Pa)	9.20	9.614	0.01	
8	Wall rock, Enterprise mine.	(Mu)	8.87	9.97	0.85	" " "
		(Pa)	9.17	9.645	0.09	
9	" " " "	(Mu)	8.90	9.94	0.76	" " "
		(Pa)	9.10	9.72	0.25	
10	Coarse vein mica, Enterprise Mine	(Mu)	8.90	9.937	0.76	
11	" " " , float	(Mu)	8.93	9.904	0.69	
12	Vein chlorite, Enterprise Mine - See Tables 6-8, 6-9					
13	" " " " " " "					

Abbreviations: Mu-muscovite Pa-paragonite Bt-biotite Qtz-quartz
Dol-dolomite Cal-calcite Chl-chlorite Ctd-chloritoid tr = trace

* Assuming 2M stacking configuration.

FIG. 6-13 Partial X-ray diffraction traces for six samples from the Owen Formation. Samples (11) and (13) are vein minerals (see Tables 6-8, 6-9), the others are country rocks. For description and composition of samples see Table 6-6 and text. Samples run at 1°/minute, Cu kα radiation.

FOLD OUT ⟶

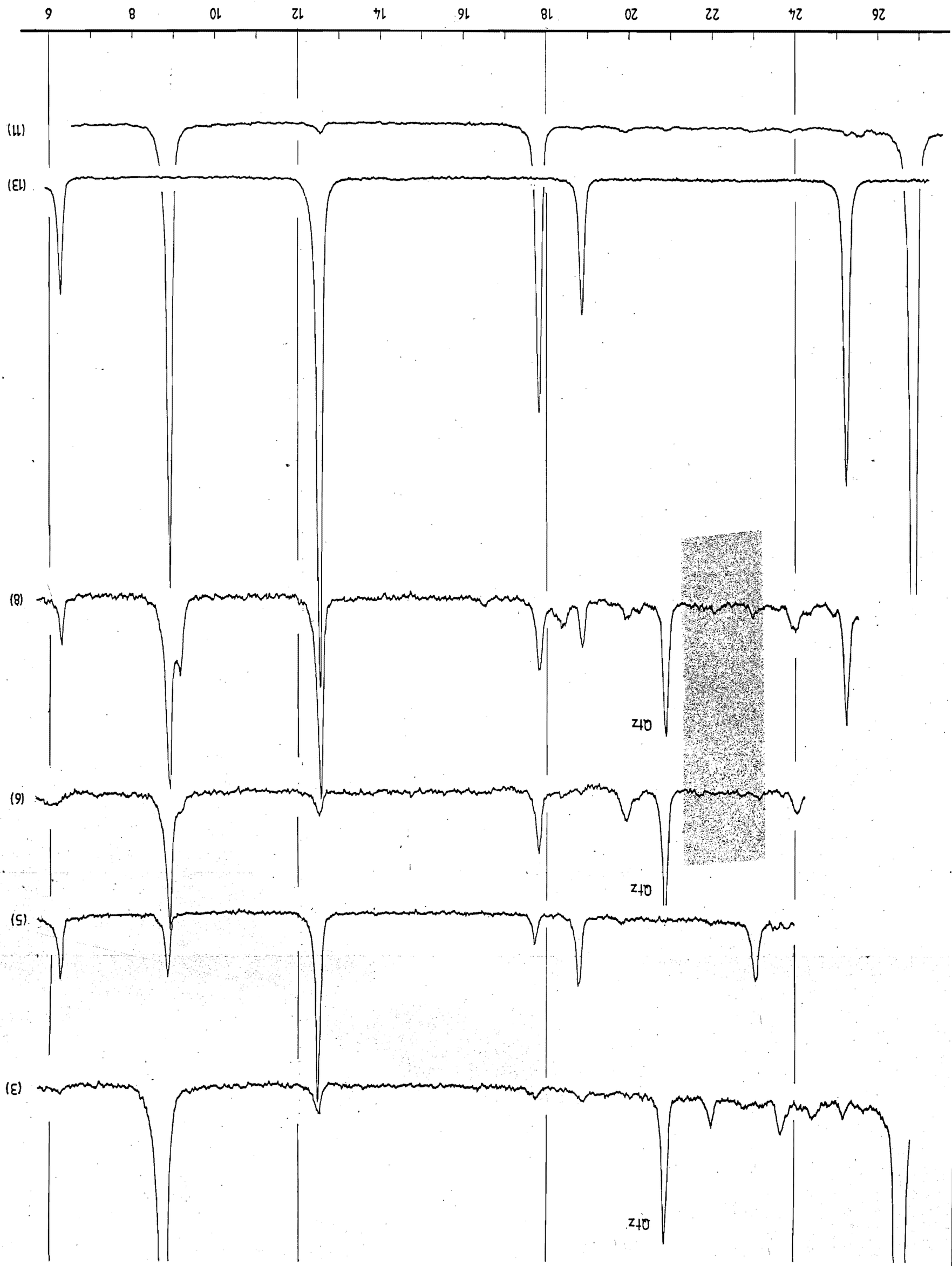
6
8
10
12
14
16
18
20
22
24
26
(11)
(13)
(8)
QTZ
(6)
QTZ
(5)
(3)
QTZ

micas, occurring as colourless to pale green flakes, show no paragonite peaks but consist of muscovite with extreme K substitution by other alkalis. The x-ray pattern for this mica is unlike any published patterns, possibly due to the highly paragonitic composition. The low-angle diffraction data for this mineral are presented in Table 6-7.

(b) Chlorite. As described in previous sections and as shown in Table 6-6, chlorite is widespread in and near the sericite zone, and abundant in the vein systems, both as a constituent of the altered wall rock and as a vein mineral. A noticeable spread in the chlorite diffraction pattern characteristics emerged when many different samples were studied. An attempt was made to investigate chlorite composition by the method of Schoen (1962), whereby both peak position and peak intensity are considered as follows:

(i) Structure factors are derived for the basal 001, 002, 003, and 004 reflections, in accordance with the expression

$$I = |F|^2 \ (L.P.)$$

where I = peak intensity, $|F|$ = structure factor, and L.P. = a combined Lorentz and polarization factor, which for a goniometer and powder mount is equivalent to

$$\left(\frac{1 + \mathrm{Cos}^2\, 2\theta}{\mathrm{Sin}^2\theta \ \mathrm{Cos}\,\theta} \right)$$

and is therefore a function of peak angle.

(ii) Ratios of F_{003}/F_{001} are compared with a table of theoretical values calculated by Schoen, and new values obtained for these structure factors. This permits the com-

putation of a scale factor, i.e.

$$\frac{F_{001}\ \text{(theoretical)}}{F_{001}\ \text{(calculated)}} \quad \text{and} \quad \frac{F_{003}\ \text{(theoretical)}}{F_{003}\ \text{(calculated}}$$

(iii) From these ratios (which should be similar in value), an average is taken and used as a multiplier to derive theoretical values for F_{002} and F_{004}. The values so obtained are applied to a table prepared from chlorites of known composition (Schoen 1962, Table 1) and the atomic Mg/Fe ratio found by interpolation.

Using this method, compositions were calculated for nine chlorite samples (Table 6-9). The results are disappointing due to the inconsistent values indicated by the final theoretical structure factor pairs. The cause of this inconsistency is not apparent, but possible sources of error are as follows:

(i) Method. Schoen's method may not be applicable to all chlorites; absorption or enhancement effects may have occurred beyond the limits considered in earlier treatments of the subject.

(ii) Measurement. An unidentified error may be incurred from the geometrical layout of the sample radiation and diffractometer system. Careful checking of sample size, sample thickness, beam dimensions and goniometer calibration suggests that such an error is unlikely to exist.

(iv) Compositional range. A variation in chlorite composition within each sample may have led to anomalous peak heights and peak positions, although this is unlikely to have

TABLE 6-7

XRD data for Vein Mica, UC8897

(See Table 6-6, sample 11)

$^{\circ}2\theta_{Cu\ k\alpha}$	d Å	I
8.90	9.94	45
17.84	4.97	28
26.85	3.32	>100

Trace not measured beyond 31° .
No other peaks in this range above I=2

TABLE 6-8

XRD data for Vein Chlorite, UC8900

(See Table 6-6, sample 12)

$^{\circ}2\theta_{Cu\ k\alpha}$	d Å	I
6.23	14.19	21
12.49	7.09	100
18.82	4.715	34
25.20	3.534	80

Trace not measured beyond 28°
No other peaks in this range above I=2

TABLE 6-9

Fe/Mg content of Chlorites as estimated by the XRD method of Schoen (1962). Sample numbers are as given in Table 6-6.

XRD No.	Description	No. of Fe atoms in octahedral positions. (Fe+Mg=12) F_{002} basis	F_{004} basis
2	Enterprise Dolomite	2.6	7.1
4	" "	3.2	6.0
5	Chloritic carbonate overlying " "	4.0	≥12
6	Sericite zone near Enterprise Mine	3.6	not measured
7	" " " " "	4.6	≥12
8	Wall rock, Enterprise Mine	3.5	6.6
9	" " " "	2.0	4.7
10	Vein mica*, " "	1.9	~12
12	Vein chlorite " "	4.6	12

*Trace of chlorite occurring with mica.

affected every result.

The indicated compositions are therefore of doubtful value. The Fe levels indicated by the F_{004} factors appear unacceptably high, and the levels from F_{002} are probably the more correct. These results may be correct in proportion, if not in absolute value. A calibration and test of the method would be possible if a chlorite of known composition was used as a standard. Such a chlorite was not available at the time of analysis. Sample 12 consisted of pure hydrothermal vein material, appearing dark green and pleochroic in thin section. A high Fe content is therefore expected. This sample produced a strong, sharp diffraction pattern, the data for which are given in Table 6-8 (cf. sample 13, Figure 6-13).

(c) The Origin and Significance of the Post-Metamorphic Silicate Assemblage. The close association of the muscovite and chlorite with the veins indicates a hydrothermal origin for these silicates. Similarly, the compositional trends noted are consistent with hydrothermal activity. The widespread development of sericite is the principal evidence for pervasive K-metasomatism, the paragonitic mica near the veins being a product of local Na-metasomatism. Under such conditions, a large range of precursor minerals could have contributed to the formation of the sericite-chlorite assemblage. Feldspars and clays are the most obvious reactant minerals in this respect, and their absence from the Owen Formation is notable. Biotite is also absent, except in the

Enterprise Dolomite. Deer et al. (1962a) indicate that the breakdown of biotite commonly contributes to the growth of both chlorite and sericite. Schwartz (1958) considers biotite to be a sensitive indicator of hydrothermal alteration, being one of the first minerals to show the effect. Surplus iron may be taken up as sulphide. The absence of quartz in many parts of the sericite zone may be due to the same metasomatic process, and suggests either removal of silica or the introduction of alumina if a feldspathic protolith is assumed.

(3) Discussion

Evidence of the metamorphic event in the Owen rocks is poor, with no definitive indication of maximum metamorphic conditions. The known metamorphic assemblage only generally indicates lower greenschist facies. Some constraints on the geochemical environment may be inferred because of the absence of certain minerals. The rocks of the goldfield contain no evidence of the formation of many of the common silicates of thermally metamorphosed carbonate rocks. The absence of talc, tremolite, diopside, wollastonite, etc. indicates that P_{CO_2} values were sufficiently high to stabilise the reactant assemblage (Skippen, 1974). The stability field of the metamorphic Ca-Mg silicates is further restricted by other mineral components. Gordon and Greenwood (1970) note a tendency for any available alumina and potash to favour the formation of chlorites and micas in preference

to other silicates. They report that '... even small activities of component $KAlSi_3O_8$ are sufficient to eliminate the stability field of talc in favour of phlogopite'. Although no phlogopite has been detected in the Owen rocks, chlorite appears to be the stable Mg-silicate.

Field evidence requires the biotite-chlorite-chloritoid assemblage to be a product of thermal metamorphism near the outer margin of the granite aureole. No evidence of earlier metamorphism can be recognised. Subsequent hydrothermal activity has undoubtedly obscured the evidence of earlier processes. The widespread metasomatism will have caused an overprinting effect, especially in the more permeable lithologies. There is doubt as to which event some minerals should be assigned. Much of the finely distributed chlorite could be due to either late metamorphism, or metasomatism. In either case, the originating environment was relatively hydrous. As both thermal metamorphism and hydrothermal activity are considered to result from granite intrusion, a continuous process of rock alteration probably took place, with 'metamorphic', and 'hydrothermal' events being only the extreme end-members of this process. An embracing term to describe the net alteration may be <u>hydrothermal metamorphism</u>, as used by Coombs (1961), i.e. 'Reconstitution confined to zones through which heated fluids are observed or inferred to have moved.'

The later hydrothermal silicates are well preserved, and reflect the operation of intense Na-metasomatism near

the active conduits. The paragonitic vein micas and the composition of coexisting muscovite-paragonite indicates the effect of local elevated temperatures (Eugster 1956). Due to the complications of the chemical systems involved, and the limited thermochemical data, no numerical estimate of temperature is drawn from this assemblage.

CHAPTER VII

EVIDENCE FROM FLUID INCLUSIONS

Introduction

The lack of good mineralogical temperature indicators and the abundance of veins at Owen prompted a search for fluid inclusions in an attempt to obtain some direct information on mineralization temperatures. This was originally intended to be a brief investigation, but to obtain useful information the work had to be greatly extended to overcome problems of laboratory technique and data interpretation. This work now comprises a major part of the entire project, and has been the subject of some minor publications and conference papers (Newman, 1975, 1976, 1977). Appendices IV, V, and VI (this work) contain additional information concerning the partial analysis of inclusion fluid, thermodynamic calculations for the fluid systems, and techniques of investigation.

At the time of writing, studies involving fluid inclusions remain uncommon, and this project is the first such study to be undertaken at the University of Canterbury. Because comparatively little is known about this specialised subject, a brief outline and discussion of the theory is given. Readers seeking a more complete introduction should

refer to the authors cited, and in particular the contributions by Edwin Roedder (1962b, 1967, 1972).

I. FLUID INCLUSION THEORY

(1) Basic Principles

Fluid inclusions are portions of fluid trapped within a mineral substance during its formation or reconstitution. They usually occur in the form of minute subspherical cavities a few microns in diameter, and rarely range up to naked eye visibility. The host substances are commonly crystalline hydrothermal minerals, which can trap inclusions when crystals grow or recrystallize. Portions of a surrounding fluid phase are trapped, either internally as large ingrown defects, or interstitially as cavities at crystal interfaces. Vein minerals frequently exhibit a very high density of fluid inclusions, particularly in the case of quartz for which the common milky translucence is evidence of their abundance.

When viewed at room temperatures, most fluid inclusions can be seen to contain a vapour bubble, which is formed by differential contraction when the liquid and host crystal cool from the temperature of formation. More than 100 years ago, the pioneering petrologist H.C. Sorby recognised this property as a means for using liquid inclusions as geothermometers (Sorby, 1858). This concept forms the basis of the homogenization method of geothermometry, undertaken by heating liquid-vapour inclusions and observing the disappearance of the vapour bubble with a hot-stage microscope adapted for the task.

The validity of all geologic evidence interpreted from the properties of fluid inclusions is primarily dependent on the validity of a single basic assumption; that the inclusions represent small portions of the original hydrothermal (or metasomatic) fluid, which have remained as closed microsystems since the time of sealing.
This embraces a number of secondary assumptions, specifically that none of the following have occurred:

(i) Leakage of inclusion fluid.

(ii) Reaction of fluid with host.

(iii) Deposition or adsorption of fluid components.

(iv) Change in inclusion volume.

In the case of quartz (the only mineral used in this study) it can be demonstrated that these effects are usually absent or insignificant.

(2) The Effect of Pressure

The hydrostatic pressure at the time of entrapment is a major factor which must be taken into account if the fluid inclusion geothermometer is to be properly exploited. Inclusions at room temperature have a liquid-vapour phase ratio which is a function of the fluid density at the time of sealing, which in turn is determined by the coexisting temperature and pressure, and also the fluid composition. Vapour filling of $<50\%$ at $0°C$ is most common, but vapour contents up to 100% have frequently been recorded.

The relation of inclusion phase ratios to liquid or gaseous sealing systems is illustrated by the two graphs

reproduced overleaf. The first (Figure 7-1), from Yermakov (1965), shows calculated curves for the 'degree of filling' versus temperature for hypothetical inclusions containing pure water. A given liquid-vapour ratio initially at 0°C will move up a path similar to one of the plotted curves as the temperature is raised. Those with more than 68% vapour at 0°C will proceed to the left, to a homogenous gas phase, while those with less initial vapour will advance to the right to homogenize as liquid-filled. Above the critical temperature (374°C) only the vapour state can exist. The compositional region about the 68% vapour point is termed the 'critical density'. On heating to the critical temperature, inclusions of this composition homogenize by phase boundary disappearance to vapour without progressive filling ('critical point homogenization').

Figure 7-2, taken from Roedder (1972), shows the phase ratios of inclusions of various degrees of filling, together with isobars and a boundary separating the two-component and one-component fields. The inclusions represented were all sealed at 540°, but at different pressures. The diagram differs from Figure 7-1 in that the horizontal axis represents inclusion density, i.e. total mass/volume. The graph of Figure 7-2 appears in an earlier publication (Roedder 1967) with the horizontal axis erroneously labelled V_L/V_L+V_G. This expression, which describes the 'degree of filling' applies to the horizontal axis of Yermakov's graph, the abscissae of Figures 7-1 and 7-2 being equivalent only at the 0°C points.

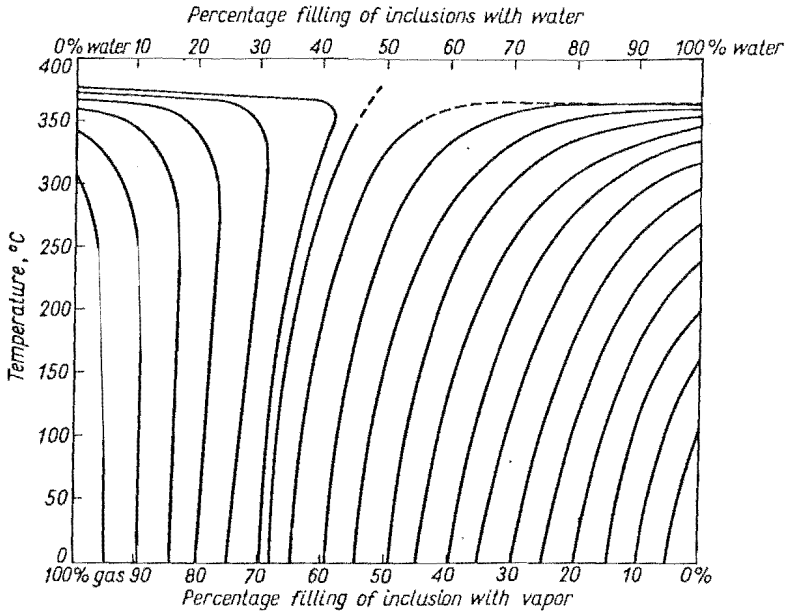

FIG. 7-1 Filling vs Temperature plot, drawn from experimental data. Reproduced from Yermakov (1965).

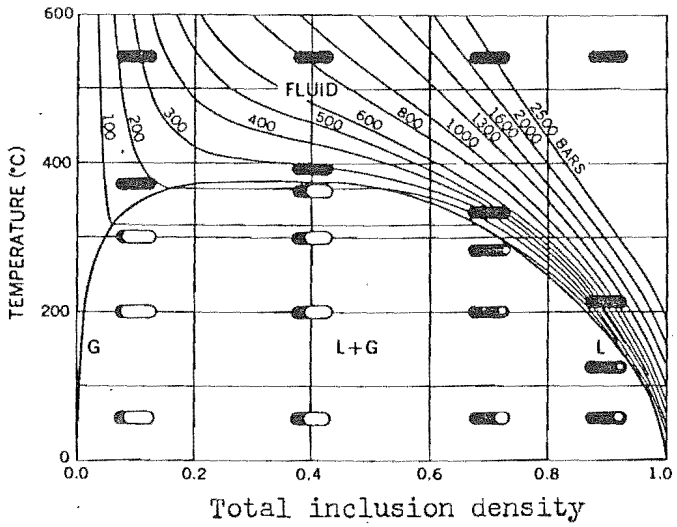

FIG. 7-2 Density vs. Temperature plot showing the filling progress of five different inclusions. From Roedder (1972). See discussion in text.

To enable a better understanding of the two figures described, the data from both are combined in Figure 7-3, plotted on Roedder's axes. The paths from Yermakov's graph now plot as straight, vertical lines within the L+G field, terminating at the phase boundary at the corresponding homogenization temperatures and pressures.

This dome-shaped boundary is termed the 'boiling curve' and describes the density of boiling water (right-hand side) or condensing vapour (left-hand side). Isobars show vapour pressures at the points of intersection with the curve. With respect to pure water, this curve marks the appearance of a second phase in cooling inclusions, the pressure and temperature conditions at the time of sealing having determined the density. Above the curve, where confining pressure exceeds equilibrium vapour pressure, compression of the fluid occurs. This results in a close isobar spacing at the dense, 'liquid' end of the fluid field (blue zone, Figure 7-3). Inclusions sealed in conditions above the curve will homogenize at the curve, at temperatures less than those of trapping.

Homogenization therefore merely provides a convenient measurement of inclusion density by showing the temperature at the 100% filling point. The sealing temperature can be determined only if the sealing pressure, and hence the displacement above the curve, is known, thereby providing a positive correction for the homogenization temperature. The pressure value is commonly established by some independent means, e.g. depth of formation. Frequently, no pressure information at all or only minimum pressure limits are avail-

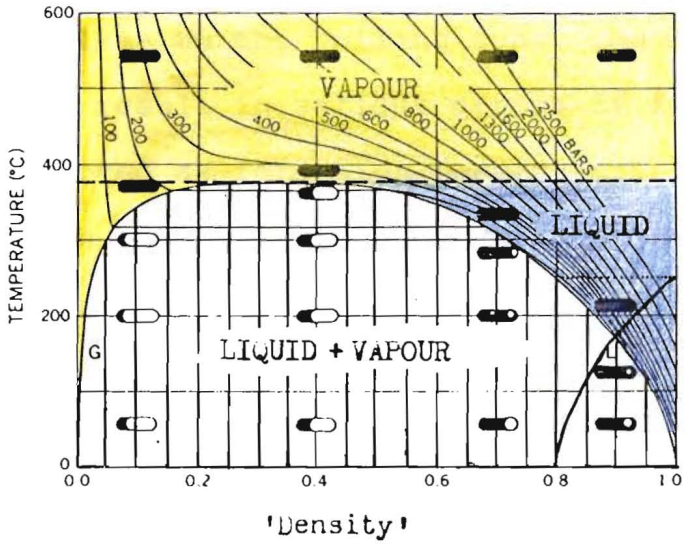

FIG. 7-3 Combined data from graphs by Yermakov and Roedder (Figures 7-1, 7-2). T_c = Critical temperature of water. See discussion in text.

able, giving rise to corresponding minimum formation temperatures.

Unless evidence exists indicating that a set of inclusions formed close to the boiling zone, the lack of pressure correction may result in serious errors if filling temperatures are accepted as formation temperatures. From the converging pattern of the isobars, it will be noted that the pressure correction is less at lower temperatures. Filling temperatures and pressures alone, however, are not sufficient for geothermometry. Fluid composition is the third important factor, as discussed in the succeeding section.

(3) The Effect of Fluid Composition

For simplicity, the discussion so far has dealt with the case of pure water; that is, the one-component system H_2O. Analysis of natural specimens shows this to be only the major component of more complex systems, as does sampling of active geothermal waters. In Sorby's time, crystalline solids were seen in fluid inclusions, and correctly interpreted as salts crystallised from the cooling, saturated fluid after trapping. Much work has been done on identifying these minute crystals ('daughter salts') from optical studies and shape recognition. Oxides, sulphides, sulphates, and carbonates have been recorded but Na and K chlorides are by far the most common. Of these, NaCl usually far exceeds KCl, and total fluid salinity is often quoted as NaCl equivalent.

As solutes change both vapour pressures and fluid compressibility from that of the pure solvent, the magnitude of

this effect must be known if pressure correction is to be applied to filling temperatures. The representative system H_2O-NaCl has been studied in detail, and a set of graphs were prepared by Lemmlein and Klevtsov (1961) to determine filling temperature corrections (See Appendix V).

At higher pressures, dissolved gases may become significant components. Both CO_2 and H_2S assume this role, and simple hydrocarbons have also been noted in inclusions (Roedder, 1963, 1972). The combination of both salts and gases with water as inclusion fluid results in complex systems, which will be discussed in a following section.

(4) The Identification and Estimation of Fluid Components

Known methods are subdivided under the headings shown below. Discussion here is limited to a brief outline, but almost all these techniques are presented in detail in Roedder (1972), which is devoted entirely to the subject of inclusion composition. Technical data for the methods used in this project are included in the appendices.

(a) Direct analysis. This involves opening the inclusions and extracting the contents, and is limited to relatively large inclusions if quantitative analysis of all major components is to be achieved. Practical difficulties are presented when minute quantities of material are involved, particularly for gaseous components. As with all microanalysis, contamination and detection limits are the restricting factors. Improved technology has greatly exten-

ded the analytical limits, with mass spectroscopy, electron probe and neutron activation methods now being used.

(b) Thermal cycling. Both heating and cooling methods can be listed under this heading, which covers all techniques involving direct observation of inclusion contents. Ordinary observation at room temperatures can be regarded as a special case. A broad subdivision of observed effects is as follows:

(i) Critical phenomena. True homogenization at a critical point is a rare occurrence, but inclusions covering a wide range of densities may homogenize very near the critical temperature (note the convergence of the homogenization curves in Figure 7-1 and the corresponding flat top of the phase boundary, Figure 7-2). When critical point behaviour can be recognised, information can be gained regarding fluid composition. Some components, e.g. immiscible liquids, may exist individually pure enough to permit identification by the recognition of characteristic critical temperatures (see Table 7-1). The composition of simple two-component mixtures may be measured from the elevation of critical temperature. The most common example of this effect is provided by saline water, where the rise in critical temperature not only permits the measurement of salinity, but also extends the useful limits of homogenization. If the critical point is observed, the salinity measurement is absolute; otherwise minimum values are indicated (Figure 7-4).

(ii) Subcritical Phase changes. When a fluid cools

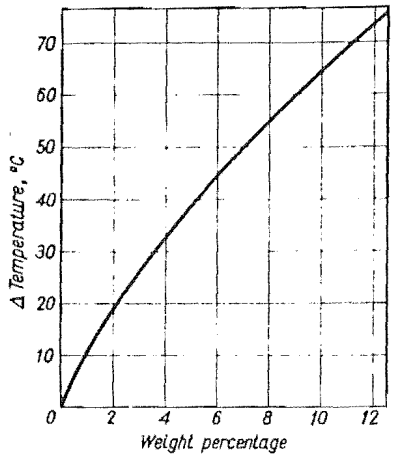

FIG. 7-4 Increase in critical temperature (ΔT_c) for aqueous solutions of NaCl (or similar univalent salts). Taken from Yermakov, (1965).

Table 7-1 Pure Substance Critical Temperatures of some Inclusion Components.

H_2O	374.2°C
H_2S	100.4°
CO_2	31.0°
Ethane	32.3°
Methane	-82.1°

after trapping, phases other than vapour bubbles may appear. As the development of such phases may be delayed by supersaturation, temperature measurements in practice are always made during heating, which therefore reverses the natural order of appearance.

Daughter salts may appear before the vapour phase on cooling, providing an improved 'minimum' value for temperature, and also a corresponding pressure, as the salinity can be estimated from temperature-solubility data. Methods for identifying salt crystals are predominantly based on crystallography, but for larger specimens optical properties can be used. When several salt species are present as crystals, these can often be distinguished by their order of disappearance on heating, in response to their relative solubility.

Cooling cycles may nucleate liquid, vapour or solid phases. So many possible combinations exist that there is insufficient space in this treatment to describe them all. Roedder (1962a, 1963, 1972) records and discusses many types. Of some importance are the solid phases, which appear at low temperatures as 'freezing' products. The most common of these is ice, which reveals the solute concentration from the depression of freezing point. This is the basis of a standard method for establishing the salinity for use in applying pressure corrections to filling temperatures. This method is prone to error, for dissolved gases may be present in concentrations sufficient to contribute significantly to the lowering of freezing point (see Browne et al.,

1975).

Higher concentrations of dissolved material may lead to the formation of hydrates, which, if distinguished from the ice, may provide useful information on the nature and concentration of the parent solutes. Halides and CO_2 are the most common hydrate formers in inclusions: CO_2 in this role is discussed later.

(c) Miscellaneous methods. Some specialised, non-destructive techniques do not fall into the two categories listed above, although they are occasionally combined with the methods outlined there. Infra-red spectroscopy is one such technique, whereby bonds characteristic of certain compounds are recognised in the inclusion fluid. Similarly, Raman spectroscopy uses back-scattered radiation, with a recent adaptation being laser beam excitation, giving an improvement in resolution and sensitivity (Rosasco et al., 1976). Finally, there are magnetic field methods for identifying magnetic or high magnetic susceptibility solids which sometimes occur as daughter products.

(5) The Genetic Classification of Fluid Inclusions

Most fluid inclusion studies have as their objective the derivation of geothermal conditions at the time of sealing. Application of the inclusion data to the original geothermal system requires some knowledge of the age of the inclusion relative to that of the system. This relationship is embodied in the following genetic classification system for fluid inclusions, which was developed mainly by Russian

workers and defined by Yermakov (1965).

(i) Primary inclusions. These are formed by the entrapment of a portion of fluid at the margin of a growing crystal, and in origin are therefore contemporaneous with the host mineral.

(ii) Pseudosecondary inclusions. Also known as primary-secondary inclusions, these are formed by the entrapment of a fluid within a healing fracture, at some stage during crystal growth. The resulting inclusions are therefore contemporaneous with the growth of at least some of the host material.

(iii) Secondary Inclusions. The healing of fluid-filled fractures at some time after crystal growth produces these structures, which may develop at relatively low temperatures.

Primaries are 'ideal' inclusions for use as paleogeothermal indicators. Pseudosecondary inclusions have a similar status, but some difficulty exists in distinguishing them from secondaries, as both types mark the sites of healed fractures. The important genetic distinction between the two is that pseudosecondary inclusions form rapidly during a time of active host deposition, whereas secondary inclusions form more slowly, spanning a greater range of temperatures.

Where a fluid-filled fracture continues to heal after a vapour phase appears, some of the resulting inclusions may trap a vapour bubble which developed from an initially larger cavity. This process is illustrated by the accompanying diagrams (Figure 7-5), originally published by Roedder (1962b).

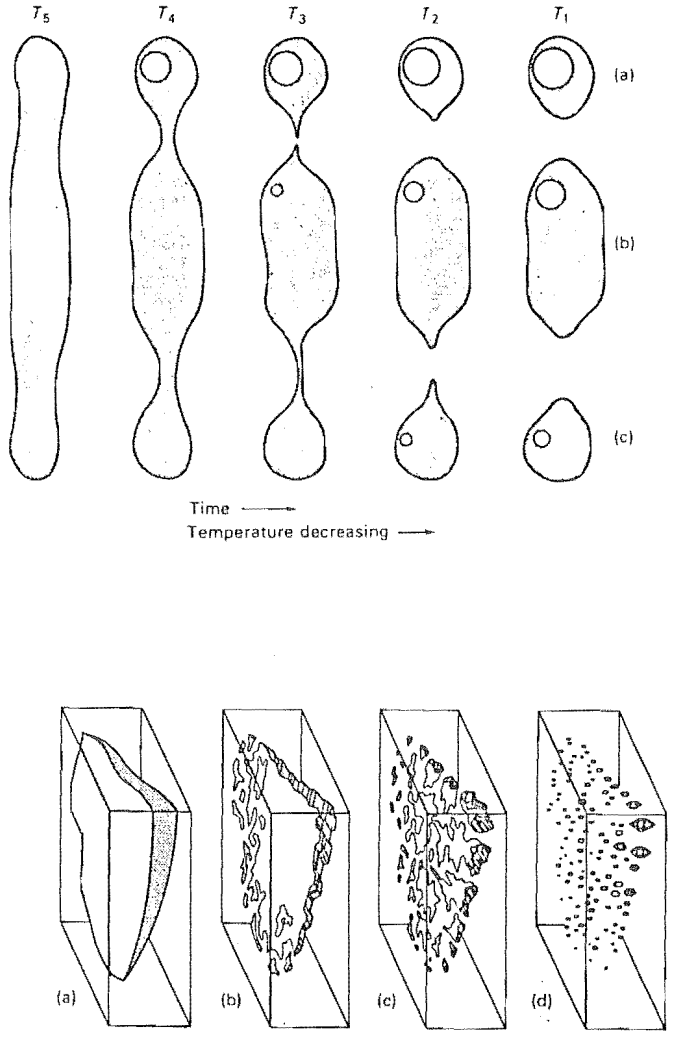

FIG. 7-5 The formation of secondary inclusions.

Upper: 'Necking-down' mechanism within an individual inclusion, producing secondary inclusions (a,b,c). These have filling temperatures both above and below the initial formational temperature T_5. See accompanying text for full description.

Lower: A healing fracture within a crystal producing a plane of secondary inclusions which finally assume negative crystal shapes.
Both illustrations from Roedder, 1967.

The same process may occur within individual inclusions having a flat or elongate shape, regardless of origin. This is shown in part (i) of Figure 7-5, and is known in the literature as 'necking down', although the adoption of the general term 'subdivision' would be welcome. As shown, inclusion (a) homogenizes far above the trapping temperature T_5, inclusion (b) fills between T_4 and T_3, while (c) fills between T_3 and T_2.

Although this example illustrates that a great range of temperatures may be indicated, only inclusions of type (a) which trap a large vapour phase in a small volume yield erroneous filling temperatures greater than that of the initial formation. Where inclusion systems seal liquid-only portions, in the presence of vapour, (i.e. below the boiling curve) the filling temperatures will equal the sealing temperatures. Useful information, therefore, can be gained from secondary inclusions, if careful selection is used to avoid anomalous cases.

When gathering inclusion data, it is important to distinguish primary and pseudosecondary inclusions from true secondary inclusions. Inclusion shape is not a good criterion for this purpose. The 'subdivision' effect and the widespread occurrence of negative crystal faces forming inclusion walls, indicates that considerable redistribution of host material within inclusions of all types is common.

Primary inclusions are often found in bands marking crystal growth zones or layers, whereas pseudosecondaries are restricted to the planes of healed fractures. Within one

sample, both types tend to have a constant degree of filling and salinity, and hence a constant filling temperature. Here lies the main distinction from secondary inclusions which have a much greater variation in all these respects. This criterion is difficult to apply when only poor material with few good inclusions is available.

(6) The Present Status of Fluid Inclusion Studies

The early approaches to fluid inclusion studies represent a considerable over-simplification of the subject, and when later complexities emerged to reveal serious errors the technique fell out of favour as a temperature and pressure indicator. A general lack of confidence persisted to the early 1960's, when sufficient data on inclusion systems began to accumulate to overcome the problems involved.

This experimental work has evolved from early attempts to evaluate inclusion systems by studying the properties of pure water. The major advance was a comprehensive understanding of the system H_2O-NaCl, culminating in Lemmlein and Klevtsov's (1961) pressure correction graphs. The importance of volatile components has long been recognised, and experiments were carried out with the principal member, CO_2. After some work of limited value involving water plus salt, and water plus CO_2 systems, all three components were combined as a ternary system H_2O-CO_2-NaCl, studied by Takenouchi and Kennedy (1965a). It is considered that this system most closely approximates natural inclusions, and data from these authors are drawn upon in the treatment of results in this project. Studies involving salts and CO_2 in inclusions are

greatly assisted by the use of cooling stages, which now complement the more familiar heating stage. The work of Edwin Roedder has provided a major contribution in this field.

More recent fluid inclusion studies make great use of cooling equipment, and seek to evaluate the effect of a greater number of components. Hollister and Burruss (1976) investigated fluid inclusions from a metamorphic complex containing abundant graphite, and include methane as a component, thus defining a quaternary system CO_2-CH_4-H_2O-NaCl.

II. RESULTS OF INVESTIGATIONS

(1) Methods Used

Many samples of quartz from the project area were collected from a number of veins, ranging from small stringers to the major lodes in which the mines were located. Suitable slabs were selected from the samples and prepared as for thin sectioning, but with the lower surface polished and the cover slip mounted with immersion oil. At this stage, examination under a microscope revealed the inclusion content. If the section proved suitable for further work, the upper surface was then polished and the section removed from the slide and cleaned by means of an alcohol bath.

The resultant wafer, having both surfaces polished, could then be transferred to a special microscope stage for examination at varying temperatures. Both heating and cooling stage apparatus was used (Appendix VI). Some thick quartz wafers were cut for an investigation of fluid inclusion composition. This was achieved by crushing the wafers, leaching the soluble salts, and analysing by atomic absorption for alkali ionic ratios. This procedure is further discussed, and the techniques involved outlined in Appendix IV.

Samples of carbonate and sphalerite from the veins were also seen to contain fluid inclusions, but these were too small to study. Quartz, being cleavage-free and colourless, proved much easier to prepare, and yielded superior images.

(2) Description of Fluid Inclusions Observed

Initial examination of the samples was disappointing, as much of the quartz collected proved quite unsatisfactory for study, due to both the small size of the inclusions and the extreme development of secondary inclusions. Figures 7-6 and 7-7 are low magnification photomicrographs to illustrate the typical distribution of inclusions in most of the initial quartz wafers prepared. These are representative of most Owen veins, with large numbers of inclusions less than 3 μ in diameter, concentrated in lines which in many cases are obviously healed fractures. Alignment of such inclusion trails or elongate inclusions often defined a penetrative, planar microfabric seen in thin section, which could occasionally be related to fracture planes within the hand specimen. Extreme examples exhibit what can best be termed a fracture cleavage (Figure 7-6). Similar examples on a much smaller scale may approach the status of Boehm lamellae. Intersecting, and possibly conjugate, fracture sets were frequently revealed by secondary inclusions (Figure 7-6b).

Figures 7-8 and 7-9 show slivers of quartz at very high magnification, photographed by means of a scanning electron microscope. This reveals a great density of small inclusions of a size extending down to the resolution limit of the instrument. Many of these inclusions would not otherwise be recognised, due to the poorer resolution of an ordinary microscope. The inclusions clearly display smooth

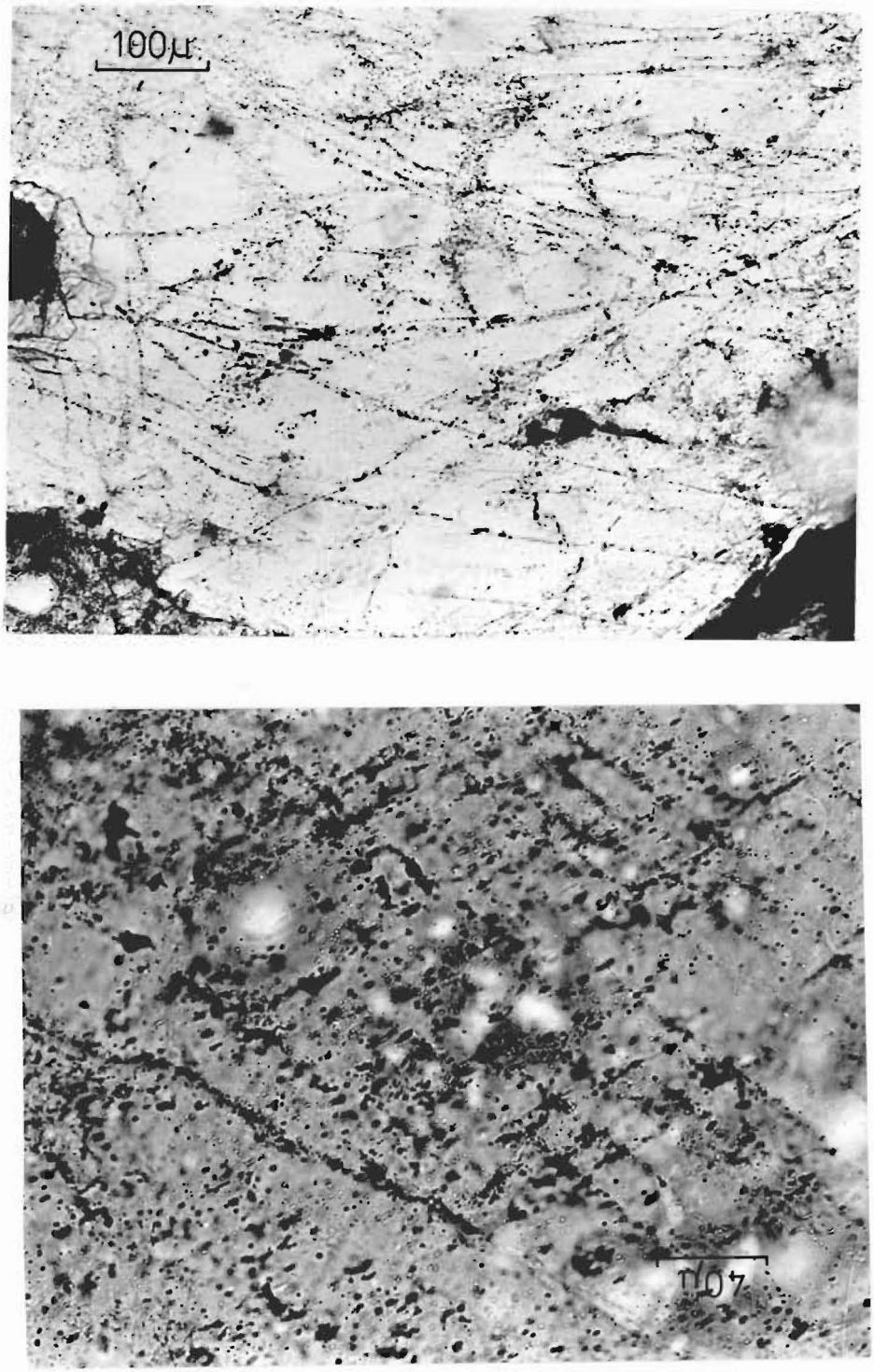

FIG. 7-6 Typical massive vein quartz. Numerous secondary inclusions scattered along healed fracture planes. Intense, parallel development of such fractures resembles fracture cleavage. Some conjugate sets have been observed (lower). Rare primary or pseudosecondary inclusions survive in less fractured zones.

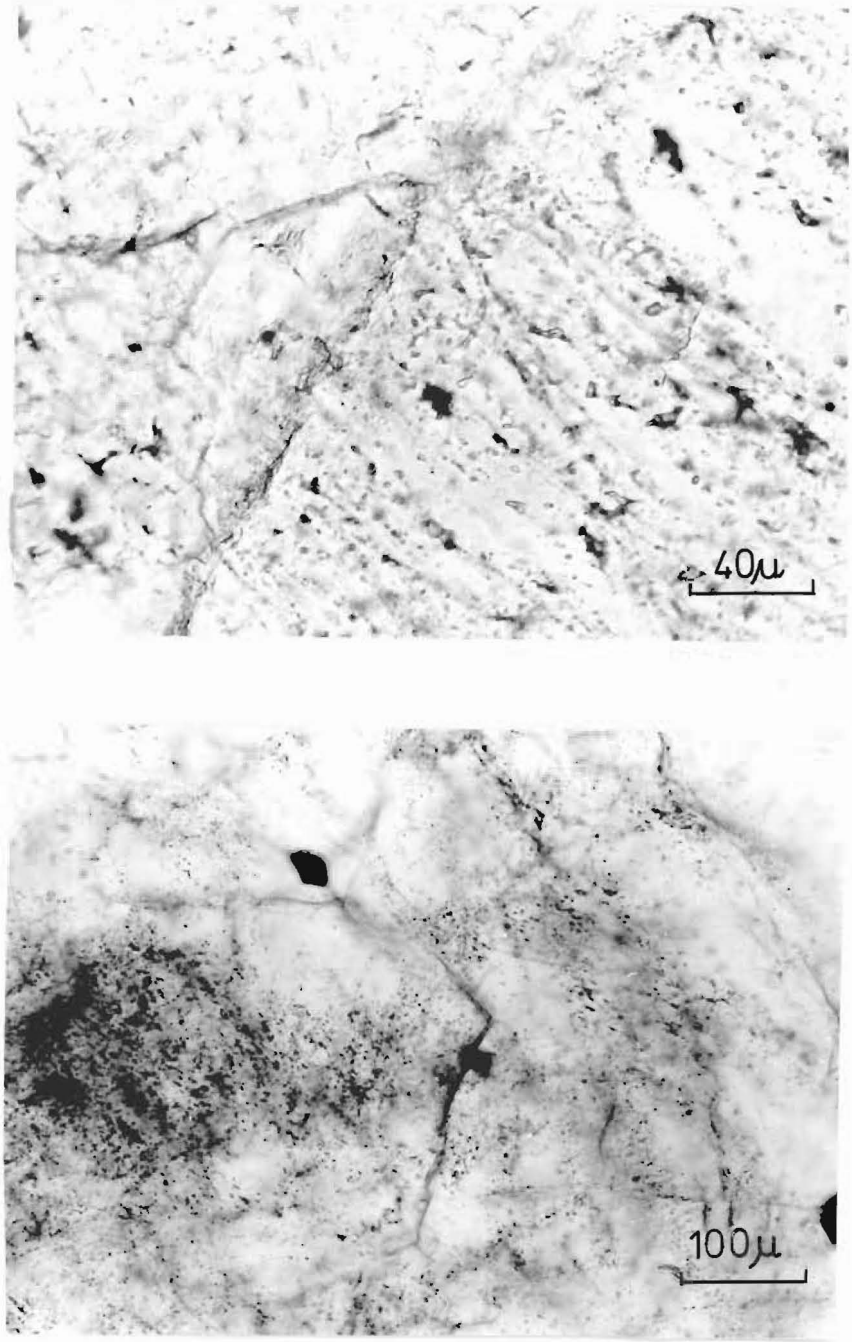

FIG. 7-7 Inclusions in quartz veins.

Upper: Sample LS-14. Quartz (right) with secondary inclusion trails marking a fracture set is cut by later calcite (left) which shows no inclusions.

Lower: Sample LS-17, from a small quartz vein in undeformed quartzite. A large proportion of these inclusions are primary. Inclusions containing dark carbonaceous matter are also present.

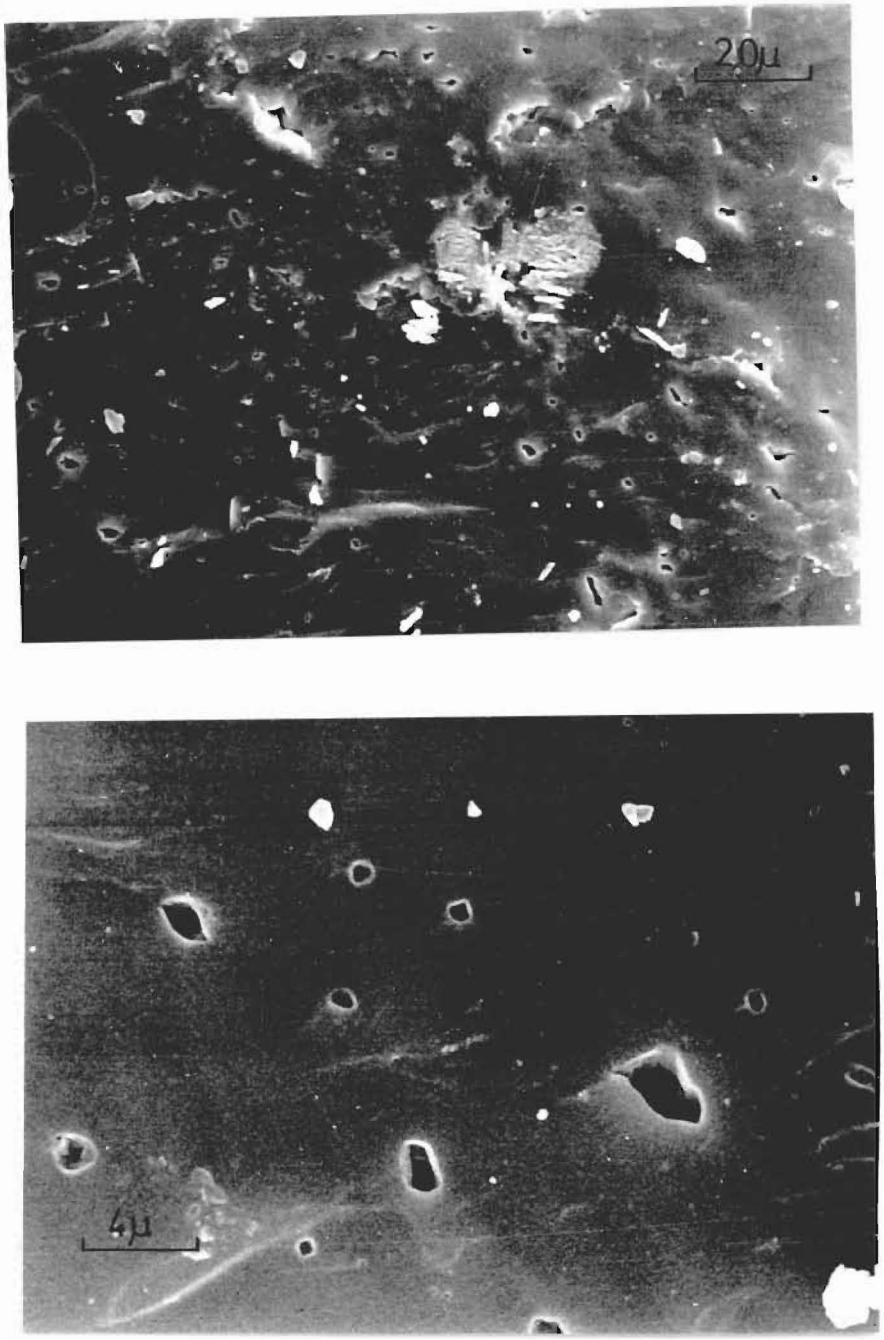

FIG. 7-8 Scanning electron microscope photographs of fracture surfaces of quartz from sample LS-13. The facility of good depth of focus at high magnification shows the opened inclusion cavities as sharp edged pits in the fresh fracture surfaces of small quartz shards broken from hand specimens. Thin sections indicate a predominance of secondary inclusions in this sample, with some rare primaries.

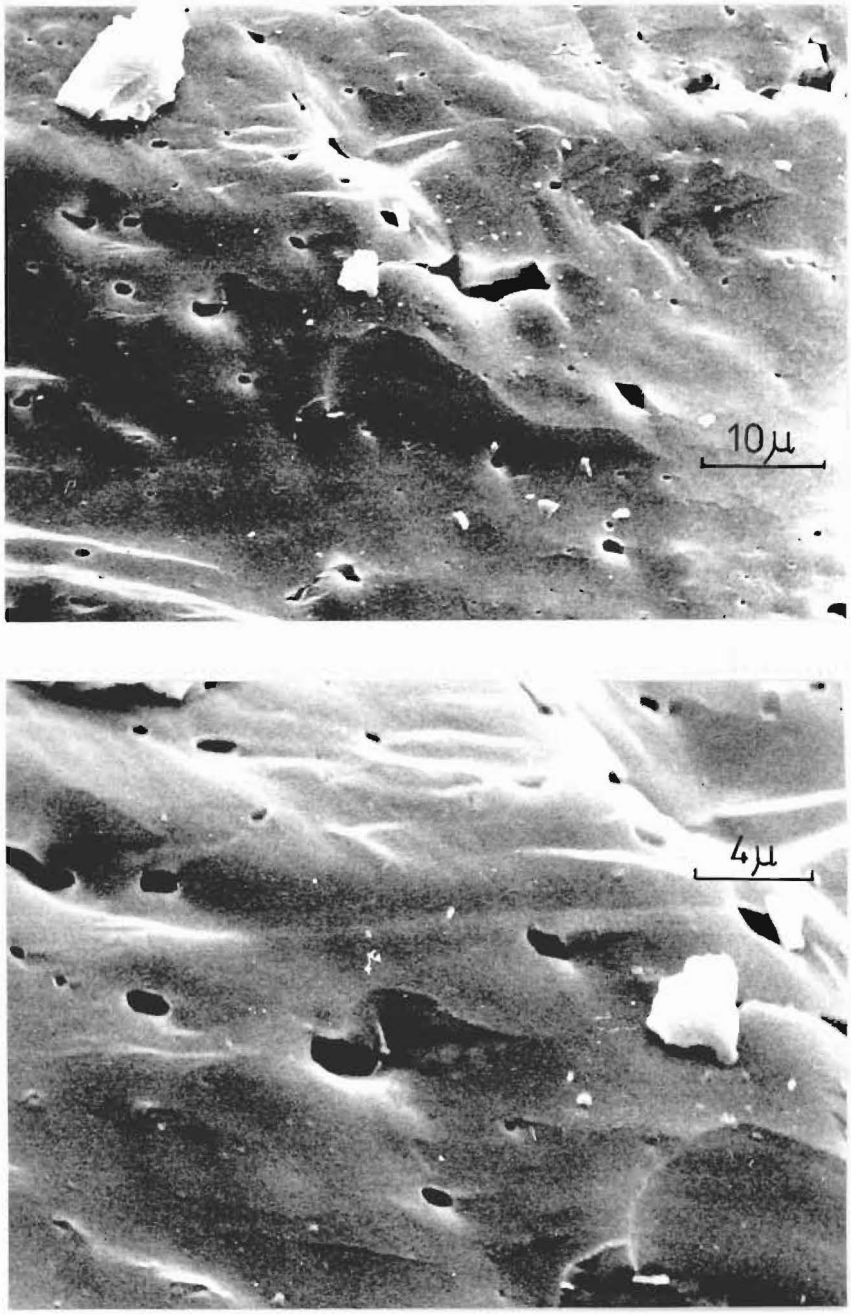

FIG. 7-9 Scanning electron microscope photographs, sample LS-13 (cont.). Alignment of secondary inclusion pits reveals the locus of healed fractures. The smallest inclusions show negative crystal shapes.

wall structures which are particularly difficult to define in transmission microscopy. Inclusions of dimensions less than approximately 3 μ tended to present shapes of negative crystals, indicating a redistribution of the host material to achieve a low-energy, equilibrium interface.

In general, the quartz from the larger lodes showed greater deformation and fewer large primary inclusions than that from small lodes and veinlets. This observation conforms with a concept of the major lodes being sites of more intense, and/or protracted shearing. The scarcity of large inclusions in deformed quartz supports the hypothesis noted by Roedder (1967) regarding the emptying of pre-existing inclusions by deformation, and the subsequent formation of secondary structures.

A small clear crystal from sample LS-12, collected from a drusy cavity near the portal of the Beilby mine, was found to contain the largest fluid inclusions encountered throughout the project (up to 50 μ in diameter, see Figures 7-10, 7-11). Many of the inclusions in this crystal were apparently related to healed fractures, yet have a constant degree of filling. These are classed as pseudosecondary inclusions, formed at a time of constant, elevated temperature and rapid fracture healing which would prevail during the time of host crystal growth. As hydrothermal indicators, these inclusions have a status equivalent to primary inclusions.

The most favourable material for primary-type inclusions

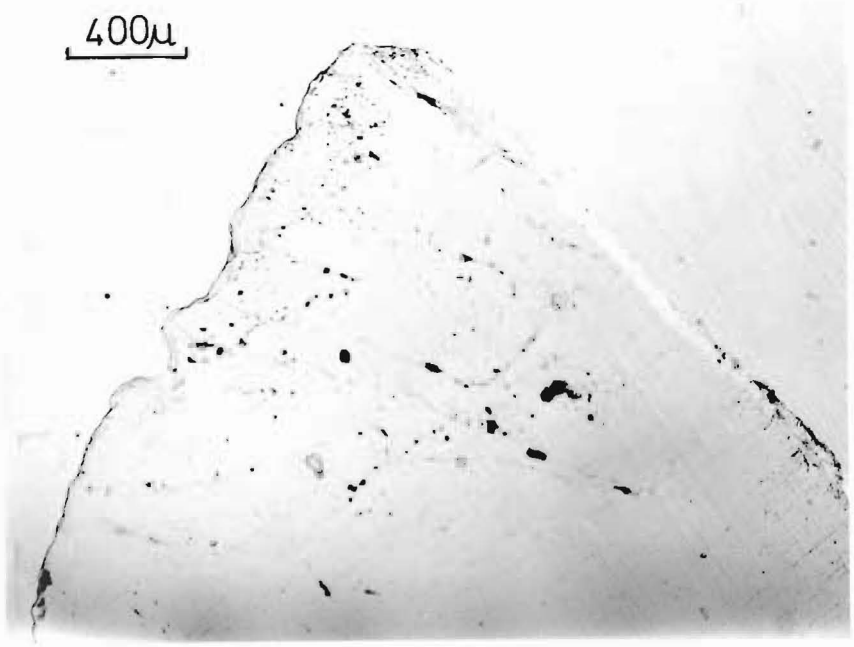

'IG. 7-10 Inclusions in sample LS-12.

Upper: The polished wafer cut from a single clear crystal.

Lower: Enlargement of area marked. A set of pseudo-secondary inclusions is shown, in which the 'bubbles' proved to be liquid CO_2. Negative crystal faces are visible.

appears to be those portions of veins which have escaped later stresses. These include some small veinlets, quartz grains within a softer matrix, and also drusy crystals such as represented by sample LS-12, described above.

No crystals or 'daughter salts' were seen in any of the inclusions, thus one may assume that none of the trapped solutions were saturated with salts at room temperature. Because of delays in developing the apparatus, cooling studies were carried out after most of the hot stage work was complete. The initial cooling experiments produced some surprising results regarding fluid composition. As the temperature was lowered, most of the large inclusions developed another phase within what had been previously interpreted as the vapour phase. The two pre-existing fluids seen at room temperature were therefore immiscible liquids. In one sample (LS-17), three phases, i.e. two liquids + vapour, coexisted at room temperature. When gradually warmed, the liquid-vapour boundary exhibited critical point disappearance at $31.0° \pm 0.5°$, which coincides closely with the published critical temperature for liquid CO_2. This substance, in the system H_2O-CO_2, is known to be sufficiently pure to exhibit critical phenomena very near this temperature. (Refer Figures 7-12, 7-13, 7-14).

This evidence, together with the similarity to other analysed inclusions (Roedder, 1972, and others) is considered sufficient for identification of the second liquid as CO_2.

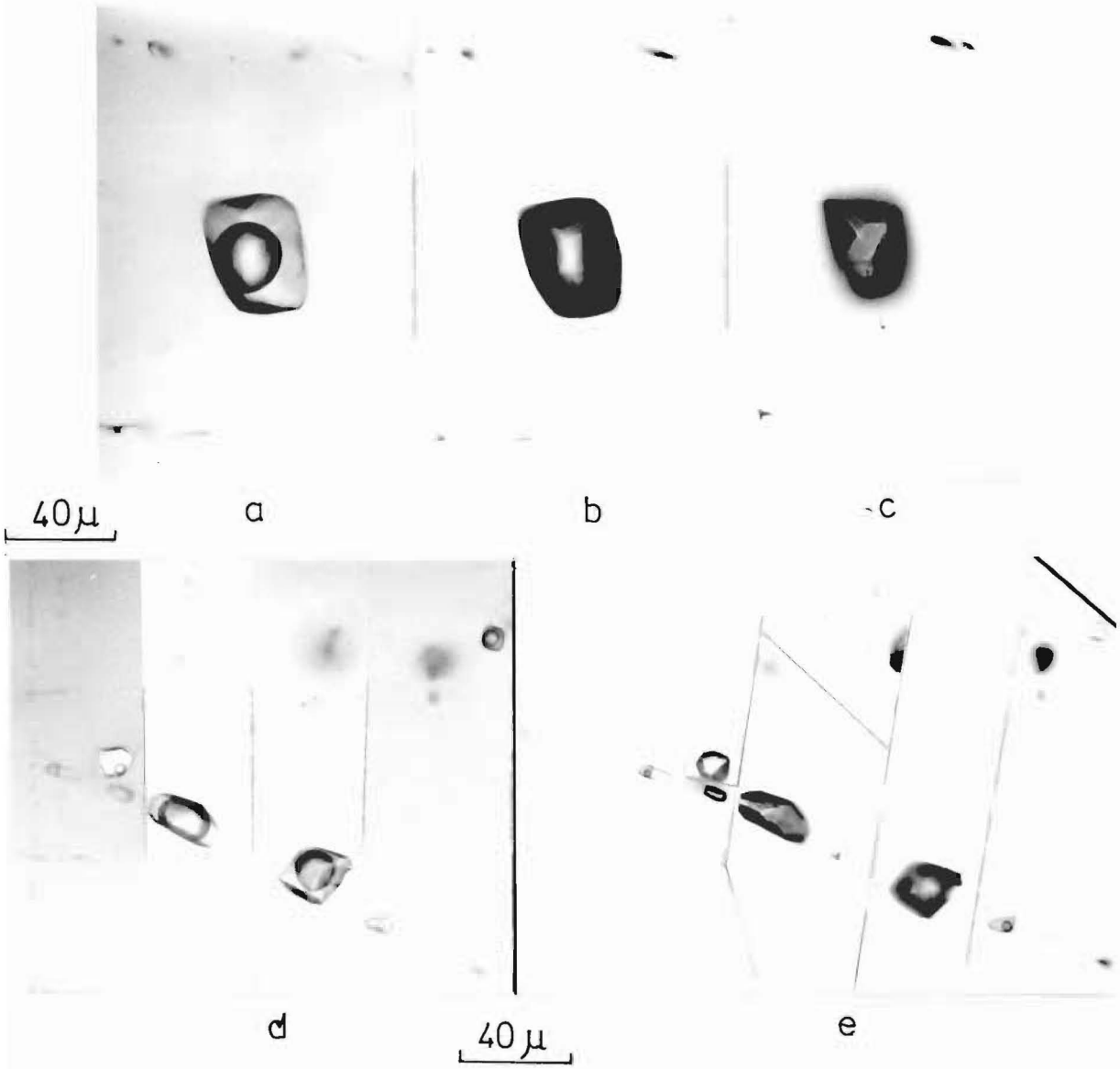

FIG. 7-11 Primary and secondary inclusions in sample LS-12.

(a) Detail of a large primary inclusion. No daughter salts are visible.

(b,c) The same inclusion after heating and consequent decrepitation. The cavity, now filled by vapour only, appears dark in transmitted light. Focus on the upper surface reveals negative crystal faces and also the minute 'blowout' vent (arrowed) through which the contents escaped.

(d) A group of secondary inclusions, showing uneven degrees of filling. (Limited depth of focus necessitated composite photographs).

(e) The same group after a heating run to 312°C. The following sequence was observed (°C):

No.2 filled at ca.140° followed by major leakage.
No.1 filled at 180° followed by slight leakage.
No.3 filled at 192° and immediately decrepitated.
No.4 decrepitated without filling at 192°. (Coincident with 3).
No.5 leaked without filling at 203°.
No.6 Filled at 228°.

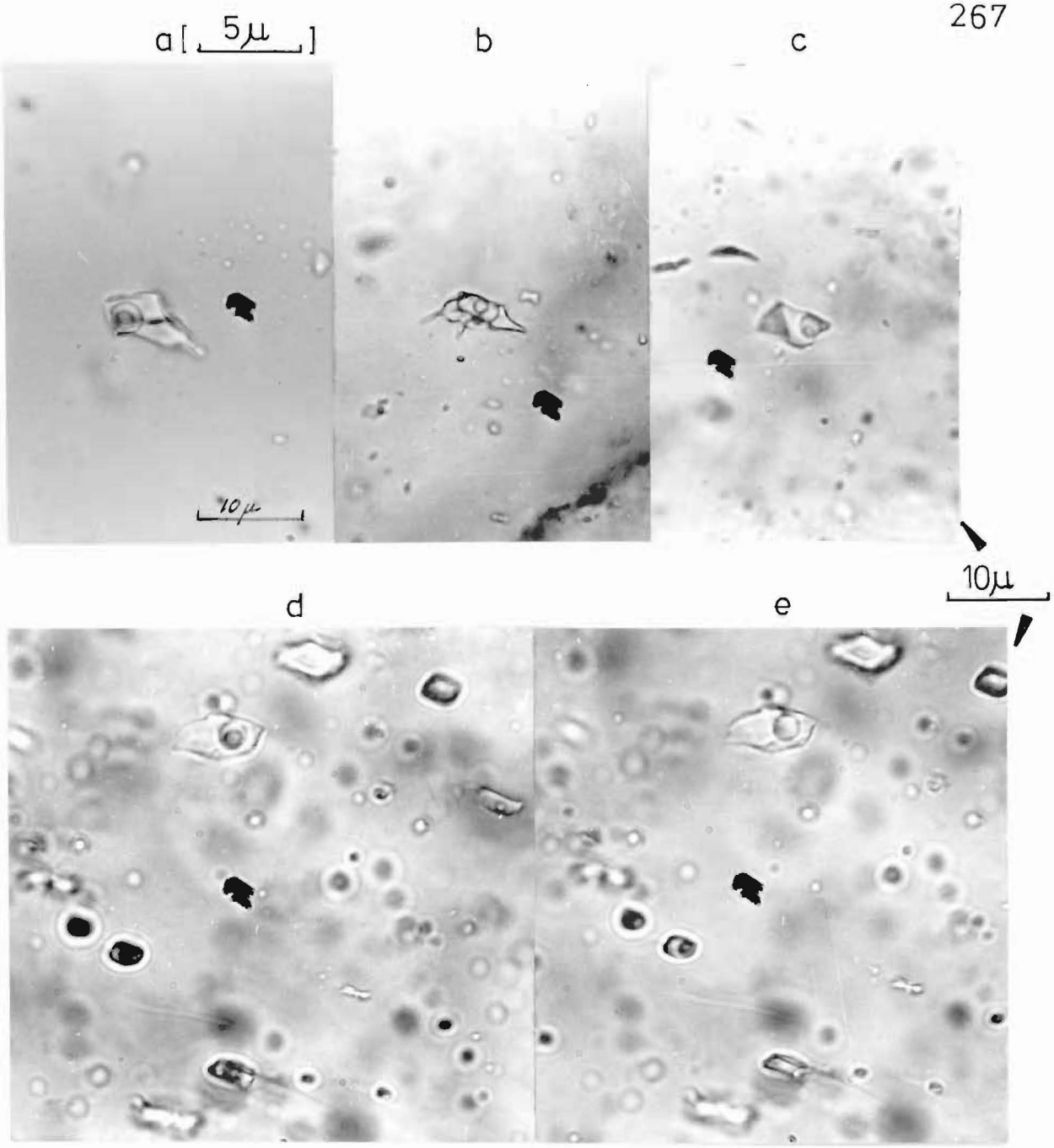

FIG. 7-12 Primary inclusions in vein LS-17. The immiscible liquid is considered to be CO_2 (see overleaf).

(a,b,c) Three examples of two component, three phase inclusions from this sample, all photographed at 7°C to reduce Brownian movement.

(d) A similar inclusion, at 7°C.

(e) The same inclusion, but at 31°C. The phase boundary in the second liquid has disappeared. Increased thermal agitation within the small inclusion to the upper right of the field has markedly reduced the image quality of the small bubble. The dark spot at the centre of all these exposures is due to dust in the optics of the camera.

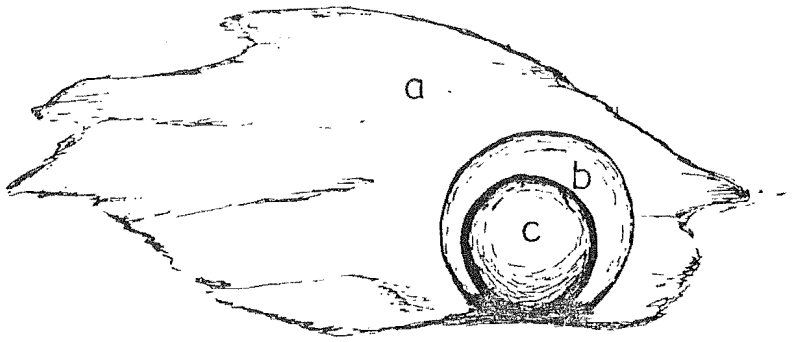

FIG. 7-13 Identification of phases in multicomponent inclusions, sample LS-17, as seen at ca.10°C.

(a) Water-rich liquid. (Mainly water, with salts and CO_2).
(b) CO_2-rich liquid. (Nearly pure CO_2).
(c) Vapour bubble. (Nearly pure CO_2).

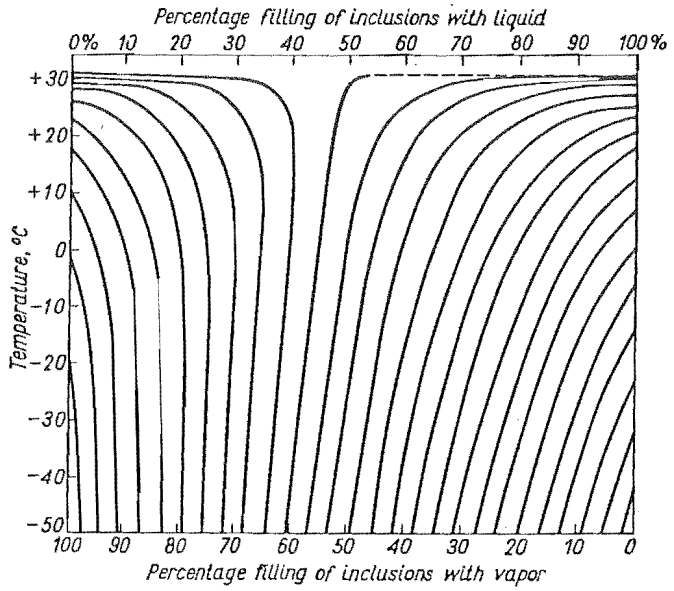

FIG. 7-14 Diagram showing homogenization behaviour for hypothetical inclusions containing only CO_2. Over the small temperature range involved, these characteristics remain valid for water-salt-CO_2 systems where immiscible liquids exist. The lines indicated represent paths for the CO_2 phases. (From Yermakov, 1965)

Photographs of these two-liquid inclusions at various temperatures are reproduced in Figures 7-15, 7-16. Photography of small vapour phases is difficult due to the intense Brownian movement at room temperature. Cooling below ca.10°C generally reduces movement sufficiently for good images to be obtained.

The inclusions illustrated from sample LS-21 (Figure 7-16) are considered to be primary, but show widely varying phase ratios. This suggests inhomogeneity in the primary hydrothermal fluid, which can arise as a result of fluid cooling and unmixing during transport, as discussed by Takenouchi and Kennedy (1965a). The resulting water-rich and CO_2-rich inclusions represent mutual components of the water-salts-CO_2 solvus (discussed in part III of this Chapter).

A similar condition of varying phase ratios is produced in secondary inclusions by the sealing of portions of an unmixing fluid. This state is illustrated overleaf in Figure 7-17. The water-rich phase always surrounds the CO_2-rich phase, and wets the walls of the inclusion cavity. The CO_2 is drawn into globules by a strong surface tension effect, avoiding small interstices and narrow necks which are filled by any available aqueous phase.

(3) Heating Stage Measurements

A summary of filling temperature measurements is shown below in Table 7-2. Much data was rejected as unreliable and not recorded in the table, resulting in a comparatively

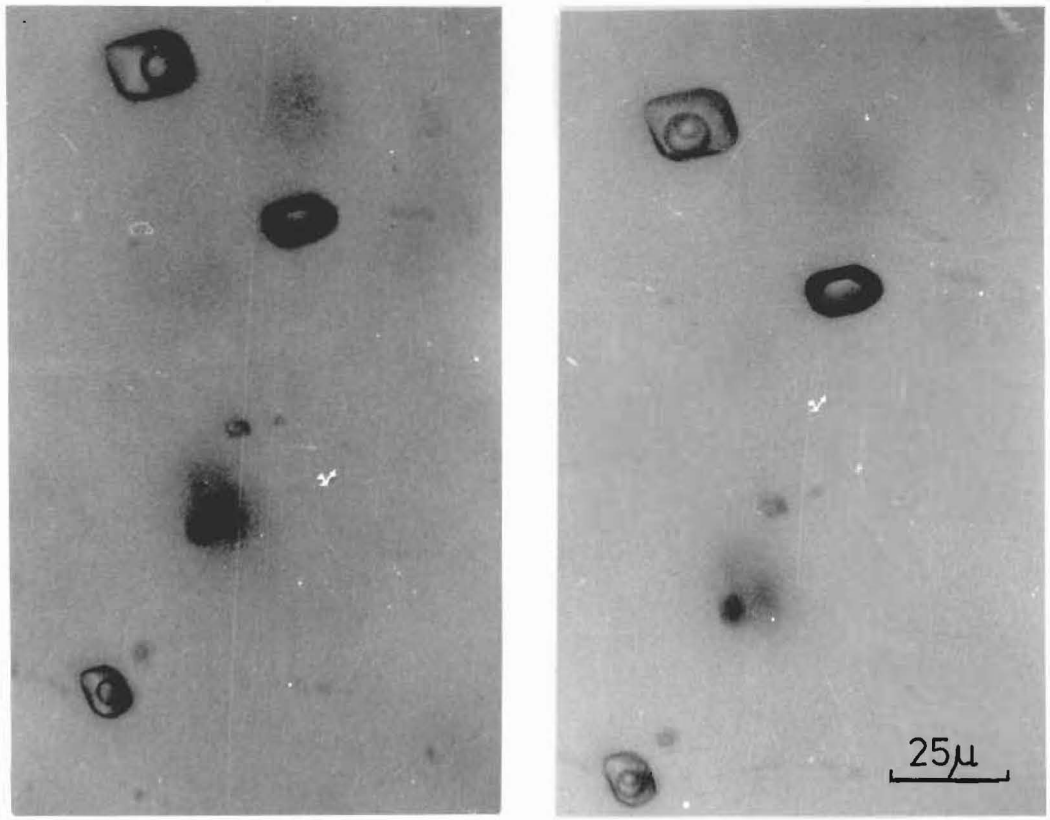

FIG. 7-15 Three inclusions from sample LS-12 (Beilby Mine portal)

(a) At room temperature (20°C).

(b) At reduced temperature (ca.8°C).

These photographs, and those on the next page (Figure 7-16) show the nucleation of vapour phases in two-liquid inclusions. Cooling was applied by means of spraying the section mount from beneath with a small jet of liquid CO_2, from a commercial spray can. Vapour nucleation temperatures, as determined with a cooling stage, were most commonly in the range 0° to +10°C.

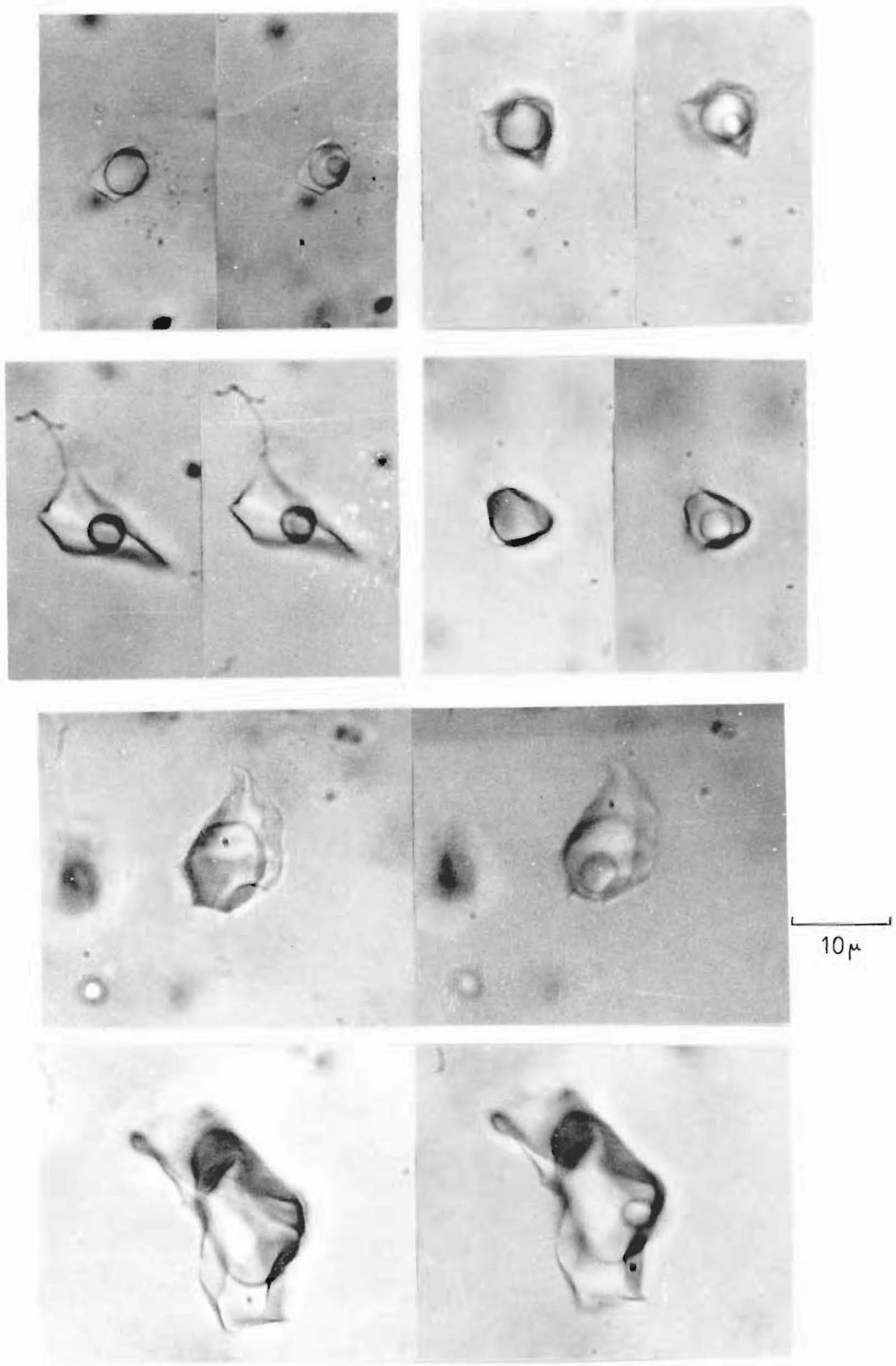

FIG. 7-16 Dual temperature, paired photographs of inclusions from sample LS-21, at room temperature (left) and 'chilled' (right). Reduced temperature causes a vapour phase to nucleate and grow, proving the original central feature to be a globule of immiscible liquid, identified as CO_2.

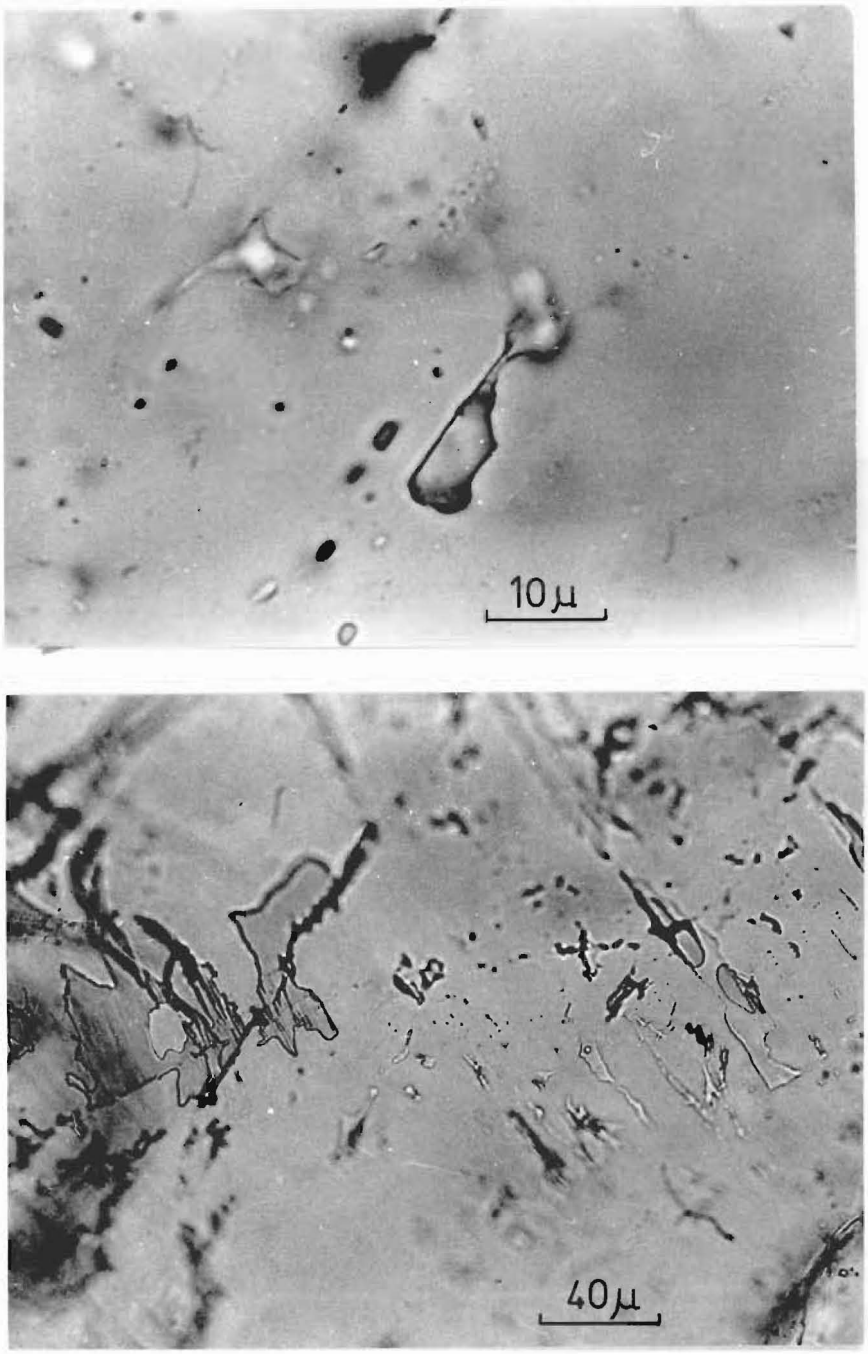

FIG. 7-17 Development of Secondary inclusions (sample LS-21).

(a), Upper: A CO_2-rich inclusion with a narrow neck in which the small hydrous phase can be seen between two globules of liquid CO_2.

(b), Lower: A thin, partially healed fracture plane viewed at a high angle. The subdividing inclusions clearly trap differing phase ratios, due to a falling temperature during the healing process instead of primary inhomogeneity.

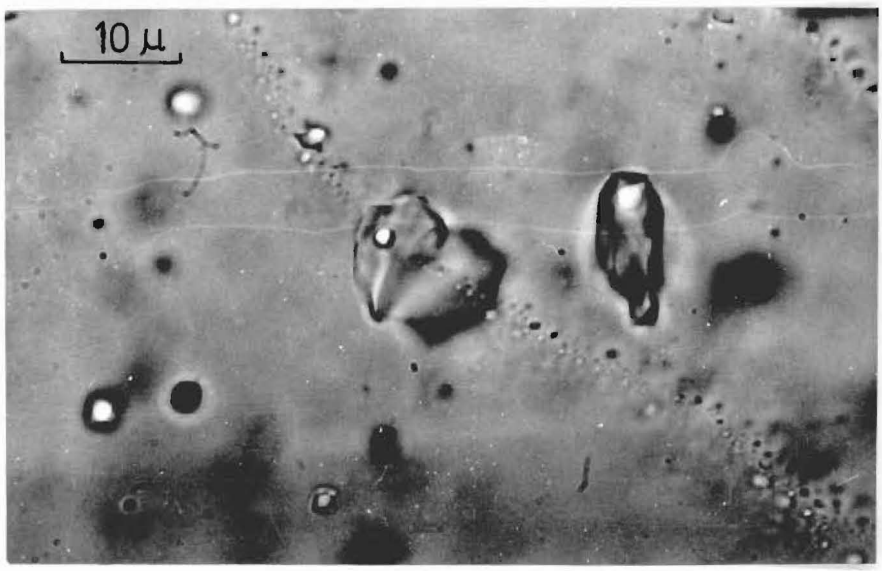

FIG. 7-18 The destruction of primary inclusions (sample LS-21).

The above photograph shows a group of primary inclusions and a fracture-derived plane defined by secondary inclusions intersecting the large primary in mid-field. The primary inclusions, being CO_2-rich, all developed vapour bubbles when chilled except the intersected one, which proved to already contain a vapour and no liquid CO_2. The central inclusion is considered to have been initially similar to its neighbour to the right, but was cut by a post-depositional fracture which permitted its contents to leak and to equilibrate with the existing system - which was no longer rich in CO_2. Thus the inclusion - after re-sealing - has suffered a change in composition, being effectively degraded from primary to secondary status.

small number of useful measurements for the number of samples prepared. No statistical treatment beyond a simple distribution graph (Figure 7-19) was attempted. The filling temperatures are considered accurate within the error limits shown, but in some cases uncertainty exists regarding the primary status of the inclusion or the fluid composition, as indicated by '?' symbols.

Data from secondary inclusions has been included as this was the only information that could be obtained from some veins. Pseudosecondary inclusions have been included with primaries, as both types belong to the same growth and temperature phase. All inclusions were checked for possible subdivision ('necking down') effects and those of suspicious appearance rejected.

(4) Cooling Stage Data

After much experimentation, a workable cooling stage was constructed, employing cold air as a refrigerant and a thermocouple for temperature measurement. As with the heating stage, it was designed to attach to the existing stage of a petrological microscope, and is more fully described in Appendix VI.

It was intended to use this stage to determine the freezing points of the inclusion fluids, and hence calculate the salinity for use in estimating a pressure correction for filling temperatures. Cooling runs with quartz wafers proved disappointing for a number of reasons. Firstly, small inclusions failed to show freezing products, even at temperatures

TABLE 7-2 Summary of filling temperature measurements.

Sample and Location	Type*	Filling T.	Composition*
(i) Wangapeka Formation veins			
LS-04: Prospect shaft east of trig EH.	P	308±5	?
LS-17: Small veins near prospect shaft.	P	285±5	CO_2
	P	290±5	"
	P	327±5	"
	S	ca.220	H_2O
LS-18: Approx 15m east of shaft.	P	310±5	CO_2
	P	332±10	"
	P	300±5	"
(ii) Owen Formation veins			
LS-01: Base metal veins south of trig C.	P	302±10	"
	P	283±5	"
LS-01: Small veins, Bulmer Ck above Beilby Stream.	S	ca.225	H_2O
LS-06: Uno workings.	P?	350±10	?
LS-09: Golden Crown mine.	P?	296±2	H_2O?
LS-10: Silverstream shaft.	P	237±5	CO_2
LS-12: Beilby mine portal (single crystal).	P	302±2	"
	P	312±2	"
	S	ca.268	H_2O
LS-21: Approx. 50m below Beilby mine.	P	286±5	CO_2
	S	ca.226	H_2O

*Notes: Type: 'P' denotes primary or pseudosecondary inclusions; 'S' denotes secondary inclusions.
Composition: 'CO_2' indicates that a second liquid was shown to exist; 'H_2O' indicates the contrary.
Where '?' is shown, the composition remains uncertain.
Values marked 'ca.' for secondary inclusions represent an average filling temperature from a number of measurements.
All measurements in ^{o}C.
A correlation of sample numbers with UC numbers is given in Appendix VII.

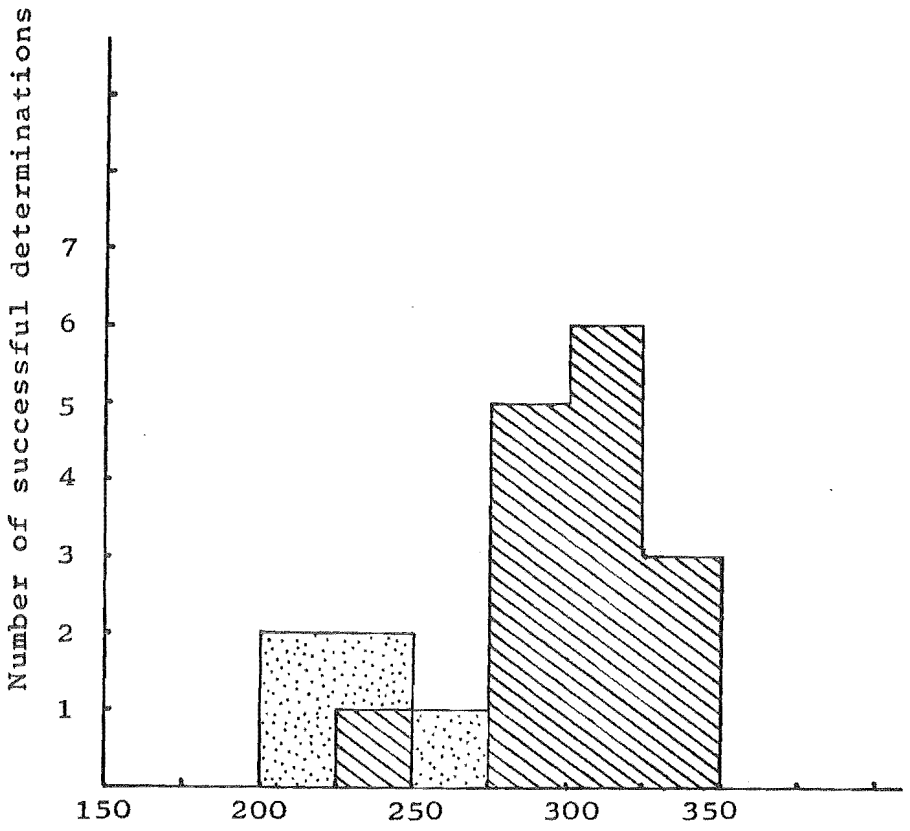

Note: Secondary inclusions not recorded below 200°C.
Representative determinations for secondary inclusions are averages from a number of measurements within a sample.

FIG. 7-19 Distribution of inclusion filling temperatures.

as low as -30°C. Some examples of continued bubble movement under these conditions were observed, which indicated that the inclusion contents were remaining liquid in a supercooled state. Even precooling plus rapid chilling by spraying with liquid CO_2 produced no detectable solids, which suggests that either liquid supercooling continued or freezing to clear 'glass-like' ice occurred. Roedder (1963), in a major paper on fluid inclusion freezing studies, records and discusses both these effects. Inclusions of small size or unfavourable shape proved very difficult to work with in cooling stage runs, where the contents are always obscured by an enlarged vapour bubble.

It is possible that most or all of these small inclusions were of a secondary origin, as all the larger inclusions cooled were seen to contain large amounts of CO_2, with a third phase appearing as described in the previous section. A simple freezing-point depression treatment for the estimation of solutes was therefore inadequate.

Cooling to around -1°C produced a rapid development of solid material to form a 'rim' at the liquid-liquid interface (Figure 7-20). Further cooling caused accumulation of solids within the aqueous portion of the inclusion, obscuring the resolution of individual phases. The observed effects were recognised as low-temperature compound formation, characteristic of H_2O-CO_2 systems where the CO_2 fraction is high enough to form an immiscible liquid.

There can be little doubt that the solid initially forming

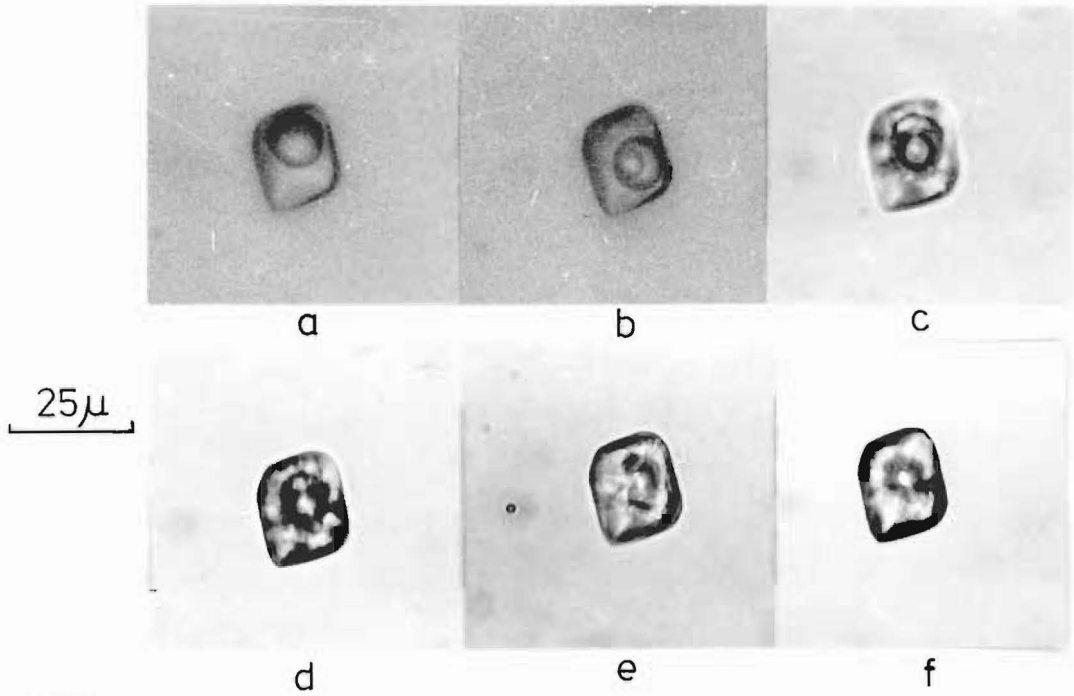

FIG. 7-20 A large, CO_2-rich inclusion from sample LS-12, photographed at various temperatures during a cooling run.

(a) 20°C. Two liquids only are present.

(b) 8°. The vapour phase well developed.

(c) -2°. A solid mass developed at the liquid-liquid interface. This solid is probably a CO_2-hydrate (see text).

(d) -10°. Solids developing in the surrounding hydrous phase.

(e) -20°. The inclusion contents are obscured by solids grown on the cavity walls. No visible change from this state was produced by further cooling.

(f) 0°. Photographed during the 'melting' cycle, after the cooling was discontinued. The inclusion walls are now ice-free, but blades of CO_2-hydrate remain at the centre. The temperature rise was too rapid to eliminate the possibility of metastable survival of solid phases.

Note: Illustrations (a) and (b) are from a different run to the remainder. Photographs taken at lower temperatures yielded inferior images to those observed during the actual experiment, due to problems caused by contraction and vibration. All temperatures were measured during warming cycles to overcome the supercooling effect.

was a CO_2- hydrate, as described by various authors in the fields of solution chemistry and fluid inclusions (Deaton and Frost, 1948; Larson, 1956; Takenouchi and Kennedy, 1965b; Roedder, 1963). This species, like other gas hydrates, is classed as a clathrate compound by Barrer and Stuart (1957) who describe these phases as "... very open crystalline structures in water, metastable with respect to ice, but stabilised by inclusion of 'fillers' within cavities in the structures." The structural formula of the compound is widely accepted as $8CO_2 \cdot 46H_2O$, corresponding to the empirical formula $CO_2 \cdot 5.75H_2O$.

Some efforts were made to measure the highest temperature of clathrate stability within the inclusions, working with the best sample only, that of LS-12. This was achieved with the cooling stage by chilling until clathrate formed, then allowing the stage to warm up, and noting the point of last clathrate survival. Measurements during the cooling part of the temperature cycle were impossible due to marked liquid metastability.

The clathrate last-melting temperature was found to be $5.0° \pm 0.5°C$, the large error estimate being due to the uncertainty in visually detecting the true end-point of the melting reaction.

Analysis of this and other measurements was then attempted, by interpreting the observations in terms of the chemical system involved.

III. TREATMENT OF RESULTS

(1) Data for the System at High Temperatures

There have been many studies of CO_2-water mixtures, but comparatively little is known of these systems at the temperatures and pressures of geothermal conditions, or in the presence of additional solutes.

At the time of writing, the only significant work of value in this respect is that by Takenouchi and Kennedy (1965a) on the solubility of CO_2 in NaCl solutions at high temperatures and pressures. Although the experimental limits were 450°C and 1400 bars, and solubility runs were made at only 0, 6, and 20 wt% NaCl, the results provide a good understanding of the system over a range of conditions typical of hydrothermal environments. The main points emerging from this study were:

(i) The addition of salt greatly inhibits the solubility of CO_2 in the solution. This is described as a 'salting-out' effect.

(ii) The solubility of CO_2 decreases as the concentration of salt increases, but the solubility curves retain a similar form to those for pure water. The graphed solubility results of these experiments are reproduced in Figures 7-21, 7-22, 7-23.

These data effectively establish the water-rich end of a set of solvus curves for the system (Figure 7-24), similar to Roedder's phase boundary diagram for water (Figure 7-2). For

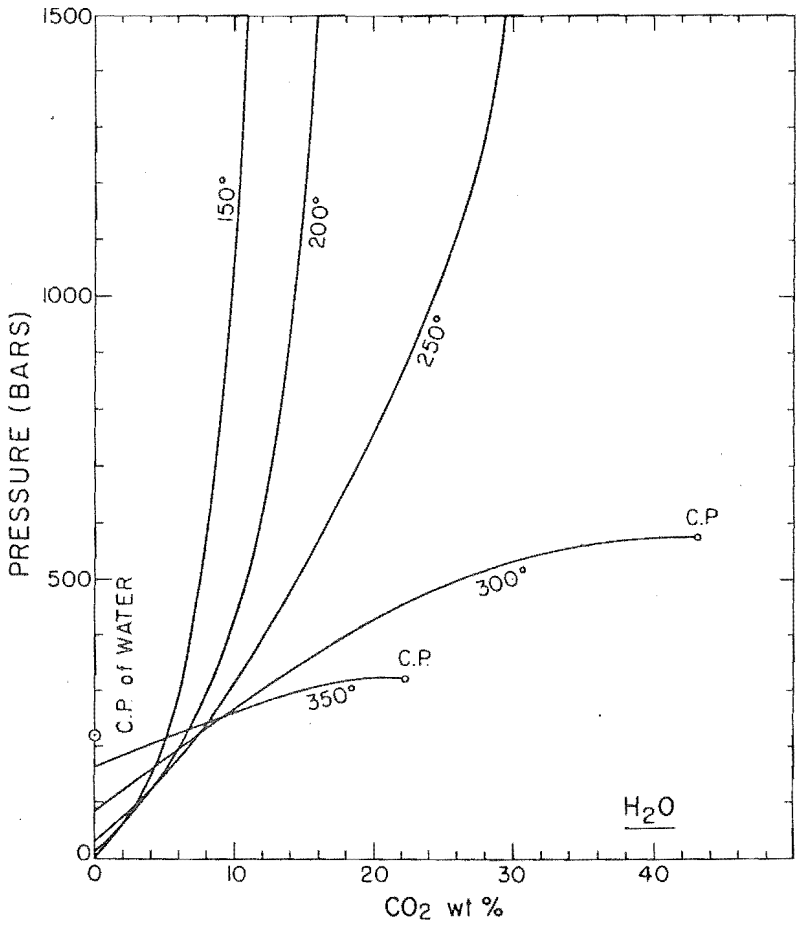

FIG.7-21 Curves expressing the solubility of CO_2 in pure water as a function of pressure and temperature. Also shown are critical points (C.P.) for the resultant solution. Except at low pressures, CO_2 solubility increases with temperature.
From Takenouchi and Kennedy (1965a).

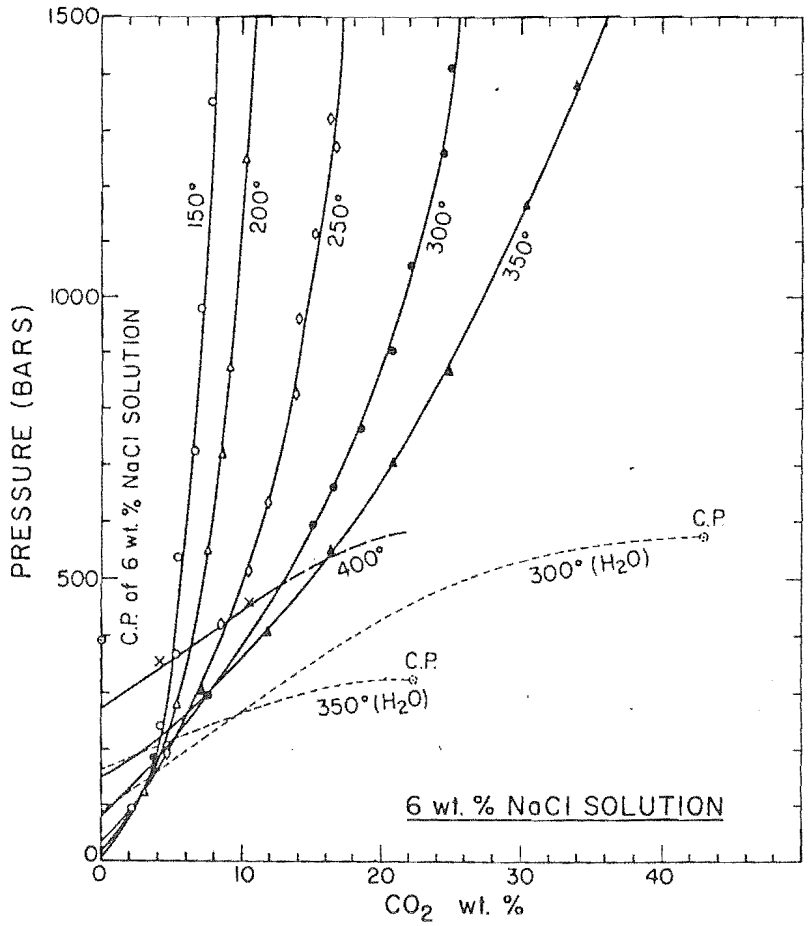

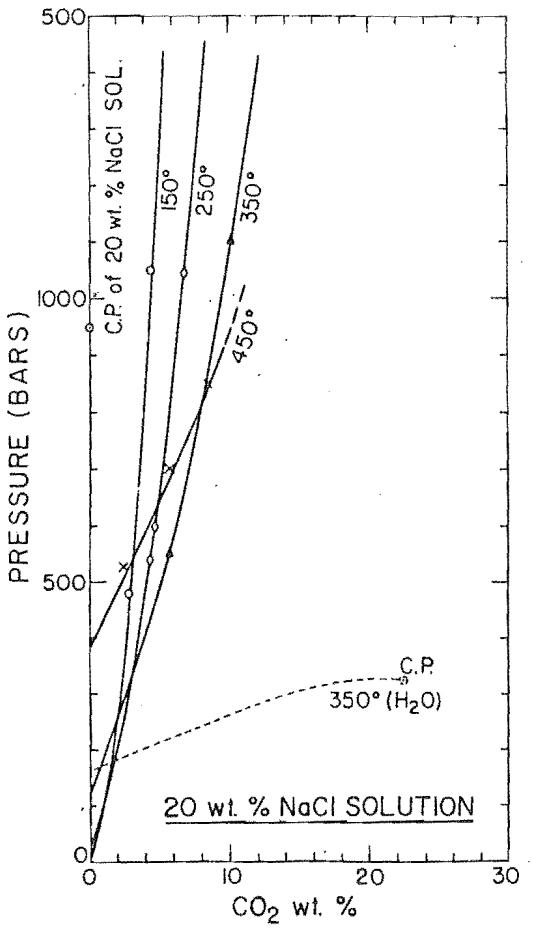

FIG. 7-22 (above)

FIG. 7-23 (left)

Takenouchi and Kennedy's solubility graphs for 6 and 20 wt. % NaCl. Although the general shape of the solubility curves is retained, the effect of the salt is to suppress both critical phenomena and solubilities.

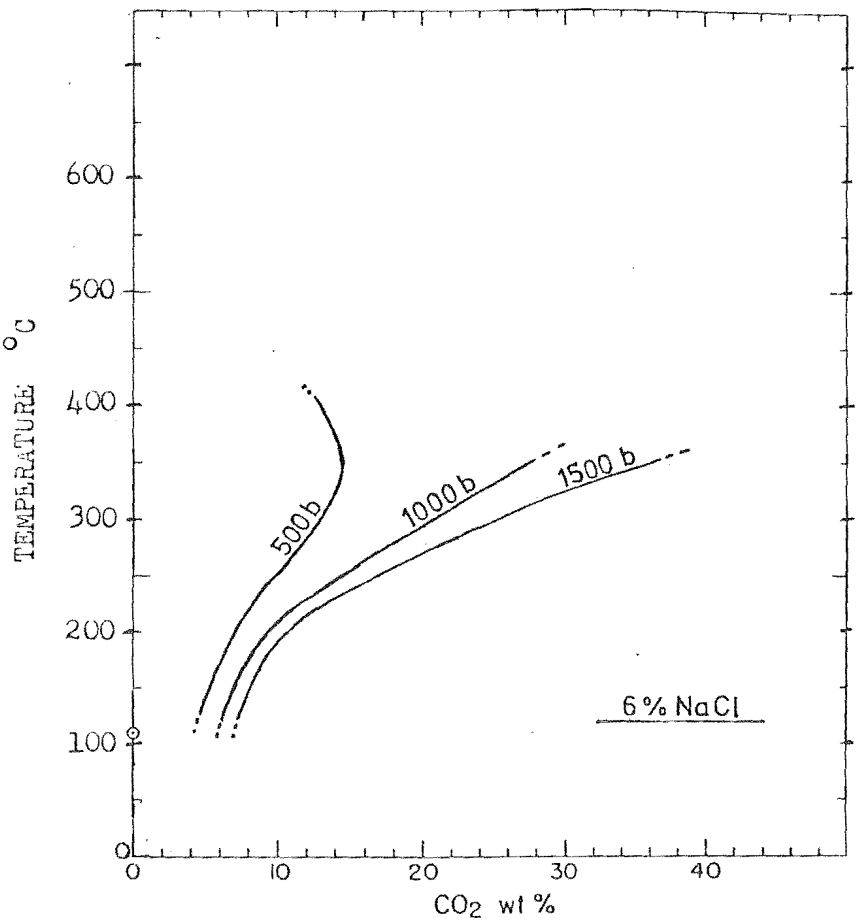

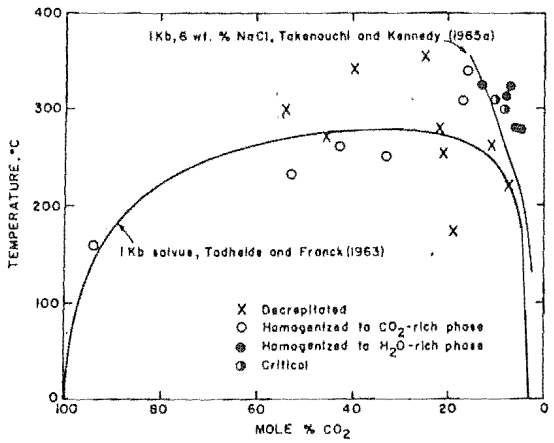

FIG.7-24

Upper: The CO_2 solubility data for the 6% salt system expressed as partial solvus boundaries, at constant pressure. Complete data is not available to delineate the crest region.

FIG. 7-25

Lower: A figure reproduced from Hollister and Burruss (1976) showing both the full solvus curve for 1 Kb pressure and no salt, and a portion of the 1 Kb 6% salt curve. The other points refer to inclusions studied by the authors (see text). (Note:the figure uses mole %, not wt.%, CO_2 and has 0% CO_2 on the right-hand side of the plot).

inclusions from both systems, the pressure-derived filling temperature correction reduces to zero if filling conditions are known to be represented by a point on the phase boundary curve. In the case of the ternary system, the solvus represents mutual saturation of the two fluid components. Over most of the range of geologically significant conditions reproduced by experiments, CO_2 in saline water behaves as a 'normal' solute, i.e. a reduction in either temperature or pressure will cause a saturated solution to unmix into two fluids.

As has been shown in the previous section, inclusions representative of the two unmixing products are preserved, providing evidence that the fluid phase of the Owen hydrothermal system did achieve saturation with respect to CO_2. Inclusions representing the water-rich side of the solvus can be considered a 'normal' type of inclusion, having a composition corresponding to the principal hydrothermal fluid. These are recognisable as having around 12-15 wt.% CO_2 for the Owen inclusions (refer to Figures 7-10, 7-11). The other, minor, fluid component gives rise to CO_2-rich inclusions, such as are shown in Figure 7-16. These inclusions show CO_2 contents varying from around 50-90%; this variation can be accounted for by local inhomogeneity at the time of sealing. As the aqueous phase always wets the walls of the host material, it appears that the CO_2-rich inclusions must inevitably be trapped as a mixture.

Over the course of moderate cooling, depressurization,

or both, the parent fluids will remain mutually saturated and their individual compositions will remain on the solvus curve, this being the analogue of a boiling curve for a simple binary (water-halide) system. Homogeneous inclusions of either composition will be isolated from external pressure changes on sealing, but will unmix immediately when the temperature falls. It is apparent that no pressure correction is required for these inclusions; as long as saturation is maintained at the time of sealing, filling temperatures equal sealing temperatures.

This concept is readily understood from studying the results of Takenouchi and Kennedy's experiments. A search of the literature revealed that such a concept was developed prior to these experiments, by Smith (1953) and later expounded by Smith and Little (1959), apparently to little effect on fluid inclusion research.

Takenouchi and Kennedy's solubility data can be put to greater use than merely to support the above postulate. As P-T-Composition data is provided for the system, an excellent opportunity is presented to evaluate the inclusion sealing pressure.

(2) Data for the System at Low Temperatures

Sealing temperature has been determined, thus only fluid composition is required to derive sealing pressure from the known solvus data. The liquid components are easily determined, as the immiscible CO_2 phase can be measured visually (see Appendix V). Estimation of the dissolved salts,

however, requires the use of low temperature techniques, since the small volumes of fluid preclude direct quantitative analysis.

As with the high-temperature data, most experimental fluid studies investigating natural systems employed binary systems of either H_2O-CO_2 or H_2O-NaCl. Research of published work on this subject indicates that to date, only Larson (1956) has recorded the effect of dissolved halide on low-temperature carbonated systems. Although Larson's original data were unobtainable at the time of writing, these have been summarised on a P-T diagram by Hollister and Burruss (1976). A modified version of this graph is reproduced as Figure 7-26, overleaf. This shows the stability field boundaries of the phases ice, water, CO_2 liquid, CO_2 vapour, and clathrate. Intersections of these boundaries produce two invariant points. Point (a) is where all the phases except CO_2 liquid may coexist. During a cooling cycle, this point would be marked by the appearance of ice, but would be of little value for investigating inclusion fluids, the first or last ice not being readily distinguishable from clathrate. Furthermore, the effect of salts on this point is not well known. Point (d) however, is buffered by the CO_2 liquid-vapour boundary and is easily recognised in inclusions, being marked by the appearance of clathrate when vapour is present.

The curved field boundary between these invariant points has been shown by Larson to be displaced to the left by dissolved salts (curve f.). As this has a negligible

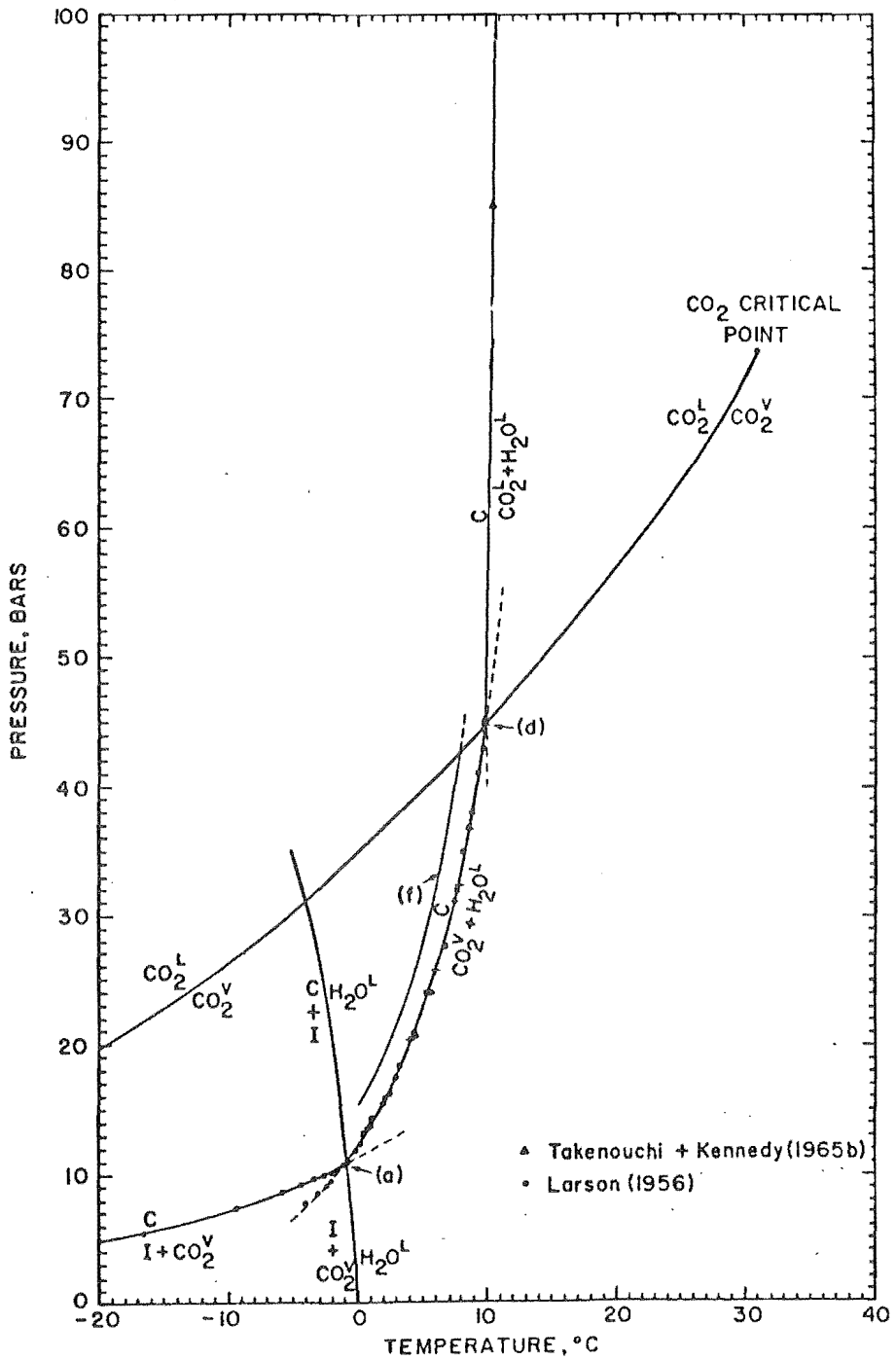

FIG. 7-26 Phase stability diagram for the system H_2O-CO_2, showing conditions of clathrate formation.

H_2O^L	:	Water
I	:	Ice
CO_2^V	:	CO_2 vapour
CO_2^L	:	CO_2 liquid
C	:	Clathrate.

(a) and (d) are invariant points. Curve (f), from Larson, refers to 1 molar NaCl.
Adapted from Hollister and Burruss (1976).

effect on the CO_2 liquid-vapour curve, the useful invariant point (d) is displaced downwards along this curve to lower temperatures.

Larson notes that the presence of 1 molar univalent electrolyte (equivalent to 5.5 wt. % NaCl) lowers the temperature of clathrate formation approximately 2°C. By reasoning that this temperature depression was due to a reduction of the chemical potential of water by the dissolved electrolyte, an expression was derived to account for this effect. The method of this calculation is recorded in Appendix V. The theoretical temperature depression for 1 molar NaCl is found to be 2.4°C. As Larson's corresponding value is stated to be 'approximately 2°C', it is apparent that his measurements were not sufficiently precise to permit a useful comparison with the calculated result. The quoted temperature for the invariant point (d) is 10°C, therefore a clathrate last-melting temperature of 5.0± 0.5° corresponds to a temperature depression of the same numerical value, 5.0± 0.5°C. By calculation, this converts to a salinity value of 11.3± 1.1 wt % NaCl equivalent.

(3) The Evaluation of Pressure

To derive pressure values from salinity data, an isothermal curve has been constructed for the specific system of the LS-12 inclusions at homogenization, vis. 312°C, 15 wt. % CO_2. This is shown as a graph (Figure 7-27), wherein the accuracy of the curve is limited by there being only three data points available. The point at 2120 bars was obtained

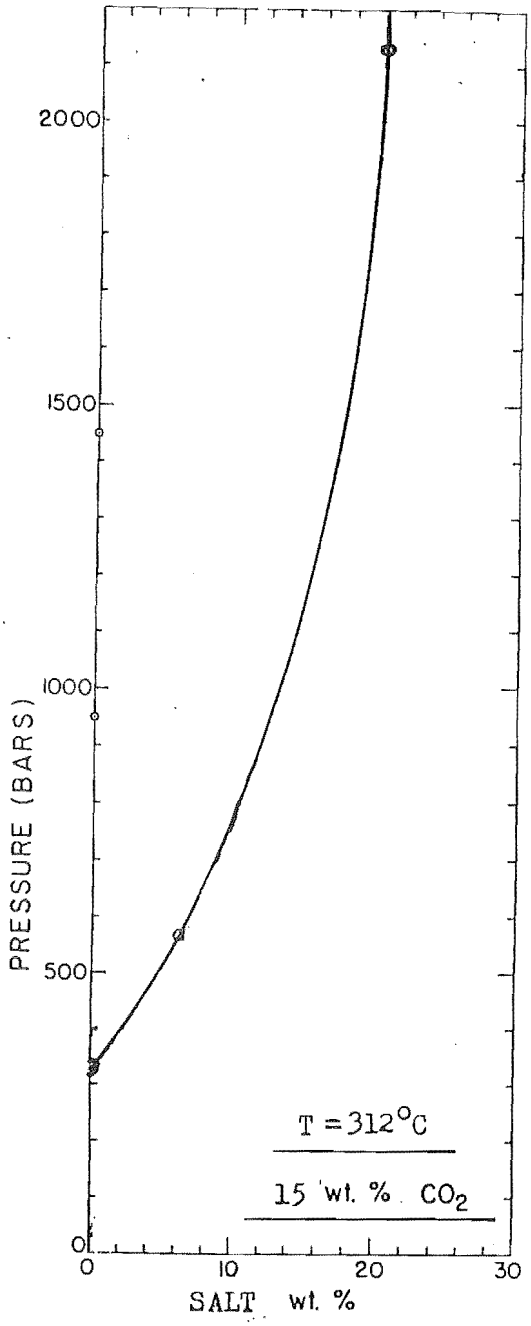

FIG. 7-27 An isothermal curve for inclusions from sample LS-12, showing fluid pressure at homogenization versus fluid salinity for a saturated system containing 15 wt. % CO_2, prepared from the data of Takenouchi and Kennedy, (1965a). See text for details. For practical purposes, the use of the straight line plot Log_e P vs wt. % salt is recommended. The application of such graphs for the derivation of fluid inclusion data requires that a curve (or line) be plotted for the specific homogeneous system, for which the components are quantitatively determined, and the homogenization temperature known.

by extrapolation and may be theoretical, but was used for supporting the location of the plotted curve. The area of the measurements lies within the limits of the experimental data.

This graph was used to obtain preliminary results for use in a paper read at a geochemistry conference (N.Z. Geochemical Group, Auckland, May 1977) and later published as an abstract (Newman, 1977). At that time, the salinity value was applied per se and indicated a pressure of approximately 950 b. Later consideration revealed that a step in the calculation had been overlooked, resulting in a pressure value that was too high. The salinity result of 11.3 wt % refers to only the aqueous liquid at low temperatures, but is distributed throughout the entire inclusion volume at homogenization.

Assuming that:

(i) The density of the homogeneous fluid does not differ greatly from that of the aqueous component under freezing conditions.

(ii) The volume ratio of the two components at 5° does not differ greatly from the measured ratio at 20°C (18 vol. % CO_2). The resulting salinity will be -

$$(11.3 \pm 1.1) \times \frac{82}{100} = 9.3 \pm 0.9 \text{ wt \% NaCl equivalent.}$$

For the actual measurement of pressure from salinity, it is more accurate to use a graph of Log_e P vs Salt wt %, which plots as a straight line (Appendix VI). The modified salinity value thus converts to a pressure of 790 bars.

This figure must be accompanied by a span of error arising from the uncertainties of the measurements, which are discussed in detail and assessed in the next section.

IV. DISCUSSION

(1) Errors of Concept

(a) Fluid saturation. The fundamental basis for the derivation of temperature and pressure in this work is the concept of fluid saturation at the time of sealing. For the inclusions which have been used for the principal measurements, there is good evidence for the existence of this situation. This evidence is found in the direct observations as recorded in this Chapter, and supported by experimental work. Theroretical considerations suggest that once achieved, saturation would be sustained as a 'self buffering' system throughout a considerable range of waning geothermal conditions. Any one fluid from such a system could become undersaturated only if a process operates which consumes all the available complementary fluid. Such a process could occur by: (i) Reheating, (ii) Recompression, (iii) Net increase of one component, or (iv) Net decrease of one component. For the Owen hydrothermal system, processes (i) and (ii) were probably negligible during the mineralizing phase, and (iii) is likely to be significant only at shallow depths where mixing with groundwater is possible. Process (iv) is largely unevaluated, but would be of importance only where consumption of the minor components (CO_2 or salts) took place. Such a process would be controlled by fluid reactions with the host rock, and could be expected to achieve significance only where the fluid traversed a boundary of sharply contrasting rock types. No such bound-

ary can be recognised at Owen; the almost ubiquitous carbonate-sericite mineralogy probably buffered the system with respect to these minor components (see Appendix IV for observations on dissolved salts in the inclusion fluid).

The best indication of fluid saturation is the record of fluid unmixing, but as this evidence is available for a few inclusions only, this condition must be assigned to the remainder of the CO_2-bearing inclusions with a degree of uncertainty.

(b) Sealing of a Homogeneous Phase. Similar phase ratios and homogenization temperatures for a number of inclusions within the same sample is evidence for this postulate, as previously described. Conversely, the presence of CO_2-rich inclusions is required as evidence of fluid saturation. The scarcity of these latter features is probably due to the surface tension effect inhibiting the filling of small cavities by CO_2-rich fluid. The sealing of heterogeneous fluid in the inclusions used for the major measurements can be considered highly improbable, but this cannot be entirely discounted where single measurements are made.

(c) Fluid Equilibrium at the Time of Sealing. Errors due to disequilibrium at sealing are restricted to those of fluid supersaturation. Cooling after homogenization under the microscope shows that this effect must be very small, as demonstrated by the phase nucleation lag. This amounted to an extreme of around 20°C for the smallest inclusions studied, but less than 2° for the larger, CO_2-bearing inclu-

sions. In the even greater fluid volume of the active vein systems, the degree of supersaturation can be expected to be insignificant.

(d) Fluid equilibrium during measurements. At both homogenization and clathrate temperatures, it is possible that a small amount of low-solubility solute of the original fluid remained as an undetected, undissolved solid. At room temperatures and above, the only evidence to support this is the doubtful identification of sulphide crystals in some of the largest inclusions. At low temperatures, clathrate development obscures the inclusions, inhibiting the detection of any other solid phase which may develop on a small scale. If any such undetected solids were present at the time of measurement, this would lower the homogenization temperatures and salinity values, and thereby produce pressure estimates which would be lower than true sealing pressures.

(e) Clathrate stability. This represents the part of the method which is least well known, being only roughly evaluated by experimental systems. Only approximate data are available for the invariant points for water (plus CO_2) and 1 molar electrolyte, the projected values for greater concentrations being entirely theoretical. This therefore provides the greatest possible source of error, the magnitude of which must remain unknown until more information is available from experimental systems.

(f) Additional gaseous components. Reference has been

made to observations by Roedder (1963) and Hollister and Burruss (1976) regarding the presence of inclusion volatiles other than water and CO_2. The black-shale type lithology could give rise to hydrocarbons, and if these or any other extra volatile constituent are present in the inclusion fluids the fundamental P-T interpretation must take this into account or incur error. The single observation of critical phenomena for coexisting CO_2 phases, which was found to be very near the pure-substance value of 30°C, suggests that extra volatiles are not present in significant amounts. Proper analysis utilising mass spectrometry would be required to provide complete data on the volatiles present.

(g) Inclusion Type. All possible care was taken to select only primary or pseudosecondary inclusions for measurements. As mentioned in (b), it is possible that some of the single measurements may refer to secondary inclusions. So far as the sealing of a single phase can be assumed, measurements made on secondary inclusions will provide valid information regarding the host system, although this system may be no more than a larger subdividing inclusion. This category would include the majority of secondary inclusions, the derived information referring to conditions at the time of sealing, post-dating the main hydrothermal event.

(2) Errors of Measurement

(a) Heating Stage Measurements. The calibration of the

heating stage was checked by noting the melting points of pure chemicals. This indicated an error of ±1°C or less, when slow heating rates were used. The use of the silicone oil and a stage muff is considered to greatly contribute to this accuracy by reducing the thermal gradient between stage hotplate and specimen (see Appendix VI).

Errors can also arise from the uncertainty of identifying the exact filling temperature. This difficulty is aggravated by small or obscured inclusions, but in the better examples this error reduced to around ±1°. The best measurements are therefore quoted in Table 7-2 as ±2°C, with larger errors for the smaller inclusions.

(b) Cooling Stage Measurements. Recording the low temperature data incurred a relatively greater possible error than the heating runs. The use of a thermocouple and chart recorder for temperature measurement gave adequate precision, with an accuracy in the order of 0.1° indicated by freezing known solutions. A greater uncertainty in detecting the last melting clathrate increased the error to an estimate of ±0.5°C. As stated, this error converts to a figure of ±0.9 wt % NaCl equivalent.

(c) Estimation of the CO_2 Component. The volume of the CO_2 globule was estimated as a percentage volume of the total inclusion. This was done by measurements from photographs taken at known temperatures, with corrections applied for the three-dimensional inclusion shape which was checked visually with a microscope. The possible error of such a procedure is difficult to estimate; ±2% v/v has been

selected as an approximate value from the magnitude of the uncertainties involved. This value is retained as ±2% after conversion to wt.%, the final presentation thus being 15 ± 2 wt.% CO_2. The error associated with this value is the chief contributor to the total possible error in the pressure determination.

The combined error from the salinity and CO_2 determinations can be estimated graphically (see Appendix V) to produce a result of +205b, -175b, read to the nearest 5b interval. To allow for the graph reading uncertainty, and the corresponding homogenization temperature error of ±2°C, an additional 10% is considered justified, leading to a final pressure determination of 790b $^{+225b}_{-192b}$. As these figures are obtained by reading linear increments on a logarithmic axis, the error span is not symmetrical about the pressure value. For approximate quotation, the error could be centred and rounded off to ±205b.

(3) Interpretation of Results

(a) Reconstruction of the Hydrothermal Environment.

The correlative data from sample LS-12, used for the principal measurements, can be summarised as follows:

Temperature: 302-312°C

Pressure: 790b $^{+225b}_{-192b}$

Bulk fluid composition: aqueous solution of 15 ± 2 wt. % CO_2, 9.3 ± 1.1 wt.% salts, measured as NaCl equivalent. The solution was probably saturated with respect to CO_2 and unmixed during vein formation in response to a reduction in

temperature, pressure or both simultaneously. The unmixing product was a small volume of fluid of which CO_2 was the principal component. Semiquantitative analysis indicates the dissolved salts to be predominantly NaCl with lesser amounts of K and Ca compounds (Appendix IV).

The above information was derived from a number of measurements from a wafer cut from a single crystal, and provides the only numerical pressure estimation. Of the remainder of the homogenization temperatures, many of those noted as having a CO_2 component may originate from saturated parent fluids, thereby requiring no pressure correction. The wide range of temperatures supports the concept of the veining activity spanning a wide range of geothermal conditions, in general agreement with the mineralogical and field evidence. It appears unlikely that any of the measured inclusions are representative of the maximum temperature veining events. The single, clear crystal of sample LS-12 definitely post-dates the surrounding milky quartz which showed evidence of brecciation. There is a notable maximum of primary inclusions homogenizing within the interval 300-332°C, which may record a final episode in a sequence of multiphase veining. Below 285°, the only primary homogenization recorded was at 237°, for a sample from the remote Silverstream lode. Secondary inclusions filled at temperatures from around 268° down to little more than room temperatures, but homogenizations below 200° were not recorded. Although rare, poorly formed secondary inclusions containing a CO_2 liquid were noted (Figure 7-17b).

These can be recognised as late stage structures which merely redistribute primary inclusion fluid. The CO_2 liquid phase could not be formed in any secondary inclusions used for measurements, therefore these homogenizations must be regarded as uncorrected for pressure. If a 790bar correction is applied to the secondaries of sample LS-12, the indicated temperature at any salinity exceeds that of the primaries in the same crystal (see correction graphs from Lemmlein and Klevtsov 1961, reproduced in Appendix V). This evidence, together with the lack of CO_2 liquid in normal secondary inclusions, suggests that the confining pressure was substantially lower during secondary inclusion formation.

(b) Depth of the Hydrothermal System. The magnitude of the fluid pressure in past hydrothermal activity is commonly evaluated by speculative estimation regarding the depth of burial. Alternatively, pressure-dependent mineral reactions may be recognised from the suite of vein or wall rock minerals. For ancient, eroded systems, either of these methods may involve a very large degree of uncertainty. Both tend to indicate the maximum pressure event for the rocks, which is frequently not coincident with the hydrothermal event.

Fortunately, fluid inclusions provide a direct, numerical pressure value for at least one veining phase of the Owen system. This value can now be used as a basis for models which attempt to reconstruct the depth of the former

activity. The true pressure-depth relationship for hydrothermal systems is more difficult to establish (to the same error) than for the deeper, metamorphic situations. Hydrothermal veining is a product of the flow of hot solutions through fissures of various restriction and vertical extent. In the case of shallower systems such as hot springs and boreholes in modern geothermal provinces, the known channelways are usually free-flowing and emerge at the ground surface. A vertical column of water of the same temperature and composition is a satisfactory model for such occurrences. For the extinct systems represented by veins and ore deposits, an additional factor must be considered,— the'degree of confinement' for the system.

Consider the hypothetical situations illustrated below (Figure 7-28). This diagram depicts three possible emplacements of hydrothermal systems where fluid flow rates are negligible, within an ideal, nondeformational environment. The common depth horizon 'd' intersects all three systems. The pressure at this point will differ for each case. For (a), a relatively unrestricted column of fluid extends to the surface. The pressure at depth 'd' will be hydrostatic, determined by the depth and density of the fluid. If an upward flow exists, the pressure is not solely hydrostatic, possessing an additional hydrodynamic component which is a function of flow restriction and flow rate. This extra component is contributed by lithostatic pressure from the host rock surroundings, transmitted via

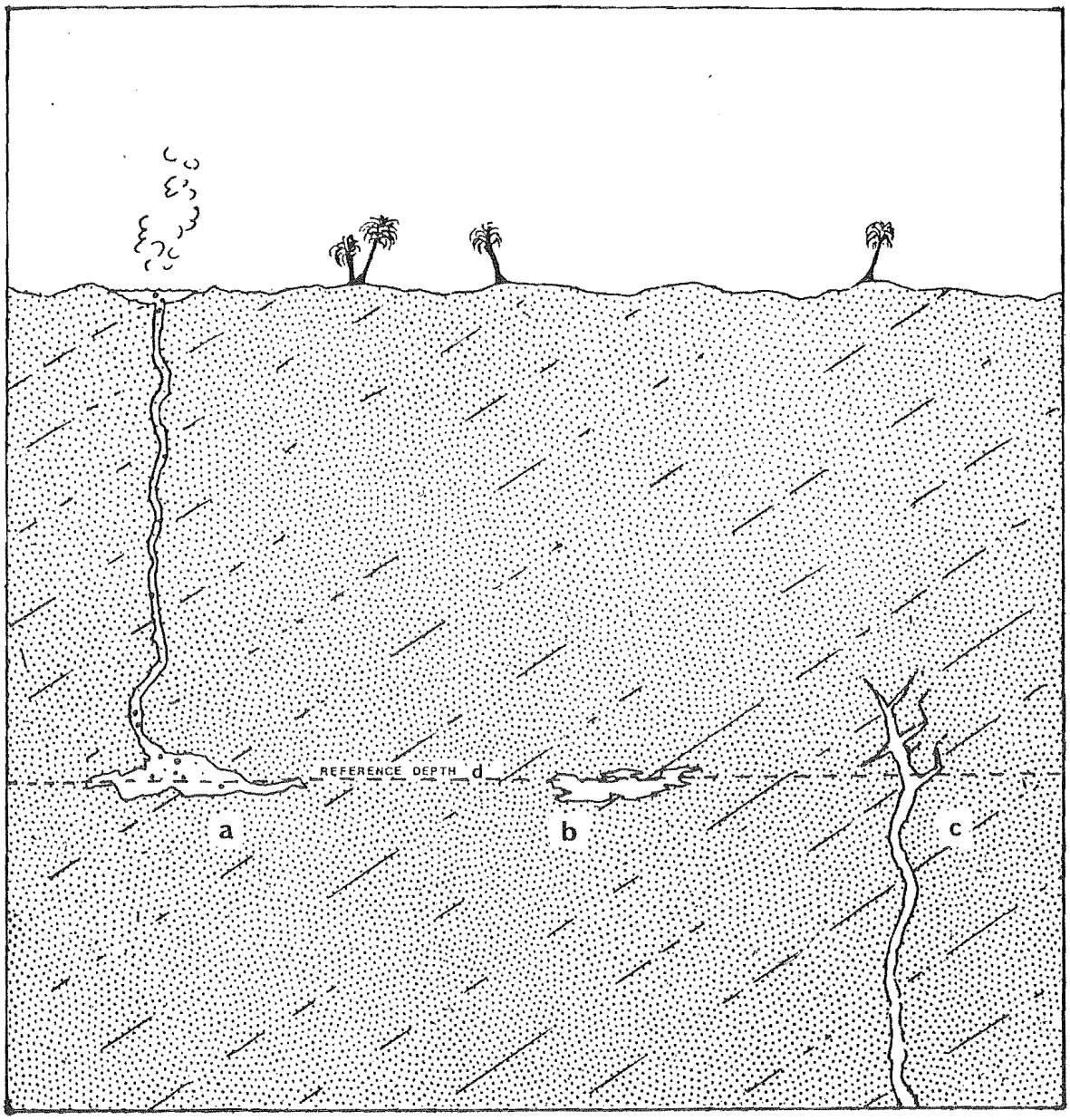

FIG. 7-28 A theoretical section of three possible hydrothermal systems, intersected by a common depth horizon 'd'. The pressure at this level will differ for each situation, particularly between (a) and (b). Situation (c) involves hydraulic fracture. Refer to the accompanying text for detailed discussion of this diagram.

pore fluids which supply the hydrothermal ducts. Flow restriction is taken to an extreme in (b) where the fluid is considered to be completely enclosed, with no flow to the surface possible. The fluid pressure will be entirely lithostatic, approximately $2\frac{1}{2}$ times that of the hydrostatic system at the same depth.

Most hydrothermal orebodies of shallow emplacement can be represented by some depth-pressure model intermediate between (a) and (b), but a further possibility exists as shown in (c). If the hydrothermal duct extends over a significant interval and the upper portions are totally restricted, lithostatic pressures from deep within the system will be hydraulically transmitted to the shallower zones. Thus the pressure at horizon 'd' will exceed the lithostatic pressure for that depth in system (c). Total upper restriction is not required for this effect. The condition created is unstable, and is limited in magnitude and duration by the strength of the confining rock. Rock failure by this mechanism is termed hydraulic fracturing (Philips 1972), and has been described from modern geothermal systems by Grindley and Browne (1976).

The models described above are ideal cases, most unlikely to be duplicated by nature. If hydrothermal systems are considered in a dynamic sense, involving movement of fluids, accumulation of deposits, and fracturing of the host rock, the particular combination of factors for any one occurrence may be continuously changing, with consequent

fluctuations in fluid pressure. The three examples illustrated may be considered as end-members of series of such factor combinations. Using the depth-pressure equation quoted by Miyashiro (1973), i.e.

Pressure (bars) = 98 x Density x Depth (km)

- and applying the computed pressure of 790b to the three situations, results in the corresponding depth values of:

(a) 8.0 km (Assuming fluid density = 1)
(b) 3.0 km (Assuming average rock density = 2.68)
(c) <3.0 km (" " " " ")

The result for situation (a) seems quite unreasonable. The existence of an unrestricted system over a vertical interval of 8 km is most unlikely, and such a depth is difficult to envisage in terms of known stratigraphic thickness, even if tectonic thickening is invoked. Case (b) presents a more realistic depth, as 3 km of sedimentary cover at the time of vein formation is conceivable, but would suggest some tectonic thickening. A model involving hydraulic pressure transmission as in (c) is supported by field evidence indicating hydraulic fracturing, and the general geologic setting of hydrothermalism marginal to an active granite batholith.

The single sample which provides the basis for this discussion of pressure (sample LS-12) consists of small, clear quartz crystals formed in the voids of brecciated vein quartz, and associated with minor base metal mineralization. This sample may be interpreted as representing a stable period of mineral deposition, following an event of

intense fracturing which was almost certainly accompanied by a sharp reduction of pressure. This interpretation indicates a fluctuating fluid pressure which at times exceeded the value derived from the sample. Clearly, the evaluation of depth from a single value of pressure remains complicated by the limited information. For hydraulic fracturing to commence, the fluid pressure must exceed the least compressive stress by an amount equal to the tensile strength of the lithology involved. Periodic hydraulic fracturing would result in pressure fluctuations of the order of only a few tens of bars, so long as major openings to the surface were not produced.

From the evidence available, the best interpretation appears to be that in which the indicated pressure of 790 bars is considered to be not greatly less than that which caused hydraulic fracturing. In this situation, the measured pressure would be expected to closely follow lithostatic pressure, inferring a depth of approximately 3 km.

The relationship of mineralization, pressure fluctuation, and hydraulic fracturing are discussed in Chapter VIII.

(c) The Effect of Fluid Composition in the Hydrothermal Process. The composition of the hydrothermal fluid has been evaluated by a number of approaches. The dissolved salts have been investigated by crushing and leaching to derive relative abundances of the principal alkalis. Sodium, potassium and calcium chlorides are present in the usual order of abundance, with sodium predominating in all cases. The full report of this work is confined to Appendix

IV. For the specific case of sample LS-12, total dissolved salts were estimated as 9.3 wt.% as NaCl equivalent. For the same inclusions, CO_2 was estimated as 15 wt %, and observed in similar proportions in the inclusions of many other samples.

Takenouchi and Kennedy (1965a) described the water-CO_2-salt fluids as 'extremely corrosive' at high temperature and pressure. This effect was sufficient to force the termination of measurements, due to the deterioration of their stainless steel equipment, accompanied by the growth of siderite crystals on the walls of the autoclave vessel. As this system closely approximates the fluid of the Owen, and many other hydrothermal situations, one may speculate on the effect in the natural environment. It is apparent that such a fluid contains chemical species of considerable chemical activity, and may be an important agent in promoting the hydrothermal effects. Although ore transport chemistry will not be debated in detail in this work, the following observations seem pertinent at this point. Laboratory and mineralogical studies indicate that most hydrothermal ore minerals are transported as either chlorides or sulphides, probably in complex species (Barnes and Czamanske, 1967, see also Chapter VIII). If sulphides are the principal transport species, the highly carbonated-chloride characteristic of the solution may remain significant in an intermediate role, such as the attack and alteration of source or host rock, or by providing a catalytic reaction. The development of the abundant vein carbonates

is consistent with the measured fluid composition as both dissolved CO_2 and halide increase the solubility of these minerals (Ellis, 1963, and Chapter VIII).

The importance of solutions of this type in the hydrothermal process appears to be neglected by geochemists, as very little published work on equivalent experimental systems is available. Fluid inclusion investigators - who frequently observe highly carbonated fluids - remain the principal, if not only, source of speculation on the significance of such fluids in orebody formation (e.g. Rankin, 1975).

(d) Future Work. Fluid inclusion research as a means of investigating the Owen hydrothermal province can be continued to good effect, as the present project has by no means exhausted this aspect. The limitation of time for collecting and preparing samples has restricted the amount of useful material studied. As previously discussed, much of the project time spent on inclusion work involved developing methods of preparation and study, and determining the type of sample material to select. Further study could follow the procedures already developed, as additional data would reduce the remaining uncertainties and more completely evaluate such aspects as the temperature and pressure history of the field, and the correlation of these measurements with episodes of mineralization. This work could ideally be combined with a thermodynamic laboratory study to provide better data on the freezing characteristics of the system H_2O-CO_2-salt, to supplement the meagre information of Larson (1956).

The inclusions could be studied by techniques not attempted in this project, by using more sophisticated methods of analysing the inclusion fluid, including isotope measurements. Should more information become available regarding the fluid system at either high or low temperatures, the original data from this present study could be recalculated to obtain more certain and accurate results, and any new measurements processed with greater facility.

V. CONCLUSIONS

(1) The Method

Conventional fluid inclusion studies involve only the measurement of filling temperatures as a means of geothermometry, occasionally supported by salinity-pressure corrections. In this study, evidence indicating a second fluid component in saturation proportions at homogenization has permitted a more sophisticated treatment. The concepts and procedures used, lead to a set of results which in the ideal case present precise, comprehensive information on the hydrothermal environment. So far as can be determined from published material, this method has not been previously proposed. It must therefore be regarded as tentative until tested by experimental work or further information from natural systems. Subsequent to the use of the concept of fluid saturation on which this temperature-pressure method is based, published work by Smith and Little (1959) was found in which the authors demonstrate the recognition of this concept, and attribute this to the earlier work of Smith (1953). An extract of the paper is reproduced as follows:

> 'In cases where a mineral grew in a one-phase H_2O-CO_2 system, the filling temperature provides a minimum temperature of formation, which, as in the case of water-water vapour inclusions, is subject to correction for pressure. The calculation of this pressure correction, however, not only requires a knowledge of the pressure at the time of formation (which at best can only be roughly approximated), but also accurate thermodynamic data on the system H_2O-CO_2 (which at present are not available in the temperature pressure range desired).

> In cases where it can be demonstrated that the mineral grew under the two-phase condition however, as was pointed out by Smith (1953), it should be possible to determine the temperature of formation directly from filling temperature measurements.'
>
> (Smith & Little 1959).

This demonstrates a clear understanding of the basic theory, and also the limitation imposed by the lack of experimental data. The effect of salinity was unknown, and no attempt could be made to evaluate pressure.

A fluid inclusion study which includes an attempt to derive pressure values was made by Hollister and Burruss (1976), using inclusions from high grade metamorphic rocks. A number of somewhat indirect approaches are employed, including the plotting of homogenization temperatures on a 1 kb solvus graph to demonstrate salinity determination (Figure 7-25). As the locus of critical point homogenizations falls near the 6% salt curve of Takenouchi and Kennedy's data, this salinity value is assumed to represent the fluid. The accuracy of such a procedure is dubious, as the solvus curves are crowded together in this region, especially when the mole % CO_2 axis is used. To the same authors, however, must go the credit for a clear representation of the low temperature phase stability diagram for the system H_2O-CO_2, which they describe as a 'petrogenetic grid'. This diagram is reproduced in this work in modified form as Figure 7-26. It also illustrates the curve displacement due to salinity from the data of Larson (1956), although this is wrongly identified in the text.

In summary, the method used in this project is a com-

posite of procedures used in others. It is based on experimental data of Larson (1956) and Takenouchi and Kennedy (1965a, 1965b), facilitated by the information gathered by Hollister and Burruss (1976), and the fundamental concept supported by the earlier work of Smith and Little (1959).

(2) The Results

The outcome of this fluid inclusion study is of considerable assistance to the project as a whole. The information gives values for temperature, pressure, and composition for specific events, which if considered together give some indication of the range and history of the hydrothermal activity. This information is of superior quality to that obtained by other means. The data from silicates, carbonates, and sulphides (Chapter VI) is of lesser certainty and precision.

Hydrothermal temperatures during vein formation probably exceeded 350°C, with a large amount of deposition occurring over the range 300-335°. This range may represent conditions of a final major veining event, with quartz deposition continuing to below 230°. Deformation accompanied and followed vein formation, probably due to a combination of tectonic and hydraulic effects, causing brecciation and intense fracturing. This resulted in the development of abundant secondary inclusions, which formed at temperatures ranging from more than 280° to less than 100°, in zones where the flow of primary hydrothermal fluid (characterised by ca.15-20 vol.% CO_2) had ceased. Hydrothermal pressures

during a late stage of the activity are known to be approximately 790±200 bars, with fluctuations in response to hydraulic and tectonic fracturing, at a depth of approximately 3 km.

CHAPTER VIII

INTERPRETATION, SUMMARY, AND CONCLUSIONS

I. A PROPOSED MODEL FOR THE MINERALIZATION

The most widespread field evidence relating mineralization to structure is the stratigraphic control of the sericite zone. This feature has the following possible origins:

(i) Alteration of a permeable and/or geochemically favourable lithology.

(ii) Restriction of fluids beneath the massive, impermeable marble, i.e. fluid confinement at a permeability boundary.

(iii) The induction of secondary permeability by differential movement at the major lithological boundary between contrasting rock types.

Although some combination of these origins is considered probable, all three involve a net effect of fluid flow within a zone of relatively high permeability, confined beneath the marble which appears to have acted as a 'capping' on the fluid-controlled processes operating beneath it, giving rise to the large difference in the degree of alteration between pelitic rocks of the Wangapeka and Owen Formations.

(1) A Reconstruction of Mineralization History

(a) The Geological Situation Prior to Intrusion (see Figure 8-1a). All available evidence suggests that the thick sequence of Paleozoic sediments exposed at Mt. Owen continued further east, at least to the position now occupied by the axial region of the batholith. Similarly, major folding of the sequence in the goldfield area cannot be inferred; therefore, for the purposes of reconstruction, Figure 8-1a depicts flat-lying units of constant thickness.

Evidence from the mudstone lithologies suggests that a water-escape process was associated with cleavage development, especially within the uppermost Owen Formation. Although this evidence is inconclusive, the expulsion of some retained pore water during pre-intrusive or early intrusive deformation must be considered a strong possibility. The movement of such pore water is of significance to processes of metal transport before or during the onset of the mineralization episode.

(b) The Intrusive Stage (Figure 8-1b). The principal phase of granite intrusion is seen as the major tectonic and thermal event in the goldfield area. A sharp rise in temperatures was accompanied by regional uplift associated with Rangitatan tectonism, probably in addition to local uplift caused by intrusion. An episode of physical dewatering probably accompanied thermal metamorphism and cleavage development. The associated desulphurization reaction is considered a potentially important element of the mineraliza-

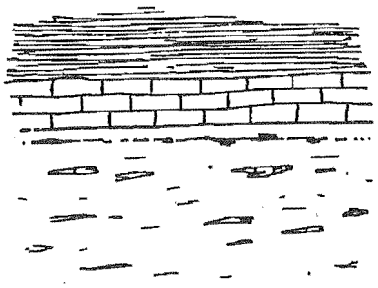

(a) Pre-intrusive Time.

Little deformation or metamorphism
High pore water content retained beneath carbonate unit ?

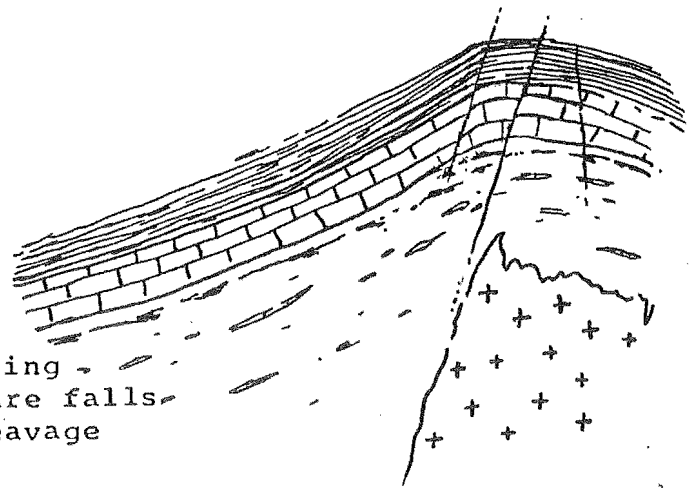

(b) Intrusive Stage.

Uplift, tilting and faulting -
Temperature rises, pressure falls-
Physical dewatering & cleavage development ?
Metamorphism, early vein formation.

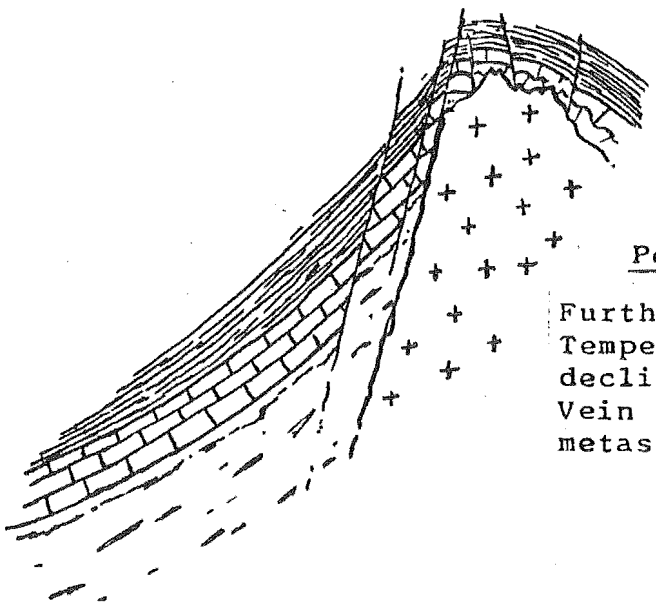

(c) Late Intrusive-

Post Intrusive Stage.

Further uplift, shearing
Temperature declines, pressure declines. Chemical dewatering
Vein formation, mineralization, metasomatism, resulphurization.

FIG. 8-1 East-west sections (not to scale) of the Mt Owen region, showing a suggested reconstruction of the metamorphic-hydrothermal history. Strata above the Wangapeka Formation (hatched) have been omitted. The rocks of the goldfield are located at the left of the sketches.

tion, as discussed below.

Major structural tilting on the flanks of the intrusion would produce the regional westward dip of both bedding and cleavage; the establishment of this configuration would determine the fluid flow pattern, and a hydrothermal system would commence to operate. Alteration would result, but vein deposition would occur only where the fluid passed down a significant pressure — temperature gradient.

(c) The Late Intrusive-Post Intrusive Stage (Figure 8-1c). Except for rare examples in the lower Owen Formation of veins which predate cleavage, the principal deposition of vein minerals is correlated with a period of alteration, shearing and brecciation, during which both temperature and pressure declined. The possibility of hydraulic fracture has been discussed. Deformed and brecciated vein structures, and multigeneration mineralization evidence, indicate that the vein-forming episode spanned a significant period of deformation. The later phases of mineralization which proceeded at the lowest temperatures gave rise to the marcasitic deposition, and possibly to the bulk of the gold deposition. Large changes in fluid chemistry are indicated, and are certainly due in part to the lowering of temperature and pressure, but possibly also due to reactions in response to specific reduction of P_{H_2O}, P_{CO_2}, or sulphur fugacity, at depth. The sulphur required for the resulphurization of pyrrhotite could have one or more of several origins, as discussed

below, but is probably derived from sulphide decomposition below the zone of deposition. Similarly, the hydrous fraction of the hydrothermal fluid may have been supplied by dehydration reactions, comprising a 'chemical dewatering' process, as distinct from the envisaged earlier physical expulsion of pore water. Development of the widespread sericitic alteration was probably contemporaneous with the principal period of vein formation.

(2) Fluid Flow Considerations

Henley (1973a) recognises two end-member models for hydrothermal fluid flow systems. The first consists of the injection of hot fluid into a dry permeable medium, commonly exemplified by the release of magmatic fluids by an igneous intrusion. The second model is one of free fluid convection in a saturated medium, the given example being the recirculatory pattern formed by groundwater surrounding a rising pluton. Neither individual model, nor any combination of these models, may be satisfactorily equated with the Owen hydrothermal system. The granite at Owen is unlikely to have supplied the bulk of the hydrothermal fluid (see below), and if the evolutionary interpretation of Figure 8-1 is correct, the structural anisotropy of the country rock precludes the operation of a convectional system. The extensive and impermeable marble flanking the granite requires an open ended, up-dip flow system, in which no fluid recharge is possible except by continued dehydration of underlying rocks. Up-dip discharge is assumed to occur

through faults and shears at or above the pluton margins.

Figure 8-2 summarises the essential elements of the envisaged fluid flow model at the time of peak hydrothermal activity (cf. Figure 8-1c). Replacement bodies within the marble and sparse quartz veins in the overlying Wangapeka Formation are envisaged as arising from penetration of the marble by high pressure fluids. CO_2-rich inclusion fluids noted in these veins suggest an origin beneath the marble, where evidence for highly carbonated fluid is abundant.

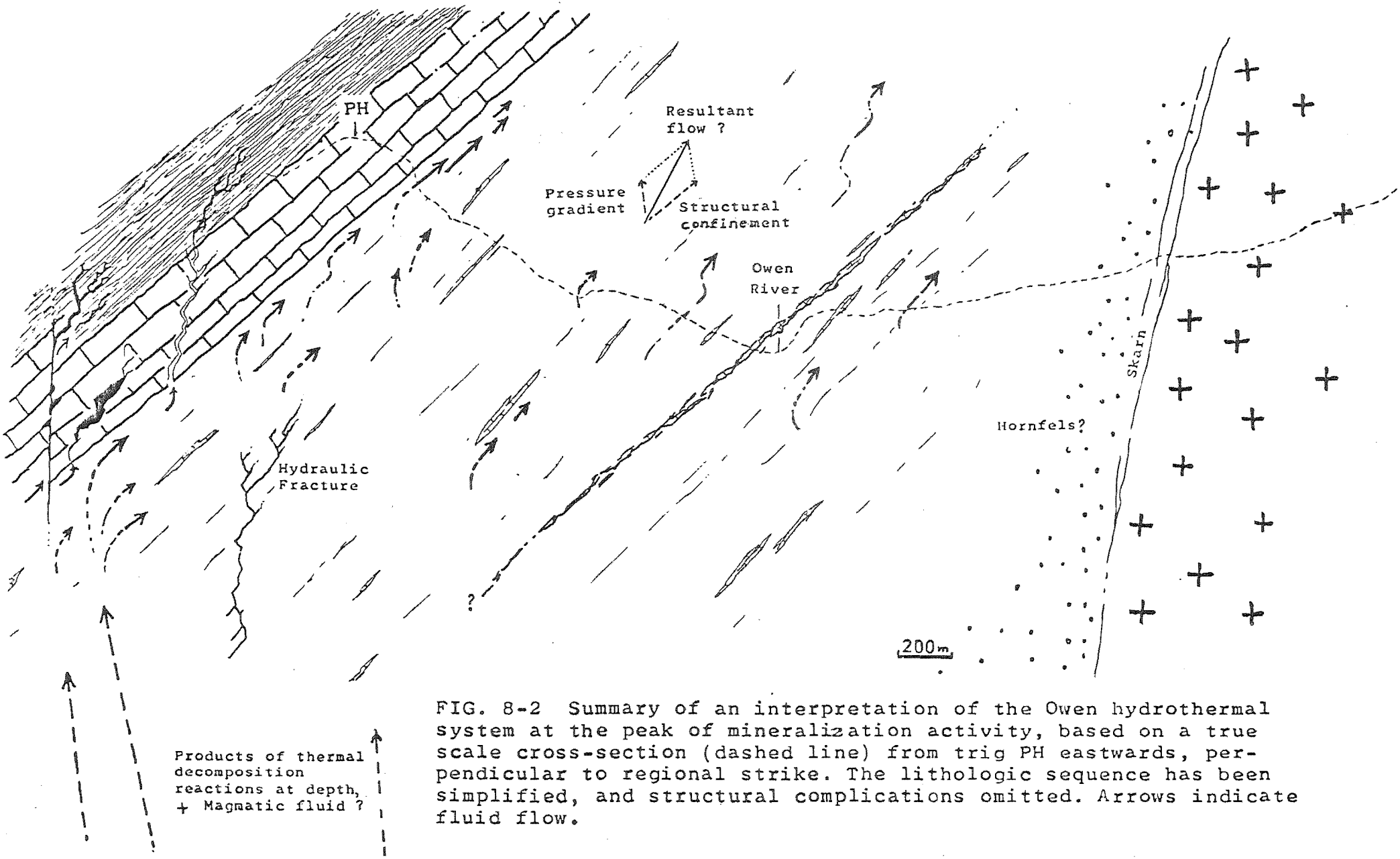

FIG. 8-2 Summary of an interpretation of the Owen hydrothermal system at the peak of mineralization activity, based on a true scale cross-section (dashed line) from trig PH eastwards, perpendicular to regional strike. The lithologic sequence has been simplified, and structural complications omitted. Arrows indicate fluid flow.

II. THE MINERALIZATION: CONCLUSIONS

(1) Source of the Mineralization Components

(a) Heat. Granite intrusion is seen as the primary thermal energy source, although heat contributed from the normal geothermal gradient must be considered in the case of pressure release and fluid flow in response to uplift. Heat flow in the country rock was probably strongly controlled by fluid flow, but closer to the intrusion, the process of conduction would dominate.

(b) Fluid. The scarcity of veins, pegmatites, and hydrous minerals near the intrusive contact suggests that the granite was a 'dry' intrusive, and did not supply significant amounts of magmatic water to the hydrothermal system. Pore water and sediment-bound water almost certainly provided the principal component of the hydrothermal fluid. Physical expulsion of this water is seen as the initially dominant fluid supply process, later progressively replaced by dehydration reactions which would proceed in response to increasing temperature/pressure ratios. Some buffering effects tending to stabilise P_{H_2O} values would occur during both the formation and decomposition of hydrated minerals. The second most abundant fluid component is CO_2, for which the most obvious source is the decomposition of carbonate minerals. The abundance of CO_2 in the sericite zone during vein formation may be due to decarbonation reactions within this zone, perhaps favoured by

the loss of ankeritic Fe and Mg to growing chlorite. A preferred alternative is the supply of CO_2 as a component of a concentrated, homogeneous fluid from a deeper source near the granite margin. Assimilation of carbonate-rich sediment by granite magma would give rise to large amounts of CO_2, which presumably migrated to the zone of mineralization via unexhumed conduits beneath the present goldfield. Unless the goldfield is underlain by an unemerged, subsidiary intrusive stock (Cf. Smale, 1976), the fluid transport path from the inferred margin of the main batholith is surprisingly long (several km) and cross-cuts the regional structure. It is conceivable that the zone of dehydration-decarbonation reactions extended westward from the granite at depth, due to a combination of intrusive heating and the normal geothermal gradient.

A problem associated with all non-recirculatory hydrothermal models is the difficulty in identifying a fluid source sufficient to emplace the mineralization observed. Special conditions of fluid supply may have existed for the Owen system, as follows:

(i) Contribution of some magmatic fluid from the granite, although unlikely, cannot be disproved.

(ii) The country rock may have retained a high proportion of water up to the time of intrusion.

(iii) The westward dipping structure of the country rocks continues for some distance west of the mineralized area. Some up-dip recharge of the hydrothermally active zones is

therefore considered possible. Inclusion and wall rock studies indicate some thermal and chemical disequilibrium of the fluids and host rocks, consistent with the channelling of fluids from greater depths.

(c) Gangue Minerals. In general, the assemblage of gangue minerals reflects the mineralogy of the altered host rocks. The absence of exotic minerals is consistent with the concept of structural confinement, and argues against the supply of fluid from the granite, unless significant dilution of such fluid occurs. Although the paragonitization may be seen as reflecting the sodic nature of the granite, a NaCl-rich fluid from original pore water must also be considered as a possible cause.

(d) Ore Minerals. A study of the disseminated minerals in the Wangapeka and Owen Formations shows the carbonaceous mudrocks to be rich in sulphide which is probably of syn-sedimentary origin. Although the total ore metal content of these rocks may not be atypical of black shale sequences, the chemical 'reworking' undergone by the Owen Formation is considered to be an important forerunner of subsequent metal-leaching processes. The desulphurization-resulphurization sequence beneath the marble is proposed as an episode in which the sediment is 'scavenged' by active sulphur species, extracting chalcophile elements which are then incorporated in easily remobilised sulphide form. The importance of metamorphic sulphur migration in this role has been stressed by several authors (McDonald,

1967, Lambert, 1973, Carpenter, 1974). An additional source of readily available ore sulphides may have been provided by inclusions incorporated in stratiform pyrite during pre-metamorphic growth. A study of the unmetamorphosed and unaltered Wangapeka formation lithologies suggests that the ultimate source of the ore metals was syndepositional accumulation in carbonaceous muds. The relatively simple mineralogy of the ore bodies, which contain Fe, Pb, Zn, and Cu sulphides, is comparable with the similar range of sulphides seen in disseminated form in the postulated source rocks. Both gangue and ore mineral assemblages therefore support the postulate that the country rocks of the Owen Formation provide both source and host for the mineralization. The exotic mineralization, Au, Ag, Sb etc., exists only as traces within the ore bodies (although these traces may comprise economic concentrations), and these metals may be attributed to the same source as the base metals.

If syngenetic-sedimentary sulphide is accepted as the ultimate source of the ore minerals, adequate sulphur accompanies the ore metals in the source rocks. On decomposition of disseminated pyrite to form pyrrhotite, a large amount of sulphur was either lost from the system or taken up in newly-formed sulphides. In either case, the resulting sulphur deficit was eliminated during the resulphurization episode due to one or both of the following reactions:

(i) <u>In situ</u> alteration of pyrrhotite to form a di-

sulphide by loss of iron, with no ingress of sulphur.

(ii) Decomposition of pyrrhotite at depth, the surplus iron being taken up by the formation of carbonates, chlorites, or higher temperature silicates, and the sulphur transported upward in solution.

Although the Owen Formation alone is considered to be adequate as a source of the mineralization, it is probable that some supply of components was provided by the sequence below that which is exposed. The possibility of metal-rich, volcanogenic rocks of the Aorere and Haupiri Groups underlying the Owen Formation cannot be neglected.

(2) Time of Mineralization

Radiometric dates for the Separation Point Granite indicate an age of ca. 90-100 m.y. This age, or a slightly younger age, may be applied to the mineralization. Winkler (1967) provides estimates of the duration of near-maximum temperatures experienced by country rocks surrounding a plate-like intrusion. This period is given by the expression $T=0.1\ D^2$,* where T is the time (years) and D is intrusion thickness (metres). The Separation Point Batholith forms a linear body of relatively constant width. Assuming the exposed width at Mt. Owen to represent thickness, D = approximately 8.8 km, indicating a high temperature duration of 7.7×10^5 years for the rocks near the centre of the goldfield. Some over-estimation is probably due to

* Not $0.01\ D^2$ as misprinted in Winkler (1967), p.83.

the significance of roof zone heat loss, i.e. a large width/depth ratio will cause departure from the thin plate model. Some compensation for this loss may be provided if the intrusion width increases with depth.

The thermal duration estimate is based on a model involving only conduction, additional complications being introduced by considerations of fluid flow. If a high temperature period of 0.5-1.0 m.y. is assumed, the cooling time representing the active hydrothermal period may have spanned several million years in view of the large temperature range indicated by the mineralization—unless rapid uplift and unroofing and/or fluid flow greatly accelerated the cooling process.

(3) Conditions of Mineralization

(a) Temperature-Pressure Information. This aspect has been examined in detail (Chapters IV-VII), and to avoid unnecessary repetition the results are summarised in condensed form in Figure 8-3. Attempts to elucidate the temperature, pressure, and chemical conditions of the hydrothermal system at the time of mineralization have been only partly successful, due to the lack of definitive mineral assemblages, insufficient mineral equilibrium data, and excessively complex mineral systems. An approach based on fluid inclusions produced good results, but much tedious preparation and measurement was required for a small number of useful values. Information from both min-

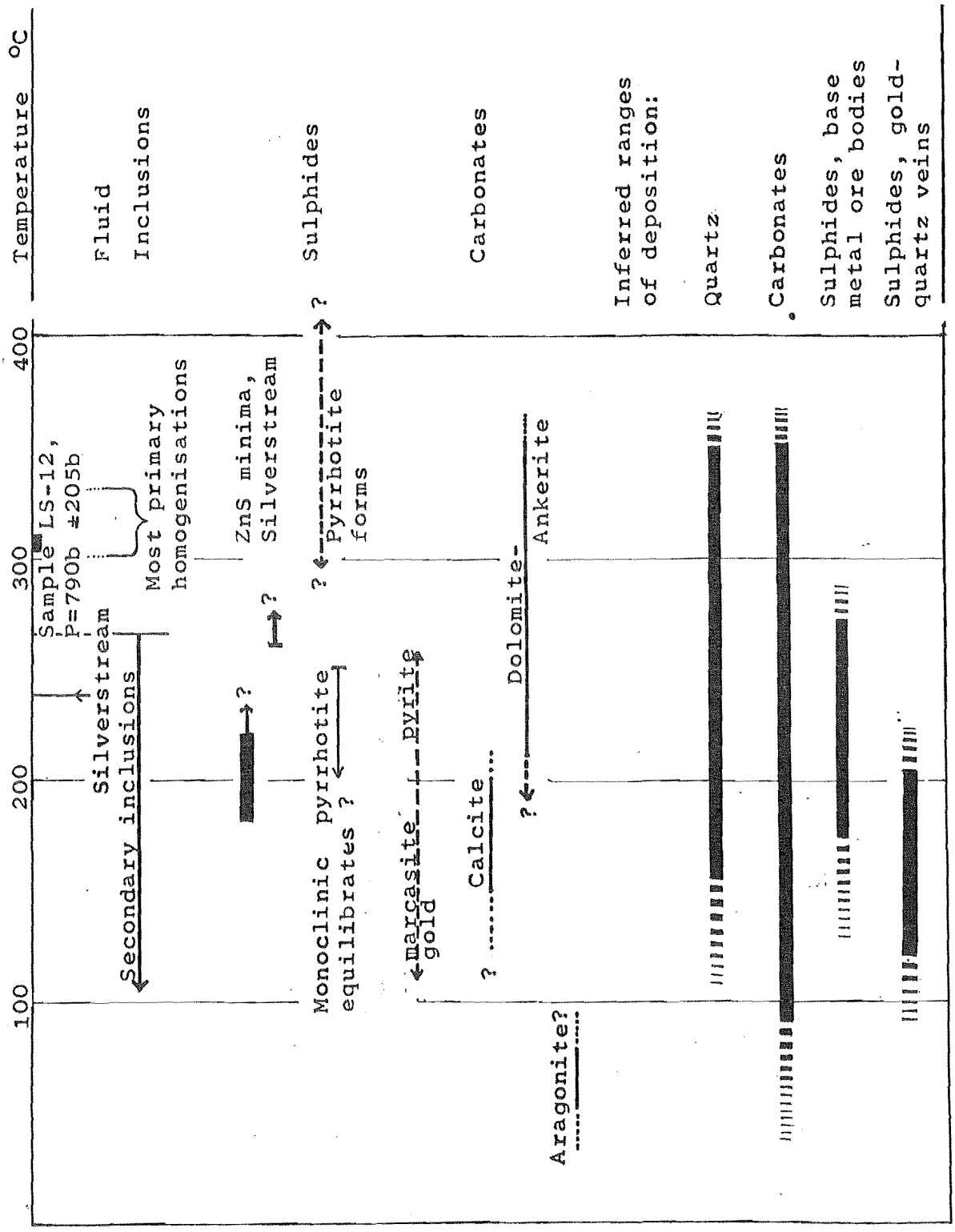

FIG 8-3 Summary of mineralization temperature-pressure evidence and inferred ranges of hydrothermal deposition.

eralogical systems and fluid inclusions indicates a range of physical and chemical conditions which is large, but consistent with the characteristics of a cooling hydrothermal system. The only satisfactory indication of pressure is a single value from fluid inclusion measurements.

(b) Fluid Composition. Some direct indication of fluid composition is available from fluid inclusion studies, but otherwise this information must be inferred from mineralogical evidence. The high CO_2 content indicated by many inclusions was probably maintained for most of the mineralization episode, the temperature and pressure in the source zone being the controlling factors. Accompanying salinities were due to mainly NaCl, the reaction of which with wall rock is suggested by paragonitization near major veins.

Both high CO_2 and high salinity favour the solution and transport of carbonates (Ellis, 1963), deposition being controlled by the reduction of one or both of these components. Cooling increases carbonate solubility under mesothermal conditions, in contrast to the response of silica and most common ore minerals. Where dolomite and ankerite are present in addition to calcite, the relative solution-deposition relationships become more complex, and will be controlled by wall rock minerals in equilibrium with the fluid. For a fluid containing Ca, Mg, and Fe at

constant pressure, a decline in temperature will favour dolomite (or ankerite) replacement by calcite (Holland, 1967). Rapid exhumation of the system during hydrothermal activity would cause a steepening of local temperature and pressure gradients, creating a situation generally favourable to mineral deposition (Henley, 1973a). Within active hydrothermal conduits, the pressure drop would lead the temperature drop until cooling occurred, thus initially favouring carbonate due to the sudden loss of CO_2 from the hydrous fluid phase. Subsequent cooling would favour quartz-sulphide deposition, forming an overall mineralization sequence consistent with that observed in some veins.

The significance of a primary, homogeneous, CO_2-rich fluid in a general metal-leaching and transport role has been discussed, and the association of such fluids with gold mineralization is recorded in a recent review of gold geochemistry (Handbook of Geochemistry, v II pt.4). The nature of chemical species enabling the transport of gold in solution remains uncertain. Opinion is chiefly divided between two possible types, namely chlorides / chloride complexes (Helgeson and Garrels, 1968; Henley, 1973a; 1973b) and sulphur-based complexes (Barnes and Czamanske, 1967; Boyle, 1969; Weissburg, 1970; Seward, 1973). This long-standing debate will not be continued here, as no definitive evidence has emerged to support any specific hypothesis. The association of gold with marcasite suggests a neutral to acid reducing environment during deposition,

but conditions of leaching and transport, which mobilised carbonate, were probably alkaline. Sulphur fugacity levels were probably buffered by pyrrhotite for much of the earlier history of the mineralization, with a gradual rise in these levels as pyrrhotite disappeared from the system. Local areas of high sulphur fugacity may have existed near the base of the marble, permitting pyrite deposition in these zones.

(4) Controls on the Mineralization

A pattern of relatively simple structural and lithological control is recognised. Almost all economically attractive concentrations of gold are found in veins within, or very near, the sericite zone. Although physical factors (e.g. promotion of fracturing and fluid confinement) dominate in this association, chemical factors may also be important. The major gold-bearing veins all show replacement of wall rock; simple infilling alone has resulted in veins which are usually small, and always poor in gold values. The large Golden Crown vein is far from the sericite zone, but is located in a zone of brecciation and adjacent to a thin carbonate lens.

The chemical effect of the Arthur Marble is dominant in locating the base metal ore bodies, all of which show prominent wall rock replacement except perhaps the Silverstream lode, where ore textures suggest infilling to have been dominant.

Local structural control of vein emplacement can be

correlated with poorly defined shear zones sub-parallel to bedding, but cannot be associated with any major tectonic structure.

(a) Gold Distribution. Assay results and mining reports indicate the gold distribution within single vein systems to be very erratic. The gold-rich ore appears to be restricted to veins of relatively carbonate-free quartz, containing marcasitic pyrite and sparse chalcopyrite. This assemblage is considered to represent a very late stage of the mineralization and to mark a large change in fluid composition. The possibility of multistage mineralization involving chemical 'reworking' of deeper parts of the vein system (see Boyle, 1969) is suggested. A period of rapid temperature and pressure decline due to unroofing of the deposit, and even the ingress of meteoric water into the system, must be considered as possible causes of the late auriferous deposition, although little supporting evidence is available.

The reef-cap zones of the ore bodies have certainly undergone some secondary enrichment, giving rise to very high values in some early assays. Although some ore bodies may have been close to the surface during early Tertiary weathering (e.g. the Golden Crown vein), most appear to bear only a thin surface zone of enriched ore which can be related to recent weathering, and is consistent with the steep topography and the relatively rapid rate of erosion.

(b) Silver distribution. All base metal ores yield

high assay values of silver, typically 200-300 oz per ton of pure sulphide (6000-9000 ppm), allowing for hand picking of the original samples. Galena is assumed to be the sole silver-carrier, except for the Silverstream ore where a silver-rich tetrahedrite is also present. Secondary enrichment of the base metal deposits is insignificant.

Silver also occurs alloyed with the argentiferous gold in the gold veins, but no other silver mineral is known.

(5) Economic Considerations

(a) Reasons for the Failure of previous Mining Attempts. Although excessive speculation and poorly directed prospecting resulted in the failure of many mining companies in the area, the more serious mining attempts by the larger companies failed because of poor gold recovery. At the Enterprise mine, large reserves of potential ore were available but the poor recovery of 2dwt/ton represented only a fraction of the overall assay value of the ore (Downey, 1928). The report of mercury loss at a rate of 60 oz/week, and the presence of visible gold in tailings remaining at the battery sites, demonstrates that severe amalgamation problems existed. These problems were variously attributed to bismuth, arsenopyrite, and pyrite. The association of gold with abundant marcasite can be recognised as a major source of the trouble. Edwards (1954) describes marcasite as a 'deleterious mineral' in both amalgamation and cyanidation processes, worse in its effect than pyrite. Rapid

oxidation of marcasite, as noticed in both the field and the laboratory, gives rise to acid sulphate solutions. The loss of mercury by 'flouring' as a result of such solutions is well known. The oxidised, free milling ores from the reef-cap zones gave good results in amalgamation tests, whereas the primary ores later proved uneconomic. The effect of depressed gold recovery by marcasitic ores may have been of equal importance to that of supergene enrichment.

Supporting evidence for this reasoning may be found in the assay results. Table 8-1 shows assays for the Enterprise mine, performed by Skey who recognised the problem of sulphides, and made amalgamation tests before and after roasting. Samples taken from various levels in the mine show a progressive divergence between the two values with increasing depth.

An additional source of amalgamation difficulty may be due to the high silver content of the gold. Edwards (1954) notes a tendency for argentiferous gold to develop a layer of silver chloride which inhibits amalgamation. Sufficient chloride for this layer to form could be derived from inclusion fluid, released during post-depositional fracturing. Conceivably, roasting would destroy any chloride layer because of the low melting point of this compound.

Although inadequate sampling, nonselective mining, and improper ore treatment are seen as the principal reasons for the failure of the mining operations, structural factors may

TABLE 8-1 Results of amalgamation tests on ore samples from the Enterprise mine. (Lab No. 4743, Twenty-third Annual Report of the Colonial Museum and Laboratory, 1889)

Sub-No.	Sample	Gold per ton, before roasting	Gold per ton, after roasting	Percentage increase on roasting.
1	Level 1	3dwt	3dwt 6gr	8.3
4	Level 1	6oz Odwt 6gr	6oz 12dwt	6.6
6	Level 2	2dwt 18gr	3dwt 4gr	15.1
9	level 2	1dwt	1dwt 6gr	25.0
14	Winze, 2-3	15gr	26gr	73.3
5	Level 3	trace	5dwt 2gr	>100

also be recognised. The lack of vein continuity can be attributed to both pinchouts and faulted dislocations. The failure to appreciate these complications resulted in poorly planned prospecting and mine development.

None of the silver mining ventures are known to have discovered workable deposits, except perhaps at the Welcome lease where the small, rich ore body was rapidly worked out, and the ore sent away for processing. The total output and results of the smelting are unknown.

(b) Recommendations for Future Prospecting.

(i) Attempts to locate further gold deposits should be concentrated on the Owen Formation, within a zone between the Enterprise Dolomite and the Beilby Quartzite. Recognition of intensification of alteration within the country rock may locate unexposed veins. Chlorite composition, the Na content of sericite, or trace metal levels may be useful in this respect. Cu may serve as a short distance pathfinder element, in view of the gold-chalcopyrite association. As the gold is highly argentiferous, a sensitive determination of silver levels may reveal oxidising reef-cap zones.

(ii) Considerable scope for further prospecting lies in the re-evaluation of abandoned leases where known gold-bearing veins exist. Many such veins are well exposed by prospecting or mining operations, and could be properly sampled with little difficulty. A re-examination of the major veins in the light of the mineralization associations noted in this report may delineate economic ore reserves.

(iii) In the event of any ore body evaluation, careful consideration should be given to the unusual characteristics of the primary ore, and appropriate treatment methods selected.

(iv) Some of the known base metal prospects could be re-examined, and further deposits sought. The Beilby's Reef prospect is unlikely to contain any economic ore body, but extensions of the Silver King and Silverstream deposits may exist. Geophysical methods (self potential, induced potential) could be useful on a local scale.

(v) The use of stream sediment geochemical techniques is not recommended for streams which drain the base of the Arthur Marble, because of the widespread abundance of very small mineralized occurrences at this horizon.

(vi) Further searches for disseminated gold mineralization should include a detailed examination of the sericite zone and adjacent rocks. The use of biogeochemical techniques and trace element distributions is suggested.

(c) Reasons for the Location of the Owen Goldfield. No equivalent of the Owen-type mineralization in the Nelson Paleozoic rocks is known. The possibly unique features which locate the mineralization are reviewed as follows:

(i) The structural 'window' at Mt. Owen, where thick sediments beneath the marble are exposed. At all other locations along the flank of the batholith, marble lies in contact with the granite.

(ii) The existence of water-rich sediments within the

Owen Formation at Mt. Owen. Many other Paleozoic localities further north show evidence of Paleozoic regional metamorphism (Shelley, 1975), and hence may already have been too dewatered to develop hydrothermal systems during Cretaceous intrusion.

(iii) The existence of favourable source rocks. The marble at Mt. Owen is underlain by a thick sedimentary sequence which includes 'black shale' lithologies. This thickness of source rocks may be absent further north. The source rocks at Mt. Owen may be further enhanced by metal-rich rocks of the Aorere Group and Haupiri Group underlying the Owen Formation.

(d) Relation to Other Mineralized Areas. Fault-located veins containing both auriferous quartz and silver-rich base metal sulphides occur in the Wangapeka goldfield, 8 km north of Mt. Owen, where prospecting was carried out about the time of mining at the Owen field (Henderson, 1924; Downey, 1928; Henderson et al., 1959). This mineralization can be interpreted as an extension of the Owen hydrothermal system, where 'breakthrough' has occurred, via faults communicating with the system which is otherwise confined by thick marbles. Other mineralized veins in the Mt. Arthur-Lodestone area, where the slates are now thought to be underlain by marble, may bear a similar relationship. At several such localities near the western margin of the Separation Point Granite, concealed Owen-type alteration may exist, although mineralization is probably absent except where adequate temperature-

pressure gradients permitted hydrothermal deposition.

III. RECOMMENDATIONS FOR FUTURE RESEARCH

Many aspects of the mineralization at Mt. Owen warrant further study, by the use of both specialised techniques and conventional structural and petrological examinations. An extension of the methods developed in the course of this project could provide a better understanding of the nature and origin of the mineralization; the limitation of field and laboratory time has resulted in a superficial coverage of many important features. Future investigations should therefore examine the following topics:

(i) Detailed structural mapping of the area, to clarify the relationships between dewatering events, cleavage formation, and the tectonic and metamorphic history on both a local and regional scale.

(ii) An extension of fluid inclusion studies, to improve the knowledge of the pressure-temperature history of the hydrothermal system.

(iii) The application of isotope studies, especially for oxygen and sulphur, to obtain further thermal data and to provide information concerning the source of mineral and fluid components. Combined fluid inclusion and isotope studies may be especially useful.

(iv) A continued study of the ore minerals and their textures using both conventional microscopy and micro-analysis, to identify the remaining unknown phases and clarify the origin of many minerals, including gold.

(v) Further geochemical studies to improve the know-

ledge concerning the source, transport, and deposition of the hydrothermal minerals, and the alteration of the host rocks.

ACKNOWLEDGEMENTS

In concluding this report, my foremost thanks must go to my former supervisor, the late Dr. Walter Oldershaw, who provided encouragement and direction during the early stages of the project, but unfortunately did not live to see the work completed. More recently, Mr. D.H. Bell reviewed the manuscript and made many useful suggestions which led to improvements. Advice concerning specific aspects of the work was kindly provided by Drs. D.W. Lewis, J.D. Bradshaw, D. Shelley, S.D. Weaver, and Mrs. J.K. Campbell, all of the Geology Department, University of Canterbury. Dr. A. Metcalfe of the Chemistry Department assisted with thermodynamic considerations.

Special thanks go to Dr. R.A. Cooper and Mr. J.E. Simes of the N.Z. Geological Survey, for paleontological data. Dr. R.P. Suggate (NZGS) provided old mapping records. A brief acquaintance was made with the late H.E. Fyfe, who related fond memories of mapping the Murchison Subdivision for the Geological Survey 50 years earlier.

Useful discussion and assistance in field excursions was given by my student colleagues, in particular Messrs. A.W. Burgess, H.N.C. Cutten, and R.B. Stewart. My thanks go also to the people of the Owen Valley, for free access through their properties, and especially to Mr. K. Farrell who was most helpful in advising on access routes in the area and on the location of old mine workings.

I am grateful for the help of the technical staff of

the Geology Department; Messrs. A.L. Smith, K.M. Swanson, and A. Downing produced many of the photographs.

I gratefully acknowledge the willing assistance of my wife, Jane, who provided help with field work, the preparation of photographs, and general support during the 'last days' of the preparation of this report.

The typist was Mrs. Helen Deverson, whose excellent work is evident to the reader.

ARNOLD, M. and others (1973) Diagenetic pyrite and associated sulphides at the Almadén mercury mine, Spain. In Amstutz, G. C.; Bernard, A.J., (Eds) Ores in sediments. International union of geological sciences, series A, No. 3. Springer-Verlag.

ARNOLD, R.G. (1962) Equilibrium relations between pyrrhotite and pyrite from 325° to 743°C. Econ. Geol., 57: 72-90.

_____ (1966) Mixtures of hexagonal and monoclinic pyrrhotite and the measurement of the metal content of pyrrhotite by X-ray diffraction. American Mineralogist, 51: 1221-1227.

_____; REICHEN, L.E. (1962) Measurement of the metal content of naturally occurring, metal deficient, hexagonal pyrrhotite by an X-ray spacing method. American Mineralogist, 47: 105-111.

BARNES, H.L.; CZAMANSKE, G.K. (1967) Solubilities and transport of ore minerals. In Barnes, H.L. (Ed) Geochemistry of hydrothermal ore deposits. Holt, Rinehart and Winston, New York.

BARRER, R.M.; STUART, W.I. (1957) Non-stoichiometric compounds of water. Proc. Roy. Soc. Aust., 242: 172-189.

BARRON, B.J. (1974) The use of coexisting calcite-ankerite solid solutions as a geothermometer. Contrib. Min. Petr., 47: 77-80.

BARTON, P.B. Jr; SKINNER, B.J. (1967) Sulphide mineral solubilities. In Barnes, H.L. (Ed) Geochemistry of hydrothermal ore deposits. Holt, Rinehart and Winston, New York.

BENNET, C.E.G.; GRAHAM, J.; THORNBER, M.R. (1972) Natural Pyrrhotites. (1) Mineragraphic techniques. American Mineralogist, 57; 445-462.

BERGLUND, S.; EKSTRÖM, T.K. (1974) Sphalerite composition in relation to the stress distribution in a boudinage. Lithos, 7: 1-6.

BERNARD, A.J. (1964)
In Amstutz, G.C. (Ed) Ores in sediments. Developments in sedimentology. 2. Elsevier.

BERNER, R.A. (1970) Sedimentary pyrite formation. Am. Jour. Sci., 268: 1-23.

BIRD, F. (1887) Warden's Reports - Nelson goldfields. In Reports on the mining industry of N.Z., 1887. Govt. printer. p. 133-135.

BIRD, F. (1888) Warden's Reports - Nelson goldfields. In Reports on the mining industry of N.Z., 1888. Govt. printer. p. C6/25-26.

BISHOP, D.G. (1967) The structural geology of the Mt Burnet dolomite deposit, north-west Nelson. N.Z. Jour. Geol. Geoph., 10: 870-892.

BITTER, F. (1931) Inhomogeneities in the magnetization. Phys. Review, 38: 1903-1905.

BLACK, J.G. (1887) Goldfields classes and Schools of Mines. In Reports on the mining industry of N.Z., 1887. Govt. printer. p. 173-187.

BOAR, P.L. (1970) Trace element analysis by atomic absorption spectroscopy. In Atomic absorption spectroscopy symposium, 1970. Varian Techtron Pty Ltd, Australia.

BODWITCH, D.C. (1973) See AMDEL Bulletin 15.

BOWEN, F.E. (1964). Sheet 15, Buller. Geological map of N.Z. 1:250,000. D.S.I.R., Wellington.

BOYLE, R.W. (1968) The geochemistry of silver and its deposits. Geol. Survey of Canada Bull. 160.

_____ (1969) Hydrothermal transport and deposition of gold - comment. Econ. Geol., 64: 112-114.

BROWN, M.C. (1976) Difficult country. An informal history of Murchison. Murchison Historical and Museum Soc.

BROWNE, P.R.L.; ROEDDER, E.; WODZICKI, A. (1975) Comparison of past and present geothermal waters from a study of fluid inclusions, Broadlands field, N.Z. Proc. Int. Symposium on water-rock interaction, Prague.

CAMERON, E.N.; Van RENSBERG, W.C.J. (1965) Chemical-mechanical polishing of ores. Econ. Geol., 60: 630-632.

CARPENTER, R.H. (1974) Pyrrhotite isograd in southeastern Tennessee and southwestern North Carolina. Bull. Geol. Soc. Am., 85: 451-456.

COLEMAN, A.C. (In press) Sheet S19, Tadmor. Geological map of N.Z. 1:63360. D.S.I.R. Wellington.

COOMBS, D. S. (1961) Some recent work on the lower grades of metamorphism. Aust. Jour. Sci., 24: 203-215.

COOPER, R.A. (1975) New Zealand and south east Australia in the early Paleozoic. N.Z. Journ. Geol. Geoph., 18: 1-20.

DEATON, W.M.; FROST, E.M. Jr (1948) Gas hydrates and their relation to the operation of natural gas pipelines. U.S. Bur. Mines Monograph 8.

DEER, W.A.; HOWIE, R.A.; ZUSSMAN, J. (1962a) Rock forming minerals. Volume 3: Sheet silicates. Longmans, London.

_____ (1962b) Rock forming minerals. Volume 5: non-silicates. Longmans, London.

DEGRAZIA, A.R.; HASKEN, L. (1964) On the gold content of rocks. Geochim. Cosmochim. Acta, 28: 559-564.

DESBOROUGH, G.A. (1970) Silver depletion indicated by micro-analysis of gold from placer occurrences, western United States. Econ. Geol., 65: 304-311.

_____ ; CARPENTER, R.A. (1965) Phase relations of pyrrhotite. Econ. Geol., 60: 1431-1450.

DESBOROUGH, G.A.; HEIDEL, R.A.; RAYMOND, W.H.; TRIPP, J. (1971) Primary distribution of silver and copper in native gold from six deposits in the western United States. Min. Deposita, 6: 321-334.

DOWNEY, J.F. (1928) Quartz reefs of the West Coast mining district of N.Z. Govt. printer.

ELLIS, A.J. (1963) The solubility of calcite in sodium chloride solutions at high temperatures. Am. Journ. Sci., 2(259-267.

EDWARDS, A.B. (1954) Textures of the ore minerals and their significance. 2nd ed. A.I.M.M., Melbourne. 242 p.

EUGSTER, H.P. (1956) Muscovite-paragonite join and its use as a geologic thermometer. (Abstract) Bull. Geol. Soc. Am., 67: 1693.

FARMER, R.T. (1967) Stratigraphy and structure of Paleozoic rocks near Springs Junction, south-west Nelson. Unpublished M.Sc. thesis, University of Canterbury, Christchurch.

FOURNIER, R.O.; TRUESDELL, A H. (1973) An empirical Na-K-Ca geothermometer for natural waters. Geochim. Cosm. Acta, 37: 1255-1275.

FRYKLUND, V.C. (1964) Ore deposits of the Coeur d'Arlene district. Shoshone County, Idaho. USGS Prof. pap. 445.

FYFE, H.E. (1968) Geology of Murchison Subdivision. (R.P. Suggate, Ed.) N.Z. Geol Survey Bull. n.s. 36.

GHENT, E.D. (1968) Petrology of metamorphosed pelitic rocks and quartzites, Pikikiruna Range, north-west Nelson, N.Z. Trans. Roy Soc. N.Z., 5:193-213.

GOLDSMITH, J.R.; GRAF, D.L. (1958) Structural and compositional variation in some natural dolomites. Jour. Geol., 66: 678-693.

_____; _____ ; JOENSUU, O.I. (1955) The occurrence of magnesian calcites in nature. Geochim. Cosm. Acta, 7: 212-230.

_____; _____ ; WITTERS, J.; NORTHROP, D.A. (1962) Studies in the system $CaCo_3$-$MgCO_3$-$FeCO_3$: 1. phase relations; 2. a method for major element spectrochemical analysis; 3. compositions of some ferroan dolomites. Jour. Geol., 70: 659-688.

GORDON, H.A. (1888) Reports on goldfields etc. Reports on the mining industry of N.Z., 1888. Govt. printer. p.C5/33-34.

GORDON, T.M.; GREENWOOD, H.J. (1970) The reaction: dolomite + quartz + water = talc + calcite + carbon dioxide. Am. Jour. Sci., 268: 225-242.

GRAF, D.L.; GOLDSMITH, J.R. (1955) Dolomite-magnesian calcite relationships at elevated temperatures and CO_2 pressures. Geochim. Cosm. Acta, 7: 109-128.

GRAF, D.L.; SKINNER, B.J. (1970) Strength and deformation of pyrite and pyrrhotite. Econ. Geol., 65: 206-215.

GRINDLEY, G.W. (1961) Sheet 13, Golden Bay. Geological map of N.Z. 1:250,000. D.S.I.R., Wellington.

_____; BISHOP, D.G.; COOPER, R.A. (1971) Sheet S1, S3, and pt. S4, Farewell-Collingwood. Geological map of N.Z. 1:63360, (appendix) D.S.I.R., Wellington.

_____ ; BROWNE, P.R.L. (1976) Structural and hydrological factors controlling the permeabilities of some hot-water geothermal fields. Proc. 2nd U.N. Symposium on development and use of geothermal resources, 1975.

_____ ; WODZICKI, A. (1960) Base metal and gold-silve mineralization on the south-east side of the Aorere Valley, north-west Nelson. N.Z. Jour. Geol. Geoph., 3: 585-592.

GARRELS, R.M.; RICHTER, D.H. (1955) Is carbon dioxide an ore-forming fluid under shallow earth conditions? Econ. Geol., 50: 447-458.

GROVES, D.I. and others (1972) A century of tin mining at Mount Bischoff, 1871-1971. Geol. Survey Bull. 54, Tasmania Dept. of Mines.

von HAAST, J. (1861) Report of a topographical and geological exploration of the western districts of the Nelson Province, N.Z. 150 p.

HALFERDAHL, L.B. (1961) Chloritoid: its composition, X-ray and optical properties, stability, and occurrence. Jour. Petr., 2: 49-135.

HARKER, R.I.; TUTTLE, O.F. (1955a) Studies in the system $CaO-MgO-CO_2$ part 1. The thermal dissociation of calcite, dolomite and magnesite. Am. Jour. Sci., 253: 209-224.

_____; _____; (1955b) Studies in the system $CaO-MgO-CO_2$ part 2. Limits of solid solution along the binary join $CaCO_3-MgCO_3$. Am. Jour. Sci., 253: 274-282.

HAYNES, S.J.; HILL, P.A. (1970) Pyrrhotite phases and pyrrhotite-pyrite relationships: Renison Bell, Tasmania. Econ. Geol., 65: 838-848.

HECTOR, J. (1888) Report on the Owen District. Rep. Geol. Expl., 19: p.xx-xxv.

HELGESON, H.C.; GARRELS, R.N. (1968) Hydrothermal transport and deposition of gold. Econ. Geol., 63: 622-635.

HENDERSON, J. (1924) The Rolling River lodes. 18th Ann. Rep. N.Z. Geol. Surv. Govt. Printer.

_____; FYFE, H.E. (1927) Murchison Subdivision. 21st Ann. Rep. N.Z. Geol. Surv., p. 4-7.

_____; _____ (1935) Maps to accompany Murchison Subdivision. N.Z. Geol. Surv. Bull. n.s. 36. Govt. Printer.

(Re-published as Fyfe, 1968).

HENLEY, R.W. (1973a) Some fluid dynamics and ore genesis. Trans. Inst. Min. Met., 82: B1-B8.

_____ (1973b) Some thoughts on chemical transport processes, with particular reference to gold. Minerals, Science, Engineering, 5: 295-303.

HOLLAND, H. (1967) Gangue minerals in hydrothermal deposits. In Barnes, H.L. (Ed) Geochemistry of hydrothermal ore deposits. Holt, Rinehart and Winston, New York.

HOLLISTER, L.S.; BURRUSS, R.C. (1976) Phase equilibria in fluid inclusions from the Khtada Lake metamorphic complex. Geochim. Cosm. Acta, 40: 163-175.

HILDON, M.A.; SULLY , G.R. (1971) See Anal. chim. Acta, 54: 245-251.

HUFFMAN, C. Jr.; MENSINK, J.D.; RILEY, L.B. (1967) Determination of gold in geologic materials by solvent extraction and atomic absorption spectrophotometry. U.S. Geol. Surv. Circular 544.

HULSTON, J.R.; McCABE, W.J. (1972) N.Z. potassium-argon age list -1. N.Z. Jour. Geol. Geoph., 15: 406-432.

JOHNSTON, M.R.; LAIRD, M.G.; SKWARKO, S.K. (1965) Age of the Wangapeka Formation and Mt Arthur Marble, Mount Owen, north-west Nelson. N.Z. Jour. Geol. Geoph., 8: 854-858.

KEAR, D. (1954) Geology of the upper Owen River area, Nelson. N.Z. Jour. Sci. Tech., B36: 258-267.

KEIDEL, F.A. (1959) Determination of water by direct amperometric measurement. Anal. Chem., 31: 2043-2048.

KISSIN, S.A.;SCOTT, S.D. (1972) Phase relations of intermediate pyrrhotites, (Abstract). Econ. Geol., 67: 1007.

_____ ; (1953) The FeS-ZnS system: a geological thermometer. Norsk. Geol. Tidsskr., 32: 61-147.

KULLERUD, G. (1959) Sulphide systems as geological thermometers. In Abelson, P.H. (Ed) Researches in geochemistry. Wiley, New York.

_____; YODER, H.S. (1959) Pyrite stability relations in the Fe-S system. Econ. Geol., 54: 533-572.

LAMBERT, I.B. (1973) Post-depositional availability of sulphur and metals and formation of secondary textures and structures in stratiform sedimentary sulphide deposits. Jour. Geol. Soc. Aust., 20: 205-215.

LARSON, S.L. (1956) Phase studies of the two-component carbon dioxide-water system involving the carbon dioxide hydrate. University microfilms, Ann Arbor, Michigan. Dissertation Abstr., 16: 248.

LEMMLEIN, G.G.; KLEVTSOV, P.V. (1961) Relations among the principal parameters in a part of the system H_2O-NaCl. Geochemistry, 1961. (2): 148-158.

LOVE, L.G. (1964) In AMSTUTZ, G.C. (Ed) Ores in sediments. Developments in Sedimentology, 2. Elsevier.

_____ (1967) Diagenesis and the origin of ores. In Brown, J.S. (Ed) Genesis of stratiform lead-zinc-barite-fluorite deposits. Economic Geology Monograph 3. Economic Geology Publishing Co., Lancaster, Pennsylvania.

LOWRY, H.H.; ERICKSON, W.R. (1927) Densities of coexisting liquid and gaseous CO_2. Jour. Am. Chem. Soc., 49: 2729-2733.

LYONS, J.H. (1952) Faring south; memories of a pioneer family including gold mining and the Kokopu. Reed.

McDONALD, J.A. (1967) Metamorphism and its effects on sulphide assemblages. Min. Deposita, 2: 200-220.

MIYASHIRO, A. (1973) Metamorphism and metamorphic belts. George Allen and Unwin, London.

MORGAN, P.G.; BARTRUM, J.A. (1913) List of the minerals of N.Z. Govt. Printer.

NAKAZAWA, H.; MORIMOTO, N.; WATANABE, E. (1975) Direct observation of metal vacancies by high-resolution electron microscopy. Pt. 1: 4c type pyrrhotite (Fe_7S_8). American Mineralogist, 60: 359-366.

NEUMANN, H. (1950) Pseudomorphs of pyrrhotine after pyrite in the Ballichulish slates. Min. Mag., 29: 234-238.

NEWHOUSE, W.H. (1925) The paragenesis of marcasite. Econ. Geol., 20: 54-66.

NEWMAN, N.A. (1975) Apparatus for fluid inclusion studies. N.Z. Geochem. Group Newsletter, 36: 80-81.

_____ (1976) Some observations on fluid inclusion studies. N.Z. Geochem. Group Newsletter, 43: 47-48.

_____ (1977) A study of fluid composition from an extinct, deep-level hyrothermal system at Mt Owen, central Nelson (abstract). N.Z. Geochemical Group Newsletter, 48: 69-70.

NOBLE, E.A. (1963) Formation of ore deposits by water of compaction. Econ. Geol., 58: 1145-1156.

PARK, J. (1888) On the geology of the Owen and Wangapeka goldfields. Rep. Geol. Expl., 19: 82-88.

PATERSON, C.J. (1971) Structure, metamorphism and mineralization in the Haast Schist at Bendigo, Central Otago. Unpublished BSc (Hons) thesis, University of Otago, Dunedin.

PETROVSKAYA, N.V. (1971) Growth and subsequent changes in native gold crystals. Mineralogical Soc. Japan, Special Paper 1 (Proc. IMA-IAGOD meetings 1970: IMA volume, p. 116-123).

PHILIPS, W.J. (1972) Hydraulic fracturing and mineralization. Jour. Geol. Soc. Lond., 128: 337-355.

POWER, L.F.; FINE, H.A. (1976) The iron-sulphur system. Part 1; the structures and physical properties of the compounds of the low-temperature phase fields. Minerals, Science, Engineering, 8: 106-128.

RADTKE, A.S.; SCHEINER, B.J. (1970) Studies of hydrothermal gold deposition: 1. Carlin gold deposit, Nevada; the role of carbonaceous materials in gold deposition. Econ. Geol., 65: 87-102.

_____ and others (1972) Data in major and minor elements in host rocks and ores, Carlin gold deposit, Nevada. Econ. Geol., 67: 975-978.

RAMDOHR, P. (1969) Ore minerals and their intergrowths. Pergamon Press.

RANKIN, A.H. (1975) Fluid inclusion studies in apatite from carbonatites of the Wasaki area of western Kenya. Lithos, 8: 123-136.

REED, J.J. (1958) Granites and mineralization in N.Z. N.Z. Jour. Geol. Geoph., 1: 47-64.

ROEDDER, E. (1962a) Studies of fluid inclusions I: low temperature applications of a dual-purpose freezing and heating stage. Econ. Geol. 57: 1045-1061.

_____ (1962b) Ancient fluids in crystals. Scientific American, 207(4): 38-47.

_____ (1963) Study of fluid inclusions II: freezing data and their interpretation. Econ. Geol., 58: 167-211.

_____ (1967) Fluid inclusions as samples of ore fluids. In Barnes, H.L. (Ed) Geochemistry of hydrothermal ore deposits. 515-574. Holt, Rinehart, and Winston, New York.

_____ (1972) Composition of fluid inclusions. Data of geochemistry, 6th ed. Chapter JJ. U.S. Geol. Surv. Prof. Paper 440-JJ.

ROSASCO. G.J.; ROEDDER, E.; SIMMONDS, J.H. (1975) Laser-excited Raman spectroscopy for nondestructive partial analysis of individual phases in fluid inclusions in minerals. Science, 190: 557-560.

ROSENBERG. P.E. (1963a) Subsolidus relations in the system $CaCO_3$-$FeCO_3$. Am. Jour. Sci., 261: 683-690.

_____ (1963b) Synthetic solid solutions in the systems $MgCO_3$-$FeCO_3$ and $MnCO_3$-$FeCO_3$. American Mineralogist, 48: 1396-1400.

_____ (1967) Subsolidus relations in the system $CaCO_3$-$MgCO_3$-$FeCO_3$ between 350° and 550°C. American Mineralogist, 52: 787-796.

_____ (1968) Subsolidus relationships on the dolomite join $CaMg(CO_3)_2$-$CaFe(CO_3)_2$-$CaMn(CO_3)_2$. American Mineralogist, 53: 880-889.

SCHWARTZ, G.M. (1958) Alteration of biotite under mesothermal conditions. Econ. Geol., 53: 164-177.

SCOTT, S.D. (1973) Experimental calibration of the sphalerite geo-barometer. Econ. Geol., 68: 466-474.

_____; BARNES, H.L. (1971) Sphalerite geothermometry and geobarometry. Econ. Geol., 68: 466-474.

SEWARD, T.M. (1973) Thio complexes of gold and the transport of gold in hydrothermal ore solutions. Geochim. Cosm. Acta, 40: 73-83.

SHELLEY, D. (1975) Metamorphic belt and volcanic arc migration in N.Z. Nature, 258:668-672.

SKEY, W. (1887) On the occurrence of bismuth at the Owen, N.Z. Trans. Proc. N.Z. Institute, 19: 459-60.

_____ (1888a) See 23rd. Rep. Colonial Museum and Laboratory, N.Z.

_____ (1888b) On the occurrence of bismuthic gold at the Owen goldfields. Trans. Proc. N.Z. Institute, 20: 453-454.

SKIPPEN, G. (1974) An experimental model for low-pressure metamorphism of siliceous dolomitic marble. Am. Jour. Sci., 274: 487-509.

SMALE, D. (1976) Hydrothermal alteration around younger intrusives near Karamea Bend, north-west Nelson, N.Z. Aust. Inst. Min. Met., 260: 53-58.

SMITH, F.G. (1953) Historical development of inclusion thermometry. University of Toronto Press, Toronto, Canada.

_____;LITTLE, W.M. (1959) Filling temperatures of H_2O-CO_2 fluid inclusions and their significance in geothermometry. Canadian Mineralogist, 6: 380-388.

SMYTHE, J.A.; DUNHAM, K.C. (1947) Ankerites and chalybites from the northern Pennine orefield and the northeast coalfield. Min. Mag., 28: 53-74.

SORBY, H.C. (1858) On the microscopic structure of crystals, indicating the origin of minerals and rocks. Jour. Geol. Soc. Lond., 14: 453-500.

SPRY, A. (1969) Metamorphic textures. Pergamon Press.

STANTON, R.L. (1972) Ore petrology. McGraw-Hill, 713 p.

STILLWELL, F.L.; EDWARDS, A.B. (1943) Mineral composition of the tin ores of Renison Bell, Tasmania. Proc. Aus. Inst. Min. Met., 131-132: 173-186.

STRELOW, F.W.E. and others (1966) Determination of gold in cyanide waste solution by solvent extraction and atomic absorption spectrophotometry. Anal. Chem., 38: 115-

TAKENOUCHI, S.; KENNEDY G.C. (1965a) The solubility of carbon dioxide in NaCl solutions at high temperatures and pressures. Am. Jour. Sci., 263: 445-454.

_____; _____ (1965b) Dissociation pressures of the phase $CO_2.5.75H_2O$. Jour. Geol., 73: 383-390.

TINDALL, F.M. (1965) Silver and gold assay by atomic absorption spectrophotometry. Atomic Absorption Newsletter, 4: 339-340.

TURNER, F.J. (1975) Biaxial calcite: occurrence, optics, and associated minor strain phenomena. Contrib. Min. Petrol., 50: 247-255.

Van SICKLE, G.H.; LAKIN, H.W. (1968) An atomic absorption method for the determination of gold in large samples of geologic materials. U.S. Geol. Surv. Circular 561.

VINE, J.D.; TOURTELOT, E.B. (1970) Geochemistry of black shale deposits - a summary report. Econ. Geol., 65: 253-272.

WARREN, H.V.; HAJEK, J.H. (1973) An attempt to discover a 'Carlin-Cortez' type of gold deposit in British Columbia. Western Mining October 1973.

WEISSBURG, B.G. (1970) Solubility of gold in hydrothermal alkaline sulphide solutions. Econ. Geol., 65: 551-556.

WELLS, J.R.; STOISER, L.R.; ELLIOT, J.E. (1969) Geology and geochemistry of the Cortez gold deposit, Nevada. Econ. Geol., 64: 526-537.

WHITE, D.E. (1965) Saline waters of sedimentary rocks. In Fluids in subsurface environments - a symposium. A.A.P.G. Mem. 4: 342-366.

_____ (1968) Environments of generation of some base metal ore deposits. Econ. Geol., 63: 301-355.

WILLIAMS, G.J. (1965) Economic Geology of N.Z. 8th Commonwealth and Mining Congress, Australia and N.Z. 1965; publication - volume 4. Aus. I. Min. Met., Melbourne.

WINCHELL, A.N. (1951) Elements of optical mineralogy, 4th ed. Wiley & Sons, New York.

WINKLER, H.G.F. (1967) Petrogenesis of metamorphic rocks, 2nd ed. Springer-Verlag.

WISE, F.M. (1964) Gold: recovery, properties and applications. Van Nostrand, New York.

WRIGHT, J.B. (1966) Studies on the pyrrhotite and paragenesis of the Moke Creek sulphide lode, Wakatipu District. N.Z. Jour. Geol. Geoph., 9: 301-322.

YERMAKOV, and others (1965) Research on the nature of ore-forming fluids. Pergamon Press.

ZEN, E-an.; ALBEE (1964) Coexisting muscovite and paragonite in pelitic schists. American Mineralogist, 49: 904-925.

APPENDIX I

PLACENAMES

In the course of this project, many of the streams and other geographic features have been named for the purposes of mapping and location description. For many others, use has been made of existing names which appear on old mining lease maps, but have been omitted on later published maps. The derivation of these names is as follows:

Advance Creek: After the Advance mining Company.

*Baigent Fault: After Baigent Creek which it intersects, and the nearby Baigent farm property (now Ben Nevis), taken up as a grazing run in the 1860's.

*Beilby's Stream, ____ Reef: After C.S. Beilby, a prospector employed to examine the base metal mineralization south of Trig C, 1911-1913.

Bonanza Ridge: After the Bonanza mining company.

Bulmer Creek, *___ Tarn: After Charles Bulmer, the principal prospector of the party which discovered the field.

*Byrne Stream: After Mathew Byrne, partner to Bulmer.

Carroll's Creek: After E. Carroll, hotel proprieter at Owen Township.

Carton's Creek: After C. Carton, prospector and leaseholder.

Deep Creek: Appears on lease maps.

*Fagan's Stream: After Fagan, prospector and leaseholder in silver mining ventures.

Fire Creek: Appears on lease maps.

*Mount Peru: The mountain surmounted by Trigs F and PH was named 'Peru Hill' at the time of the original surveys, when the Peru mining company took out a silver mining lease near the summit. The name 'Peru' is retained in local usage.

Spring Creek: Appears on lease maps.

Sunrise Peak: After the Mount Owen and Rising Sun Mineral Company, which prospected Beilby's reef. The name 'Rising Sun' may have been used for this peak prior to the formation of this company.

Uno Creek: After the Uno mining company.

Zealandia Creek: After the Zealandia mining company.

* Denotes new name

APPENDIX II

THE QUANTITATIVE ANALYSIS OF GOLD IN ORES AND ROCKS

(1) Choice of Method

Perhaps the earliest accurate chemical analysis developed by mankind was the fire assay for gold, a traditional and specialised analysis which owes its reliability to a fusion-type sample decomposition, a solvent extraction-type concentration, and freedom from interferences at the detection stage. Disadvantages of the method comprise a poor detection limit (rarely less than 0.25 ppm), and the need for a high level of operator skill. Several modern laboratory methods (emission spectroscopy, X-ray fluorescence, colourimetry) offer an improved detection limit if concentration is employed, but have interference problems which limit the usefulness of this operation. Since the mid-1960's, atomic absorption has provided an analytical method which combines good sensitivity with a low level of interference. The method gives good results for gold in ores, and with some refinements and careful sample preparation, can be extended to determine the background gold content of rocks.

(2) Gold Determination by Atomic Absorption: The Basic Method

The basic method of gold analysis used in the course of this project is similar to that recommended in the Varian Techtron handbook, Analytical Methods for Flame Spectroscopy (1972). The method adopted was as follows:

(a) Sample Preparation. Physical preparation consists of fine grinding and weighing, followed by a roasting treatment. The roasting of the sample assists extraction of gold during subsequent leaching by oxidising sulphides and

carbonaceous matter, and therefore should be carried out in shallow crucibles or trays to allow free access to air. To avoid sintering clay minerals and other silicates, the temperature should not exceed 650°C. Oxidation of carbon, however, is slow at this temperature, and for highly carbonaceous samples, roasting at higher temperatures followed by regrinding appears to be worth investigation.

(b) Extraction of Gold into Solution. There is a number of possible methods of leaching the gold from the sample material. If wet-chemical methods are used, the use of HF is required for complete decomposition of silicates. Such a step may be essential for the accurate analysis of igneous samples, but is unnecessary for vein materials and fine grained sedimentary rocks, where very little gold is bound in silicate lattices.

A very simple extraction procedure consists of leaching by a dilute cyanide solution which is continuously aerated (Huffman et al, 1967), but this method is not suitable for complex ores or rocks. Better extraction, and avoidance of the use of cyanide, is possible by the use of a bromine-ether leach (VanSickle and Lakin, 1968), although sample decomposition remains poor. A more vigorous extraction is provided by leaching with hot aqua regia (Tindall, 1965; Bodwitch, 1973), a process which is carried out by a preliminary sample digestion in hot HCl followed by the addition of HNO_3 to form aqua regia. The mixture is evaporated to dryness, preferably on a waterbath, and further HCl added to return the soluble products into solution, followed by dilution by water. After cooling, gold is stabilised in solution by the addition of a small amount of HBr, and the liquid filtered off. A fine filter is recommended, to ensure minimum solids

in the filtrate. A special advantage of this method is the facility of using the same filtrate for the analysis of many other metals.

(c) Concentration. Samples containing high gold levels may not require concentration of the filtrate, permitting direct analysis of the aqueous solution. Solvent extraction by organic liquids permits an overall concentration factor of 20 or greater, depending on the nature of the sample. Methyl isobutyl ketone (MIBK, 4-methylpentan-2-one) has been established as the best solvent for this purpose (Strelow et al, 1966). A standard liquid separation technique is used, but the operation should be carried out in a fume cupboard because of the hazards of exposure to MIBK vapour.

(d) Detection. The MIBK-atomic absorption method is remarkably free from interferences, but a slight depression of absorbance is produced by large amounts of Fe, Ni, and Cu (Hildon and Sully, 1971). If samples contain a high proportion of acid-soluble components, non-atomic absorption may affect the results of the analyses. These problems can be largely overcome by the use of internal standards, i.e. the addition of gold standards to sample duplicates. Where the samples are of similar composition, standardised extracts from a representative number of samples may suffice.

Flame stoichiometry is important if good sensitivity is required, and the flame controls should be carefully adjusted for maximum absorbance. The MIBK acts as additional fuel, and should be aspirated during mixture adjustments. The flame runs very lean during the interval between samples, and may extinguish or even flash back into the mixing chamber if pressures and mixture are incorrectly set.

A chart recorder is the preferred form of readout,

providing a permanent and detailed record of the absorbance/time characteristics, which is often essential because of 'noise' and standardisation drifts, especially when small MIBK extracts must be used and the aspiration time is short.

(3) Special Requirements for the Analysis of Very Low Gold Concentrations

The analysis of background levels of gold in rocks is normally done by isotope methods, i.e. neutron activation analysis and radioisotope dilution analysis. Where access to these methods is unavailable, atomic absorption must be used. The atomic absorption method outlined above may be extended to the analysis of gold background levels, but due to the much greater concentration required, special modifications must be employed as outlined below:

(i) To maintain a useful signal/noise ratio from the absorbance readout, the MIBK analyte should contain a minimum of 0.1 µg Au/ml. If the final MIBK volume is 2 ml (a practical minimum), sample sizes should be not less than 50 g for gold concentrations in the order of 0.005 ppm.

(ii) The acid digestion and leaching process is unchanged except where a large proportion of acid-solubles is present. Such components (usually Fe or carbonate minerals) cause problems by consuming a large amount of acid before leaching is complete, and by interfering with the evaporation stage, in addition to causing non-atomic absorption during detection. If more than 10% of the sample is acid-soluble, efforts should be made to remove some of the products by crystallization or precipitation methods.

(iii) The MIBK extract should be washed by shaking with 30 ml portions of 10% HCl until light yellow or clear. This process removes unwanted components accumulated during solvent

extraction. Some allowance should be made for the slight solubility of MIBK in aqueous solution, which may cause variations in the final analyte volumes. The degree of solubility appears to be affected by the concentration of other solute (i.e. a 'salting out' effect) and the final volume is difficult to predict, even when MIBK-saturated wash solutions are used. It is therefore advisable to measure and standardise the analyte volumes before aspiration, by either diluting with more MIBK, or by partial evaporation.

(iv) When operating atomic absorption equipment near the sensitivity limit, very careful adjustment for optimum performance is essential, and the running of tests with low-concentration MIBK standards is suggested, the best settings being found by experiment. The factor of operator skill therefore becomes important.

(v) Contamination problems rarely appear in the analysis of gold ores, but may easily affect the results of background determination. Care should be taken to avoid contact with glassware, etc. which has been in contact with solutions or standards containing gold. The metal will adsorb onto surfaces from where it will be readily extracted by contact with the aqua regia or HBr solutions. When collecting and preparing samples, inclusion of, and contact with, high-gold samples or any type of vein material should be avoided. At all stages of sample collection, processing, and analysis, gold rings should not be worn.

(vi) Several refinements of the basic atomic absorption equipment have been developed, wherein the conventional slot-burner has been replaced by devices which greatly enhance the detection sensitivity, especially for the noble metals. Various types of such accessories, described by Boar (1970), are suitable for the analysis of gold.

APPENDIX III

SOLID SOLUTION DATA FOR CARBONATES

Four figures referred to in the discussion of carbonate composition (Chapter VI part II) are shown.

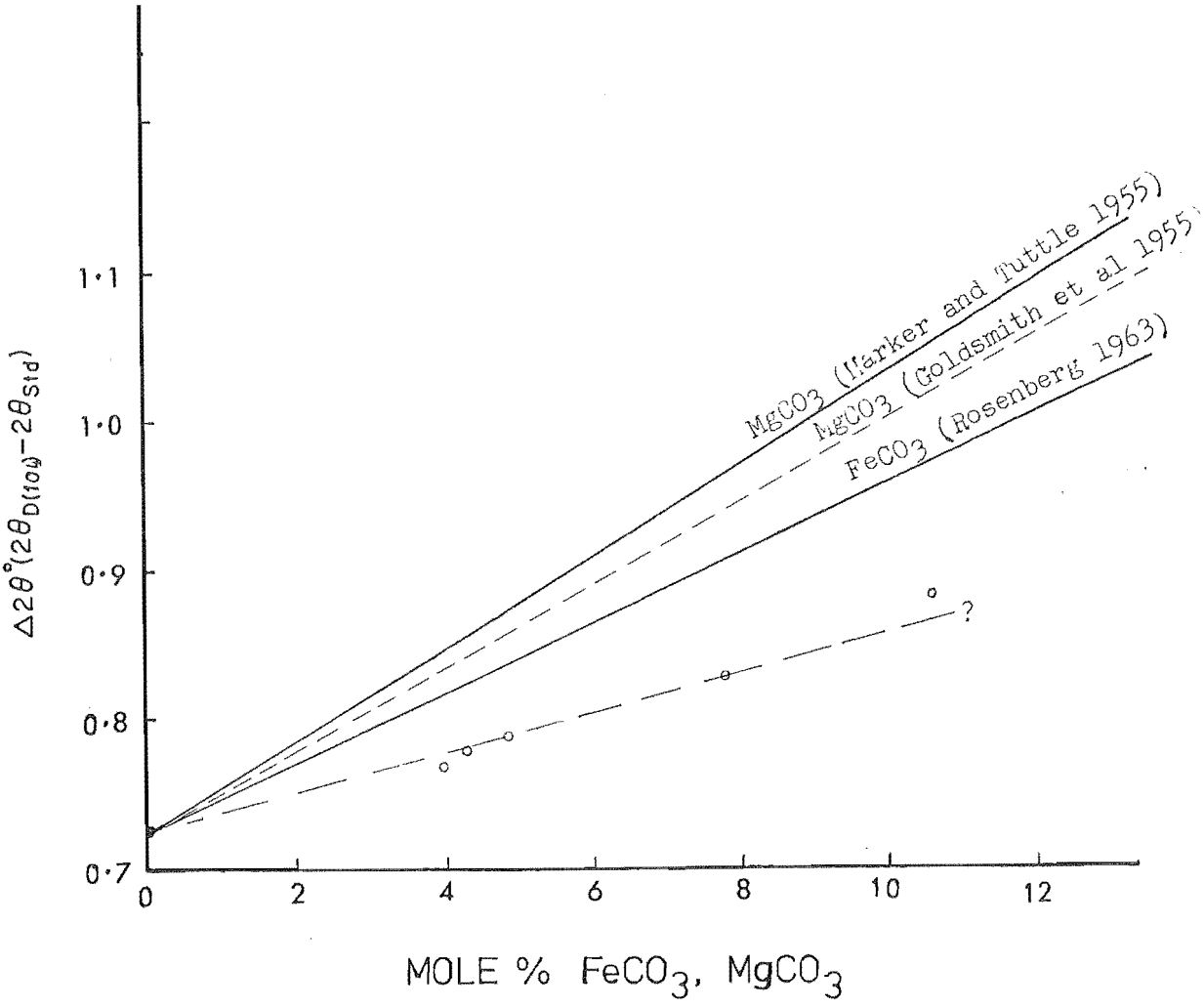

FIG. III-1 Graph for converting (104) X-ray peak shifts to substitution values for $FeCO_3$ and $MgCO_3$ in calcite, using Cu kα radiation. The $\Delta 2\theta$ values are quoted as a difference from the principal peak of a standard, CdF_2 ($2\theta = 28.70^{\circ}$). The heavy lines are from the data selected for interpreting the composition of natural calcites, and are those used in this report. The small circles are Barron's erroneous values for $MgCO_3$ (see Table 6-5).

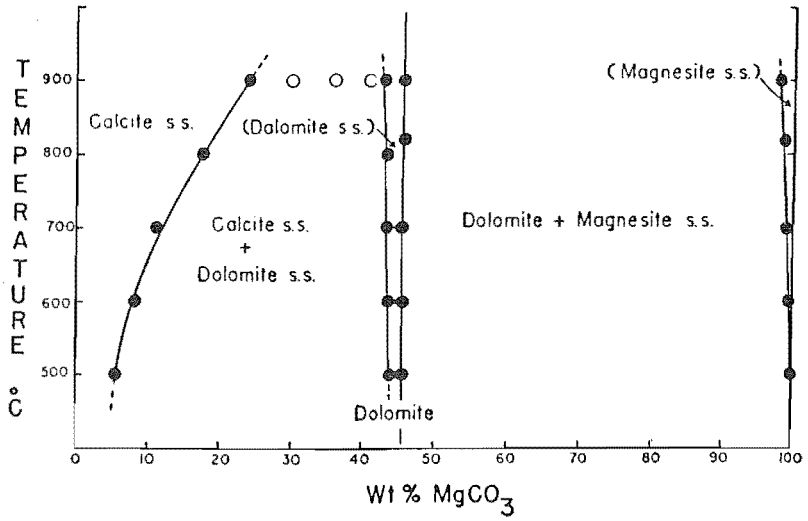

Limits of solid solution in the system $CaCO_3$—$MgCO_3$ between 500 and 900°C.

FIG. III-2 $CaCO_3$-$MgCO_3$ binary from Harker and Tuttle (1955, Figure 3). Note that the $MgCO_3$ values are quoted in weight %.

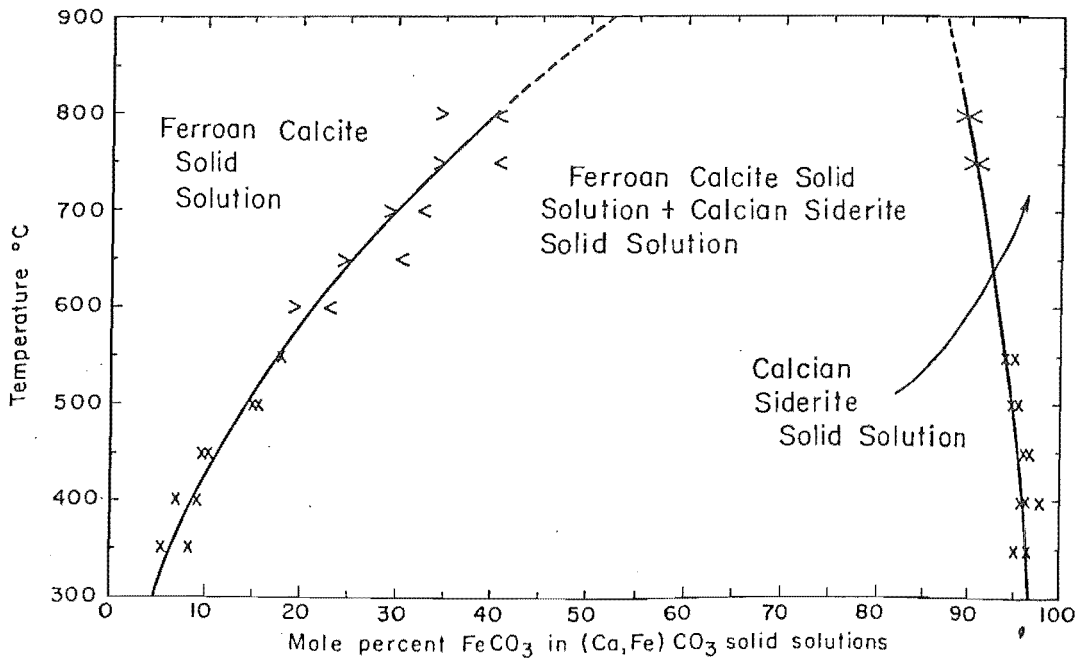

The binary system $CaCO_3$-$FeCO_3$. The small crosses at 550° C. and lower temperatures are data of Rosenberg (1960*b*, table 3). The "less than" and "more than" symbols at higher temperatures are derived from the runs plotted in figs. 1–5 of this paper.

FIG. III-3 $CaCO_3$-$FeCO_3$ binary from Goldsmith et al, (1955, Figure 6).

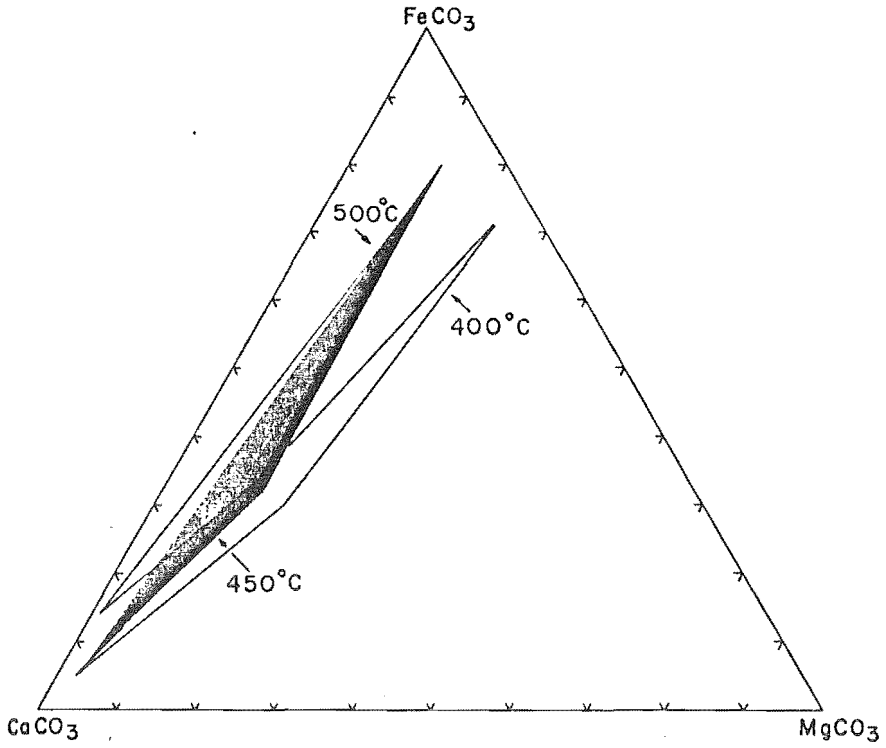

Three-phase triangles for temperatures of 400°C, 450°C (shaded), and 500°C shown superimposed.

FIG. III-4 From Rosenberg (1967, Figure 4). Barron (1974) plotted calcite T-X data to 0.1 mole % from measurements of the lower apices of the superimposed triangles. See Figure 6-3 for the complete ternary for 450°C.

APPENDIX IV

PARTIAL ANALYSIS OF INCLUSION FLUID

(1) Aim

A brief series of analyses was carried out to obtain some estimate of the relative proportions of dissolved salts in the inclusion fluid. A large number of published analyses show Na, K, and Ca to be the dominant cations in hydrothermal fluids, and the present investigation was limited to these elements. Alkali metal analysis provides an opportunity to attempt geothermometry by the method of ionic abundance ratios.

(2) Theory of Ionic Ratio Geothermometry

This method is based on the partitioning of alkali metals between hydrothermal solutions and solid mineral phases. The relative partitioning ratio for hydrothermal fluids which are in equilibrium with wall rocks is known to be temperature-dependent. White (1965) first published a curve to show such a relationship, using K/Na measurements from natural waters. Later work by White (1968) advanced this idea with additional curves from other sources, including some fluid inclusion measurements. Other workers also published supporting evidence from natural systems and experiments, all based on the atomic K/Na ratio.

A more intensive study was undertaken by Fournier and Truesdell (1973) to account for the lack of agreement between curves from different systems. A new empirical thermometry method was devised by including a factor for Ca, in addition to Na and K. Their principal criticism of the simple Na-K geothermometer was that it is accurate only for each individual set of rea ions for which it is calibrated. As Ca enters into

silicate reactions in competition with Na and K, the concentration of Ca will influence the amount of dissolved Na and K. As Na is almost always more abundant than K, it is the K concentration which is most affected, with a resultant change in the K/Na ratio.

An equilibrium equation -

$$\text{Log}\mathcal{K} = \text{Log}\ (\text{Na/K}) + \beta\ \text{Log}\ \left[\sqrt{(\text{Ca})}/\text{Na}\right]$$

- was derived by Fournier and Truesdell, as an approximate expression to cover all geothermal reactions involving the ions Ca^{+2}, Na^{+}, and K^{+}; β is a numerical factor. The equation is used in a procedure as follows:

(i) The concentration of the alkalis in the fluid is expressed as molality and Log $\left[\sqrt{(\text{Ca})}/\text{Na}\right]$ is calculated. If the result is negative, β is given the value $\frac{1}{3}$.

(ii) The value of Log$\mathcal{K}$ is calculated and converted to a temperature by the use of the graph reproduced as Figure IV-1. Should Log $\left[\sqrt{(\text{Ca})}/\text{Na}\right]$ be positive, $\beta = 1\frac{1}{3}$ is used.

(iii) If the result of the determinations from step (ii) is greater than 100°C, the value is rejected and recalculated by reverting to $\beta = \frac{1}{3}$.

(3) Method

As the analysis of dissolved salts in inclusion fluid involves only minute amounts of material, care must be taken to use a sensitive analytical method and a contamination-free preparation. To extract sufficient alkali to analyse by common laboratory methods required a treatment of crushing the host crystal and leaching the salts from the released inclusion fluid. This type of extraction has been used by other workers. Paterson (1971) ground several hundred grams of quartz in a laboratory grinder, but on analysing the leachate, he obtained an unreasonably high temperature result, using the

calibration of White (1968). Bulk treatment such as this is undesirable for the following reasons:

(i) Larger samples are more prone to contamination from either accumulated and absorbed surface material, or included foreign mineral species.

(ii) Larger samples are more likely to contain planes or other concentrations of secondary inclusions, or perhaps fractures filled with groundwater.

(iii) The process of grinding may yield alkali contaminants from the surfaces of the grinding vessel.

To overcome these problems, a micro-crushing method was devised. The quartz to be analysed was carefully selected so as to be free from surface organic matter, other minerals, and fracture zones. From the selected pieces, wafers 2-3 mm in thickness were cut and broken into fragments of approximately 100 mm^2 area. These were cleaned in hot acid, rinsed with de-ionised water, and carefully dried, being handled with forceps only. Single pieces were placed in a clean steel piston-mortar and loaded to compression failure in a hydraulic press. The resulting explosive disintegration of the wafer produced an even textured, penetrative microfracturing, with almost complete absence of abrasive contact with the crushing equipment. The quartz powder from this operation was leached in acid-cleaned flame photometry beakers, using a minimum (typically 2-3 ml) of de-ionised water.

(4) Results

The data from these measurements are shown in Table IV-1 where the ppm values refer to the concentration of the leachate. The method cannot reveal the absolute concentration of the alkalis in the inclusion fluid, as required by the factor $\sqrt{(Ca)}/Na$ in the Fournier and Truesdell expression.

It is therefore impossible in this case to obtain Ca-corrected values for Log K. Ca was determined in four of the samples, to obtain some indication of the concentration relative to Na and K.

As the Ca concentrations were relatively low (Ca/Na $\leqslant$0.162), an attempt has been made to plot Log (Na/K) values, neglecting the effect of Ca. Reference to Figure IV-2, taken from Fournier and Truesdell (1973) will show that almost all of the natural waters measurements, when plotted as Log K (=Log (Na/K), β=0), fall between two geometrically simple boundaries. The upper boundary is marked by a linear concentration of points from ca.400°-ca.100°C, while the lower one progressively diverges over this range. The authors show this spread to be due to contribution by Ca in some cooler natural waters. If Ca is assumed to be neglible, there is some justification for using the graph of Figure IV-2 as a Na-K geothermometer calibration, by inserting a 'best fit' line parallel to the upper boundary, through the linear concentration of points. This straight-line plot may be useful as an 'ideal case' calibration, instead of plotting simple K/Na ratios on one of the many curves published for individual experimental or natural systems. By the use of Log (Na/K) vs $10^3/T°K$, a straight line is obtained. The linear upper boundary of the field in Figure IV-2 can be considered to represent reactions in which Ca plays little or no part, with the 'best fit' line being slightly lower to allow for point scatter. Figure IV-3 shows calibrations of both the 'best fit' line (b), and the fully Ca-corrected line (a) of Fournier and Truesdell (Figure IV-1). The calibration lines intersect near the point $10^3/T$=2.5 (=127°C): at higher temperatures, the 'best fit' line gives the higher values, causing a differential of 74°C

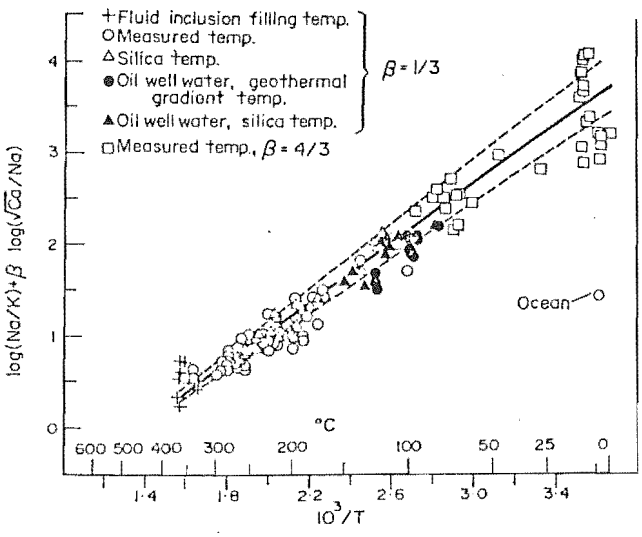

FIG. IV-1 Measured geothermal temperatures plotted as a function of Log$K$ in Fournier and Truesdell's geothermometry method. The dashed lines represent +15°C.
From Fournier and Truesdell (1973).

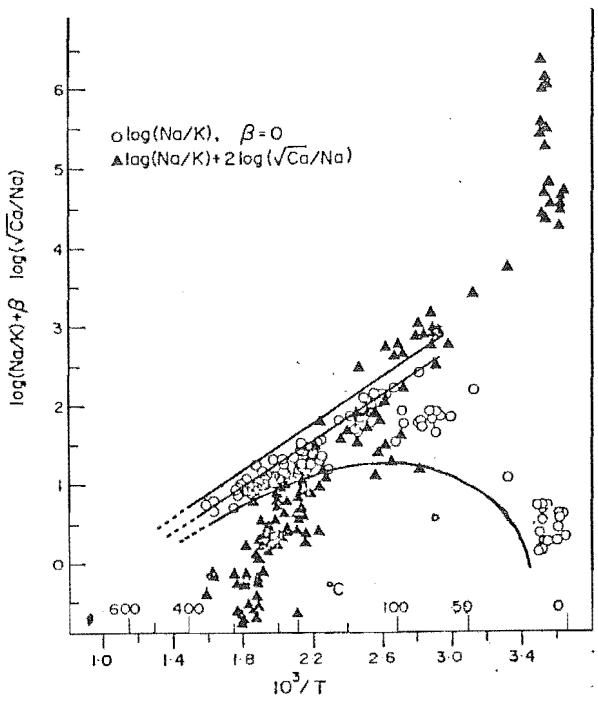

FIG. IV-2 Experimental graph used by Fournier and Truesdell in devising the formula for a Ca-corrected geothermometry method. The lines have been added (see text).

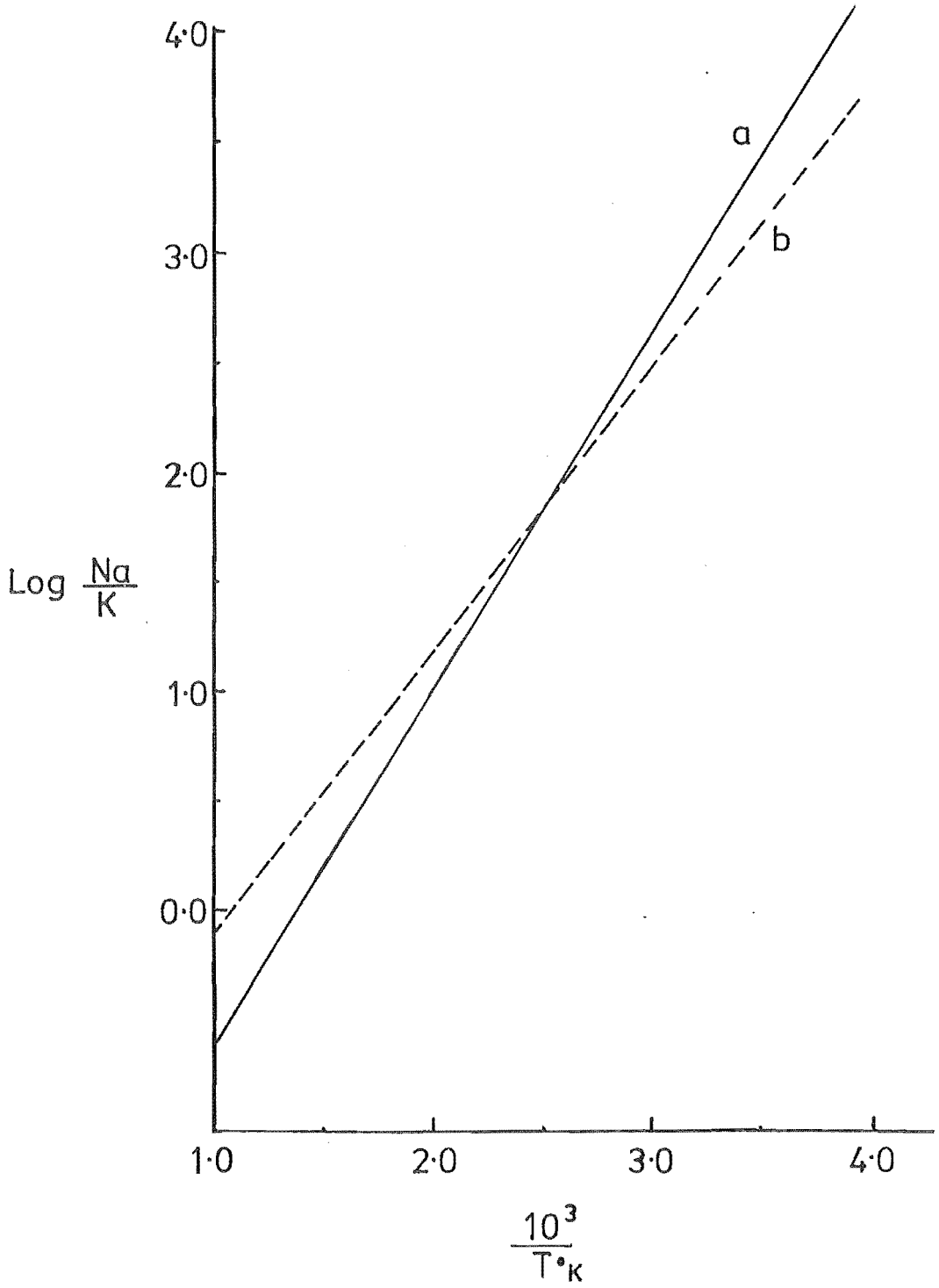

FIG. IV-3 Calibration lines for the alkali ratio geothermometer.

(a) Fournier and Truesdell (1973), Ca-corrected.

(b) 'Best fit' line for uncorrected data, neglecting Ca. See text for details.

TABLE IV-1 Inclusion Fluid Composition Data

Sample	Na ppm	K ppm	Ca ppm	K/Na	Ca/Na	Log Na/K	T°C line (a)	T°C line (b)
LS-09	3.7	0.67	-	0.107	-	0.97	234	276
LS-12	1.4	0.42	-	0.177	-	0.75	271	332
LS-14	0.53	0.21	-	0.24	-	0.63	294	368
LS-15	6.00	0.72	-	0.071	-	1.15	207	237
LS-17	4.00	1.15	0.88	0.17	0.126	0.77	268	326
"	6.82	0.80	-	0.069	-	1.16	206	235
LS-18	19.7	1.10	5.57	0.033	0.162	1.48	164	178
"	3.47	1.18	-	0.20	-	0.70	281	346
LS-19	2.8	0.39	-	0.082	-	1.09	216	249
LS-20	9.3	0.39	-	0.025	-	1.61	150	160
"	8.4	0.40	-	0.028	-	1.55	156	167
"	7.3	0.50	-	0.040	-	1.39	175	193
"	3.87	0.40	-	0.061	-	1.21	199	225
"	3.75	0.42	-	0.066	-	1.18	202	231
"	8.5	0.32	-	0.022	-	1.65	145	153
"	12.66	0.85	0.19	0.039	0.008	1.40	174	191
"	7.70	0.25	0.95	0.019	0.071	1.72	138	143
LS-23	1.88	0.72	-	0.226	-	0.65	290	361
					Average for LS-20		167	183

Note: All ratios computed from molar concentrations.
ppm values refer to leachate solution.

for the highest temperature measurement (sample LS-14). Temperature measurements based on both calibrations are presented in Table IV-1.

(5) Discussion

Much of the alkali in the samples analysed is considered to be from secondary inclusions, and to reflect equilibration of fluid with silicates at temperatures below that indicated by primary inclusion homogenization. The temperatures derived from the 'best fit' line, which are comparable with homogenization temperatures (Table IV-2), are therefore considered too high, unless secondary inclusions formed largely by redistribution and resealing of primary inclusion fluid which failed to re-equilibrate. Temperatures from line (a) appear more realistic, but because the factor $(+\beta[\sqrt{(Ca)}/Na$ has been neglected, these results may be too high also. Some degree of correlation between homogenization temperatures and Na-K temperatures is shown by the few samples where the results of both determinations are available (Table IV-2).

TABLE IV-2 Comparison of Alkali Ratio and Homogenizatio Temperatures (^{o}C).

Sample	T, line (a)	T, line (b)	T, homogenization
LS-09	234	276	P? 289*
LS-12	271	332	P 302, 312 S ca268
LS-17	268, 206	326, 235	P 238-327 S ca220
LS-18	164, 281	178, 346	P 300-335

P:primary S:secondary

* Not CO_2-saturated ? (may require positive correction for pressure).

Repeat analyses of LS-20 were made to examine consistency of results. The choice of sample for such a test proved unfortunate, as subsequent thin sectioning showed concentrations of extremely large secondary inclusions, as suggested by the generally low temperature measurements. A greater inconsistency is shown by the duplicate analyses of sample LS-18. In one of these analyses, a very high Na content may be due to an unusual amount of secondary inclusion fluid, as suggested by the corresponding high Ca value. Alternatively, sample contamination may have occurred.

There is a number of geochemical factors -largely unevaluated- which may affect the application of this geothermometer. These consist mainly of solution pH changes, dissolved CO_2, and the presence of large proportions of anion species other than chlorides (principally sulphates). Alkali ratio geothermometry has only rarely been applied to fossil geothermal systems, but more commonly to modern geothermal springs and bores, where the problems of low temperatures and shallow depth are more acute. Such problems include high Ca contents and complications arising from disequilibrium effects (rapid cooling, mixing of groundwater, the lining of conduits by silica, etc.).

Such effects may not be significant for the veins at Owen, where there is independent evidence for moderate temperatures and pressures. Although hydrothermal carbonates are abundant, they are usually present in phases distinct from the quartz, and care was taken during sampling to avoid material associated with carbonate. In addition, the mineral assemblages indicate that low oxygen fugacities prevailed, preventing the formation of sulphates during vein formation.

Although feldspars may have been absent in the sericitised zones of deposition, coexisting muscovite-paragonite probably maintained sufficient Na-K solid component in equilibrium with the fluid for thermal control of composition at the time of inclusion formation.

The results of the analyses are sufficiently encouraging to warrant further investigation of the method, using smaller samples, and better sample material containing fewer secondary inclusions. It is unfortunate that more determinations of Ca were not made, as it is noteworthy that the Ca levels for sample LS-20 reflect the Na-K temperatures. Refinements of the method may be possible, leading to absolute quantitative analysis of Ca and the use of the full Log K expression. Such analyses would be possible if the amount of liberated inclusion water were measured, perhaps by microgravimetric means. Alternatively, if the sample was crushed under a water-miscible organic liquid, or in a carrier gas flow, the liberated water could be absorbed onto a catalytic surface and estimated electrochemically (Keidel, 1959).

APPENDIX V

THE TREATMENT OF FLUID INCLUSION DATA

(1) Pressure Correction in 2-Component Systems

Simple water-halide fluid inclusions may be successfully corrected for sealing pressure by the use of the graphs shown in Figure V-2, taken from Lemmlein and Klevtsov (1961). Such a correction, however, requires a knowledge of the fluid salinity, which can be estimated by the use of freezing techniques published by Roedder (1962, 1963), and outlined below.

(a) Salinity Determination by Freezing Point Depression.

The final temperature of melting ice in the inclusion fluid is noted, and if the salts can be assumed to be predominantly univalent halides, Figure V-1 permits an estimation of concentration in terms of NaCl equivalent.

(b) Pressure Correction of Filling Temperatures.

The measured filling temperatures can now be given positive correction for sealing pressure, a parameter which must be estimated by some independent means, e.g. depth of burial at the time of vein formation. If such depths can be estimated by calculating the overlying lithological thickness, considerable errors may be incurred by uncertainty of the degree of restriction of the system (see Chapter VII). Hydrothermal pressures may range from near-hydrostatic pressures in the case of shallow systems, to more than lithostatic pressures in deep systems.

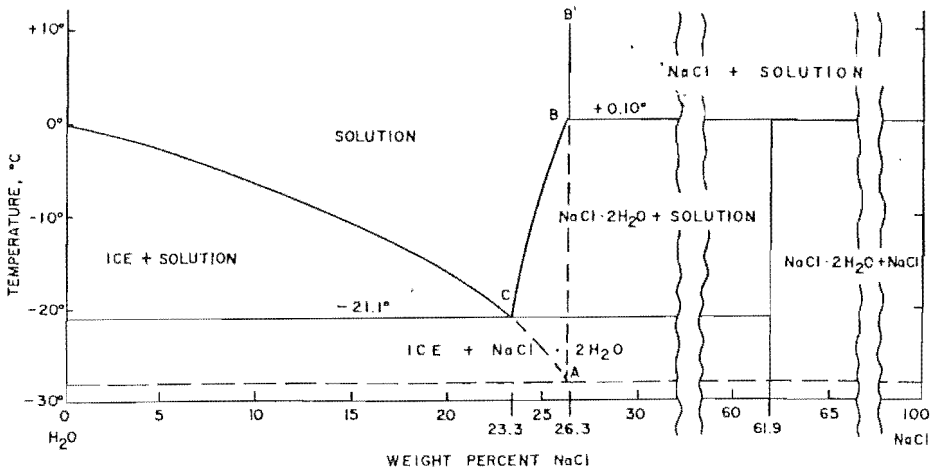

FIG. V-1 Low temperature phases of the system H_2O-NaCl, showing the depression of freezing point by salinity. Most inclusions form ice under conditions expressed by the curve at the extreme left of the diagram. In practice, the last melting temperature is used instead of the first freezing temperature, to avoid problems caused by liquid metastability.
From Roedder (1962).

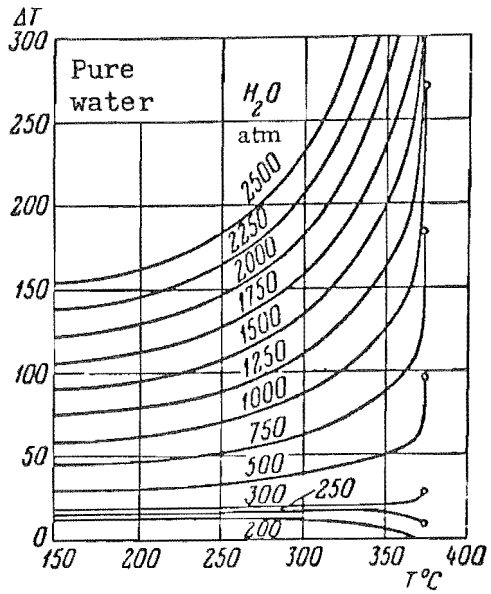

FIG. V-2 Graphs for the correction of inclusion filling temperatures for sealing pressure, from Lemmlein and Klevtsov (1961). The horizontal axes represent observed filling temperature, and the vertical axes the correction to be added. Graphs are given for pure water (above), and for 5, 10, 15, 20, 25, and 30 wt.% NaCl (overleaf).

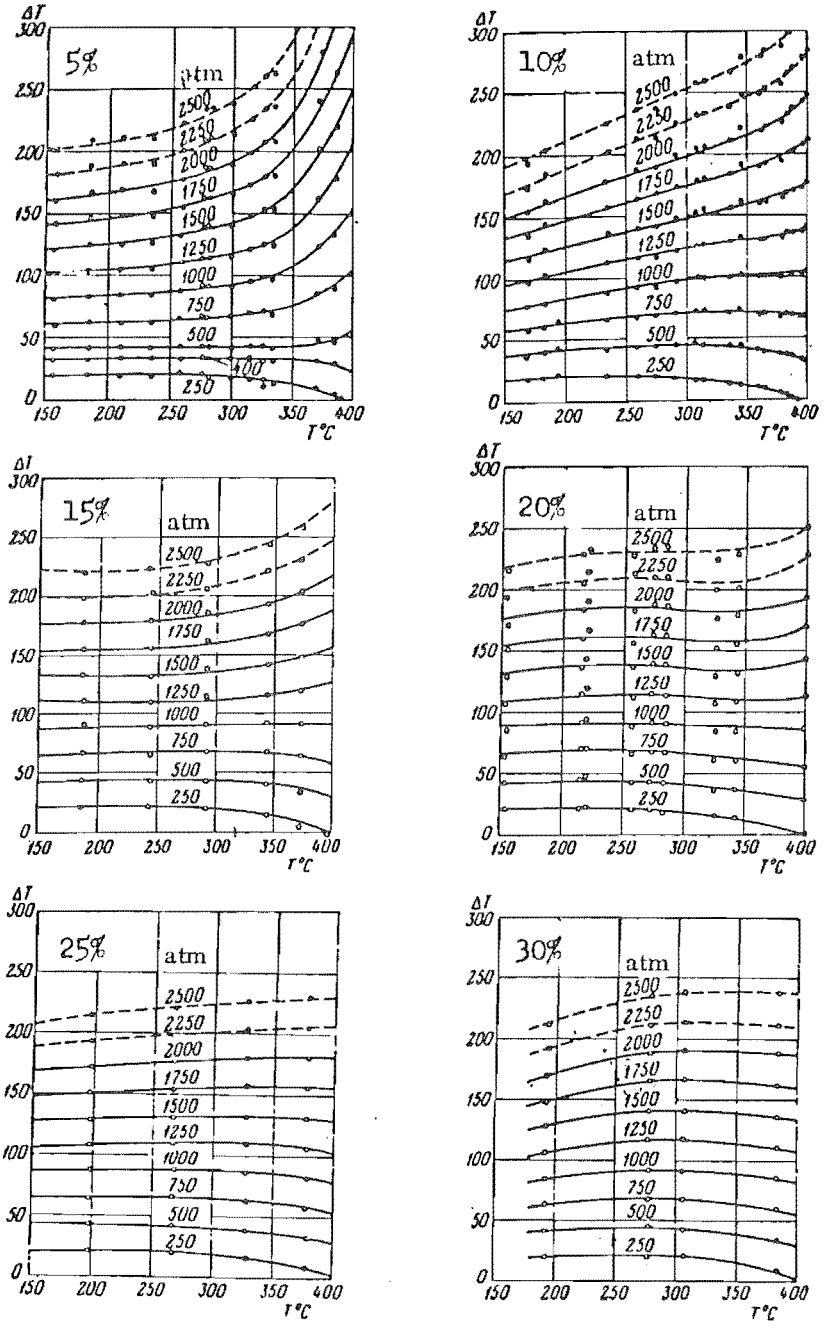

FIG. V-2 (Continued). The percentage figures represent wt.% NaCl equivalent.

(2) Calculation of Pressure for CO_2-Saturated Systems

(a) Estimation of CO_2 and Water. Where CO_2 can be recognised in inclusion fluids, the fluid fraction of this component can be estimated by measuring the vapour fraction (or immiscible liquid fraction) at various temperatures, in subspherical inclusions, by the use of Roedder's (1967) 'degree of filling' diagrams (Figure V-3). For consideration of both liquid and gaseous fluids, Figure V-4 shows the densities of the coexisting phases. A minor correction for CO_2 dissolved in the aqueous fluid fraction may be added, by using the solvus data (Figures 7-21, 7-22, 7-23) and vapour pressure data (Figure 7-26). This correction may be slightly improved on obtaining a provisional salinity estimate.

(b) Estimation of Salinity. Figure 7-26 shows the low temperature phases of the system H_2O-CO_2 in terms of temperature and pressure. Invariant point (d) marks the highest temperature at which CO_2 clathrate can coexist with gaseous CO_2 and liquid water, and the only point at which the phases $CO_{2(l)}$, $CO_{2(g)}$, $H_2O_{(l)}$, and clathrate coexist. As shown by Larsen (1956), this invariant point is displaced to lower temperatures and pressures along the $CO_{2(l)}/CO_{2(g)}$ boundary by increasing salinity of the aqueous liquid.

The temperature depression of this point can be expressed in terms of fluid composition as follows:

$$\text{Log}_e \frac{(1-X_{CO_2}-X_{sol})^{5.75}}{(1-X_{CO_2})^{5.75}} = \frac{-\Delta H^o_{fc}}{R}\left(\frac{1}{T'_o}-\frac{1}{T_i}\right) \quad \ldots\ldots(i)$$

(Dr A. Metcalfe*, pers. comm.)

* Chemistry Department, University of Canterbury.

The symbols of the above equation (i) are as shown:

X_{CO_2} : mole fraction of CO_2 in solution (i.e. reactant for clathrate formation).

X_{sol} : mole fraction of solute (dissolved salts).

ΔH^o_{fc} : energy of formation of clathrate at observed temperature (see Takenouchi and Kennedy 1965b).

R : gas constant.

T_i : temperature of invariant point for a solution without salt, approximately 283°K.

T'_o : observed temperature of invariant point, modified to a theoretical value (°K). As equation (i) is derived from a consideration of energy changes accompanying clathrate formation at constant pressure, the invariant point temperature measured with the freezing-stage (T_o) must be modified by the following procedure:

(i) Construct a graph of $\text{Log}_e P$ vs $\frac{1}{T}$ for values about the invariant point (Figure V-5).

(ii) Add the $CO_{2(l)}/CO_{2(g)}$ boundary, which will plot as a straight line (A) of slope $-\left(\frac{\Delta H^o(l \rightarrow g)}{R}\right)$

(iii) Add the clathrate/$CO_{2(g)}$ + $H_2O_{(l)}$ boundary (line E), the slope of which is

$$-\left(\frac{\Delta H^o_{fc} - \Delta H^o_{sol}}{R}\right)$$

(iv) Add E', a line parallel to E, intersecting line A at the observed invariant point. This point is established by the final melting temperature of the clathrate (T_o), in the presence of salts (see Figure 7-26, curve f).

(v) Extend a horizontal, isobaric line through point (d) to intersect line E'. This intersection defines $\frac{1}{T'_o}$.

Equation (i) can be simplified as follows:

where $X_{CO_2} + X_{sol} < 1$,

$$\text{Log}_e\,(1-X_{CO_2} - X_{sol}) - \text{Log}_e\,(1-X_{CO_2}) = \frac{-\Delta H^o_{fc}}{5.75\ R}\left(\frac{1}{T'_o} - \frac{1}{T_i}\right) \qquad \text{.....(ii)}$$

As $\text{Log}_e(1-X) \cong -X$ if $X \ll 1$,

$$-X_{CO_2} - X_{sol} - (-X_{CO_2}) = -X_{sol} \simeq \frac{-\Delta H^o_{fc}}{5.75\ R}\left(\frac{1}{T'_o} - \frac{1}{T_i}\right) \qquad \text{.....(iii)}$$

By the use of Equation (iii), the mole fraction of the solute is found. Note that the mole fraction value refers to the number of particles, which for a univalent salt is approximately twice the molal concentration;

$$\text{i.e.}\quad X_{sol} = \left(\frac{2m_{sol}}{m_{solvent} + 2m_{sol}}\right) \qquad \text{assuming ideal behaviour.}$$

A small error may be introduced by nonideal behaviour and the neglect of activity coefficients.

(c) Application of Salinity Data to the High Temperature Solvus. The salinity value found by the above procedure is converted to weight % NaCl equivalent for the inclusion fluid at homogenization; i.e.

$$\text{salinity (from (b), above)} \times \left(\frac{\text{aqueous fluid volume } (T_o)}{\text{total inclusion volume}}\right)$$

The amended salinity value may now be applied to a specific Pressure vs Salinity graph drawn up for the measured inclusion, as outlined in Chapter VII. For the purposes of measurement, this graph is best prepared by plotting Log_e P vs salinity (wt. % NaCl), which appears to yield a straight line, at least for mesothermal measurements, permitting an accurate determination by slope calculation. Figure V-6 shows an example, using the data of Figure 7-27.

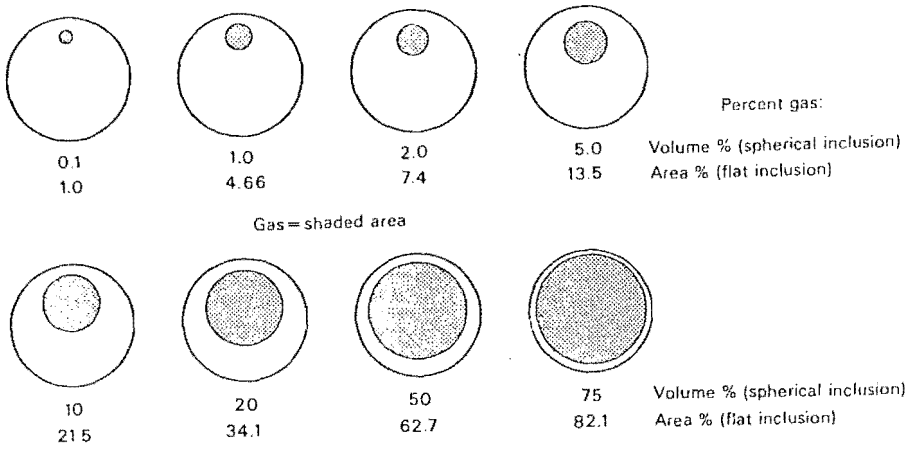

FIG. V-3 'Degree of filling' diagrams from Roedder (1967) showing the appearence of inclusions of ideal shape, partly filled by a vapour (or immiscible liquid) phase.

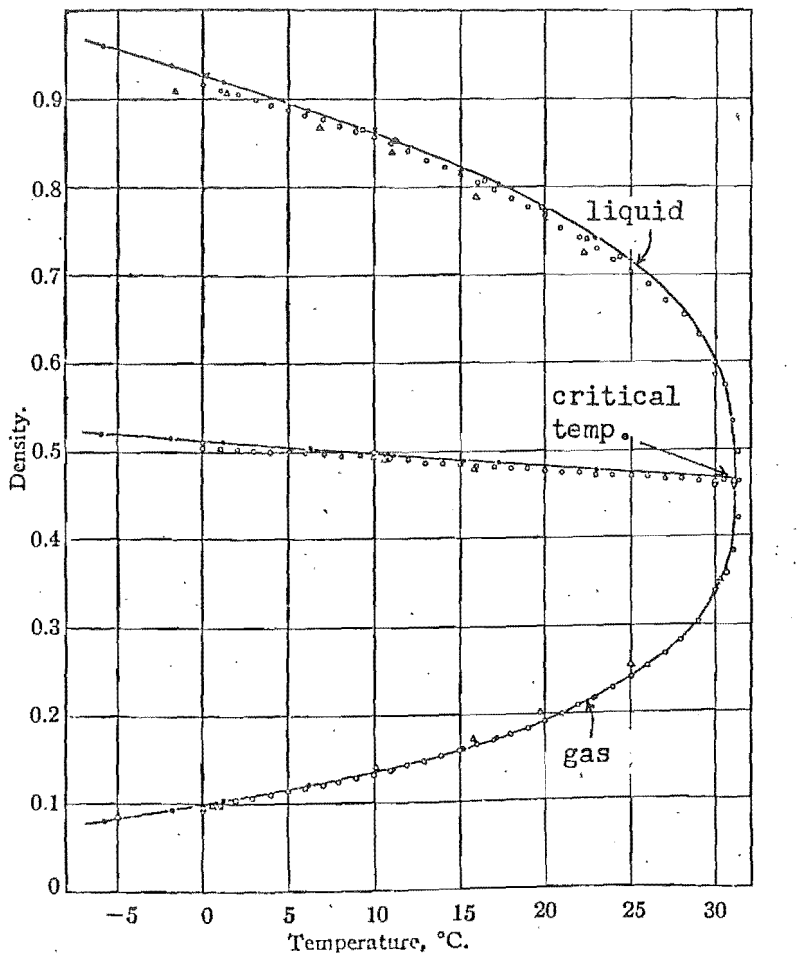

FIG. V-4 Densities of coexisting liquid and gaseous CO_2, adapted from Lowry and Erikson (1927).

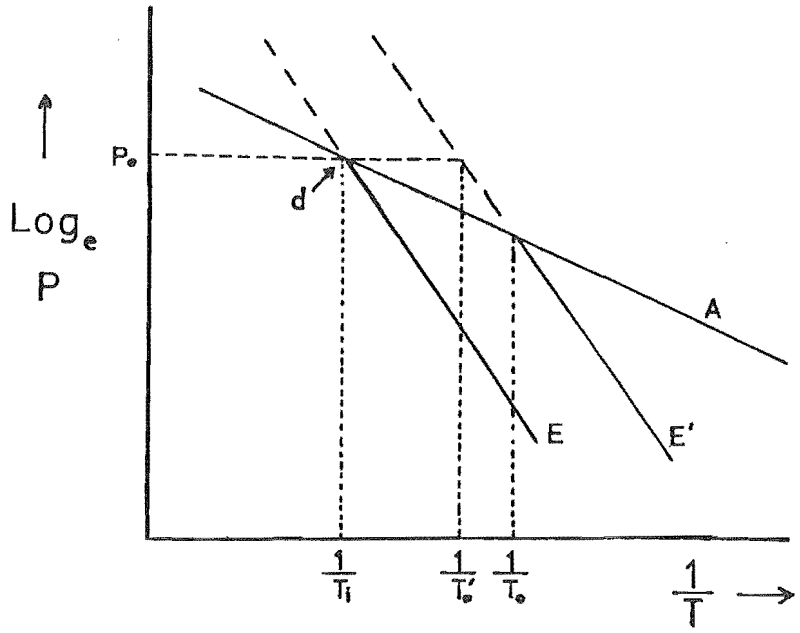

FIG. V-5 The derivation of $\frac{1}{T'_o}$ from $\frac{1}{T_o}$. See text.

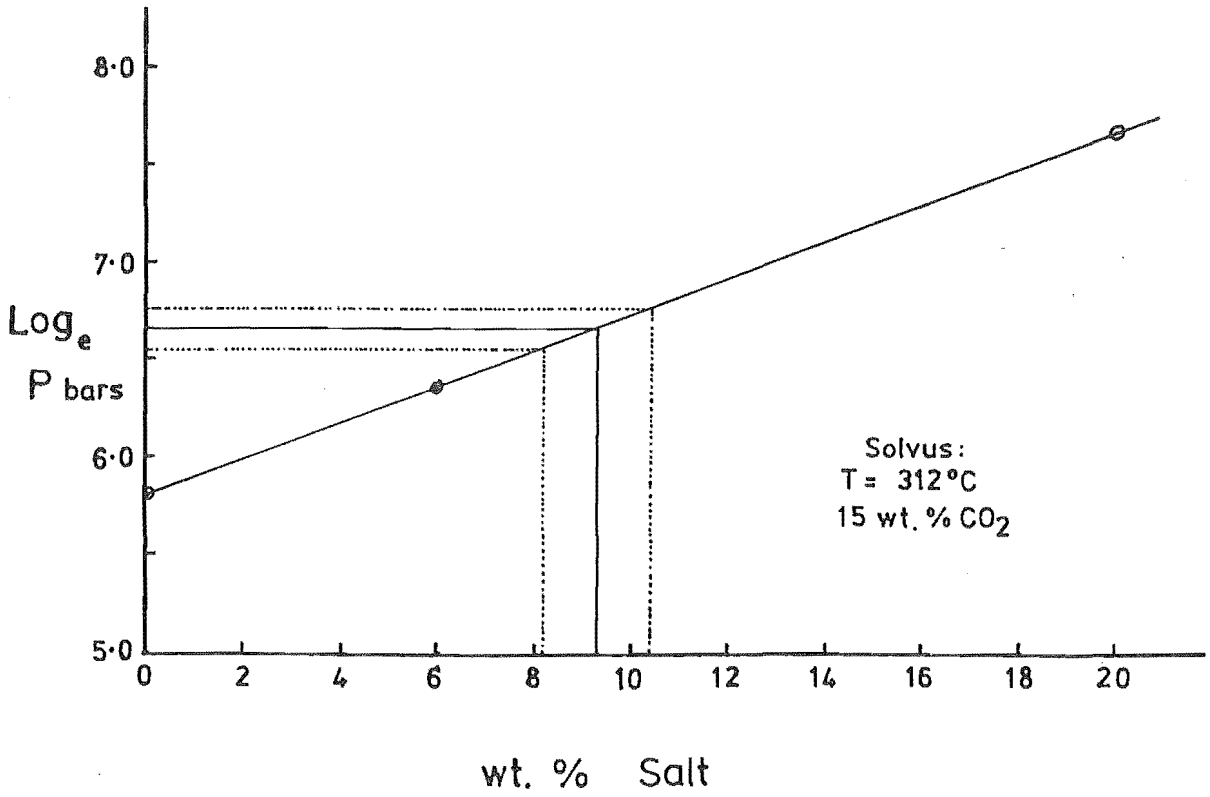

FIG. V-6 The derivation of sealing pressure from salinity, using the line plotted for the solvus of the specific system represented by the measured inclusion.
The data shown above is for the sample LS-12 (compare with Figure 7-26).

APPENDIX VI

FLUID INCLUSION RESEARCH TECHNIQUES

(1) High Temperature Techniques

Roedder (1962) described heating and cooling stages for fluid inclusion studies. Such stages are commercially available, but due to their comparatively high cost, they remain uncommon except where research organisations specialis in this type of investigation. For small projects, a satisfactory stage for heating can be obtained by adapting cheaper equipment as outlined by Newman (1974), and shown in Figure VI-1. A good microscope is essential, especially if small inclusions are to be studied. For typical inclusions in the size range 5-50 μ, an objective power of x40 to x50 is required, preferably of the 'long working distance' type. Binocular eyepiece attachments are desirable due to the long viewing periods required when making homogenization measurements.

Sample preparation has been described in Chapter VII. Careful polishing of both sides of a quartz wafer greatly improves the image quality, although partial polishing is adequate if the inclusions are very large, and especially if silicone oil is used as a sample immersion medium (Newman, 1974). A rapid examination of the sample wafer should be made before polishing is complete, so as to ensure that useable inclusions are present. This step can be carried out by simply mounting a cover slip on the sample with a small drop of water or immersion oil.

For the accurate determination of homogenization temperatures, a heating rate of less than 2^{o}C/minute is recommended for temperatures within ca. 10^{o} of the filling point.

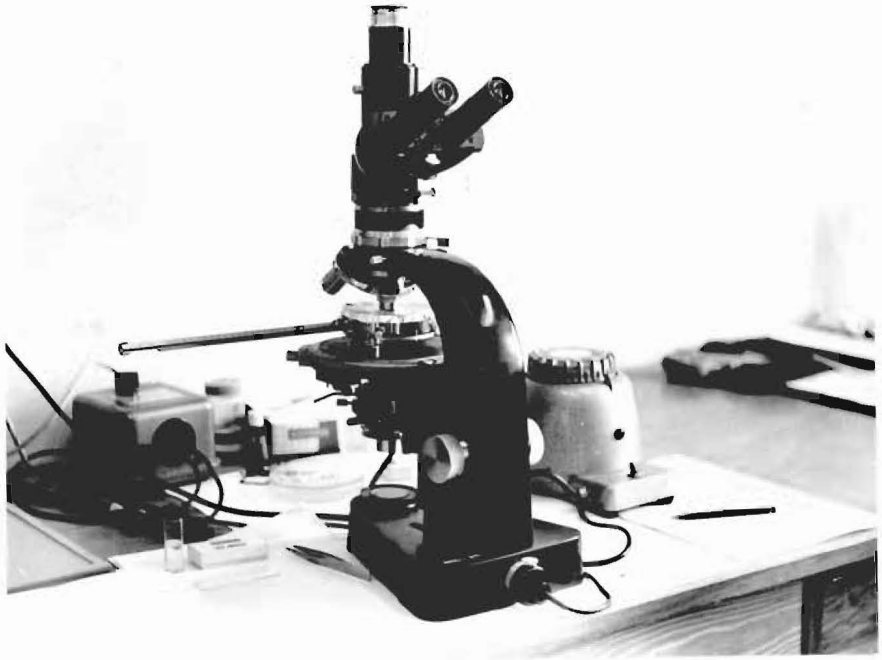

FIG. VI-1 Hot-stage apparatus as used in this project. The microscope is a Leitz Dialux-Pol* with a x44 N.A.=0.65 objective (this lens was intended for polished section use, but provided satisfactory images for inclusions within quartz sections and beneath cover slips). A x25 objective was also fitted for locating inclusions prior to heating; other objectives were removed to provide more working space near the stage. Both x10 and x20 oculars were used. The hot-stage is a standard Reichert stage intended for the determination of melting points and thermal decomposition, etc. of chemical substances. An aluminium foil lid has been added to reduce convection above the hotplate, and to reduce heating of the microscope. Temperature is measured with a mercury thermometer supplied with the stage. Other apparatus shown includes a variac transformer (right) to supply the heating element, and forceps and silicone oil (left) for use in mounting the sample.

* Not Ortholux as previously stated in error (Newman, 1974).

It is not advisable, however, to maintain high temperatures for long periods, as vapourising silicone oil will condense on the objective, and excessive heating of the microscope may incur damage. Unless special cooling accessories are fitted, a cooling period between thermal runs is advised.

Illumination when using the hot-stage is complicated by the increase in distance between sample and condenser, and the consequent lack of conoscopic illumination is especially noticeable when examining very small inclusions. The addition of a small condenser lens directly beneath the hotplate would overcome this problem.

(2) Low Temperature Techniques

(a) Examination of Inclusions without Temperature Measurement. Routine examination of fluid inclusions at low temperatures, advocated by Newman (1975), is easily carried out by spraying the underside of the glass slide sample mount with a small jet of liquid CO_2 while the sample is in place on a conventional microscope stage, and under observation. The CO_2 refrigerant is commercially available in a spray can, from which the contents are discharged through a small, flexible plastic tube which can be carefully passed above the microscope condenser to chill a small area about the field of view. Care should be taken when chilling samples mounted as thin sections, as the balsam mountant may 'craze' and possibly detach from the slide due to thermal shock.

(b) Cooling Studies involving Temperature Measurement. The precise measurement of temperature with cooling stages involves a number of potential difficulties, including thermal gradients within the stage or between sample and stage, sample heating by the illumination, misting and icing of sample and objective surfaces, and problems associated with maintaining

a controlled flow of refrigerant. Many of these difficulties and the need for any cooling stage at all, are eliminated by refrigerating the entire microscope in a large, 'walk in' freezer. A very accurate measurement of temperature may be obtained by simply reading the ambient air temperature near the microscope. Further advantages include the use of the standard conoscopic illuminator, and of oil immersion. Also, the dry atmosphere prevents misting and icing problems. For the low temperature study of very small inclusions, this method is unsurpassed, but for general use there are considerable disadvantages. The operator must endure the low temperatures while examining the sample, and temperature changes are very slow due to the large thermal capacity involved. The method may be employed with minimum discomfort if the operator enters the freezer for a short time at regular intervals to check the appearence of the inclusion contents. The microscope used in this manner (a Leitz Dialux-Pol) withstood temperatures down to -20°C without damage, but removal of unnecessary objectives is advisable. The disadvantages of the method could be overcome if a small freezing chamber was constructed to hold the microscope alone, with suitable ports through which the ocular tubes could project, and with extended controls for the remote operation of focus adjustment.

A conventional cooling stage is more convenient to use, and will produce satisfactory results if care is taken to prevent the problems noted above. The design of a cooling stage which should produce good results is shown in Figure VI-2. A stage of this type was constructed and used for this project, but lacked some of the refinements shown.

Filtering of the illumination by a blue filter will greatly reduce the heating of the sample, but the use of the

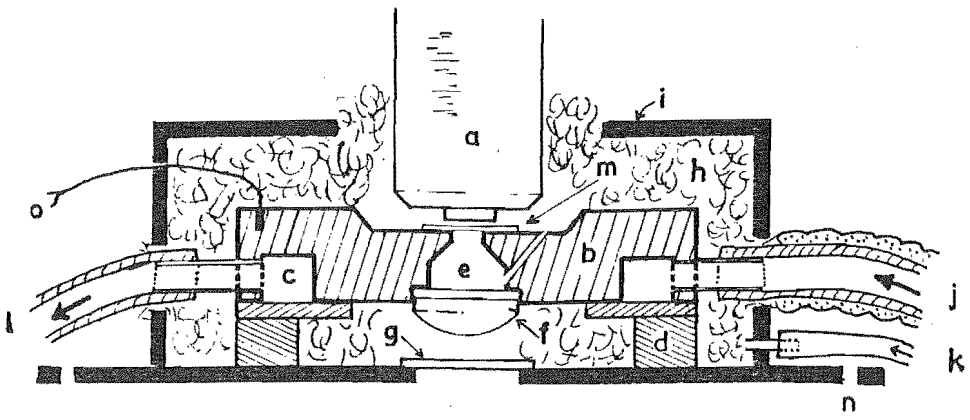

FIG. VI-2 Practical design of a cooling stage, shown in section, approximately natural size.

(a) Microscope objective.
(b) Cooling block (aluminium, brass, or copper).
(c) Annular passage for gas flow.
(d) Non-conducting support blocks and annular sealing disk ('tufnel' or similar).
(e) Cell of low freezing temperature liquid, with relief vent.
(f) Accessory condenser lens.
(g) Plane glass window.
(h) Insulation (cotton or dacron wool).
(i) Outer case ('perspex' or plastic).
(j) Refrigerant gas inlet tube (plastic, insulated).
(k) Small tube for flushing gas entry.
(l) Refrigerant gas exhaust.
(m) Sample wafer, mounted in suitable immersion medium between cover slips.
(n) Holes for mounting screws, for attachment to microscope.
(o) Line to thermocouple.

lowest adequate level of illumination is recommended. If photography of the chilled inclusions is required, a flash type illumination will prevent image blurring caused by volume changes and Brownian movement. An accessory condenser lens below the sample will greatly improve image quality, but this lens should be combined with the liquid-filled cell shown in Figure VI-2, to provide good thermal equilibrium between sample and stage. If such a cell is used, a small vent channel must be provided to prevent air bubbles being drawn in beneath the sample during contraction of the liquid.

The most suitable refrigerant was found to be the vapour from boiling liquid air or liquid nitrogen. Flow rates, and hence stage cooling rates, can be controlled by the following methods:

(i) The exhaust vent of the stage can be connected to a tap aspirator, and the input tube immersed in the liquid refrigerant in an open container. With this configuration, a long inlet tube length must be exposed to the air to allow the liquid to boil before reaching the stage. The flow is controlled by a pinchclamp on the exhaust tube, but 'bumping' of the boiling liquid is difficult to prevent.

(ii) A more satisfactory method involves venting the stage exhaust freely, and sealing the liquid refrigerant flask to the stage input line by means of a rubber bung and glass tube. The refrigerant gases may now be boiled off and forced through the stage under slight positive pressure by the use of a small electric heating element immersed in the liquid. A heating-stage variac transformer is adequate to power such an element, and provides excellent control of gas flow rate. If this method is used, a second tube through the flask bung should be provided, terminating in a lightly

stoppered seal, to act as a safety valve in case of the accumulation of excessive pressure. This precaution is necessary because the main flask bung usually becomes firmly cemented in place by accumulated ice. Care should be taken to ensure that the boiling-off process is not continued to the point where the liquid level falls below the heating element; should this occur, the element will rapidly burn out. No oxidisable substance should be allowed in the flask if liquid air is used as ignition by an overheated element in such circumstances can have destructive consequences.*

Misting and icing is greatly reduced by packing the space around the objective with insulation, and entirely eliminated if the stage chamber is periodically flushed by a small flow of dry refrigerant gas. Leakage around the annular sealing ring may provide sufficient gas for this purpose during a cooling run, but adequate flushing before cooling begins is recommended, to remove all water vapour from the chamber.

Stage temperature is easily monitored by using a thermocouple cemented into the cooling block, and standardised by a reference junction in melting ice. Connection to the high-impedence input of a chart recorder provides a convenient readout. Temperature calibration may be checked by freezing small drops of saline water. All temperature measurements made with a cold-stage should be taken from melting points, because of the common liquid metastability encountered in small inclusions.

*The writer has personal experience of such an incident.

APPENDIX VII

CORRELATION OF SAMPLE NUMBERS

Writer's LS number	UC number *
LS-01	UC8933a
LS-06	UC8933b
LS-09	UC8933c
LS-12	UC8934
LS-13	UC8933d
LS-14	UC8933e
LS-15	UC8933f
LS-17	UC8933g
LS-20	UC8933h
LS-21	UC8933i

Polished specimens	UC number
PS500	UC8872
PS501	UC8868
PS503	UC8890
PS504	UC8888
PS505	UC8888
PS506	UC8889
PS507	UC8894
PS508	UC8895
PS509	UC8896
PS510	UC8893
PS511	UC8886

Notes.
UC numbers and PS numbers are catalogued at the Geology Department, and the specimens retained in collections.

*Gaps in the LS series are due to the discarding of unimportant material, and some specimens referred to in the text are not catalogued because insufficient sample remained.